



Ludwig-Maximilians-Universität München

Department Biologie I

Bereich Genetik

Evolutionary repurposing of cAMP and PKA signaling pathways in kinetoplastids

Sabine Bachmaier

**Inaugural-Dissertation
zur Erlangung des Doktorgrades
der Fakultät für Biologie
der Ludwig-Maximilians-Universität München
Eingereicht am 16.03.2015**

Erster Gutachter: **Prof. Dr. Michael Boshart**
Biozentrum der Ludwig-Maximilians-Universität München
Bereich Genetik

Zweiter Gutachter: **Prof. Dr. Martin Parniske**
Biozentrum der Ludwig-Maximilians-Universität München
Bereich Genetik

Datum der Abgabe: 16.03.2015

Datum der mündlichen Prüfung: 23.04.2015

Eidesstattliche Erklärung

Ich versichere hiermit an Eides statt, dass die vorgelegte Dissertation von mir selbstständig und ohne unerlaubte Hilfe angefertigt wurde. Des Weiteren erkläre ich, dass ich nicht anderweitig ohne Erfolg versucht habe, eine Dissertation einzureichen oder mich der Doktorprüfung zu unterziehen. Die folgende Dissertation liegt weder ganz, noch in Teilen einer anderen Prüfungskommission vor.

München, 16.03.15

Sabine Bachmaier

Statutory declaration

I declare that I have authored this thesis independently, that I have not used other than the declared sources/resources. As well I declare that I have not submitted a dissertation without success and not passed the oral exam. The present dissertation (neither the entire dissertation nor parts of it) has not been presented to another examination board.

Munich, 16.03.15

Sabine Bachmaier

Table of contents

Eidesstattliche Erklärung	III
Statutory declaration	III
Table of contents	IV
Abbreviations	VI
Publications and Manuscripts Originating from this Thesis	IX
Contribution to Publications and Manuscripts Presented in this Thesis	X
Summary	XII
Zusammenfassung	XIV
1. Introduction	16
1.1 The cAMP/PKA signal transduction pathway	16
1.1.1 Evolutionary conservation of the cAMP/PKA signal transduction pathway	17
1.1.2 Activation mechanism of PKA	20
1.1.3 Downstream functions of cAMP/PKA signaling	21
1.2 Signal transduction in <i>T. brucei</i>	21
1.2.1 The model organism <i>Trypanosoma brucei brucei</i>	21
1.2.2 Putative components of the <i>T. brucei</i> cAMP/PKA signal transduction pathway	23
1.2.3 Life cycle stage differentiation of <i>T. brucei</i>	24
1.3 Scope of this thesis	27
1.4 References for introduction	28
2. Cyclic AMP production in <i>T. brucei</i> – the adenylyl cyclases.	39
2.1 Cytokinesis of <i>Trypanosoma brucei</i> bloodstream forms depends on expression of adenylyl cyclases of the ESAG4 or ESAG4-like subfamily.	39
2.2 Adenylate cyclases of <i>Trypanosoma brucei</i> inhibit the innate immune response of the host.	41
3. Cyclic AMP effectors in African trypanosomes revealed by genome-scale RNA interference library screening for resistance to the phosphodiesterase inhibitor CpdA.	43
4. Unconventional activation of <i>T. brucei</i> PKA.	45
4.1 Cyclic AMP-independent signaling from a conserved PKA.	45
4.2 A cold-inducible protein kinase A regulates stage differentiation of trypanosomes.	85
5. Bidirectional axenic differentiation of <i>Leishmania</i> implicates changes in protein kinase A signaling.	117
6. Concluding Discussion	136
6.1 Why is there such a diversity of ACs in <i>T. brucei</i> ?	137
6.2 Unconventional upstream activation mechanism(s) of <i>T. brucei</i> PKA	138
6.2.1 No activation by cAMP – predictable from the primary amino acid sequence of <i>T. brucei</i> PKAR?	138
6.2.2 Possible mechanisms of cold shock-induced PKA activation	139
6.2.3 Ligand-dependent activation of <i>T. brucei</i> PKA.	141

Content

6.2.4	Is there a physiological connection between cold shock- and purine nucleoside-dependent PKA activation?	144
6.3	The special properties of the catalytic PKA isoform C3	145
6.4	Downstream signaling of <i>T. brucei</i> PKA	146
6.5	A kinetoplastid-specific cAMP downstream pathway	149
6.6	Evolutionary conservation of the unconventional cAMP and PKA signal transduction pathways within kinetoplastids?	150
6.7	References for discussion	150
	Supplemental material – Chapter 4.1	160
	Supplemental material – Chapter 4.2	208
	Supplemental material – Chapter 5	241
	Supplemental material – Discussion	242
	Acknowledgements	248
	Curriculum Vitae	250

Abbreviations

7-TM	7-transmembrane
AC	adenylyl cyclase
AKAP	A-kinase anchoring protein
AMP	adenosine monophosphate
ATP	adenosine triphosphate
BioID	proximity-dependent biotin identification
BLAST	basic local alignment search tool
BLE	bleomycin resistance protein
BSD	blasticidin S deaminase
BSF	bloodstream form
CaMKII	calmodulin-dependent kinase II
cAMP	cyclic adenosine monophosphate
CARP	cAMP response protein
CCA	citrate/cis-aconitate
cGMP	cyclic guanosine monophosphate
CK	casein kinase
CLK	cdc2-like kinase
CNB	cyclic nucleotide binding
cNMP	cyclic nucleotide monophosphate
CpdA	compound A
CRP	cAMP receptor protein
CS	cytoskeleton
CSD	cold shock domain
CSP	cold shock protein
DAPI	4,6-Diamidino-2-phenylindole
DD	dimerization/docking
DMP	dimethyl pimelimidate
DMSO	dimethyl sulfoxide
DTT	dithiothreitol
EDTA	ethylenediaminetetraacetic acid
ENT	equilibrative nucleoside transporter
Epac	exchange protein activated by cAMP
FACS	fluorescence activated cell sorting
FBS	fetal bovine serum
GAF	cGMP-specific and -stimulated phosphodiesterases, <i>Anabaena</i> adenylylate cyclases and <i>E. coli</i> FhtA
GC	guanylyl cyclase
FDR	false discovery rate
GKIP	G-kinase interacting protein
GMP	guanosine monophosphate

Abbreviations

GO	gene ontology
GPCR	G protein coupled receptor
GSK	glycogen synthase kinase
GST	glutathione S-transferase
HA	hemagglutinin
HAT	Human African Trypanosomiasis
HMM	Hidden Markov Model
HSP	heat shock protein
HYG	hygromycin phosphotransferase
IFT	intraflagellar transport protein
IP	immunoprecipitation
I κ B	inhibitor of NF κ B
LEXSY	<i>Leishmania tarentolae</i> expression system
LRR	leucine rich repeat
LS	long slender
MAPK	mitogen activated protein kinase
MCP3	mitochondrial carrier protein 3
MS	mass spectrometry
MS/MS	tandem mass spectrometry
MST	Microscale Thermophoresis
MT	microtubule
MW	molecular weight
NEO	neomycin phosphotransferase
NF κ B	nuclear factor 'kappa-light-chain-enhancer' of activated B-cells
ORF	open reading frame
PAC	puromycin N-acetyl transferase
PAD	protein associated with differentiation
PBC	phosphate binding cassette
PBP	periplasmic binding protein
PBS	phosphate buffered saline
PCF	procyclic form
pCPT	para-chlorophenylthio
PCR	polymerase chain reaction
PDE	phosphodiesterase
PDT	population doubling time
PEK	pancreatic eIF-2 α kinase
PFC	paraflagellar rod component
PFR	paraflagellar rod
PIP39	PTP1-interacting protein with a MW of 39 kDa
PKA	cAMP-dependent protein kinase, protein kinase A
PKAC	PKA catalytic subunit
PKAR	PKA regulatory subunit

PKB	protein kinase B
PKC	protein kinase C
PKG	protein kinase G
PKI	protein kinase inhibitor (PKA specific)
PM	plasma membrane
PTM	posttranslational modification
PTP1	protein tyrosine phosphatase 1
PVDF	polyvinylidene difluoride
RBP	RNA-binding protein
RDK	repressor of differentiation kinase
RIPA	radioimmunoprecipitation assay
RNAi	RNA interference
RNAseq	RNA sequencing
RSK	ribosomal S6 kinase
SDS	sodium dodecyl sulfate
SIF	stumpy induction factor
SS	short stumpy
Tet	tetracycline
TGF- β	transforming growth factor beta
TMD	transmembrane domain
TRP	transient receptor potential
UTR	untranslated region
VASP	vasodilator stimulated phosphoprotein
VSG	variant surface glycoprotein
wt	wild type
Y2H	yeast 2-hybrid
ZFK	zinc finger kinase

Publications and Manuscripts Originating from this Thesis

Chapter 2.1

Salmon D., Bachmaier S., Krumbholz C., Kador M., Gossmann J. A., Uzureau P., Pays E., Boshart M. (2012). Cytokinesis of *Trypanosoma brucei* bloodstream forms depends on expression of adenylyl cyclases of the ESAG4 or ESAG4-like subfamily. *Mol Microbiol* 84(2): 225-42.

Chapter 2.2

Salmon D., Vanwalleghem G., Morias Y., Denoëud J., Krumbholz C., Lhomme F., Bachmaier S., Kador M., Gossman J. A., Dias F. B., De Muylder G., Uzureau P., Magez S., Moser M., De Baetselier P., Van Den Abbeele J., Beschin A., Boshart M., Pays E. (2012). Adenylate cyclases of *Trypanosoma brucei* inhibit the innate immune response of the host. *Science* 337(6093): 463-6.

Chapter 3

Gould, M. K.*, Bachmaier, S.*, Ali, J. A., Alsford, S., Tagoe, D. N., Munday, J. C., Schnauffer, A. C., Horn, D., Boshart, M., de Koning, H. P. (2013). Cyclic AMP effectors in African trypanosomes revealed by genome-scale RNA interference library screening for resistance to the phosphodiesterase inhibitor CpdA. *Antimicrob Agents Chemother* 57: 4882-4893.

* these authors contributed equally to this article.

Chapter 4.1

Bachmaier, S., Kramer, S., Githure, G., Scharf, F., Klöckner, T., Krumbholz, C., Böttger, F., Pepperl, J., Schulte zu Sodingen, C., Schwede, F., Gunasekera, K., Ochsenreiter, T., Genieser, H.-G., Boshart, M. (2015). Cyclic AMP-independent signaling from a conserved PKA. *Manuscript*.

Chapter 4.2

Bachmaier, S., Kramer, S., Pepperl, J., Githure G., Israel, L., Imhof, A., Boshart, M. (2015). A cold-inducible protein kinase A regulates stage differentiation of trypanosomes. *Manuscript*.

Chapter 5

Bachmaier, S.*, Witztum, R.*, Tsigankov, P., Koren, R., Boshart, M., Zilberstein, D. (2015). Bidirectional axenic differentiation of *Leishmania* implicates changes in protein kinase A signaling. *Manuscript* submitted to *Int J Parasitol*.

* these authors contributed equally to this article.

Contribution to Publications and Manuscripts Presented in this Thesis

Chapter 2.1

D.S., S.B., E.P., and M.B. designed research; D.S., S.B., C.K., M.K., J.A.G., and P.U. performed research; D.S., S.B., C.K., M.K., J.A.G., E.P., and M.B. analyzed data; D.S., E.P., and M.B. wrote the paper.

Chapter 2.2

D.S., A.B., M.B., and E.P. designed research; D.S., G.V., A.B., Y.M., J.D., C.K., F.L., S.B., M.K., J.A.G., F.B.S.D., G.D.M., P.U., S.M., M.M., and J.V.D.A. performed research; D.S., G.V., A.B., J.V.D.A., M.B., and E.P. analyzed data; D.S., A.B., M.B. and E.P. wrote the paper.

Chapter 3 (shared first authorship)

M.K.G., S.B., M.B., and H.P.d.K. designed research; M.K.G., S.B., J.A.A., D.N.T., and J.C.M. performed research; M.K.G., S.B., S.A., A.C.S., M.B., and H.P.d.K. analyzed data; M.K.G., S.B., M.B., and H.P.d.K. wrote the paper.

Chapter 4.1

S.B., S.K., G.G., and M.B. designed research; S.B., S.K., G.G., F. Scharf, T.K., C.K., F.B., J.P., C.S.z.S., and K.G. performed research; F. Schwede and H.-G.G. contributed new reagents; S.B., S.K., G.G., F. Scharf, F. Schwede, K.G., T.O., and M.B. analyzed data; S.B. wrote the paper.

Chapter 4.2

S.B., S.K., and M.B. designed research; S.B., S.K., J.P., G.G., and L.I. performed research; S.B., S.K., L.I., A.I., and M.B. analyzed data; S.B. wrote the paper.

Chapter 5 (shared first authorship)

S.B., M.B., and D.Z. designed research; S.B., R.W., P.T., and R.K. performed research; S.B., R.W., P.T., R.K., M.B., and D.Z. analyzed data; S.B., M.B., and D.Z. wrote the paper.

Contribution

I hereby confirm the above statements

Sabine Bachmaier

Matthew Kenneth Gould

Ronit Witztum

Prof. Dr. Michael Boshart

Summary

The protein kinase A (PKA) signal transduction pathway is highly conserved from lower unicellular eukaryotes such as *Saccharomyces cerevisiae* to mammals. The evolutionary distance from yeast to mammals is, however, relatively low compared to the evolutionary distance to the first primitive eukaryotic organisms. In the protozoan parasite *Trypanosoma brucei*, which belongs to the evolutionary early branching order of *Kinetoplastida*, not a single complete signal transduction pathway has been uncovered yet. Since *T. brucei* is the causative agent of Human African Sleeping Sickness, a life threatening neglected tropical disease very difficult to treat, there is a strong demand for discovery, design and development of new drugs. Parasite-specific signal transduction components might represent promising drug targets. Previous work from this laboratory provided indications for retooling of cAMP/PKA signaling in *T. brucei*. The scope of this work was to identify and characterize known and novel components of cAMP/PKA signaling in the parasite. Cyclic AMP is produced by a large family of receptor-type adenylate cyclases (ACs) with atypical sequence and structural features. We could show that by regulation of cytokinesis and modulation of the host immune response, the second messenger plays an important intracellular as well as extracellular role in *T. brucei*. Surprisingly, the parasite PKA orthologue was insensitive to cAMP and thereby represents the first example of a PKA uncoupled from this second messenger. Instead, the kinase was activated by low temperature, a known inducer in the parasite's life cycle. *T. brucei* shuttles between a mammalian host and an insect vector and hence faces dramatic and rapid alterations in the environmental conditions, e.g. changes in temperature, pH or nutrient availability. We provide evidence that *T. brucei* PKA is involved in signaling during temperature-dependent differentiation from the bloodstream to the insect stage in culture. Similarly, in the related kinetoplastid parasite *Leishmania donovani*, the causative agent of visceral leishmaniasis, PKA signaling showed strong stage-specificity with a rapid change in the abundance of PKA-specific downstream phosphorylations upon induction of promastigote (in the insect vector) to amastigote (in the mammalian host) differentiation. Moreover, we observed indirect activation of *T. brucei* PKA by the adenosine antimetabolite dipyrindamole *in vivo* providing strong evidence for activation of PKA by (an) endogenous, purine nucleoside-related ligand(s). A small-scale chemical screen aiming to define the chemical space of the putative ligand(s) resulted in identification of several activators and inhibitors, which were subsequently used as tool to identify downstream components of PKA signaling in *T. brucei*. Expression profiling and phosphoproteomics analysis revealed involvement of the kinase in regulation of metabolism, ribosome biogenesis and translation, transport, protein folding, and motility, reminiscent of PKA downstream functions in other organisms. However, a substantial amount of the identified PKA downstream components were kinetoplastid- or even *Trypanosoma*-specific with mostly unknown function and hence point to parasite-specific functions of the kinase. The absence of genes with similarity to any known alternative cAMP receptors from trypanosomal genomes indicated the presence of unknown cAMP effectors. By a whole genome RNAi library screen selecting for cells resistant to elevated intracellular cAMP levels, we identified several novel cAMP response proteins (CARPs). Most importantly, CARP1, a protein exclusively found in kinetoplastids, acts as cAMP acceptor and might represent the entry point into a novel, kinetoplastid-specific cAMP signaling

Summary

pathway. Since the discovered peculiarities of cAMP and PKA signaling in *T. brucei* are likely to be conserved within the kinetoplastid order, components of these pathways represent promising targets for drug development against kinetoplastid-caused diseases (Human African Sleeping Sickness, Chagas disease, Leishmaniasis).

Zusammenfassung

Der Protein Kinase A (PKA) Signaltransduktionsweg ist hoch konserviert von niederen, einzelligen Eukaryoten wie z. B. der Bäckerhefe *Saccharomyces cerevisiae* bis hin zu Säugern. Die evolutionäre Distanz der Hefe zum Säuger ist jedoch relativ zur evolutionären Distanz zu den ersten, ursprünglichen Eukaryoten ziemlich gering. In *Trypanosoma brucei*, einem parasitischen Protozoen der Ordnung *Kinetoplastida*, welche sich in der Evolution sehr früh abgespalten hat, konnte bislang kein einziger kompletter Signaltransduktionsweg entschlüsselt werden. Da *T. brucei* die Afrikanische Schlafkrankheit verursacht, eine lebensbedrohliche, vernachlässigte tropische Erkrankung, welche nur schwer behandelbar ist, herrscht ein enormer Bedarf an der Entdeckung und Entwicklung neuer Therapeutika. Hierbei könnten Trypanosomen-spezifische Komponenten von Signaltransduktionswegen erfolgversprechende Zielstrukturen darstellen. Da vorhergehende Arbeiten aus diesem Labor einen Hinweis auf Besonderheiten der cAMP/PKA Signaltransduktion in *T. brucei* lieferten, war das Ziel der vorliegenden Arbeit, bekannte sowie neue Komponenten dieses Signalweges in *T. brucei* zu identifizieren und zu charakterisieren. Der sekundäre Botenstoff cAMP wird in dem Parasiten von einer großen Familie membranständiger, rezeptorartiger Adenylatzyklen hergestellt, welche untypische Sequenz- und Struktureigenschaften aufweisen. Wir konnten zeigen, dass die Adenylatzyklen intrazellulär für die Regulation der Zytokinese verantwortlich sind. Darüber hinaus konnten wir nachweisen, dass *T. brucei* cAMP nutzt, um das Immunsystem des Wirtes zu manipulieren und damit seine eigene Verbreitung zu optimieren. Überraschenderweise zeigte die *T. brucei* PKA im Gegensatz zu allen bisher charakterisierten PKAs aus den verschiedensten Organismen keine Sensitivität gegenüber cAMP. Stattdessen konnte die Kinase durch Temperaturenniedrigung, einem sogenannten Kälteschock, aktiviert werden, ein Stimulus, der eine wichtige Rolle bei der Stadiendifferenzierung des Parasiten spielt. *T. brucei* durchläuft während seines komplexen Lebenszyklus einen Wechsel zwischen einem Säugewirt und einem Insektenvektor und ist deshalb gravierenden Änderungen der Umgebungsbedingungen, wie z. B. Temperatur, pH-Wert oder Nährstoffangebot, ausgesetzt. Tatsächlich konnten wir zeigen, dass die *T. brucei* PKA bei der Kälte-induzierten Differenzierung der Blutstromform (im Säugewirt) in die prozyklische Form (in der Tsetse-Fliege) in Kultur eine Rolle spielt. Auch in dem verwandten Kinetoplastiden *Leishmania donovani*, dem Erreger der viszeralen Leishmaniose, wies der PKA Signalweg eine starke Stadienspezifität auf mit rapider Änderung PKA-spezifischer Phosphorylierungen nach Induktion der Differenzierung vom promastigoten (im Insektenvektor) zum amastigoten (im Säugewirt) Stadium, was möglicherweise auf eine Beteiligung an der Regulation der Stadiendifferenzierung hinweisen könnte. Darüber hinaus konnten wir beobachten, dass die *T. brucei* PKA *in vivo* indirekt durch den Adenosin-Antimetaboliten Dipyridamol aktiviert wird. Dies deutet auf Regulierbarkeit der Kinase durch einen (oder auch mehrere) endogenen Liganden, welcher Ähnlichkeit zu Purin-Nukleosiden aufweist, hin. Um die Struktur des/der möglichen endogenen Liganden weiter einzuzugrenzen, wurde ein chemischer Screen durchgeführt, anhand dessen mehrere Aktivatoren und Inhibitoren der *T. brucei* PKA identifiziert wurden. Diese eignen sich als hervorragende Werkzeuge, um nachfolgende Komponenten des PKA Signalweges zu identifizieren. Mittels Transkriptom- und Phosphoproteomanalysen konnten wir zeigen, dass die Kinase an der Regulierung von Stoffwechsel,

Ribosomen-Biogenese und Translation, Transport, Proteinfaltung und Motilität von *T. brucei* beteiligt ist. Diese Prozesse werden auch in anderen Eukaryoten durch PKA reguliert. Allerdings ist ein beträchtlicher Anteil der identifizierten Proteine Kinetoplastiden- oder sogar Trypanosomen-spezifisch, was auf einzigartige Funktionen der PKA in diesen Organismen hinweist. Da das Trypanosomengenom keine Gene mit Ähnlichkeit zu bekannten, alternativen cAMP Rezeptoren aus anderen Organismen enthält, ist es sehr wahrscheinlich, dass bislang unbekannte cAMP Effektorproteine vorhanden sind. Mittels eines RNAi Screens, welcher auf Selektion von Zellen mit Resistenz gegenüber erhöhter intrazellulärer cAMP-Konzentration basierte, konnten wir mehrere neue „cAMP response proteins“ (CARPs) identifizieren. Besonders hervorzuheben ist dabei die Identifizierung von CARP1, ein cAMP-bindendes Protein, welches ausschließlich in Kinetoplastiden vorkommt und damit höchstwahrscheinlich die Eintrittsstelle in einen neuen, Kinetoplastiden-spezifischen cAMP Signaltransduktionsweg darstellt. Da die Besonderheiten der cAMP und PKA Signaltransduktionswege in *T. brucei* offensichtlich innerhalb der Ordnung der *Kinetoplastida* konserviert sind, stellen Komponenten beider Signalwege vielversprechende Zielstrukturen zur Medikamentenentwicklung gegen Krankheiten, welche durch Kinetoplastiden verursacht werden (Afrikanische Schlafkrankheit, Chagas Krankheit, Leishmaniose), dar.

1. Introduction

1.1 The cAMP/PKA signal transduction pathway

The ability to specifically respond to changes in the extracellular environment is pivotal for unicellular as well as multicellular organisms. This is accomplished by various mechanisms of signal transduction with protein kinases representing major components of most signaling pathways. The cyclic AMP-dependent protein kinase PKA has been identified almost 50 years ago (Walsh et al., 1968), ten years after the identification of its activator, the second messenger cyclic AMP (cAMP) (Rall and Sutherland, 1958), and is now one of the best studied protein kinases from a variety of eukaryotes. Together with the cGMP-dependent protein kinase PKG it belongs to the group of cyclic nucleotide-regulated kinases. Several highly conserved components comprise the conventional cAMP/PKA signal transduction pathway of most eukaryotes (Figure 1.1, left): binding of an extracellular ligand, e.g. a hormone, to a 7-transmembrane (7-TM) G protein-coupled receptor (GPCR) induces dissociation of the alpha subunit ($G_s\alpha$) of an associated heterotrimeric G protein, which subsequently activates a transmembrane adenylate cyclase (AC) to produce the second messenger cAMP. By binding to the regulatory subunits of PKA, cAMP induces a conformational change resulting in dissociation of active catalytic PKA subunits, which consequently phosphorylate a variety of downstream substrates (Skalhegg and Tasken, 2000). Deregulation of the cAMP/PKA signal transduction pathway has been implicated in a variety of human diseases including Carney complex (Kirschner et al., 2000), Cushing's syndrome (Groussin et al., 2002; Beuschlein et al., 2014; Cao et al., 2014; Goh et al., 2014; Sato et al., 2014), or cancer (Gordge et al., 1996; Cho et al., 2000; Naviglio et al., 2010; Beristain et al., 2014). Hence, spatiotemporal specificity is crucial for cellular and organismal viability. This is accomplished by generation of cAMP microdomains via several independent mechanisms (Skalhegg and Tasken, 2000): 1) cAMP produced by ACs can be hydrolyzed by several different classes of phosphodiesterases (PDEs) or can be exported via specific transporters. 2) Distinctive isoforms of regulatory (PKAR) and catalytic (PKAC) PKA subunits with differences e.g. in their tissue-specific expression pattern, subcellular localization or substrate specificity constitute the PKA holoenzyme. 3) A-kinase anchoring proteins (AKAPs) provide spatial control of PKA activation by tethering PKAR and other components of the cAMP/PKA signaling pathway to specific subcellular sites (Dessauer, 2009; Welch et al., 2010).

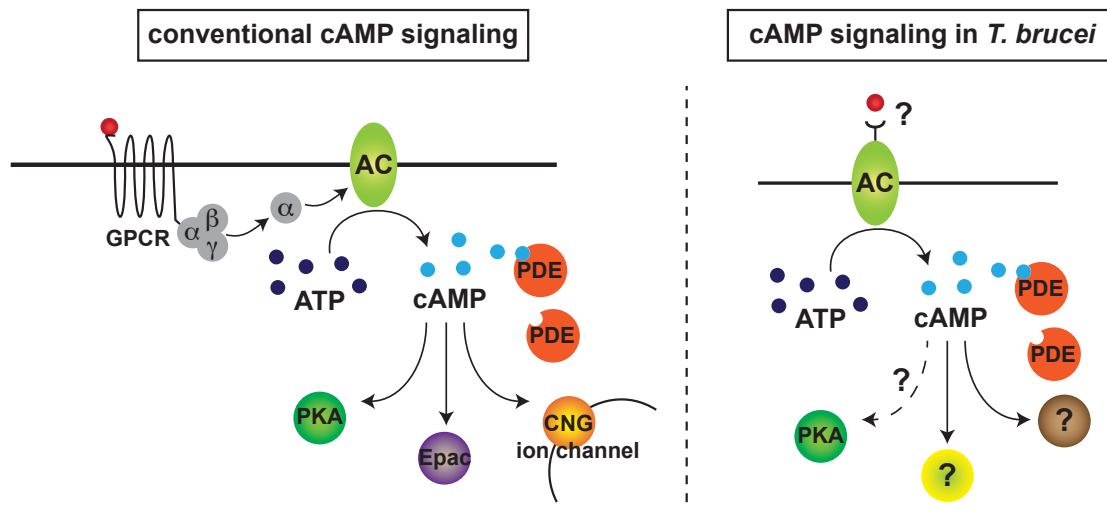


Figure 1.1: Eukaryotic cyclic cAMP signaling pathways. Comparison of the conventional cAMP signaling pathway found in most eukaryotes (left) with cAMP signaling in *Trypanosoma brucei* (right).

1.1.1 Evolutionary conservation of the cAMP/PKA signal transduction pathway

Whereas ACs, PDEs and cAMP are ubiquitous signaling molecules suggested to be present in all kingdoms of life, the occurrence of a cAMP-regulated kinase is restricted to eukaryotes. The cAMP/PKA signal transduction pathway including all components described in chapter 1.1 has been identified and characterized in many eukaryotes ranging from protozoa like *Dictyostelium discoideum* to humans. However, there are a few exceptions: while in plants the existence of conventional GPCRs is under debate, and plant heterotrimeric G proteins are suggested to function independent of 7-TM receptors (Lagerstrom and Schioth, 2008; Tuteja, 2009; Urano et al., 2013; Taddese et al., 2014), genes encoding these signaling molecules seem to be completely absent from the genomes of parasitic protozoa of the order of *Kinetoplastida* (e.g. *Trypanosoma brucei*, *Trypanosoma cruzi*, *Leishmania donovani*) (El-Sayed et al., 2005; Parsons et al., 2005). It is speculated that in these organisms ACs might replace the receptor function of GPCRs (Gould and de Koning, 2011). A variable intracellular N-terminal domain, two membrane-spanning cassettes composed of six transmembrane domains each, and two large cytoplasmic catalytic domains comprise the common secondary structure of mammalian transmembrane ACs (Cooper, 2005; Dessauer, 2009) (Figure 1.2). In contrast, kinetoplastid ACs consist of a large variable extracellular N-terminal domain, followed by a single membrane-spanning region and a well-conserved intracellular, C-terminal catalytic domain (Gould and de Koning, 2011). In general, transmembrane ACs are activated by the alpha subunit of heterotrimeric G proteins ($G_s\alpha$) to generate cAMP from ATP. In addition, isoform-specific regulation by the alpha subunit ($G_i\alpha$) of inhibitory heterotrimeric G proteins or by G protein $\beta\gamma$ subunits has been observed (Defer et al., 2000; Hanoune and Defer, 2001). Moreover, AC activity can be controlled by calcium or by phosphorylation mediated by kinases such as PKA or PKC (Defer et al., 2000; Hanoune and Defer, 2001).

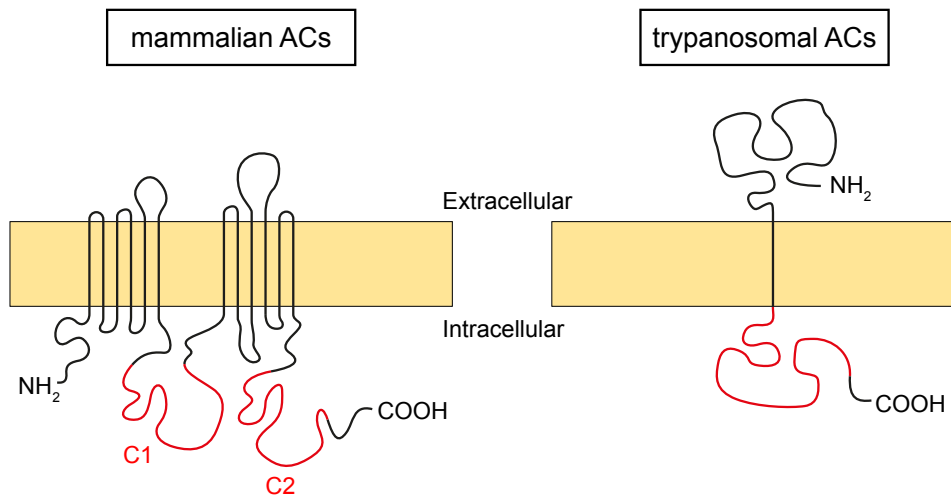


Figure 1.2: Schematic representation of the structures of mammalian (left) compared to trypanosomal (right) transmembrane adenylate cyclases. The picture was adapted from Naula and Seebeck (2000). Catalytic domains are indicated in red. In mammalian ACs, the two closely related subdomains C1 and C2 together form the catalytic domain.

Cyclic nucleotide phosphodiesterases are found in all kingdoms of life and catalyze the hydrolytic cleavage of the 3' phosphodiester bond of cAMP or cGMP, resulting in formation of 5'AMP or 5'GMP, respectively (Bender and Beavo, 2006; Conti and Beavo, 2007; Francis et al., 2011). Typically, PDEs have an N-terminal regulatory domain and a conserved C-terminal catalytic domain encompassing several invariant residues. Based on differences in the primary amino acid sequence of the catalytic domain, PDEs are grouped into three classes. In unicellular organisms, all classes of PDEs have been identified, whereas metazoa express predominantly class I PDEs. The different classes can be further subdivided into families with differences in subcellular localization, regulatory properties, and catalytic characteristics. PDE activity can be regulated by diverse processes including phosphorylation by different kinases such as PKA or PKG, cyclic nucleotide binding to allosteric GAF domains, changes in expression levels, or interaction with other proteins. The major downstream effector of cAMP in eukaryotes is the cAMP-dependent protein kinase PKA. All PKA orthologues analyzed to date consist of regulatory and catalytic subunits. Whereas the mammalian genome encodes four different PKAR (RI α , RI β , RII α , RII β) and two to three different PKAC isoforms (C α , C β , C γ (only in primates)) with differences in their primary amino acid sequence, their tissue-specific expression pattern, sub-cellular localization and affinity to cAMP (Skalhegg and Tasken, 2000), the genomes of most unicellular eukaryotes contain only one *PKAR* gene and a variable number of *PKAC* genes. The regulatory PKA subunit PKAR shows a characteristic domain structure: an N-terminal dimerization/docking (DD) domain important for homodimerization and for interaction with A kinase anchoring proteins (AKAPs) is connected to two C-terminal cyclic nucleotide binding (CNB) domains, CNB-A and CNB-B, by a flexible linker, which contains an inhibitory pseudosubstrate (PKARI) or autophosphorylation site (PKARII) (Scholten et al., 2008). PKAC isoforms belong to the AGC kinase family, which is characterized by specific structural and sequence motifs within the kinase core and the C-terminal tail of the kinase. The N-terminal, in contrast, is unique to PKA and

1. Introduction

highly variable between PKAC isoforms from different organisms (Haste et al., 2012). Almost all PKA holoenzymes analyzed to date are heterotetrameric proteins consisting of a dimer of regulatory subunits and two associated catalytic subunits. However, in some lower eukaryotes like *Dictyostelium discoideum* (Mutzel et al., 1987), *Paramecium tetraurelia* (Hochstrasser and Nelson, 1989) or the dinoflagellate *Amphidinium operculatum* (Leighfield et al., 2002), heterodimeric PKA holoenzymes have been described. The PKAR orthologue of the apicomplexan parasite *Plasmodium falciparum* lacks the N-terminal DD domain, suggesting either a dimeric R-C holoenzyme or heterotetramer formation by a so far unknown mechanism (Haste et al., 2012). Besides mediating homodimerization, the DD domain serves as docking site for interaction with AKAPs. AKAPs are important structural molecules ensuring spatiotemporal specificity of the cAMP/PKA signal transduction pathway in eukaryotes by tethering PKAR as well as other signaling components to defined sub-cellular organelles and membranes (Dessauer, 2009; Welch et al., 2010). So far, AKAPs have almost exclusively been identified in multicellular eukaryotes. However, in *Chlamydomonas reinhardtii* and *Saccharomyces cerevisiae*, functional AKAP homologues have been discovered, which structurally differ from their counterparts in multicellular eukaryotes (Gaillard et al., 2001; Griffioen et al., 2001; Griffioen et al., 2003; Sivadas et al., 2012). Whereas PKA orthologues have been identified in many eukaryotes ranging from primitive protozoa to humans, their existence in plants is highly questionable. Initially, it was commonly believed that plants completely lack signal transduction via cyclic AMP. However, in the last few decades its existence in various plant species has been proposed by a considerable number of reports (Lemtiri-Chlieh et al., 2001; Talke et al., 2003; Newton and Smith, 2004; Bridges et al., 2005; Kaplan et al., 2007; Lomovatskaya et al., 2008; Gehring, 2010). Although there is some indirect, biochemical evidence for cAMP-dependent kinase activities in plants (Lemtiri-Chlieh et al., 2001; Talke et al., 2003; Newton and Smith, 2004), genes with significant sequence similarities to putative PKAR orthologues have not been identified in plant genomes. Interestingly, however, BLAST searches with the consensus sequence for the CNB domain (Pfam PF00027) revealed the existence of two highly similar genes (AT2G20050.1 and AT2G20050.2 (<http://www.arabidopsis.org/>)) with a tandem arrangement in the *Arabidopsis* genome bearing a serine/threonine kinase domain, two cAMP-binding domain-like domains, and one phosphatase domain (domain analysis tool: <http://supfam.cs.bris.ac.uk/SUPERFAMILY/index.html>). Whether the encoded proteins act as cAMP-dependent kinases is yet to be confirmed. Most of the *Arabidopsis* proteins carrying a CNB domain are annotated as cyclic nucleotide activated ion channels. Several studies demonstrate that these channels can be regulated by cyclic nucleotides, are able to conduct specific mono- and divalent cations, and are implicated in regulation of diverse cellular processes such as Ca²⁺ homeostasis, development, and defense responses (Balague et al., 2003; Talke et al., 2003; Ali et al., 2006; Gao et al., 2014). However, direct binding of cAMP has not been shown by any of these studies. It is speculated that a cyclic nucleotide-dependent change in the intracellular Ca²⁺ concentration might regulate calcium-dependent protein kinases and hence provide a crosstalk between cyclic nucleotide and calcium signaling (Talke et al., 2003). This would represent an example of cyclic nucleotide-dependent signaling involving kinases other than PKA. Apart from plants, cyclic nucleotide activated ion channels have also been identified in vertebrates and invertebrates with main functions in photo- and chemoreception as well as neuronal signal transmission (Kaupp and Seifert,

2002). In recent years, ion channels regulated by cAMP have also been discovered in prokaryotes (Karpen, 2004; Caldwell et al., 2010; Brams et al., 2014; Kowal et al., 2014). Another, just recently discovered class of cAMP effector proteins is the cAMP-regulated guanine nucleotide exchange factor Epac (exchange protein directly activated by cAMP) (isoforms Epac1 and Epac2) that regulates the activity of the small G-protein Rap1. Epacs have been identified in vertebrates and some invertebrates (Gancedo, 2013) and are implicated in regulation of diverse cellular processes including cell adhesion, differentiation, and apoptosis (Cheng et al., 2008). In prokaryotes, the main cAMP downstream effectors are transcription factors of the CRP (cAMP receptor protein) family (Kannan et al., 2007; Gancedo, 2013), which regulate the expression of a number of downstream genes and thereby control processes such as utilization of alternative sugars, motility, or virulence. Interestingly, the processes regulated by CRP family proteins are highly diverse between different types of bacteria. Finally, some pathogenic bacteria regulate their virulence by excretion of cAMP or ACs into host cells, resulting in manipulation of innate immune functions by modulating inflammatory mediator expression (McDonough and Rodriguez, 2012).

1.1.2 Activation mechanism of PKA

In the absence of cAMP, PKA exists as an inactive heterotetrameric R_2C_2 holoenzyme in most eukaryotes (exceptional R-C heterodimers in some lower eukaryotes: see chapter 1.1.1). The kinase is activated by the cooperative binding of two molecules of cAMP to each PKAR subunit: one molecule of cAMP binds to the C-terminal binding pocket (B domain) thereby rendering the N-terminal binding pocket (A domain) accessible for cAMP (Skalhegg and Tasken, 2000). This induces a conformational change and consequently displacement of the internal pseudosubstrate (PKARI) or autophosphorylation motif (PKARII) resulting in the release of an R subunit dimer and two free, catalytically active PKAC subunits, which subsequently phosphorylate serine and threonine residues on a variety of downstream substrates. The cyclic nucleotide-binding domain (CNB domain) is a highly conserved module of all cAMP-binding proteins from both pro- and eukaryotes. The phosphate binding cassette (PBC) is the hallmark motif for all CNB domains and ensures proper binding of cAMP by the presence of several invariant residues including a conserved arginine interacting with the exocyclic phosphate of cAMP and a glutamate mediating binding to the ribose 2'OH (Kannan et al., 2007). A few examples of cAMP-independent activation of PKA have been described such as cross-activation of PKA by cGMP (Shabb, 2001; Francis et al., 2010; Shabb, 2011) or activation of PKA via TGF- β (Wang et al., 1998; Yang et al., 2013), NF κ B/I κ B (Zhong et al., 1997) or AKAP110 (Niu et al., 2001). Moreover, *Saccharomyces cerevisiae* PKA can be activated independently of cAMP by another, as yet unknown mechanism: under conditions of nitrogen or phosphate starvation, the addition of the limiting nutrient induces rapid activation of PKA by a cAMP- and PKAR-independent mechanism, also called the 'Fermentable-Growth Medium (FGM) Pathway' (Fuller and Rhodes, 2012).

1.1.3 Downstream functions of cAMP/PKA signaling

In mammalian cells, PKA is involved in regulation of a large variety of cellular processes including metabolism, differentiation, apoptosis, sperm motility, or cell cycle progression (Skalhegg and Tasken, 2000; Shabb, 2001; Pearce et al., 2010). Hence, deregulation of the cAMP/PKA signal transduction pathway plays a major role in the pathogenesis of cancer and other severe diseases. Several of these downstream functions of PKA are even conserved in unicellular eukaryotes. The PKA orthologues of the non-pathogenic fungus *Saccharomyces cerevisiae* and the protozoa *Dictyostelium discoideum* and *Plasmodium falciparum* are among the best-examined representatives in unicellular organisms. In *Saccharomyces cerevisiae*, the cAMP/PKA pathway is mainly controlled by the availability of extracellular nutrients and regulates growth, metabolism, differentiation, apoptosis, cell cycle progression, and stress responses (Wilson et al., 2010; Tamanoi, 2011; Fuller and Rhodes, 2012; Lastauskiene et al., 2014). In the slime mold *Dictyostelium discoideum*, the cAMP/PKA signaling pathway controls the transition from growth to development as well as the differentiation to subsequent developmental stages (Primpke et al., 2000; Saran et al., 2002). The PKA orthologue of the protozoan parasite *Plasmodium falciparum* has been implicated in a number of processes in malarial pathogenesis e.g. by modification of membrane permeability of red blood cells thereby ensuring survival in the host (Haste et al., 2012). PKA regulates downstream processes either directly at the level of substrate phosphorylation or at the level of protein synthesis involving all steps from transcriptional (via phosphorylation of transcription factors) (Shabb, 2001), posttranscriptional (via phosphorylation of RNA-binding proteins with transcript stabilizing/destabilizing functions) (Huang et al., 1995; Mizunuma et al., 2013), or translational control (Vaidyanathan et al., 2014).

1.2 Signal transduction in *T. brucei*

1.2.1 The model organism *Trypanosoma brucei brucei*

Subspecies of *Trypanosoma brucei*, a unicellular, flagellated protozoan parasite belonging to the *Kinetoplastida*, an evolutionary early branching eukaryotic order, are the causative agents of Human African Trypanosomiasis (HAT) (*T. brucei gambiense*, *T. brucei rhodesiense*) and Nagana in cattle (*T. brucei brucei*) (Brun et al., 2010). The prevalence of these diseases is restricted to sub-Saharan African countries and correlates with the geographical extension of the tsetse fly (*Glossina spp.*), a blood-sucking insect responsible for transmission of *T. brucei*. HAT is a severe disease, usually fatal if untreated and is subdivided into two stages: the early stage is characterized by unspecific symptoms such as fever, headache, or itching at the site of the tsetse bite. As soon as the parasites cross the blood brain barrier, they infect the central nervous system initiating the late stage of the disease hallmarked by severe neurological dysfunctions ultimately resulting in coma and death. Treatment of HAT is complicated due to the high costs and the toxicity of some of the available drugs as well as the increasing emergence of drug-resistant trypanosome strains (Brun et al., 2010). Since *T. brucei* possesses a highly effective combination of independent and complementary mechanisms of immune evasion (Leung et al., 2014), preventive vaccination is not possible against HAT. The *T. brucei* cell is characterized by a single flagellum, which is connected to the cell body along the length of the cell (Figure 1.3). The flagellum exits the cytoplasm at the so-called flagellar pocket, an invagination of the

plasma membrane and the only site of endo- and exocytosis (Field and Carrington, 2009). The densely packed mitochondrial DNA constitutes the name-giving kinetoplast, which is located in close proximity to the basal body of the flagellum. The surface of *T. brucei* bloodstream forms (BSFs) living in the mammalian bloodstream is covered by a densely packed coat of variant surface glycoproteins (VSGs) (Manna et al., 2014). Whereas the trypanosomal genome encodes >1000 VSG genes, only one is expressed at a certain time. As soon as the mammalian immune system produces antibodies against the VSG coat, most of the parasites get eliminated. However, by antigenic variation involving mechanisms of homologous recombination and transcriptional silencing and activation, trypanosomes can exchange their VSG coat (Glover et al., 2013). Hence, periodical switching of the VSG coat is accompanied by periodical extinction of most of the parasites resulting in the typical, observed waves of parasitemia. This ensures a prolonged survival of the host and thereby increases the transmissibility to a new host. In addition, a recent study showed that antibodies against VSGs bound to the trypanosomal surface are moved by hydrodynamic forces related to motility to the posterior end of the cell and are internalized by endocytosis at the flagellar pocket (Engstler et al., 2007).

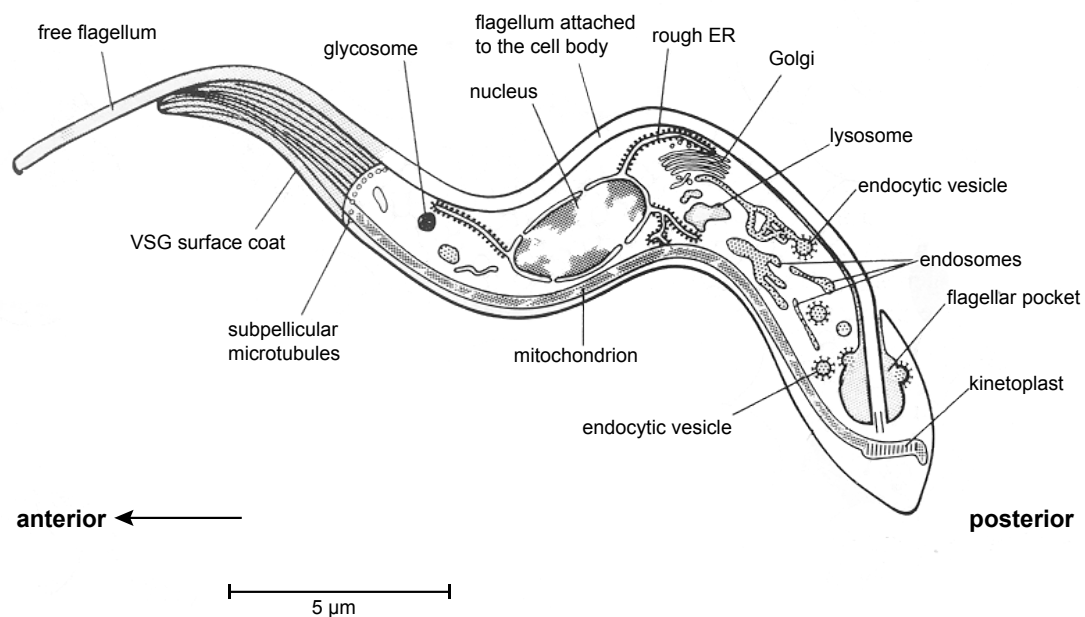


Figure 1.3: Schematic representation of a *T. brucei* cell. The picture was adapted from <http://www.ilri.org/InfoServ/Webpub/fulldocs/Ilr90/Figures/fig%2025%20p45.gif>. The arrow indicates the swimming direction.

Its early evolutionary divergence and several special molecular and cellular features such as antigenic variation (Glover et al., 2013) or a highly unconventional polycistronic gene expression exclusively regulated at the posttranscriptional level (Clayton, 2002; Haile and Papadopoulou, 2007) as well as the existence of a subspecies non-pathogenic for humans made *T. brucei* an interesting model organism. Furthermore, complete genome sequences of an increasing number of species and strains (www.tritrypdb.org) combined with the available variety of tools for genetic manipulation, e.g. gene replacement by homologous recombination (Carruthers et al., 1993; Li and Gottesdiener, 1996;

McCulloch et al., 2004) or RNAi-mediated gene silencing (Ngo et al., 1998; Bringaud et al., 2000; Shi et al., 2000; Clayton et al., 2005), provide an excellent opportunity to study unique as well as evolutionary conserved cellular mechanisms in these evolutionary early branching eukaryotes.

1.2.2 Putative components of the *T. brucei* cAMP/PKA signal transduction pathway

Whereas conventional cAMP/PKA signaling pathways are found in several unicellular eukaryotes such as *Saccharomyces cerevisiae* (Santangelo, 2006) or *Dictyostelium discoideum* (Saran et al., 2002), kinetoplastid cAMP signaling seems to be significantly different (Figure 1.1, right). First evidence for the presence of cAMP in trypanosomes dates back to the year 1974 when Walter and co-workers reported AC and PDE activities in *T. b. gambiense* (Walter, 1974; Walter et al., 1974) followed by the discovery of changes in the intracellular cAMP concentration between different life cycle stages of *T. lewisi* by Strickler and Patton (1975). In the following decades, multiple reports analyzed putative components and functions of cAMP signaling in kinetoplastids (e.g. Naula and Seebeck, 2000; Seebeck et al., 2001; Seebeck et al., 2004; Laxman and Beavo, 2007; Oberholzer et al., 2007; Bhattacharya et al., 2008, 2009; Biswas et al., 2011; Gould and de Koning, 2011; Bhattacharya et al., 2012; de Koning et al., 2012; Salmon et al., 2012a; Salmon et al., 2012b; Gould et al., 2013; Lopez et al., 2014; Saada et al., 2014; Vij et al., 2014). Apart from the apparent absence of genes encoding GPCRs or heterotrimeric G proteins from kinetoplastid genomes (see chapter 1.1.1), the existence of a cAMP-dependent kinase activity in kinetoplastids is an open question. As in most other eukaryotes, cAMP is produced by ACs and degraded by PDEs. Kinetoplastid ACs, however, diverge from their mammalian orthologues in structure and sequence (see chapter 1.1.1) and were suggested to replace the receptor function of GPCRs. Yet, no ligand has been identified to date. Activation of trypanosomal ACs has been observed upon exposure to stress conditions such as acid treatment or osmotic lysis (Voorheis and Martin, 1980; Rolin et al., 1996; Nolan et al., 2000). Interestingly, there is a remarkable expansion of the AC family in the genomes of the African trypanosomes *T. brucei* and *T. congolense* (www.tritrypdb.org), which live extracellularly in the mammalian bloodstream, in contrast to *T. cruzi* or *L. donovani*, kinetoplastid parasites developing intracellularly in host cells. Four families of cAMP-specific class I PDEs have been characterized in *T. brucei* with structural similarities to mammalian PDEs within their catalytic domain (Seebeck et al., 2001; Seebeck et al., 2004; Laxman and Beavo, 2007; Gould and de Koning, 2011). The two members of the *T. brucei* PDEB family, PDEB1 and PDEB2, are encoded by two tandemly arranged genes with high sequence similarity and represent the major cAMP-degrading activity in BSFs. The lethal phenotype resulting from genetic or pharmacological inhibition of both enzymes simultaneously in contrast to absence of a phenotype upon inhibition of a single PDEB suggests functional redundancy and indicates that deregulation of cAMP signaling is detrimental to the parasites (Oberholzer et al., 2007; Bland et al., 2011; de Koning et al., 2012). This validates the trypanosomal cAMP-specific PDEs as excellent drug targets. The reported predominant localization of ACs (Paindavoine et al., 1992; Salmon et al., 2012b; Saada et al., 2014) and PDEs (Oberholzer et al., 2007) to the parasite flagellum suggests this organelle as a center for cAMP signaling. As in most other kinetoplastids, the *T. brucei* genome encodes one orthologue of a regulatory and three isoforms of catalytic subunits of

PKA. Two closely related *PKAC* genes are arranged in tandem and most likely result from a recent gene duplication event (Kramer et al., 2007). The few amino acid differences between the two isoforms are located at the very N- and C-terminal ends (Bachmaier and Boshart, 2013). The third *PKAC* gene (*PKAC3* in *T. brucei*) is more distant and is located on a different chromosome. Surprisingly, it has been shown that *in vitro* kinase activity is not stimulated by cAMP but by unphysiologically high concentrations of cGMP (Shalaby et al., 2001). This is in contrast to the *Leishmania donovani* orthologue, which according to a recent study seems to be activated by cAMP *in vitro* (Bhattacharya et al., 2012). An involvement of cAMP/PKA signaling in kinetoplastid differentiation has been shown for *Leishmania donovani* (Bhattacharya et al., 2012) and suggested for *Trypanosoma cruzi* (Rangel-Aldao et al., 1987; Gonzales-Perdomo et al., 1988; Rangel-Aldao et al., 1988; Naula and Seebeck, 2000; de Godoy et al., 2012). Several observations led to the assumption that cAMP signaling also plays a role in life cycle stage differentiation of *T. brucei* (see chapter 1.2.3).

1.2.3 Life cycle stage differentiation of *T. brucei*

The shuttling between a mammal and an insect vector requires the ability to quickly adapt to dramatic changes in the environmental conditions. The parasites live in an environment with plenty of glucose as energy source (Bringaud et al., 2006) and a constant temperature of 37°C in the mammalian bloodstream. Upon uptake by a tsetse fly, the parasites encounter significant environmental changes such as a drop in temperature and altered carbon source availability. The host switch is accompanied by a complex life cycle involving dividing as well as cell cycle-arrested stages with the latter being pre-adapted to the life in the next host compartment (Figure 1.4). In the mammalian bloodstream, *T. brucei* cells proliferate extracellularly as long slender (LS) forms, which differentiate into cell cycle-arrested short stumpy (SS) forms by a density-dependent, quorum sensing-like mechanism (Reuner et al., 1997; MacGregor et al., 2011). This differentiation step is accompanied by morphological, biochemical and metabolic changes such as repositioning of nucleus and kinetoplast as well as expression of procyclin, the major surface protein of PCFs, and of enzymes crucial for utilization of available carbon sources in the fly (Fenn and Matthews, 2007). Upon a blood meal on an infected mammal, tsetse flies take up LS and SS trypanosomes. The latter, pre-adapted to the life in the insect vector, differentiate within 48-72 hours into the dividing PCF stage characterized by synchronous re-entry into the cell cycle, exchange of the stage-specific surface coat as well as morphological and metabolic changes (Fenn and Matthews, 2007). The fully developed mitochondrion including all enzymes required for utilization of proline as main energy source enables ATP generation via oxidative phosphorylation. LS cells, in contrast, are attacked and killed by proteases in the fly midgut (Nolan et al., 2000). Within the tsetse vector, *T. brucei* cells differentiate from the procyclic stage colonizing the fly midgut to the infectious metacyclic stage inhabiting the tsetse salivary glands via several different intermediate stages (Sharma et al., 2009). Until recently, it was not possible to reproduce these differentiation steps *in vitro*. A major break-through was the identification of RBP6, an RNA-binding protein, which promotes differentiation of PCFs upon overexpression in culture (Kolev et al., 2012).

1. Introduction

There are many studies investigating life cycle stage differentiation of *T. brucei*. Several of these studies use monomorphic cell lines, i.e. cells that have been passaged several times through rodents and as a consequence have lost the ability to differentiate to the short stumpy bloodstream form. Instead, they develop into so-called stumpy-like forms. Naturally occurring trypanosomes, which efficiently differentiate into stumpy forms, are called pleomorphic.

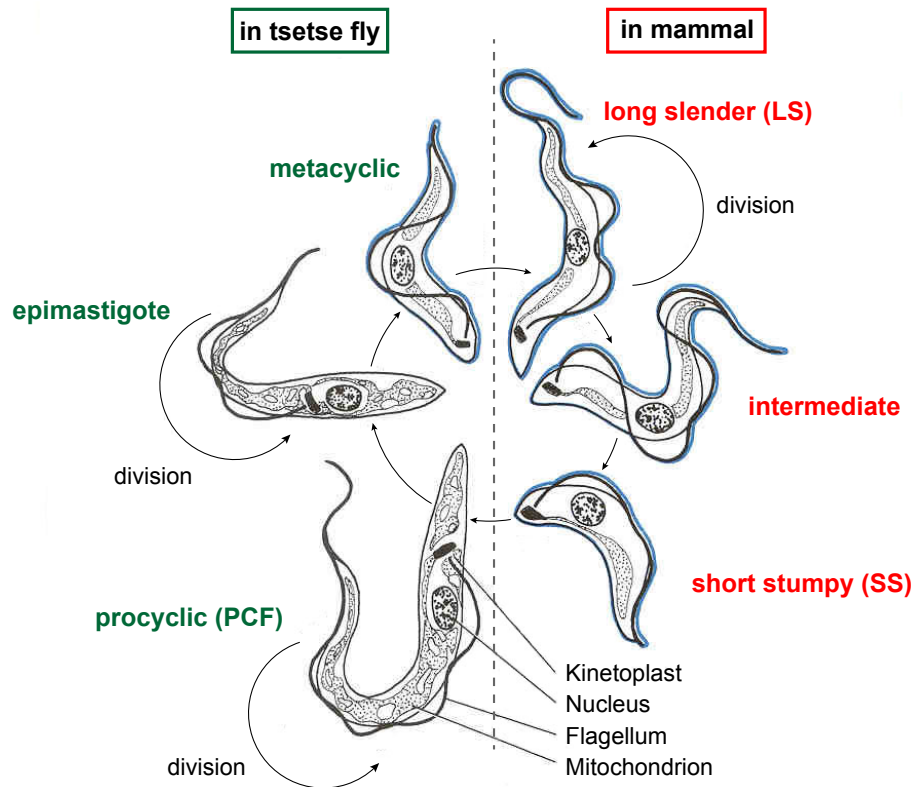


Figure 1.4: Life cycle of *T. brucei*. The picture was adapted from <http://www.ilri.org/InfoServ/Webpub/fulldocs/Irad90/Figures/fig%2018%20p35.jpg>. The VSG surface coat is indicated in blue.

1.2.3.1 Signaling during LS to SS differentiation

The observation that intracellular cAMP levels change according to the parasitemia in rats led to the speculation that cAMP signaling might play a role in the density-dependent differentiation from LS to SS (Mancini and Patton, 1981). This hypothesis was strengthened by the discovery of a putative, as yet unknown 'stumpy induction factor' (SIF), a heat-stable, low molecular weight compound (or compounds) extracted from medium of a BSF culture at maximal density (Vassella et al., 1997). The effect of SIF could be mimicked by treatment of LS forms with the membrane-permeable cAMP derivative 8-pCPT-cAMP (Vassella et al., 1997; Breidbach et al., 2002; Laxman et al., 2006). Furthermore, exposure of LS cells to conditioned medium containing SIF resulted in a two- to threefold increase in the intracellular cAMP concentration. However, the finding that the effect of SIF cannot be mimicked by treatment with hydrolysis-resistant but only with hydrolysable cAMP

derivatives and even more effectively with their degradation products, namely the respective 5'AMP and adenosine derivatives, indicated that these molecules are likely to be the key players in the signaling cascade rather than cAMP (Laxman et al., 2006). A recent whole-genome RNAi library screen selecting for cells resistant to 8-pCPT-cAMP or 8-pCPT-2'O-me-5'AMP and hence defective in stumpy formation identified several proteins with putative involvement in the process of LS to SS differentiation (Mony et al., 2014). Notably, RBP7, an RNA-binding protein identified by the screen, is likely to be a positive regulator of stumpy formation, since RNAi-mediated repression of *RBP7* caused loss of LS to SS differentiation and overexpression resulted in cell cycle arrest and increased differentiation competence. Apart from these putative positive regulators, several kinases have been proposed to negatively regulate stumpy formation such as ZFK (Vassella et al., 2001), MAPK5 (Domenicali Pfister et al., 2006), and TbTOR4 (Barquilla et al., 2012). A family of putative citrate transporters, the PAD (protein associated with differentiation) proteins, has been shown to play an important role in the differentiation process from BSF to PCF in the insect host (Dean et al., 2009) (see chapter 1.2.3.2). One member of the PAD proteins, PAD1, is only expressed at significant levels in differentiation-competent SS cells and hence serves as stage-specific marker. This property of PAD1 is currently being exploited to identify small molecule compounds, which either inhibit or promote differentiation and hence might serve as promising leads for drug development against diseases caused by African trypanosomes (MacGregor et al., 2014).

1.2.3.2 Signaling during SS to PCF differentiation

In vitro, the differentiation process from SS to PCF can be induced by treatment with millimolar concentrations of citrate/*cis*-aconitate (CCA) (Ziegelbauer et al., 1990), mild acid stress (Rolin et al., 1998), or proteases (Hunt et al., 1994; Sbicego et al., 1999; Szöör et al., 2013). In addition, a temperature drop of >15°C (cold shock) sensitizes stumpy trypanosomes to low, putatively physiological concentrations of CCA (Engstler and Boshart, 2004). The molecular mechanisms and signaling pathways underlying these differentiation processes are only partially uncovered. A family of putative citrate transporters, the PAD proteins, is required for perception of the CCA stimulus (Dean et al., 2009). PAD proteins are encoded by an array of eight genes, and simultaneous knockdown of all members results in reduced ability to differentiate to the insect form and eliminates CCA hypersensitivity under cold shock conditions. Stumpy cells exposed to cold shock show increased expression as well as surface routing of PAD2, which might act as CCA receptor. Moreover, a phosphatase cascade involving PTP1 and PIP39 controls differentiation from SS to PCF (Szöör et al., 2006; Szöör et al., 2010) with PTP1 being a negative and PIP39 a positive regulator. Phosphorylation of PIP39 at Y278 is a prerequisite for differentiation to the insect stage. As long as SS forms reside in the mammalian bloodstream, PTP1 inactivates PIP39 by dephosphorylation at Y278 and thereby prevents differentiation. PIP39 activates PTP1 and thereby promotes its own inhibition. Szöör et al. (2013) propose a model in which the feedback inhibition of PIP39 by PTP1 is blocked by a CCA-dependent mechanism upon uptake of SS cells by a tsetse fly: CCA entering the cells via transporters of the PAD family localized at the surface of SS cells promotes interaction between PIP39 and PTP1 and independently blocks the ability of PIP39 to enhance PTP1 activity. In

1. Introduction

addition, expression of PIP39 in SS is induced by cold shock (Szöör et al., 2010). These combined events eventually result in increased amounts of phosphorylated PIP39, which localizes to the glycosomes and consequently promotes efficient differentiation into PCFs. So far, the kinase responsible for phosphorylation of PIP39 at Y278 as well as the downstream pathway ultimately resulting in differentiation to the PCF stage is unknown. Kinases negatively regulating BSF to PCF differentiation have recently been discovered by a global kinome RNAi library screen (Jones et al., 2014): RDK1, repressor of differentiation kinase 1, has been shown to act in conjunction with the PTP1/PIP39 pathway blocking uncontrolled BSF to PCF differentiation, whereas RDK2 might act upstream of RDK1 and PTP1.

1.3 Scope of this thesis

Although multiple studies investigating cAMP/PKA signaling in kinetoplastids have been published in recent years (e.g. Naula and Seebeck, 2000; Seebeck et al., 2001; Seebeck et al., 2004; Laxman and Beavo, 2007; Oberholzer et al., 2007; Bhattacharya et al., 2008, 2009; Biswas et al., 2011; Gould and de Koning, 2011; Bhattacharya et al., 2012; de Koning et al., 2012; Salmon et al., 2012a; Salmon et al., 2012b; Gould et al., 2013; Lopez et al., 2014; Saada et al., 2014; Vij et al., 2014) and the general interest in this field is increasing, there are still many open questions concerning various putative steps in this/these signaling pathway/s.

1) Is *T. brucei* PKA activated by cAMP?

Whereas *Leishmania donovani* PKA is apparently activated by cAMP *in vitro* (Bhattacharya et al., 2012), previous work from our laboratory (S. Kramer PhD thesis, 2004) as well as published data from Shalaby et al. (2001) indicate that the *T. brucei* orthologue is cAMP independent. In order to confirm these *in vitro* observations under physiological conditions, a previously established *in vivo* PKA reporter assay will be used to investigate PKA activity when intracellular cAMP levels are elevated ([chapter 4.1](#)). This assay will be furthermore exploited to identify possible alternative ligands.

2) Are there alternative cAMP downstream effectors?

A cAMP-independent PKA would suggest uncoupling of cAMP and PKA signaling in *T. brucei* and hence would raise the question about the existence of alternative downstream effectors of cAMP. In the absence of genes encoding orthologues of known cAMP receptor proteins of other organisms such as CRP, Epac or CNGs from the trypanosomal genome, alternative downstream effectors are most likely novel, maybe even kinetoplastid-specific proteins. The study presented in [chapter 3](#) aims at identification of cAMP response proteins in *T. brucei* by a whole-genome RNAi library screen.

3) Which functional role does cAMP play in *T. brucei*?

The putative absence of known cAMP receptor proteins raises the question whether cAMP has any intracellular function in *T. brucei*. Since manipulation of the intracellular cAMP concentration by simultaneous inhibition of *T. brucei* PDEB1 and PDEB2 either genetically (by RNAi; Oberholzer et al., 2007) or pharmacologically (by the PDE inhibitor CpdA; de Koning et al., 2012) causes cytokinesis defects eventually resulting in cell death, increased intracellular cAMP levels seem to be

detrimental to the parasites. The studies presented in [chapters 2.1](#) and [2.2](#) will shed light on downstream functions of cAMP in *T. brucei* by genetic manipulation of ACs, the enzymes producing cAMP from ATP.

4) How is *T. brucei* PKA activated and to which purpose?

The absence of activation of *T. brucei* PKA by cAMP asks for the identification of alternative activators or activating conditions. Previous work from the laboratory has shown that the kinase is activated *in vivo* by a drop in temperature (S. Kramer PhD thesis, 2004), a known differentiation trigger in the parasite's life cycle (see [chapter 1.2.3.2](#)). [Chapter 4.2](#) aims to extend the specificity of activation of *T. brucei* PKA by cold shock as well as to prove the suggested role of the kinase in the differentiation from BSF to PCF.

5) Is PKA downstream signaling conserved between *T. brucei* and other organisms?

Hundreds of substrates phosphorylated by PKA are known from a variety of eukaryotes (Skalhegg and Tasken, 2000). There is even a high overlap between processes regulated by PKA in lower, unicellular eukaryotes like *Saccharomyces cerevisiae* and higher eukaryotes like mammals, such as regulation of metabolism or differentiation (Sonneborn et al., 2000; Bockmuhl and Ernst, 2001; Wilson et al., 2010; Tamanoi, 2011; Lastauskiene et al., 2014). Since *T. brucei* PKA has apparently lost its upstream activation by cAMP, it is possible that the kinase acts in a completely different pathway thereby regulating a different set of downstream processes. Alternatively, the unconventional upstream activation mechanism could be combined with a downstream pathway conserved from trypanosomes to humans. [Chapters 4.1](#) and [4.2](#) will provide insight into downstream components of *T. brucei* PKA signaling.

6) Is the unconventional cAMP/PKA signaling in *T. brucei* conserved in other kinetoplastids?

T. brucei PKA is the first example of a PKA not regulated by cAMP. The parasite belongs to the order of *Kinetoplastida*, evolutionary early branching eukaryotes. The loss of the evolutionary conserved upstream regulatory mechanism of PKA could have occurred directly after the early branching of the *Kinetoplastida*. Alternatively, it could be a unique feature of the *T. brucei* kinase. Analysis of cAMP/PKA signaling in the related kinetoplastid parasites *L. donovani* and *T. cruzi* will shed light on the evolutionary conservation of these signal transduction pathways ([chapter 5](#) and [discussion](#)).

1.4 References for introduction

- Ali, R., Zielinski, R.E., and Berkowitz, G.A. (2006). Expression of plant cyclic nucleotide-gated cation channels in yeast. *J Exp Bot* 57, 125-138.
- Bachmaier, S., and Boshart, M. (2013). Kinetoplastid AGC Kinases. In *Protein Phosphorylation in Parasites* (Wiley-VCH Verlag GmbH & Co. KGaA), pp. 99-122.
- Balague, C., Lin, B., Alcon, C., Flottes, G., Malmstrom, S., Kohler, C., Neuhaus, G., Pelletier, G., Gaymard, F., and Roby, D. (2003). HLM1, an essential signaling component in the

1. Introduction

- hypersensitive response, is a member of the cyclic nucleotide-gated channel ion channel family. *Plant Cell* *15*, 365-379.
- Barquilla, A., Saldivia, M., Diaz, R., Bart, J.M., Vidal, I., Calvo, E., Hall, M.N., and Navarro, M. (2012). Third target of rapamycin complex negatively regulates development of quiescence in *Trypanosoma brucei*. *Proc Natl Acad Sci U S A* *109*, 14399-14404.
- Bender, A.T., and Beavo, J.A. (2006). Cyclic nucleotide phosphodiesterases: molecular regulation to clinical use. *Pharmacol Rev* *58*, 488-520.
- Beristain, A.G., Molyneux, S.D., Joshi, P.A., Pomroy, N.C., Di Grappa, M.A., Chang, M.C., Kirschner, L.S., Prive, G.G., Pujana, M.A., and Khokha, R. (2014). PKA signaling drives mammary tumorigenesis through Src. *Oncogene*.
- Beuschlein, F., Fassnacht, M., Assie, G., Calebiro, D., Stratakis, C.A., Osswald, A., Ronchi, C.L., Wieland, T., Sbiera, S., Faucz, F.R., *et al.* (2014). Constitutive activation of PKA catalytic subunit in adrenal Cushing's syndrome. *N Engl J Med* *370*, 1019-1028.
- Bhattacharya, A., Biswas, A., and Das, P.K. (2008). Role of intracellular cAMP in differentiation-coupled induction of resistance against oxidative damage in *Leishmania donovani*. *Free Radic Biol Med* *44*, 779-794.
- Bhattacharya, A., Biswas, A., and Das, P.K. (2009). Role of a differentially expressed cAMP phosphodiesterase in regulating the induction of resistance against oxidative damage in *Leishmania donovani*. *Free Radic Biol Med* *47*, 1494-1506.
- Bhattacharya, A., Biswas, A., and Das, P.K. (2012). Identification of a protein kinase A regulatory subunit from *Leishmania* having importance in metacyclogenesis through induction of autophagy. *Mol Microbiol* *83*, 548-564.
- Biswas, A., Bhattacharya, A., and Das, P.K. (2011). Role of cAMP Signaling in the Survival and Infectivity of the Protozoan Parasite, *Leishmania donovani*. *Mol Biol Int* *2011*, 782971.
- Bland, N.D., Wang, C., Tallman, C., Gustafson, A.E., Wang, Z., Ashton, T.D., Ochiana, S.O., McAllister, G., Cotter, K., Fang, A.P., *et al.* (2011). Pharmacological validation of *Trypanosoma brucei* phosphodiesterases B1 and B2 as druggable targets for African sleeping sickness. *J Med Chem* *54*, 8188-8194.
- Bockmuhl, D.P., and Ernst, J.F. (2001). A potential phosphorylation site for an A-type kinase in the Efg1 regulator protein contributes to hyphal morphogenesis of *Candida albicans*. *Genetics* *157*, 1523-1530.
- Brams, M., Kusch, J., Spurny, R., Benndorf, K., and Ulens, C. (2014). Family of prokaryote cyclic nucleotide-modulated ion channels. *Proc Natl Acad Sci U S A* *111*, 7855-7860.
- Breidbach, T., Ngazoa, E., and Steverding, D. (2002). *Trypanosoma brucei*: *in vitro* slender-to-stumpy differentiation of culture-adapted, monomorphic bloodstream forms. *Exp Parasitol* *101*, 223-230.
- Bridges, D., Fraser, M.E., and Moorhead, G.B. (2005). Cyclic nucleotide binding proteins in the *Arabidopsis thaliana* and *Oryza sativa* genomes. *BMC Bioinformatics* *6*, 6.
- Bringaud, F., Riviere, L., and Coustou, V. (2006). Energy metabolism of trypanosomatids: adaptation to available carbon sources. *Mol Biochem Parasitol* *149*, 1-9.

- Bringaud, F., Robinson, D.R., Barradeau, S., Biteau, N., Baltz, D., and Baltz, T. (2000). Characterization and disruption of a new *Trypanosoma brucei* repetitive flagellum protein, using double-stranded RNA inhibition. *Mol Biochem Parasitol* 111, 283-297.
- Brun, R., Blum, J., Chappuis, F., and Burri, C. (2010). Human African trypanosomiasis. *Lancet* 375, 148-159.
- Caldwell, D.B., Malcolm, H.R., Elmore, D.E., and Maurer, J.A. (2010). Identification and experimental verification of a novel family of bacterial cyclic nucleotide-gated (bcNG) ion channels. *Biochim Biophys Acta* 1798, 1750-1756.
- Cao, Y., He, M., Gao, Z., Peng, Y., Li, Y., Li, L., Zhou, W., Li, X., Zhong, X., Lei, Y., *et al.* (2014). Activating hotspot L205R mutation in PRKACA and adrenal Cushing's syndrome. *Science* 344, 913-917.
- Carruthers, V.B., van der Ploeg, L.H.T., and Cross, G.A.M. (1993). DNA-mediated transformation of bloodstream-form *Trypanosoma brucei*. *Nucleic Acids Research* 21, 2537-2538.
- Cheng, X., Ji, Z., Tsalkova, T., and Mei, F. (2008). Epac and PKA: a tale of two intracellular cAMP receptors. *Acta Biochim Biophys Sin (Shanghai)* 40, 651-662.
- Cho, Y.S., Park, Y.G., Lee, Y.N., Kim, M.K., Bates, S., Tan, L., and Cho-Chung, Y.S. (2000). Extracellular protein kinase A as a cancer biomarker: its expression by tumor cells and reversal by a myristate-lacking Calpha and RIbeta subunit overexpression. *Proc Natl Acad Sci U S A* 97, 835-840.
- Clayton, C., Estévez, A., Hartmann, C., Alibu, V., Field, M., and Horn, D. (2005). Down-Regulating Gene Expression by RNA Interference in *Trypanosoma brucei*. In *RNA Silencing*, G. Carmichael, ed. (Humana Press), pp. 39-59.
- Clayton, C.E. (2002). Life without transcriptional control? From fly to man and back again. *Embo j* 21, 1881-1888.
- Conti, M., and Beavo, J. (2007). Biochemistry and physiology of cyclic nucleotide phosphodiesterases: essential components in cyclic nucleotide signaling. *Annu Rev Biochem* 76, 481-511.
- Cooper, D.M. (2005). Compartmentalization of adenylate cyclase and cAMP signalling. *Biochem Soc Trans* 33, 1319-1322.
- de Godoy, L.M., Marchini, F.K., Pavoni, D.P., Rampazzo Rde, C., Probst, C.M., Goldenberg, S., and Krieger, M.A. (2012). Quantitative proteomics of *Trypanosoma cruzi* during metacyclogenesis. *Proteomics* 12, 2694-2703.
- de Koning, H.P., Gould, M.K., Sterk, G.J., Tenor, H., Kunz, S., Luginbuehl, E., and Seebeck, T. (2012). Pharmacological validation of *Trypanosoma brucei* phosphodiesterases as novel drug targets. *J Infect Dis* 206, 229-237.
- Dean, S., Marchetti, R., Kirk, K., and Matthews, K.R. (2009). A surface transporter family conveys the trypanosome differentiation signal. *Nature* 459, 213-217.
- Defer, N., Best-Belpomme, M., and Hanoune, J. (2000). Tissue specificity and physiological relevance of various isoforms of adenylyl cyclase. *Am J Physiol Renal Physiol* 279, F400-416.
- Dessauer, C.W. (2009). Adenylyl cyclase--A-kinase anchoring protein complexes: the next dimension in cAMP signaling. *Mol Pharmacol* 76, 935-941.

1. Introduction

- Domenicali Pfister, D., Burkard, G., Morand, S., Renggli, C.K., Roditi, I., and Vassella, E. (2006). A Mitogen-activated protein kinase controls differentiation of bloodstream forms of *Trypanosoma brucei*. *Eukaryot Cell* 5, 1126-1135.
- El-Sayed, N.M., Myler, P.J., Blandin, G., Berriman, M., Crabtree, J., Aggarwal, G., Caler, E., Renauld, H., Worthey, E.A., Hertz-Fowler, C., *et al.* (2005). Comparative genomics of trypanosomatid parasitic protozoa. *Science* 309, 404-409.
- Engstler, M., and Boshart, M. (2004). Cold shock and regulation of surface protein trafficking convey sensitization to inducers of stage differentiation in *Trypanosoma brucei*. *Genes Dev* 18, 2798-2811.
- Engstler, M., Pfohl, T., Herminghaus, S., Boshart, M., Wiegertjes, G., Heddergott, N., and Overath, P. (2007). Hydrodynamic flow-mediated protein sorting on the cell surface of trypanosomes. *Cell* 131, 505-515.
- Fenn, K., and Matthews, K.R. (2007). The cell biology of *Trypanosoma brucei* differentiation. *Curr Opin Microbiol* 10, 539-546.
- Field, M.C., and Carrington, M. (2009). The trypanosome flagellar pocket. *Nat Rev Microbiol* 7, 775-786.
- Francis, S.H., Blount, M.A., and Corbin, J.D. (2011). Mammalian cyclic nucleotide phosphodiesterases: molecular mechanisms and physiological functions. *Physiol Rev* 91, 651-690.
- Francis, S.H., Busch, J.L., Corbin, J.D., and Sibley, D. (2010). cGMP-dependent protein kinases and cGMP phosphodiesterases in nitric oxide and cGMP action. *Pharmacol Rev* 62, 525-563.
- Fuller, K.K., and Rhodes, J.C. (2012). Protein kinase A and fungal virulence: a sinister side to a conserved nutrient sensing pathway. *Virulence* 3, 109-121.
- Gaillard, A.R., Diener, D.R., Rosenbaum, J.L., and Sale, W.S. (2001). Flagellar Radial Spoke Protein 3 Is an a-Kinase Anchoring Protein (Akap). *The Journal of Cell Biology* 153, 443-448.
- Gancedo, J.M. (2013). Biological roles of cAMP: variations on a theme in the different kingdoms of life. *Biol Rev Camb Philos Soc* 88, 645-668.
- Gao, Q.-F., Fei, C.-F., Dong, J.-Y., Gu, L.-L., and Wang, Y.-F. (2014). *Arabidopsis* CNGC18 Is a Ca²⁺-Permeable Channel. *Molecular Plant* 7, 739-743.
- Gehring, C. (2010). Adenyl cyclases and cAMP in plant signaling - past and present. *Cell Commun Signal* 8, 15.
- Glover, L., Hutchinson, S., Alford, S., McCulloch, R., Field, M.C., and Horn, D. (2013). Antigenic variation in African trypanosomes: the importance of chromosomal and nuclear context in VSG expression control. *Cell Microbiol* 15, 1984-1993.
- Goh, G., Scholl, U.I., Healy, J.M., Choi, M., Prasad, M.L., Nelson-Williams, C., Kunstman, J.W., Korah, R., Suttorp, A.C., Dietrich, D., *et al.* (2014). Recurrent activating mutation in PRKACA in cortisol-producing adrenal tumors. *Nat Genet* 46, 613-617.
- Gonzales-Perdomo, M., Romero, P., and Goldenberg, S. (1988). Cyclic AMP and adenylate cyclase activators stimulate *Trypanosoma cruzi* differentiation. *Exp Parasitol* 66, 205-212.

- Gordge, P.C., Hulme, M.J., Clegg, R.A., and Miller, W.R. (1996). Elevation of protein kinase A and protein kinase C activities in malignant as compared with normal human breast tissue. *Eur J Cancer* 32a, 2120-2126.
- Gould, M.K., Bachmaier, S., Ali, J.A., Alsford, S., Tagoe, D.N., Munday, J.C., Schnauffer, A.C., Horn, D., Boshart, M., and de Koning, H.P. (2013). Cyclic AMP effectors in African trypanosomes revealed by genome-scale RNA interference library screening for resistance to the phosphodiesterase inhibitor CpdA. *Antimicrob Agents Chemother* 57, 4882-4893.
- Gould, M.K., and de Koning, H.P. (2011). Cyclic-nucleotide signalling in protozoa. *FEMS Microbiol Rev* 35, 515-541.
- Griffioen, G., Branduardi, P., Ballarini, A., Anghileri, P., Norbeck, J., Baroni, M.D., and Ruis, H. (2001). Nucleocytoplasmic distribution of budding yeast protein kinase A regulatory subunit Bcy1 requires Zds1 and is regulated by Yak1-dependent phosphorylation of its targeting domain. *Mol Cell Biol* 21, 511-523.
- Griffioen, G., Swinnen, S., and Thevelein, J.M. (2003). Feedback inhibition on cell wall integrity signaling by Zds1 involves Gsk3 phosphorylation of a cAMP-dependent protein kinase regulatory subunit. *J Biol Chem* 278, 23460-23471.
- Groussin, L., Jullian, E., Perlemoine, K., Louvel, A., Leheup, B., Luton, J.P., Bertagna, X., and Bertherat, J. (2002). Mutations of the PRKAR1A gene in Cushing's syndrome due to sporadic primary pigmented nodular adrenocortical disease. *J Clin Endocrinol Metab* 87, 4324-4329.
- Haile, S., and Papadopoulou, B. (2007). Developmental regulation of gene expression in trypanosomatid parasitic protozoa. *Current Opinion in Microbiology* 10, 569-577.
- Hanoune, J., and Defer, N. (2001). Regulation and role of adenylyl cyclase isoforms. *Annu Rev Pharmacol Toxicol* 41, 145-174.
- Haste, N.M., Talabani, H., Doo, A., Merckx, A., Langsley, G., and Taylor, S.S. (2012). Exploring the *Plasmodium falciparum* cyclic-adenosine monophosphate (cAMP)-dependent protein kinase (PfPKA) as a therapeutic target. *Microbes Infect* 14, 838-850.
- Hochstrasser, M., and Nelson, D.L. (1989). Cyclic AMP-dependent protein kinase in *Paramecium tetraurelia*. Its purification and the production of monoclonal antibodies against both subunits. *J Biol Chem* 264, 14510-14518.
- Huang, D., Hubbard, C.J., and Jungmann, R.A. (1995). Lactate dehydrogenase A subunit messenger RNA stability is synergistically regulated via the protein kinase A and C signal transduction pathways. *Mol Endocrinol* 9, 994-1004.
- Hunt, M., Brun, R., and Kohler, P. (1994). Studies on compounds promoting the *in vitro* transformation of *Trypanosoma brucei* from bloodstream to procyclic forms. *Parasitol Res* 80, 600-606.
- Jones, N.G., Thomas, E.B., Brown, E., Dickens, N.J., Hammarton, T.C., and Mottram, J.C. (2014). Regulators of *Trypanosoma brucei* cell cycle progression and differentiation identified using a kinome-wide RNAi screen. *PLoS Pathog* 10, e1003886.
- Kannan, N., Wu, J., Anand, G.S., Yooseph, S., Neuwald, A.F., Venter, J.C., and Taylor, S.S. (2007). Evolution of allostery in the cyclic nucleotide binding module. *Genome Biol* 8, R264.

1. Introduction

- Kaplan, B., Sherman, T., and Fromm, H. (2007). Cyclic nucleotide-gated channels in plants. *FEBS Lett* 581, 2237-2246.
- Karpen, J.W. (2004). Ion channel structure and the promise of bacteria: cyclic nucleotide-gated channels in the queue. *J Gen Physiol* 124, 199-201.
- Kaupp, U.B., and Seifert, R. (2002). Cyclic nucleotide-gated ion channels. *Physiol Rev* 82, 769-824.
- Kirschner, L.S., Carney, J.A., Pack, S.D., Taymans, S.E., Giatzakis, C., Cho, Y.S., Cho-Chung, Y.S., and Stratakis, C.A. (2000). Mutations of the gene encoding the protein kinase A type I-alpha regulatory subunit in patients with the Carney complex. *Nat Genet* 26, 89-92.
- Kolev, N.G., Ramey-Butler, K., Cross, G.A., Ullu, E., and Tschudi, C. (2012). Developmental progression to infectivity in *Trypanosoma brucei* triggered by an RNA-binding protein. *Science* 338, 1352-1353.
- Kowal, J., Chami, M., Baumgartner, P., Arbeit, M., Chiu, P.L., Rangl, M., Scheuring, S., Schroder, G.F., Nimigean, C.M., and Stahlberg, H. (2014). Ligand-induced structural changes in the cyclic nucleotide-modulated potassium channel MloK1. *Nat Commun* 5, 3106.
- Kramer, S., Klockner, T., Selmayr, M., and Boshart, M. (2007). Interstrain sequence comparison, transcript map and clonal genomic rearrangement of a 28 kb locus on chromosome 9 of *Trypanosoma brucei*. *Mol Biochem Parasitol* 151, 129-132.
- Lagerstrom, M.C., and Schiöth, H.B. (2008). Structural diversity of G protein-coupled receptors and significance for drug discovery. *Nat Rev Drug Discov* 7, 339-357.
- Lastauskiene, E., Zinkeviciene, A., and Citavicius, D. (2014). Ras/PKA signal transduction pathway participates in the regulation of *Saccharomyces cerevisiae* cell apoptosis in an acidic environment. *Biotechnol Appl Biochem* 61, 3-10.
- Laxman, S., and Beavo, J.A. (2007). Cyclic nucleotide signaling mechanisms in trypanosomes: possible targets for therapeutic agents. *Mol Interv* 7, 203-215.
- Laxman, S., Riechers, A., Sadilek, M., Schwede, F., and Beavo, J.A. (2006). Hydrolysis products of cAMP analogs cause transformation of *Trypanosoma brucei* from slender to stumpy-like forms. *Proc Natl Acad Sci U S A* 103, 19194-19199.
- Leighfield, T.A., Barbier, M., and Van Dolah, F.M. (2002). Evidence for cAMP-dependent protein kinase in the dinoflagellate, *Amphidinium operculatum*. *Comp Biochem Physiol B Biochem Mol Biol* 133, 317-324.
- Lemtiri-Chlieh, F., Thomas, L., Marondedze, C., Irving, H., and Gehring, C. (2001). Cyclic Nucleotides and Nucleotide Cyclases in Plant Stress Responses. In *Abiotic Stress Response in Plants - Physiological, Biochemical and Genetic Perspectives*, A. Shanker, ed.
- Leung, K., Manna, P., Boehm, C., Maishman, L., and Field, M. (2014). Cell Biology for Immune Evasion: Organizing Antigenic Variation, Surfaces, Trafficking, and Cellular Structures in *Trypanosoma brucei*. In *Trypanosomes and Trypanosomiasis*, S. Magez, and M. Radwanska, eds. (Springer Vienna), pp. 1-39.
- Li, F., and Gottesdiener, K.M. (1996). An efficient method for stable transfection of bloodstream-form *Trypanosoma brucei*. *Nucleic Acids Research* 24, 534-535.
- Lomovatskaya, L.A., Romanenko, A.S., and Filinova, N.V. (2008). Plant adenylate cyclases. *J Recept Signal Transduct Res* 28, 531-542.

- Lopez, M.A., Saada, E.A., and Hill, K.L. (2014). Insect stage-specific adenylate cyclases regulate social motility in African trypanosomes. *Eukaryot Cell*.
- MacGregor, P., Ivens, A., Shave, S., Collie, I., Gray, D., Auer, M., and Matthews, K.R. (2014). High-throughput chemical screening for antivirulence developmental phenotypes in *Trypanosoma brucei*. *Eukaryot Cell* *13*, 412-426.
- MacGregor, P., Savill, N.J., Hall, D., and Matthews, K.R. (2011). Transmission stages dominate trypanosome within-host dynamics during chronic infections. *Cell Host Microbe* *9*, 310-318.
- Mancini, P.E., and Patton, C.L. (1981). Cyclic 3',5'-adenosine monophosphate levels during the developmental cycle of *Trypanosoma brucei brucei* in the rat. *Mol Biochem Parasitol* *3*, 19-31.
- Manna, P.T., Boehm, C., Leung, K.F., Natesan, S.K., and Field, M.C. (2014). Life and times: synthesis, trafficking, and evolution of VSG. *Trends Parasitol* *30*, 251-258.
- McCulloch, R., Vassella, E., Burton, P., Boshart, M., and Barry, J.D. (2004). Transformation of monomorphic and pleomorphic *Trypanosoma brucei*. *Methods Mol Biol* *262*, 53-86.
- McDonough, K.A., and Rodriguez, A. (2012). The myriad roles of cyclic AMP in microbial pathogens: from signal to sword. *Nat Rev Microbiol* *10*, 27-38.
- Mizunuma, M., Tsubakiyama, R., Ogawa, T., Shitamukai, A., Kobayashi, Y., Inai, T., Kume, K., and Hirata, D. (2013). Ras/cAMP-dependent protein kinase (PKA) regulates multiple aspects of cellular events by phosphorylating the Whi3 cell cycle regulator in budding yeast. *J Biol Chem* *288*, 10558-10566.
- Mony, B.M., MacGregor, P., Ivens, A., Rojas, F., Cowton, A., Young, J., Horn, D., and Matthews, K. (2014). Genome-wide dissection of the quorum sensing signalling pathway in *Trypanosoma brucei*. *Nature* *505*, 681-685.
- Mutzel, R., Lacombe, M.L., Simon, M.N., de Gunzburg, J., and Veron, M. (1987). Cloning and cDNA sequence of the regulatory subunit of cAMP-dependent protein kinase from *Dictyostelium discoideum*. *Proc Natl Acad Sci U S A* *84*, 6-10.
- Naula, C., and Seebeck, T. (2000). Cyclic AMP signaling in trypanosomatids. *Parasitol Today* *16*, 35-38.
- Naviglio, S., Di Gesto, D., Illiano, F., Chiosi, E., Giordano, A., Illiano, G., and Spina, A. (2010). Leptin potentiates antiproliferative action of cAMP elevation via protein kinase A down-regulation in breast cancer cells. *J Cell Physiol* *225*, 801-809.
- Newton, R.P., and Smith, C.J. (2004). Cyclic nucleotides. *Phytochemistry* *65*, 2423-2437.
- Ngo, H., Tschudi, C., Gull, K., and Ullu, E. (1998). Double-stranded RNA induces mRNA degradation in *Trypanosoma brucei*. *Proc Natl Acad Sci U S A* *95*, 14687-14692.
- Niu, J., Vaiskunaite, R., Suzuki, N., Kozasa, T., Carr, D.W., Dulin, N., and Voyno-Yasenetskaya, T.A. (2001). Interaction of heterotrimeric G13 protein with an A-kinase-anchoring protein 110 (AKAP110) mediates cAMP-independent PKA activation. *Curr Biol* *11*, 1686-1690.
- Nolan, D.P., Rolin, S., Rodriguez, J.R., Van Den Abbeele, J., and Pays, E. (2000). Slender and stumpy bloodstream forms of *Trypanosoma brucei* display a differential response to extracellular acidic and proteolytic stress. *Eur J Biochem* *267*, 18-27.

1. Introduction

- Oberholzer, M., Marti, G., Baresic, M., Kunz, S., Hemphill, A., and Seebeck, T. (2007). The *Trypanosoma brucei* cAMP phosphodiesterases TbrPDEB1 and TbrPDEB2: flagellar enzymes that are essential for parasite virulence. *FASEB J* 21, 720-731.
- Paindavoine, P., Rolin, S., Van Assel, S., Geuskens, M., Jauniaux, J.C., Dinsart, C., Huet, G., and Pays, E. (1992). A gene from the variant surface glycoprotein expression site encodes one of several transmembrane adenylyl cyclases located on the flagellum of *Trypanosoma brucei*. *Mol Cell Biol* 12, 1218-1225.
- Parsons, M., Worthey, E.A., Ward, P.N., and Mottram, J.C. (2005). Comparative analysis of the kinomes of three pathogenic trypanosomatids: *Leishmania major*, *Trypanosoma brucei* and *Trypanosoma cruzi*. *BMC Genomics* 6, 127.
- Pearce, L.R., Komander, D., and Alessi, D.R. (2010). The nuts and bolts of AGC protein kinases. *Nat Rev Mol Cell Biol* 11, 9-22.
- Primpke, G., Iassonidou, V., Nellen, W., and Wetterauer, B. (2000). Role of cAMP-dependent protein kinase during growth and early development of *Dictyostelium discoideum*. *Dev Biol* 221, 101-111.
- Rall, T.W., and Sutherland, E.W. (1958). Formation of a cyclic adenine ribonucleotide by tissue particles. *J Biol Chem* 232, 1065-1076.
- Rangel-Aldao, R., Allende, O., Triana, F., Piras, R., Henriquez, D., and Piras, M. (1987). Possible role of cAMP in the differentiation of *Trypanosoma cruzi*. *Mol Biochem Parasitol* 22, 39-43.
- Rangel-Aldao, R., Triana, F., Comach, G., Abate, T., Fernandez, V., and McMahon-Pratt, D. (1988). Intracellular signaling transduction in the differentiation of *Trypanosoma cruzi*: role of cAMP. *Arch Biol Med Exp (Santiago)* 21, 403-408.
- Reuner, B., Vassella, E., Yutzy, B., and Boshart, M. (1997). Cell density triggers slender to stumpy differentiation of *Trypanosoma brucei* bloodstream forms in culture. *Mol Biochem Parasitol* 90, 269-280.
- Rolin, S., Hancocq-Quertier, J., Paturiaux-Hanocq, F., Nolan, D.P., and Pays, E. (1998). Mild acid stress as a differentiation trigger in *Trypanosoma brucei*. *Mol Biochem Parasitol* 93, 251-262.
- Rolin, S., Hancocq-Quertier, J., Paturiaux-Hanocq, F., Nolan, D., Salmon, D., Webb, H., Carrington, M., Voorheis, P., and Pays, E. (1996). Simultaneous but independent activation of adenylyl cyclase and glycosylphosphatidylinositol-phospholipase C under stress conditions in *Trypanosoma brucei*. *J Biol Chem* 271, 10844-10852.
- Saada, E.A., Kabututu, Z.P., Lopez, M., Shimogawa, M.M., Langousis, G., Oberholzer, M., Riestra, A., Jonsson, Z.O., Wohlschlegel, J.A., and Hill, K.L. (2014). Insect stage-specific receptor adenylyl cyclases are localized to distinct subdomains of the *Trypanosoma brucei* flagellar membrane. *Eukaryot Cell* 13, 1064-1076.
- Salmon, D., Bachmaier, S., Krumbholz, C., Kador, M., Gossmann, J.A., Uzureau, P., Pays, E., and Boshart, M. (2012a). Cytokinesis of *Trypanosoma brucei* bloodstream forms depends on expression of adenylyl cyclases of the ESAG4 or ESAG4-like subfamily. *Mol Microbiol* 84, 225-242.

- Salmon, D., Vanwalleghem, G., Morias, Y., Denoëud, J., Krumbholz, C., Lhomme, F., Bachmaier, S., Kador, M., Gossmann, J., Dias, F.B., *et al.* (2012b). Adenylate cyclases of *Trypanosoma brucei* inhibit the innate immune response of the host. *Science* 337, 463-466.
- Santangelo, G.M. (2006). Glucose signaling in *Saccharomyces cerevisiae*. *Microbiol Mol Biol Rev* 70, 253-282.
- Saran, S., Meima, M.E., Alvarez-Curto, E., Weening, K.E., Rozen, D.E., and Schaap, P. (2002). cAMP signaling in *Dictyostelium*. Complexity of cAMP synthesis, degradation and detection. *J Muscle Res Cell Motil* 23, 793-802.
- Sato, Y., Maekawa, S., Ishii, R., Sanada, M., Morikawa, T., Shiraishi, Y., Yoshida, K., Nagata, Y., Sato-Otsubo, A., Yoshizato, T., *et al.* (2014). Recurrent somatic mutations underlie corticotropin-independent Cushing's syndrome. *Science* 344, 917-920.
- Sbicego, S., Vassella, E., Kurath, U., Blum, B., and Roditi, I. (1999). The use of transgenic *Trypanosoma brucei* to identify compounds inducing the differentiation of bloodstream forms to procyclic forms. *Mol Biochem Parasitol* 104, 311-322.
- Scholten, A., Aye, T.T., and Heck, A.J. (2008). A multi-angular mass spectrometric view at cyclic nucleotide dependent protein kinases: *in vivo* characterization and structure/function relationships. *Mass Spectrom Rev* 27, 331-353.
- Seebeck, T., Gong, K., Kunz, S., Schaub, R., Shalaby, T., and Zoraghi, R. (2001). cAMP signalling in *Trypanosoma brucei*. *Int J Parasitol* 31, 491-498.
- Seebeck, T., Schaub, R., and Johner, A. (2004). cAMP signalling in the kinetoplastid protozoa. *Curr Mol Med* 4, 585-599.
- Shabb, J.B. (2001). Physiological substrates of cAMP-dependent protein kinase. *Chem Rev* 101, 2381-2411.
- Shabb, J.B. (2011). Cyclic Nucleotide Specificity and Cross-Activation of Cyclic Nucleotide Receptors. In *Transduction mechanisms in Cellular Signaling*, Dennis, and Bradshaw, eds.
- Shalaby, T., Liniger, M., and Seebeck, T. (2001). The regulatory subunit of a cGMP-regulated protein kinase A of *Trypanosoma brucei*. *Eur J Biochem* 268, 6197-6206.
- Sharma, R., Gluenz, E., Peacock, L., Gibson, W., Gull, K., and Carrington, M. (2009). The heart of darkness: growth and form of *Trypanosoma brucei* in the tsetse fly. *Trends Parasitol* 25, 517-524.
- Shi, H., Djikeng, A., Mark, T., Wirtz, E., Tschudi, C., and Ullu, E. (2000). Genetic interference in *Trypanosoma brucei* by heritable and inducible double-stranded RNA. *Rna* 6, 1069-1076.
- Sivadas, P., Dienes, J.M., St. Maurice, M., Meek, W.D., and Yang, P. (2012). A flagellar A-kinase anchoring protein with two amphipathic helices forms a structural scaffold in the radial spoke complex. *The Journal of Cell Biology* 199, 639-651.
- Skalhegg, B.S., and Tasken, K. (2000). Specificity in the cAMP/PKA signaling pathway. Differential expression, regulation, and subcellular localization of subunits of PKA. *Front Biosci* 5, D678-693.
- Sonneborn, A., Bockmuhl, D.P., Gerads, M., Kurpanek, K., Sanglard, D., and Ernst, J.F. (2000). Protein kinase A encoded by TPK2 regulates dimorphism of *Candida albicans*. *Mol Microbiol* 35, 386-396.

1. Introduction

- Strickler, J.E., and Patton, C.L. (1975). Adenosine 3',5'-monophosphate in reproducing and differentiated trypanosomes. *Science* *190*, 1110-1112.
- Szöör, B., Dyer, N.A., Ruberto, I., Acosta-Serrano, A., and Matthews, K.R. (2013). Independent pathways can transduce the life-cycle differentiation signal in *Trypanosoma brucei*. *PLoS Pathog* *9*, e1003689.
- Szöör, B., Ruberto, I., Burchmore, R., and Matthews, K.R. (2010). A novel phosphatase cascade regulates differentiation in *Trypanosoma brucei* via a glycosomal signaling pathway. *Genes Dev* *24*, 1306-1316.
- Szöör, B., Wilson, J., McElhinney, H., Taberner, L., and Matthews, K.R. (2006). Protein tyrosine phosphatase TbPTP1: A molecular switch controlling life cycle differentiation in trypanosomes. *J Cell Biol* *175*, 293-303.
- Taddese, B., Upton, G.J., Bailey, G.R., Jordan, S.R., Abdulla, N.Y., Reeves, P.J., and Reynolds, C.A. (2014). Do plants contain G protein-coupled receptors? *Plant Physiol* *164*, 287-307.
- Talke, I.N., Blaudez, D., Maathuis, F.J., and Sanders, D. (2003). CNGCs: prime targets of plant cyclic nucleotide signalling? *Trends Plant Sci* *8*, 286-293.
- Tamanoi, F. (2011). Ras signaling in yeast. *Genes Cancer* *2*, 210-215.
- Tuteja, N. (2009). Signaling through G protein coupled receptors. *Plant Signal Behav* *4*, 942-947.
- Urano, D., Chen, J.G., Botella, J.R., and Jones, A.M. (2013). Heterotrimeric G protein signalling in the plant kingdom. *Open Biol* *3*, 120186.
- Vaidyanathan, P.P., Zinshteyn, B., Thompson, M.K., and Gilbert, W.V. (2014). Protein kinase A regulates gene-specific translational adaptation in differentiating yeast. *RNA*.
- Vassella, E., Kramer, R., Turner, C.M., Wankell, M., Modes, C., van den Bogaard, M., and Boshart, M. (2001). Deletion of a novel protein kinase with PX and FYVE-related domains increases the rate of differentiation of *Trypanosoma brucei*. *Mol Microbiol* *41*, 33-46.
- Vassella, E., Reuner, B., Yutzy, B., and Boshart, M. (1997). Differentiation of African trypanosomes is controlled by a density sensing mechanism which signals cell cycle arrest via the cAMP pathway. *J Cell Sci* *110 (Pt 21)*, 2661-2671.
- Vij, A., Biswas, A., Bhattacharya, A., and Das, P.K. (2014). A Soluble Phosphodiesterase in *Leishmania donovani* Regulates cAMP-dependent Protein Kinase A Signaling in a Unique Way. *Int J Biochem Cell Biol*.
- Voorheis, H.P., and Martin, B.R. (1980). 'Swell dialysis' demonstrates that adenylylase in *Trypanosoma brucei* is regulated by calcium ions. *Eur J Biochem* *113*, 223-227.
- Walsh, D.A., Perkins, J.P., and Krebs, E.G. (1968). An adenosine 3',5'-monophosphate-dependant protein kinase from rabbit skeletal muscle. *J Biol Chem* *243*, 3763-3765.
- Walter, R.D. (1974). 3':5'-cyclic-AMP phosphodiesterase from *Trypanosoma gambiense*. *Hoppe Seylers Z Physiol Chem* *355*, 1443-1450.
- Walter, R.D., Nordmeyer, J.P., and Konigk, E. (1974). Adenylylase from *Trypanosoma gambiense*. *Hoppe Seylers Z Physiol Chem* *355*, 427-430.
- Wang, L., Zhu, Y., and Sharma, K. (1998). Transforming growth factor-beta1 stimulates protein kinase A in mesangial cells. *J Biol Chem* *273*, 8522-8527.

- Welch, E.J., Jones, B.W., and Scott, J.D. (2010). Networking with AKAPs: context-dependent regulation of anchored enzymes. *Mol Interv* 10, 86-97.
- Wilson, W.A., Roach, P.J., Montero, M., Baroja-Fernandez, E., Munoz, F.J., Eydallin, G., Viale, A.M., and Pozueta-Romero, J. (2010). Regulation of glycogen metabolism in yeast and bacteria. *FEMS Microbiol Rev* 34, 952-985.
- Yang, H., Li, G., Wu, J.J., Wang, L., Uhler, M., and Simeone, D.M. (2013). Protein kinase A modulates transforming growth factor-beta signaling through a direct interaction with Smad4 protein. *J Biol Chem* 288, 8737-8749.
- Zhong, H., SuYang, H., Erdjument-Bromage, H., Tempst, P., and Ghosh, S. (1997). The transcriptional activity of NF-kappaB is regulated by the IkappaB-associated PKAc subunit through a cyclic AMP-independent mechanism. *Cell* 89, 413-424.
- Ziegelbauer, K., Quinten, M., Schwarz, H., Pearson, T.W., and Overath, P. (1990). Synchronous differentiation of *Trypanosoma brucei* from bloodstream to procyclic forms *in vitro*. *Eur J Biochem* 192, 373-378.

2. Cyclic AMP production in *T. brucei* – the adenylyl cyclases.

2.1 Cytokinesis of *Trypanosoma brucei* bloodstream forms depends on expression of adenylyl cyclases of the ESAG4 or ESAG4-like subfamily.

Didier Salmon^{1**†}, Sabine Bachmaier², Carsten Krumbholz^{2‡}, Markus Kador², Jasmin A. Gossmann², Pierrick Uzureau¹, Etienne Pays^{1§} and Michael Boshart^{2*§}

¹Laboratory of Molecular Parasitology, Institute of Molecular Biology and Medicine, Université Libre de Bruxelles, 12, rue de Professeurs Jeener et Brachet, B-6041 Gosselies, Belgium.

²Biocenter, Section Genetics, University of Munich (LMU), Grosshaderner Str. 2-4, D-82152 Martinsried, Germany.

To whom correspondence should be addressed:

*E-mail boshart@lmu.de; Tel. (+49) 89 2180 74600; Fax (+49) 89 2180 74629

**E-mail salmon@bioqmed.ufrj.br; Tel. (+55) 21 25626756; Fax (+55) 21 38814155

Present addresses:

[†]Institute of Medical Biochemistry, Centro de Ciências e da Saude, Federal University of Rio de Janeiro, Av. General Trompowsky, Rio de Janeiro, 21941-590, Brazil.

[‡]Human GmbH, Berlin, Germany.

[§]These authors contributed equally to this work.

Abstract

Antigenic variation of the parasite *Trypanosoma brucei* operates by monoallelic expression of a variant surface glycoprotein (VSG) from a collection of multiple telomeric expression sites (ESs). Each of these ESs harbours a long polycistronic transcription unit containing several expression site-associated genes (*ESAGs*). *ESAG4* copies encode bloodstream stage-specific adenylyl cyclases (AC) and belong to a larger gene family of around 80 members, the majority of which, termed genes related to *ESAG4* (*GRESAG4s*), are not encoded in ESs and are expressed constitutively in the life cycle. Here we report that ablation of *ESAG4* from the active ES did not affect parasite growth, neither in culture nor upon rodent infection, and did not significantly change total AC activity. In contrast, inducible RNAi-mediated knock-down of an AC subfamily that includes *ESAG4* and two *ESAG4*-like *GRESAG4* (*ESAG4L*) genes, decreased total AC activity and induced a lethal phenotype linked to impaired cytokinesis. In the $\Delta esag4$ line compensatory upregulation of apparently functionally redundant *ESAG4L* genes was observed, suggesting that the *ESAG4/ESAG4L*-subfamily ACs are involved in the control of cell division. How deregulated adenylyl cyclases or cAMP might impair cytokinesis is discussed.

Full-text article:

<http://www.ncbi.nlm.nih.gov/pubmed/22340731>

<http://onlinelibrary.wiley.com/doi/10.1111/j.1365-2958.2012.08013.x/full>

Molecular Microbiology, Salmon D., Bachmaier S., Krumbholz C., Kador M., Gossmann J. A., Uzureau P., Pays E., Boshart M. (2012). Cytokinesis of *Trypanosoma brucei* bloodstream forms depends on expression of adenylyl cyclases of the *ESAG4* or *ESAG4*-like subfamily. Copyright 2012 by Blackwell Publishing Ltd.

doi: 10.1111/j.1365-2958.2012.08013.x

2.2 Adenylate cyclases of *Trypanosoma brucei* inhibit the innate immune response of the host.

Didier Salmon^{1,2*†}, Gilles Vanwalleghem^{1†}, Yannick Morias^{3,4}, Julie Denoeud⁵, Carsten Krumbholz⁶, Frédéric Lhommé⁷, Sabine Bachmaier⁶, Markus Kador⁶, Jasmin Gossmann⁶, Fernando Braga Stehling Dias^{1,2}, Géraldine De Muylder¹, Pierrick Uzureau¹, Stefan Magez^{4,8}, Muriel Moser⁵, Patrick De Baetselier^{3,4}, Jan Van Den Abbeele⁹, Alain Beschin^{3,4}, Michael Boshart^{6*}, Etienne Pays^{1,10*}

¹Laboratory of Molecular Parasitology, Institute for Molecular Biology and Medicine (IBMM), Université Libre de Bruxelles, 12, rue des Professeurs Jeener et Brachet, B6041 Gosselies, Belgium.

²Institute of Medical Biochemistry, Centro de Ciências e da Saude, Federal University of Rio de Janeiro, Avenida General Trompowsky, Rio de Janeiro 21941-590, Brazil.

³Myeloid Cell Immunology Laboratory, Vlaams Instituut voor Biotechnologie, Brussels, Belgium.

⁴Cellular and Molecular Immunology Unit, Vrije Universiteit Brussel, Brussels, Belgium.

⁵Laboratory of Immunobiology, IBMM, Université Libre de Bruxelles, Gosselies, Belgium.

⁶Biocenter, Section Genetics, Ludwig-Maximilians-Universität München, Martinsried, Germany.

⁷Center for Microscopy and Molecular Imaging, Gosselies, Belgium.

⁸Department of Structural Biology, VIB, Brussels, Belgium.

⁹Department of Biomedical Sciences, Unit of Veterinary Protozoology, Institute of Tropical Medicine Antwerp, Antwerp, Belgium.

¹⁰Walloon Excellence in Life Sciences and Biotechnology (WELBIO), Wavre, Belgium.

*To whom correspondence should be addressed:

E-mail: salmon@bioqmed.ufrj.br

boshart@lmu.de

epays@ulb.ac.be

†These authors contributed equally to this work.

Abstract

The parasite *Trypanosoma brucei* possesses a large family of transmembrane receptor-like adenylyl cyclases. Activation of these enzymes requires the dimerization of the catalytic domain and typically occurs under stress. Using a dominant-negative strategy, we found that reducing adenylyl cyclase activity by about 50% allowed trypanosome growth but reduced the parasite's ability to control the early innate immune defense of the host. Specifically, activation of trypanosome adenylyl cyclase resulting from parasite phagocytosis by liver myeloid cells inhibited the synthesis of the trypanosome-controlling cytokine tumor necrosis factor- α through activation of protein kinase A in these cells. Thus, adenylyl cyclase activity of lysed trypanosomes favors early host colonization by live parasites. The role of adenylyl cyclases at the host-parasite interface could explain the expansion and polymorphism of this gene family.

Full-text article:

<http://www.ncbi.nlm.nih.gov/pubmed/22700656>

<http://www.sciencemag.org/content/337/6093/463>

Science, Salmon D., Vanwalleghem G., Morias Y., Denoed J., Krumbholz C., Lhomme F., Bachmaier S., Kador M., Gossman J. A., Dias F. B., De Muylder G., Uzureau P., Magez S., Moser M., De Baetselier P., Van Den Abbeele J., Beschin A., Boshart M., Pays E. (2012). Adenylyl Cyclases of *Trypanosoma brucei* Inhibit the Innate Immune Response of the Host. Copyright 2012 by the American Association for the Advancement of Science.

doi: 10.1126/science.1222753

3. Cyclic AMP effectors in African trypanosomes revealed by genome-scale RNA interference library screening for resistance to the phosphodiesterase inhibitor CpdA.

Matthew K. Gould^{a,d}, Sabine Bachmaier^b, Juma A. M. Ali^a, Sam Alford^c, Daniel N. A. Tagoe^{a,e}, Jane C. Munday^{a,e}, Achim C. Schnauffer^d, David Horn^{c*}, Michael Boshart^b, Harry P. de Koning^a

^aInstitute of Infection, Immunity & Inflammation, College of Medical, Veterinary & Life Sciences, University of Glasgow, Glasgow, United Kingdom

^bBiocenter, Section Genetics, Ludwig-Maximilians-Universität München, Martinsried, Germany

^cFaculty of Infectious & Tropical Diseases, London School of Hygiene & Tropical Medicine, London, United Kingdom

^dCentre for Immunity, Infection & Evolution, Institute of Immunology & Infection Research, University of Edinburgh, Edinburgh, United Kingdom

^eWellcome Trust Centre for Molecular Parasitology, University of Glasgow, Glasgow, United Kingdom

To whom correspondence should be addressed:

Harry P. de Koning, Harry.De-Koning@gla.ac.uk

Michael Boshart, boshart@lmu.de.

* Present address:

David Horn, Biological Chemistry & Drug Discovery, College of Life Sciences, University of Dundee, Dundee, United Kingdom.

M.K.G. and S.B. contributed equally to this article.

Abstract

One of the most promising new targets for trypanocidal drugs to emerge in recent years is the cyclic AMP (cAMP) phosphodiesterases (PDE) activity encoded by *TbrPDEB1* and *TbrPDEB2*. These genes were genetically confirmed as essential, and a high affinity inhibitor, CpdA, displays potent antitrypanosomal activity. To identify effectors of the elevated cAMP levels resulting from CpdA action and, consequently, potential sites for adaptations giving resistance to PDE inhibitors, resistance to the drug was induced. Selection of mutagenized trypanosomes resulted in resistance to CpdA as well as cross-resistance to membrane permeable cAMP analogues but not to currently used trypanocidal drugs. Resistance was not due to changes in cAMP levels or in *PDEB* genes. A second approach, a genome-wide RNA interference (RNAi) library screen, returned four genes giving resistance to CpdA upon knockdown. Validation by independent RNAi strategies confirmed resistance to CpdA and suggested a role for the identified cAMP Response Proteins (CARPs) in cAMP action. CARP1 is unique to kinetoplastid parasites and has predicted cyclic nucleotide binding-like domains, and RNAi repression resulted in >100-fold resistance. CARP2 and CARP4 are hypothetical conserved proteins associated with the eukaryotic flagellar proteome or with flagellar function, with an orthologue of CARP4 implicated in human disease. CARP3 is a hypothetical protein, unique to *Trypanosoma*. CARP1 to CARP4 likely represent components of a novel cAMP signaling pathway in the parasite. As cAMP metabolism is validated as a drug target in *Trypanosoma brucei*, cAMP effectors highly divergent from the mammalian host, such as *CARP1*, lend themselves to further pharmacological development.

Full-text article:

<http://www.ncbi.nlm.nih.gov/pubmed/23877697>

<http://aac.asm.org/content/57/10/4882>

Antimicrobial Agents and Chemotherapy, Gould, M. K., Bachmaier, S., Ali, J. A. M., Alsford, S., Tagoe, D. N. A., Munday, J., Schnauffer, A. C., Horn, D., Boshart, M., de Koning, H. P. (2013) Cyclic AMP Effectors in African Trypanosomes Revealed by Genome-Scale RNA Interference Library Screening for Resistance to the Phosphodiesterase Inhibitor CpdA. Copyright © 2013 Gould et al. This is an open-access article distributed under the terms of the Creative Commons Attribution 3.0 Unported license.

doi: 10.1128/AAC.00508-13

4. Unconventional activation of *T. brucei* PKA.

4.1 Cyclic AMP-independent signaling from a conserved PKA.

Sabine Bachmaier¹, Susanne Kramer^{1*}, George Githure¹, Florentine Scharf¹, Thomas Klöckner¹, Carsten Krumbholz¹, Franziska Böttger^{1§}, Julia Pepper^{1§}, Cordula Schulte zu Sodingen¹, Frank Schwede², Kapila Gunasekera³, Torsten Ochsenreiter³, Hans-Gottfried Genieser², Michael Boshart^{1#}

¹ *Biocenter, Section Genetics, Ludwig-Maximilians-Universität München, D-82152 Martinsried, Germany*

² *BIOLOG Life Science Institute, D-28199 Bremen, Germany*

³ *University of Bern, Institute of Cell Biology, CH-3012 Bern, Switzerland*

** present address: Department of Cell & Developmental Biology, Biocenter of the University of Würzburg, Würzburg, Germany*

§ present address: Karolinska Institutet, Department of Microbiology, Tumor and Cell Biology (MTC), Stockholm, Sweden

§ present address: Institute of Molecular Life Sciences, University of Zürich, Zürich, Switzerland

Manuscript

To whom correspondence should be addressed

Prof. Dr. Michael Boshart
boshart@lmu.de
Tel.: 49-89-2180-74600

Abstract

The protein kinase A (PKA) signaling pathway is highly conserved among eukaryotes. Activation by cyclic AMP and regulation of a plethora of cellular processes such as metabolism, differentiation or cell cycle progression, are hallmarks of PKA in unicellular as well as multicellular eukaryotes. Here we show that in the early branching eukaryote *Trypanosoma brucei*, the PKA signaling pathway has been retooled. The kinase is completely refractory to cAMP, and transcriptome profiling revealed a large number of kinetoplastid- or *Trypanosoma*-specific downstream substrates indicating involvement in regulation of an unusual subset of downstream processes. The observation that the kinase is indirectly activated by the adenosine antimetabolite dipyridamole provided evidence that *T. brucei* PKA is activated by an alternative, endogenous ligand. To define the chemical space of the alternative ligand(s), we conducted a small-scale chemical screen using several nucleoside and nucleotide derivatives combined with an *in vivo* PKA reporter assay and identified several 7-deazapurine analogues as potent activators. The most potent compound was subsequently used as tool to successfully identify downstream components of PKA signaling in *T. brucei*. Sequence comparison revealed the presence of highly similar PKA orthologues in the related kinetoplastids *Trypanosoma cruzi* and *Leishmania donovani* indicating conservation of this unconventional pathway within kinetoplastids. The presence of a conserved PKA with unconventional properties in kinetoplastids combined with the essentiality of the kinase in *T. brucei* suggests it as an optimal drug target for kinetoplastid-caused diseases.

Introduction

The cyclic AMP-dependent protein kinase PKA has been identified almost 50 years ago (Walsh et al., 1968), ten years after the identification of its activator, the second messenger cyclic AMP (cAMP) (Rall and Sutherland, 1958), and is now one of the best studied protein kinases from a variety of eukaryotes. In most organisms, the inactive PKA holoenzyme is a heterotetramer composed of a dimer of regulatory subunits (PKAR) and two associated catalytic subunits (PKAC). However, in some unicellular eukaryotes such as *Dictyostelium discoideum* (Mutzel et al., 1987) or *Paramecium tetraurelia* (Hochstrasser and Nelson, 1989), heterodimeric holoenzymes have been described. PKAR shows a characteristic domain structure with an N-terminal dimerization/docking (DD) domain responsible for homodimerization and sub-cellular localization, an internal inhibitor site and two C-terminal cNMP-binding domains (Scholten et al., 2008). The kinase is activated by the cooperative binding of two molecules of cAMP, produced by adenylyl cyclases (ACs) activated downstream of G protein-coupled receptors (GPCRs), to each PKAR subunit (Ogreid and Doskeland, 1981b, a; Ringheim et al., 1988; Herberg et al., 1996) resulting in a conformational change, which induces displacement of the internal inhibitor site and hence dissociation and activation of the catalytic kinase subunit. Whereas the mammalian genome encodes four different PKAR (RI α , RI β , RII α , RII β) and two to three different PKAC isoforms (C α , C β , C γ (only in primates)), which differ in their tissue-specific expression pattern, sub-cellular localization and affinity to cAMP (Skalhegg and Tasken, 2000), the genomes of most unicellular eukaryotes contain only one *PKAR* gene and a variable number of *PKAC* genes. PKA fulfills pleiotropic cellular functions by phosphorylation of a plethora of different substrates. Metabolism, differentiation, apoptosis, or cell cycle progression are among the manifold processes regulated by PKA in mammalian cells (Shabb, 2001). Several of these functions (such as regulation of metabolism of differentiation) are even conserved in unicellular eukaryotes (Primpke et al., 2000; Sonneborn et al., 2000; Bockmuhl and Ernst, 2001; Saran et al., 2002; Wilson et al., 2010; Tamanoi, 2011; Lastauskiene et al., 2014). PKA controls downstream processes either directly at the level of substrate phosphorylation or at the level of protein synthesis involving all steps from transcriptional (via phosphorylation of transcription factors) (Shabb, 2001), posttranscriptional (via phosphorylation of RNA-binding proteins with transcript stabilizing/destabilizing functions) (Huang et al., 1995; Mizunuma et al., 2013) or translational control (Vaidyanathan et al., 2014).

The cAMP/PKA signaling pathway is highly conserved in most eukaryotes ranging from lower, unicellular organisms such as *Dictyostelium discoideum* or *Saccharomyces cerevisiae* to mammals. However, in *Trypanosoma brucei*, a unicellular protozoan parasite of the evolutionary early branching order of *Kinetoplastida*, this signaling pathway seems to be significantly different. Whereas several components of cAMP signaling such as ACs, which produce cAMP, or phosphodiesterases (PDEs), which degrade cAMP, have been identified and partially characterized in *T. brucei*, genes encoding GPCRs or heterotrimeric G proteins seem to be absent from trypanosomal genomes (Seebeck et al., 2001; Seebeck et al., 2004). cAMP produced by the parasite has been shown to be involved in host-parasite interaction by modulating the immune response of the host thereby enabling the establishment of an efficient infection (Salmon et al., 2012b). Furthermore, manipulation of the intracellular cAMP concentration results in cell cycle defects implying a role for the second messenger in cell division

control (Oberholzer et al., 2007; de Koning et al., 2012; Salmon et al., 2012a). Despite the presence of genes orthologous to regulatory and catalytic subunits of PKA of other organisms in the *T. brucei* genome (Shalaby et al., 2001; Kramer et al., 2007), there is no indication for a cAMP-dependent kinase activity. The recently identified alternative cAMP response protein CARP1 (Gould et al., 2013) might replace PKAR as cAMP receptor. Here we show that *T. brucei* PKA is the first example of a conserved PKA, which is completely uncoupled from the second messenger cAMP. Our results provide indications for the presence of an alternative endogenous purine nucleoside-related ligand. By a small-scale chemical screen we identified several 7-deazapurine derivatives as potent activators of *T. brucei* PKA, which were subsequently used as tools to identify downstream components of PKA signaling in *T. brucei*. Sequence comparison of *T. brucei* PKA with orthologues from the related kinetoplastids *Trypanosoma cruzi* and *Leishmania donovani* suggests conservation of the unconventional features of the kinase within kinetoplastids. Since several kinetoplastid species are the causative agents of severe, health threatening diseases (*T. brucei*: Human African Sleeping Sickness; *T. cruzi*: Chagas disease; *Leishmania spp.*: leishmaniasis) with the urgent need for the development of new therapeutics, identification of novel drug targets is highly important. We suggest the kinetoplastid PKA as ideal drug target due to its essentiality in *T. brucei*, the presence of ligand-binding sites deviating from orthologous proteins in the mammalian host, and the identification of a compound, which binds to and activates the parasite kinase in the lower nanomolar range.

Material and Methods

Trypanosome strains and culture conditions. Bloodstream forms (BSFs) of the monomorphic strain Lister 427, variant MiTat 1.2 (Cross and Manning, 1973), of *Trypanosoma brucei brucei* were cultivated at 37°C in a 5% CO₂ atmosphere in modified HMI-9 medium (Vassella et al., 1997) supplemented with 10% (v/v) heat-inactivated fetal bovine serum (FBS). Expression of T7 polymerase and Tet repressor in the cell lines 13-90 (Wirtz et al., 1999) or 1313-514 (Alibu et al., 2005) was ensured by addition of 2.5 µg/ml G418 and 5 µg/ml hygromycin B or 0.2 µg/ml phleomycin and 2 µg/ml G418, respectively, to the culture medium. Cells were counted with a hemocytometer and diluted if required to keep the cell density below 1×10⁶ cells/ml.

Cloning and generation of transgenic trypanosomes. N-terminal *in situ* tagging of *T. brucei* PKAC1 (Tb427tmp.211.2410) and PKAC2 (Tb427tmp.211.2360) subunits was achieved by transfection with plasmids containing the full-length ORFs fused to a Ty1- or HA-epitope tag, respectively, in the pUC19 backbone. For transfection, the plasmids were linearized with HindIII and SdaI or ClaI and BstZ17I, respectively, and selection was performed in the presence of 2 µg/ml phleomycin or 2 µg/ml G418, respectively. A kinase-dead mutant of PKAC1 with an N-terminal Ty1-tag was generated by replacement of N153 of PKAC1 by alanine using the type II restriction enzyme Eco31I. The correct mutation was confirmed by sequencing. For overexpression of PKAC3 (Tb427.10.13010), the *PKAC3* ORF was amplified from MiTat 1.2 genomic DNA with primers introducing a Ty1-tag at the N-terminus and cloned into pTSARib[HYG] (Xong et al., 1998). The plasmid was linearized with SphI for transfection, and cells were grown in the presence of 4 µg/ml hygromycin B. A *T. brucei* cell line with inducible overexpression of PKAR (Tb427tmp.02.2210) was generated by transfection with a plasmid based on plew82 (Wirtz et al., 1999) containing the *PKAR* ORF amplified from MiTat 1.2 genomic DNA using primers introducing a Ty1-tag at the C-terminus. The plasmid was linearized with NotI for transfection, and 1-5 µg/ml phleomycin and 1 µg/ml tetracycline were used for selection. A *T. brucei* cell line with *in situ* tagging of PKAR with a C-terminal PTP tag (Protein A-TEV-Protein C) (Schimanski et al., 2005) was generated by replacement of the U170k coding sequence of pC-PTP-NEO (kindly provided by A. Bindereif, Giessen) with the *PKAR* ORF. Linearization for transfection was done using XcmI, and selection was performed by addition of 2 µg/ml G418 to the culture medium. *PKAC1* deletion mutants were generated by replacing the *PKAC1* ORF with a blasticidin or phleomycin resistance cassette flanked by actin UTRs. Antibiotic selection was performed using 1 µg/ml blasticidin or 1 µg/ml phleomycin, respectively. Similarly, *PKAC2* alleles were deleted by replacement with neomycin and hygromycin resistance genes flanked by actin UTRs. *PKAC2* knock out cells were grown in the presence of 2 µg/ml G418 and 2 µg/ml hygromycin B. *PKAR* knock out cells were generated by exchanging the *PKAR* alleles with puromycin and hygromycin resistance cassettes flanked by actin or aldolase UTRs, respectively. Selection was done by addition of 0.05 µg/ml puromycin and 1 µg/ml hygromycin B to the culture medium. The *PKAR* knock out cell line was rescued by endogenous expression of a wild type copy of *PKAR* under phleomycin selection (2.5 µg/ml). Knockdown of *PKAC1/2* was achieved by inducible RNAi targeting an N-terminal fragment of the *PKAC1* and *PKAC2* ORFs (pos. 30-648; difference between *PKAC1* and *PKAC2* within that region is only three nucleotides; no homology to *PKAC3*)

amplified from MiTat 1.2 genomic DNA and cloned into the RNAi vector p2t7^{Ti}TAblue (Alibu et al., 2005). The plasmid was linearized with NotI and transfected into the MiTat 1.2 1313-514 cell line (Alibu et al., 2005), followed by selection with 2 µg/ml hygromycin B. *PKAR* was knocked down by inducible RNAi targeting an N-terminal fragment of the *PKAR* ORF (pos. 1-467). In order to confirm specificity of the RNAi phenotype, a non-overlapping region of the *PKAR* ORF including part of the 3'UTR (*PKAR* ORF pos. 1106-end and *PKAR* 3'UTR pos. 1-34) was chosen for generation of a second *PKAR* RNAi cell line. Both fragments were amplified from MiTat 1.2 genomic DNA and independently cloned into the vector p2t7^{Ti}A (LaCount et al., 2002). The plasmids were linearized with NotI and transfected into the tetracycline-inducible 13-90 cell line (Wirtz et al., 1999). Selection was performed using 3 µg/ml phleomycin. RNAi-mediated repression of the *T. brucei* cAMP-specific phosphodiesterases *PDEB1* and *PDEB2* was carried out as published previously (Oberholzer et al., 2007) with the exception that the Tet-inducible vector pHD615[PAC] (derivative of pHD615 (Biebinger et al., 1997) with puromycin resistance gene) was used for hairpin RNAi in the present study. The 13-90 cell line (Wirtz et al., 1999) with or without expression of the PKA reporter substrate VASP was transfected with the *PDEB1/2* RNAi construct linearized with NotI and grown in the presence of 0.1 µg/ml puromycin. *T. brucei* cell lines expressing VASP were generated by transgenic expression of the *VASP* ORF amplified from human cDNA (VASP p14/1 in pBSK-, Acc. No. Z46389; (Haffner et al., 1995) kindly provided by U. Walter, University of Würzburg Medical Clinic) and cloned into pTSARib[HYG] (Xong et al., 1998) and its derivatives pTSARib[BSD] and pTSARib[PAC] (exchange of hygromycin resistance cassette against blasticidin or puromycin). Linearization for transfection was done with SphI. Cells were grown in the presence of 4 µg/ml hygromycin B, 4 µg/ml blasticidin, or 0.1 µg/ml puromycin, respectively. An inducible version of VASP with a C-terminal Ty1 tag was cloned into the vector plew82 (Wirtz et al., 1999) and transfected into the 13-90 cell line (Wirtz et al., 1999). Antibiotic selection was performed in the presence of 1 µg/ml phleomycin. Details on primer sequences and cloning strategies are available upon request. All transfections were performed as described previously (Schumann Burkard et al., 2011).

Generation of polyclonal antibodies. Anti-PKAC1 and anti-PKAC3 antisera were produced in rabbits against GST fusion proteins (amino acids 277 to 334 for PKAC1 and 272 to 337 for PKAC3). Rabbits were immunized by Eurogentec with 500 µg GST fusion protein purified from *E. coli* BL21DE3 (Stratagene), followed by further boosts with 500 µg antigen. Full-length hexahistidine-fusion proteins expressed in *E. coli* M15 (Qiagen) and purified using Ni-NTA columns (Qiagen) were used for affinity purification of the antibodies according to the method of Olmsted (1981).

Expression of PKA catalytic subunits in 293 cells. GST-fusion proteins of full-length PKAC1, PKAC2 and PKAC3 were expressed in human 293 cells. The ORFs were amplified by PCR from MiTat 1.2 genomic DNA and cloned into the eukaryotic expression vector pSCTEV3s (Matthias et al., 1989; Seipel et al., 1992). Cultivation and transfection of human 293 cells was performed as described in Vassella et al. (2001). For antibiotic selection, 300 µg/ml hygromycin B and 250 µg/ml G418 were added to the culture medium.

4. Activation of *T. brucei* PKA

(Co-) Immunoprecipitation. PTP purification was performed according to the protocol of Schimanski et al. (2005) with a few exceptions. Briefly, 2×10^8 BSF MiTat 1.2 cells with endogenous expression of PTP-tagged PKAR were lysed in PA-150 buffer (Schimanski et al., 2005; w/o DTT, supplemented with Complete Mini EDTA-free protease inhibitor cocktail and 25 $\mu\text{g/ml}$ pepstatin A) by three sonication cycles à 30 seconds with the Bioruptor (Diagenode) at low power. After centrifugation (20 min, $20000 \times g$, 4°C), the cleared supernatant was incubated with IgG beads (pre-equilibrated with PA-150 buffer) for 4 hours to overnight by overhead rotation at low speed. After two washes with PA-150 buffer followed by a final wash with PBS, proteins bound to the IgG beads were eluted by incubation with $2 \times$ Laemmli sample buffer for 5 minutes at 95°C .

Immunoprecipitation of Ty1- or HA-tagged PKA subunits was performed by incubation of trypanosome cells in lysis buffer (50 mM Tris pH 7.2, 2 mM EGTA, 150 mM NaCl, 0.2% NP-40; supplemented with 1 mM NaVO_4 , 0.5% aprotinin, 2 $\mu\text{g/ml}$ leupeptin, 1 mM PMSF) for 10 min on ice with subsequent clearing of the supernatant by centrifugation (20 min, $20000 \times g$, 4°C). The cleared lysate was incubated with the respective epitope-tag antibody coupled covalently (using the cross-linker DMP (Thermo Scientific) according to the manufacturer's instructions) or non-covalently to protein G sepharose beads (Amersham Pharmacia) for one hour to overnight. Bound proteins were either eluted by incubation with different concentrations of cNMPs or boiled in $2 \times$ Laemmli sample buffer for 5 minutes at 95°C .

Southern blot. Total genomic DNA was isolated by phenol/chloroform extraction. Restriction enzyme digests of genomic DNA were analyzed by Southern blot with digoxigenine labeled probes (DIG DNA Labeling and Detection Kit, Roche). Details are available on request.

Western Blot. Lysates of $1\text{-}5 \times 10^6$ trypanosome cells or 10 μg protein of human 293 cells were separated on 10% polyacrylamide gels and transferred to an Immobilon-FL PVDF membrane (Millipore) by semi-dry blotting. Primary antibodies used were anti-PKAR (1:500; Bachmaier et al., submitted manuscript; see chapter 5), anti-PKAC1/2 (1:500-1:1000), anti-PKAC3 (1:500), anti-Ty1 (1:300-1:1000; Bastin et al., 1996), anti-HA (clone 12CA5; undiluted hybridoma), anti-HSP60 (1:10000; Bringaud et al., 1995), anti-PFR-A/C (1:2000; Kohl et al., 1999), anti-VASP (1:5000; ImmunoGlobe, catalogue number IG-731), and anti-Phospho-(Ser/Thr) PKA substrate antibody (1:1000; Cell Signaling Technologies, catalogue number 9621). The immunological detection was either done with enhanced chemiluminescence (ECL) using horseradish peroxidase-conjugated secondary antibodies (Amersham Pharmacia, now GE Healthcare) according to the manufacturer's instructions or with the OdysseyTM IR fluorescence scanning system (LI-COR) using fluorescently labeled secondary antibodies (Alexa Fluor® 680 goat anti-rabbit IgG (H+L) (1:5000; Life Technologies), IRDye 680LT goat anti-rabbit IgG (H+L) (1:50000; LI-COR), IRDye 800CW goat anti-mouse IgG (H+L) (1:5000; LI-COR)). Signals of *T. brucei* PKA subunit proteins or phospho-RXXS/T-containing proteins were normalized to the PFR-A/C (Kohl et al., 1999) or Hsp60 (Bringaud et al., 1995) loading control after automatic subtraction of the background values (Median Left/Right method) using the Odyssey software (LI-COR). For the *in vivo* PKA reporter assay, the signals of the upper band (phosphorylated) and the lower band (non-phosphorylated) were quantified, and the extent

of phosphorylated VASP was calculated as follows: % phosphorylated VASP = (phosphorylated VASP / (phosphorylated + non-phosphorylated VASP)) × 100.

***In vivo* PKA reporter assay (VASP assay).** Trypanosomes were harvested (10 min, 1400×g, 37°C) and resuspended in fresh HMI-9 medium (pre-heated to 37°C) at a density of 5×10⁷ cells/ml. After a 5-10 minute recovery at 37°C while slightly shaking, test compounds were added to the cell suspension followed by careful mixing. Subsequently, cells were incubated at 37°C for a specified time period. Details on incubation time and compound concentration in each experiment are given in the results section. Cells were lysed with 6× Laemmli sample buffer preheated to 95°C and incubated for 5 minutes at 95°C.

Phenotypic analysis. For microscopic analysis, 5×10⁵ cells were spread on glass slides and fixed overnight in methanol at -20°C. Cellular DNA was visualized with 4',6-diamidino-2-phenylindole (DAPI; 1 µg/ml). Image acquisition was performed with a motorized Zeiss Axiophot2 wide-field microscope equipped with a Zeiss 63×/1.4 NA Oil DIC objective, a 1.0×-2.5× optovar, and a Princeton Instruments Micromax cooled (-15°C) slow scan CCD camera (Kodak KAF-1400 CCD chip).

Inhibitors and test compounds. PKI(5-24) and myr-PKI(14-22) were obtained from Biomol. CpdA was synthesized by Geert-Jan Sterk, Mercachem. Dipyrindamole was obtained from Sigma-Aldrich, toyocamycin and sangivamycin from Berry & Associates. All other compounds were synthesized by Biolog.

Cyclic AMP measurement. Before lysis, all steps were performed identical to the *in vivo* PKA reporter assay. For lysis, 2×10⁷ cells were pipetted into 5 ml of boiling water and incubated for 5 minutes, followed by lyophilization. cAMP concentrations were determined using the Cyclic AMP XP® Assay Kit (NEB). Three independent experimental series were analyzed in duplicates.

Cell viability assay. The viability of *T. brucei* BSF cells upon treatment with various compounds was assessed using the Alamar blue assay as published previously (Gould et al., 2013) with the exceptions that the initial seeding density was reduced from 1×10⁵ to 5×10³ trypanosomes/ml, the following growth period was extended from 48 h to 72 h, and the subsequent incubation with 0.5 mM resazurin sodium salt was reduced from 24 h to 4 h.

Cultivation and transfection of *Leishmania tarentolae*, recombinant expression of PKA subunits and purification of the PKA holoenzyme. The *L. tarentolae* strain LEXSY T7-TR (Jena Biosciences) was cultivated at 26.5°C in BHI medium supplemented with 10 µg/ml hemin and 100 U/l streptomycin / 100 mg/l penicillin according to the conditions published by Jena Biosciences. For maintenance of T7 polymerase and Tet repressor, 10 µg/ml nourseothricin (NTC) and 10 µg/ml hygromycin B were added to the medium. For co-expression of *T. brucei* PKAR-10×His and Strep-PKAC1, the full length ORFs were amplified from genomic DNA using primers introducing the respective epitope tag and cloned into pLEXSY_I-ble3 and pLEXSY_I-neo3 (Jena Biosciences), respectively. Cells transfected with both constructs were cultivated in the presence of 10 µg/ml phleomycin and 10 µg/ml neomycin. 200-500 ml of *L. tarentolae* cells at mid log phase (2-3×10⁷ cells/ml) were induced with 10 µg/ml tetracycline for 24 h. Cell lysis was performed using detergent (lysis buffer: 50 mM Tris pH 7.4, 150 mM NaCl, 0.2% triton X-100, 1 mM β-mercaptoethanol) and

4. Activation of *T. brucei* PKA

douncer homogenization. Purification of the holoenzyme complex was performed in a two-step procedure: His-tag purification using Ni-NTA beads (Thermo Fisher Scientific) was followed by Strep-tag purification using gravity flow chromatography and StrepTactin sepharose beads (IBA, Göttingen), according to the manufacturers' instructions. The eluted fractions were pooled and dialyzed against the kinase storage buffer (20 mM MOPS, pH 7.0, 150 mM NaCl, 1 mM β -mercaptoethanol). Details on primer sequences and cloning strategies are available upon request.

Recombinant expression and purification of the human PKAR1 α -PKAC α holoenzyme complex. For co-expression of human PKAR1 α (with an N-terminal 6 \times His tag followed by a TEV cleavage site) and PKAC α (with an N-terminal Strep-tag) in *E. coli*, the full length ORFs were amplified from cDNA (with primers introducing the respective epitope tag and protease cleavage site) and cloned into pETDuet-1 (Novagene). Purification of the holoenzyme complex was performed according to the protocol given for the *T. brucei* PKA holoenzyme. Details on primer sequences and cloning strategies are available upon request.

In vitro kinase assay. A radioactive PKA kinase assay was performed according to Hastie et al. (2006), adapted from Witt and Roskoski (1975) using 100 μ M Kemptide (LRRASLG; Kemp et al., 1976; Kemp et al., 1977) as kinase substrate and 100 μ M ATP spiked with [γ -³²P] ATP to give 200-400 cpm/pmol. Each compound was measured at least twice, in duplicates, including two controls, one lacking the substrate and the other one lacking the kinase.

RNA isolation and transcriptome analysis. RNA extraction, library construction, and spliced leader trapping were performed as described in Nilsson et al. (2010).

Bioinformatics. Read mapping and extraction was done as described previously (Nilsson et al., 2010). The read counts per gene were normalized using the DESeq2 package (Anders and Huber, 2010). The statistical analysis was done using the R environment (<http://www.R-project.org/>). A pairwise Z statistics was computed according to the description of Kal et al. (1999) dividing the normalized read counts by the predefined size factor. The analysis was based on four comparisons per gene in the wild type cell line: from time point 0 h to 0.5 h, from 0.5 h to 1 h, from 1 h to 4 h, and from 4 h to 8 h. The four resulting Z-scores were combined to one using Stouffer's Z-score method (Stouffer, 1949) weighing them all equally. Bi-directional p-values were computed and FDR-corrected as adjustment for multiple testing (Benjamini and Hochberg, 1995). We extracted those genes that met the following criteria: 1) p-value in wild type < 0.05; 2) fold change in wild type > 1.75; 3) fold change in Rko < fold change in wild type; and 4) neither in the knock out nor in the wild type more than two changes in direction were allowed; a change in direction was defined as a fold change larger than 1.3 from one time point to the next, if previous changes showed different directions. This resulted in exclusion of transcripts showing many fluctuations. GO enrichment analysis has been performed using TriTrypDB (www.tritrypdb.org) and the bioinformatics database DAVID (<http://david.abcc.ncifcrf.gov/>) (Huang et al., 2009b, a).

Quantitative RT-PCR. Total RNA was isolated in triplicates from *T. brucei* MiTat 1.2 BSF wild type cells or the homozygous *PKAR* deletion mutant incubated with or without 2 μ M toyocamycin for 0 h and 8 h using the NucleoSpin RNA kit (Macherey-Nagel) followed by cDNA synthesis using the iScript cDNA Synthesis kit (Bio-Rad). Relative mRNA expression levels of

selected candidates (primer sequences available on request) were determined by quantitative real-time PCR according to the previously published protocol (Gould et al., 2013). *TERT* was used as reference gene (Brenndorfer and Boshart, 2010).

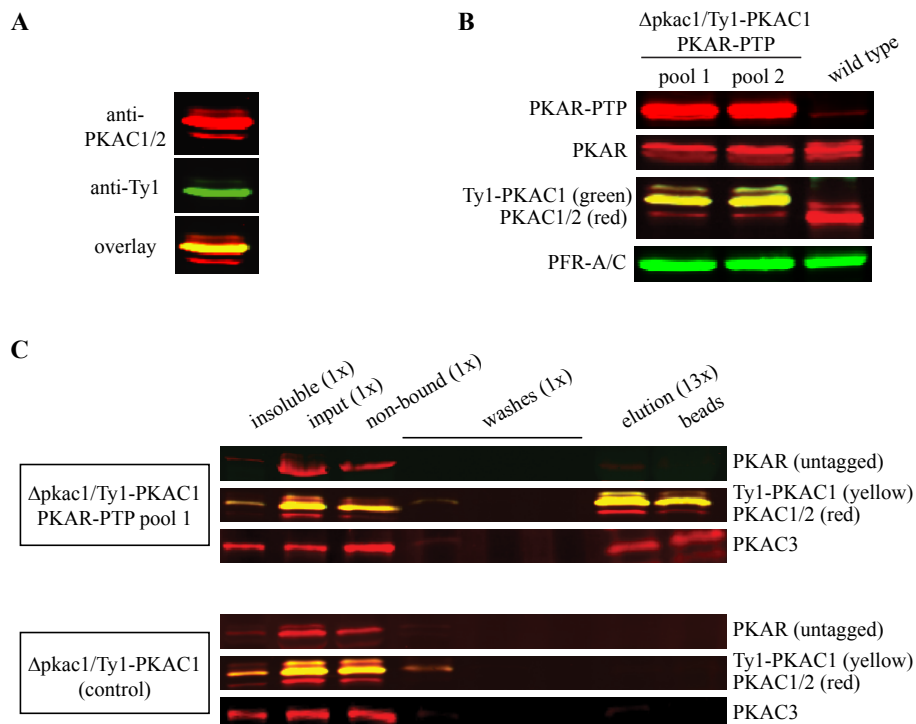
Results

Sequence analysis of putative *T. brucei* PKA subunits. The *T. brucei* genome harbors three genes (*PKAC1*, *PKAC2*, *PKAC3*; TriTrypDB entries: Tb427tmp.211.2410, Tb427tmp.211.2360, Tb427.10.13010) with highest similarity to catalytic as well as one gene (*PKAR*; GenBank AF182823; TriTrypDB Tb427tmp.02.2210) with highest similarity to regulatory subunits of cAMP-dependent protein kinases from a range of organisms (Kramer et al., 2007; Bachmaier and Boshart, 2013). While *PKAC1* and *PKAC2* share 95% sequence identity with most differences at the very N- and C-terminal ends and are arranged in tandem in the trypanosomal genome, *PKAC3* is more distant (60% and 59% sequence identity with *PKAC1* and *PKAC2*, respectively) and is located on a different chromosome. These features are found in almost all kinetoplastid genomes sequenced to date. Many important characteristics of PKAs from other organisms are conserved in the *T. brucei* orthologues (Figure S1A) such as the 11 canonical kinase subdomains (Hanks et al., 1988), the essential threonine in the kinase activation loop or residues important for binding to a regulatory PKA subunit (Taylor et al., 2004). The most obvious difference between the *T. brucei* kinases and PKACs of higher organisms is found at the N-terminus. In higher eukaryotes, the PKAC N-terminus consists of a myristoylation motif followed by an alpha helix of 21 amino acids in length (A-helix) that is thought to stabilize the catalytically active C-subunit (Herberg et al., 1997). The corresponding N-terminal sequences of the *T. brucei* kinases are significantly shorter and, in addition, contain several helix breaking amino acids. Similar truncated N-termini have been reported from PKAs of other protozoa (Siman-Tov et al., 1996; Kiriyaama et al., 1999). In addition, of the amino acids that carry post-translational modifications (PTMs) in catalytic PKA subunits from higher eukaryotes (Yonemoto et al., 1993; Gesellchen et al., 2006), only Thr-197 located in the kinase activation loop is conserved in all *T. brucei* orthologues (Nett et al., 2009; Urbaniak et al., 2013). (Auto-)phosphorylation at this site is essential for kinase activity (Steinberg et al., 1993; Adams et al., 1995; Steichen et al., 2010). PTMs of the N- and C-terminal tails of mammalian PKAC are known to confer specificity by influencing its activity, localization, and capacity to interact with other proteins. The divergence between the PTMs of the mammalian and the *T. brucei* orthologues might be an indication for differences in specificity.

T. brucei PKAR shares characteristics with mammalian PKARI and PKARII isoforms (Figure S1B). The overall sequence shows higher similarity to the mammalian isoform PKARI, but the presence of a phosphorylatable residue in the inhibitor site (RRTTV) is a hallmark of PKARII isoforms. Despite a similar overall domain organization, the kinetoplastid orthologues display several unique features compared to other regulatory PKA subunits: they have an elongated N-terminus with leucine-rich repeats (LRR) lacking a dimerization/docking (DD) domain, and they show several substitutions of highly conserved amino acids in their cNMP-binding pockets. Due to the absence of a DD domain, *T. brucei* PKA is most likely a heterodimeric holoenzyme composed of one R and one C subunit.

***T. brucei* PKAR interacts with all three PKA catalytic isoforms.** In order to examine the composition of the *T. brucei* PKA holoenzyme, the interactions between the different subunits/isoforms were studied by co-immunoprecipitation. Specific antibodies were raised in rabbits against recombinant GST-tagged PKAC1 (anti-PKAC1/2) or PKAC3 (anti-PKAC3). Specificity and cross-reactivity of anti-PKAC1/2 and anti-PKAC3 were tested on a Western blot with lysates from

human 293 cells transiently transfected with DNA containing the sequence of the complete *PKAC1*, *PKAC2* or *PKAC3* ORFs (Figure S2). Anti-PKAC3 was specific for PKAC3 and did not recognize any of the other catalytic isoforms. Since PKAC1 and PKAC2 share 95% sequence identity, the antibody raised against PKAC1 detected both isoforms but did not detect PKAC3. In addition, no cross-reactivity with human PKACs was observed. Since PKAC1 and PKAC2 have the same molecular weight and are detected by the same antibody, they cannot be distinguished on a Western blot with lysate from *T. brucei* wild type cells. Therefore, a cell line was generated with deletion of one allele of *PKAC1* and replacement of the other allele with Ty1-epitope tagged *PKAC1* (Δ pkac1/Ty1-PKAC1) resulting in an electrophoretic mobility shift and thereby allowing the distinction between the two isoforms (Figure 1A). In addition, PKAR was fused to a C-terminal PTP-tag in the cell line Δ pkac1/Ty1-PKAC1 (Figure 1B). Whereas PKAR and PKAC1/2 were almost exclusively found in the soluble fraction upon lysis, PKAC3 was equally distributed between soluble and insoluble fractions (Figure 1C). PKAR-PTP was able to pull down all three PKAC isoforms. In contrast, the same experiment in the parental Δ pkac1/Ty1-PKAC1 cell line without PTP-tagging of PKAR did not pull down any of the probed proteins indicating that PKACs do not unspecifically interact with the IgG beads. Furthermore, PKAR-PTP did not co-precipitate the endogenous, untagged PKAR, which indicates that the holoenzyme - at least in this cell line - is a heterodimer consisting of one regulatory and one of three different isoforms of a catalytic subunit. To exclude unspecific interactions of PKACs with the PTP-tag, independent co-immunoprecipitations were carried out in cell lines with Ty1-tagged PKAC1, PKAC3 or PKAR, or HA-tagged PKAC2, respectively, showing the same results as the PKAR-PTP pull-down (Figure S3A-C). Furthermore, this experiment showed that one specific PKAC isoform did not co-precipitate any of the other two isoforms supporting the idea of a heterodimeric holoenzyme.



4. Activation of *T. brucei* PKA

Figure 1: *T. brucei* PKAR interacts with all three PKA catalytic isoforms.

A. Western blot showing the discrimination between PKAC1 and PKAC2 in the cell line Δ pkac1/Ty1-PKAC1. Deletion of one allele of *PKAC1* and fusion of the other one to a Ty1-tag results in an electrophoretic mobility shift of PKAC1 allowing discrimination between PKAC1 and PKAC2 on a Western blot. Anti-PKAC1/2 and anti-Ty1 (Bastin et al., 1996) antibodies were used for detection.

B. PKAR was fused to a C-terminal PTP-tag in the cell line Δ pkac1/Ty1-PKAC1. The Western blot shows two independent pools of the cell line Δ pkac1/Ty1-PKAC1 PKAR-PTP compared to wild type cells and was probed with anti-PKAR (Bachmaier et al., submitted manuscript; see chapter 5), anti-PKAC1/2, anti-Ty1 (Bastin et al., 1996), and anti-PFR-A/C (Kohl et al., 1999) as loading control.

C. Western blot analysis of PTP purification using the cell line Δ pkac1/Ty1-PKAC1 PKAR-PTP (upper panel) and the parental cell line Δ pkac1/Ty1-PKAC1, which does not express a PTP-tagged PKAR (lower panel). Western blots were probed with anti-PKAR (Bachmaier et al., submitted manuscript; see chapter 5), anti-PKAC1/2, anti-PKAC3, and anti-Ty1 (Bastin et al., 1996). Values of x indicate relative amounts of each fraction analyzed.

***T. brucei* PKA orthologues are not activated by cAMP *in vitro*.** Since all PKA orthologues analyzed to date are activated by the second messenger cAMP, we studied cAMP-dependence of the *T. brucei* orthologues. PKA holoenzymes were purified from trypanosomes by immunoprecipitation via PKAR-Ty1. The immunoprecipitate was able to phosphorylate the PKA-specific substrate kemptide (Figure 2A, upper panel), and kinase activity was inhibited by the PKA-specific inhibitor peptide PKI(5-24). PKI is the gold standard of a PKA-specific inhibitor (Walsh et al., 1971; Glass et al., 1989; Harris et al., 1997; Dalton and Dewey, 2006). Surprisingly, even though the *T. brucei* PKA orthologues exhibit all features of a classical PKA in terms of holoenzyme composition (R-C complex) as well as substrate and inhibitor specificity, no activation by cAMP was observed, not even when the second messenger was used in mM concentrations. In contrast, the presence of high concentrations of cGMP significantly increased the activity of the *T. brucei* PKA holoenzymes. These results were confirmed by *in vitro* kinase assays with holoenzymes purified via Ty1-PKAC1 or HA-PKAC2, respectively, using antibodies against the respective epitope tag (Figure 2A, middle and lower panels). We can exclude that the measured kinase activities were due to contamination, since no substrate phosphorylation was detected with immunoprecipitate from wild type cells or with a catalytically inactive Ty1-PKAC1 mutant (dead mutant), in which the residue N153 in the kinase catalytic center was replaced by alanine (Cheek et al., 2002) (Figure S4A). In addition, the cNMPs cCMP (C = cytidine), cXMP (X = xanthosine), cIMP (I = inosine) and cUMP (U = uridine) did not show any influence on kinase activity (Figure S4B). It is unlikely that cGMP is the physiological activator since kinase activation was only detectable when cGMP was used in millimolar and thus unphysiologically high concentrations. In fact, for half maximal activation a concentration of 5-8 mM cGMP was required (Figure S4C), similar to previous observations (Shalaby et al., 2001). In addition, there are several lines of evidence arguing against the presence of cGMP or cGMP signaling in trypanosomatids (Laxman and Beavo, 2007).

As expected from the results of the *in vitro* kinase assays, addition of cAMP did not dissociate the PKAR-PKAC1 holoenzyme purified by immunoprecipitation via Ty1-PKAC1, whereas high concentrations of cGMP (1 mM) induced some release of PKAR into the supernatant (Figure 2B).

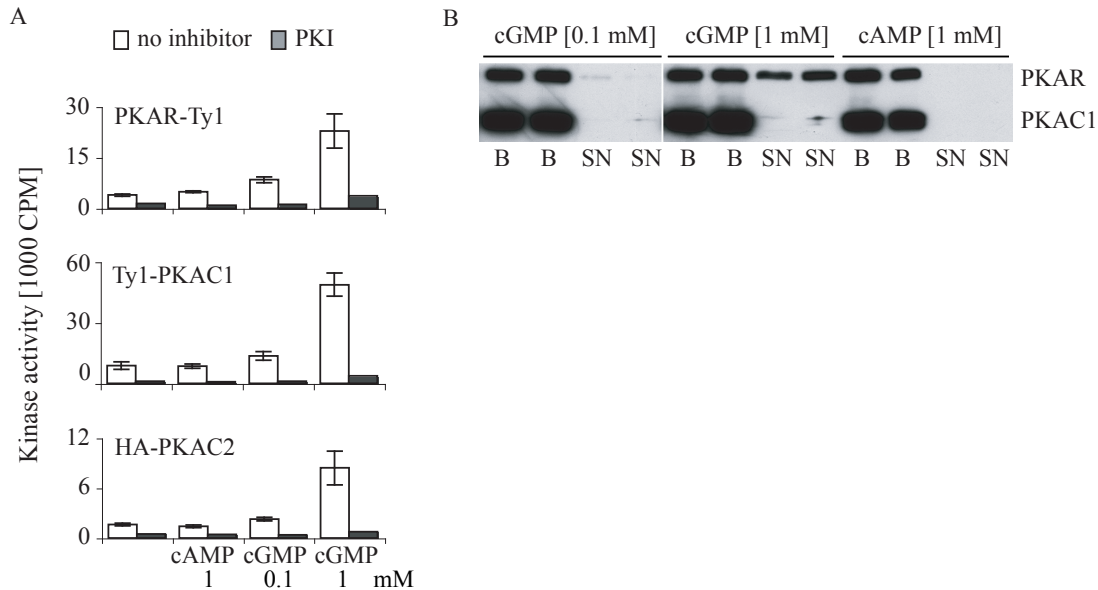


Figure 2: *T. brucei* PKA is not activated by cAMP *in vitro*.

A. *In vitro* kinase assays analyzing phosphorylation of the PKA-specific substrate kemptide by immunoprecipitated PKAR-Ty1 (upper panel), Ty1-PKAC1 (middle panel), or HA-PKAC2 (lower panel) in the presence or absence of cAMP or cGMP, respectively. Inhibition of kinase activity by 5 μ M PKI(5-24) was included as control. Each assay (except the ones with PKI) was performed in triplicate. Standard deviations are indicated by error bars.

B. Dissociation of the PKAR-PKAC1 holoenzyme, purified via Ty1-PKAC1, in the presence of cGMP or cAMP was analyzed by Western blot. Ty1-PKAC1 and PKAR bound to the beads (B) and free PKAR released into the supernatant (SN) were detected by anti-PKAC1/2 and anti-PKAR (Bachmaier et al., submitted manuscript; see chapter 5). Note that the film was over-exposed on purpose to stress the absence of any PKAR in the supernatant without cGMP.

***T. brucei* PKA orthologues are not activated by cAMP *in vivo*.** The absence of PKA dissociation and activation by cAMP *in vitro* could have different reasons e.g. a lack of an intracellular factor or an interacting protein important for kinase regulation. To exclude this possibility, an *in vivo* PKA reporter assay was established in *T. brucei*. The human, platelet-derived PKA substrate VASP (vasodilator stimulated phosphoprotein) was transgenically expressed in trypanosomes. Phosphorylation of VASP at the PKA-specific site Ser-157 causes a mobility shift in SDS gel electrophoresis from 46 to 50 kDa (Halbrugge and Walter, 1989; Butt et al., 1994). VASP, involved in organizing the actin cytoskeleton (Sechi and Wehland, 2004), has no orthologous protein in *T. brucei*. This was determined by a HMM-based search (HMMER version 2.3.2, standard parameters as set by the software; Eddy, 1998) of the *T. brucei* GeneDB (www.genedb.org/genedb/trypan/index.jsp) using the SMART family alignment of the VASP specific WH1 domain (Smart Accession SM00461; Schultz et al., 1998; Letunic et al., 2004) as template. A Western blot with lysates of wild type and VASP expressing *T. brucei* cells as well as human platelet protein was probed with a VASP-specific antibody (Figure 3A). The PKA substrate is expressed in the transgenic *T. brucei* cell line, whereas wild type cells do not express an orthologous protein. Furthermore, two bands are detected with the anti-VASP antibody in *T. brucei*, the upper one with a MW of 50 kDa corresponding to the phosphorylated and the lower one with a MW of 46 kDa representing the non-phosphorylated version

4. Activation of *T. brucei* PKA

of VASP. To prove that VASP is specifically phosphorylated by the parasite PKA orthologues, a myristoylated and hence membrane-permeable version of the PKA-specific inhibitor peptide PKI (myr-PKI(14-22)) was used to inhibit PKA activity. Upon treatment with 200 μ M myr-PKI(14-22) for 10 min, the intensity of the phosphorylated band decreased significantly (Figure 3B).

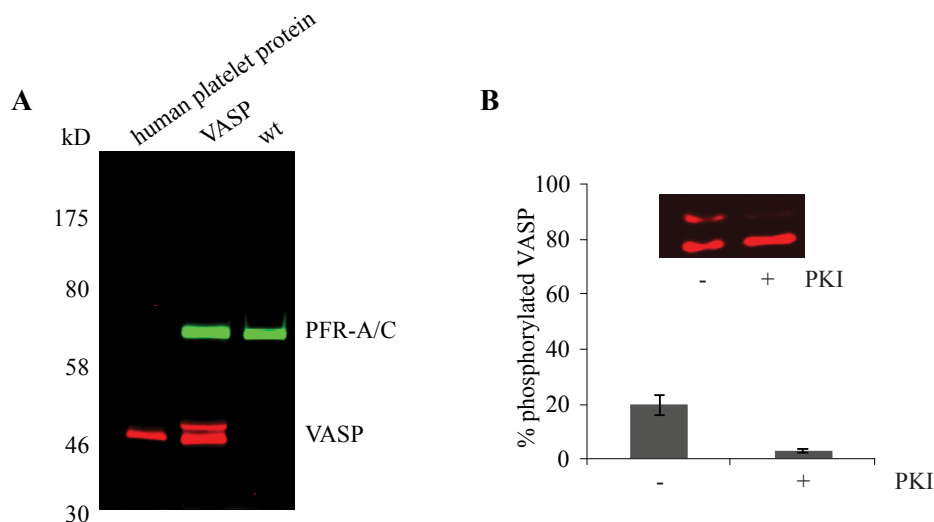


Figure 3: *T. brucei* PKA phosphorylates the transgenically expressed PKA substrate VASP *in vivo*.

A. Western blot showing the transgenic expression of the human PKA substrate VASP in *T. brucei* BSFs (VASP, lane 2). Human platelet protein (lane 1) and *T. brucei* wild type (wt) cells without expression of VASP (lane 3) were included as controls. PFR-A/C detected by the monoclonal antibody L13D6 (Kohl et al., 1999) was used as loading control.

B. *T. brucei* PKA phosphorylates VASP *in vivo*. Treatment of VASP expressing trypanosomes with the membrane-permeable PKA-specific inhibitor peptide myr-PKI(14-22) (200 μ M in TFA/H₂O, 10 min) causes repression of VASP phosphorylation. Results are derived from three independent experiments; error bars represent SD. The Western blot (inset) shows one representative experiment.

To exclude any influence of the selectable marker on VASP phosphorylation, three independent cell lines expressing the reporter substrate with different markers were generated. VASP phosphorylation was analyzed in two of these cell lines (VASP[BSD] and VASP[PAC]) in the presence or absence of myr-PKI(14-22) showing efficient inhibitor-dependent reduction in reporter substrate phosphorylation in both cell lines (Figure S5). To examine the influence of cAMP on *in vivo* PKA activity, elevation of the intracellular cAMP concentration was induced by two independent approaches: pharmacological PDE inhibition using the recently published PDE inhibitor CpdA (de Koning et al., 2012) and RNAi against the cAMP-specific phosphodiesterases (PDEs) *PDEB1* and *PDEB2* (Oberholzer et al., 2007). A >600- or ~45-fold increase in intracellular [cAMP] compared to untreated wild type cells was observed upon treatment with 10 μ M CpdA ($p \leq 0.05$) for 15 min or upon RNAi against *PDEB1* and *PDEB2* for 24h ($p \leq 0.001$), respectively (Figure 4A, C (upper panel)), corresponding to intracellular cAMP concentrations of ~200 μ M or ~14 μ M, respectively (assuming even intracellular distribution and no excretion of cAMP). Interestingly, even at these extremely high cAMP concentrations no increase in PKA activity was detected (Figure 4B, C (lower panel); Figure S6), supporting the observed lack of cAMP-dependent activation of the *T. brucei* PKA orthologues *in vitro*.

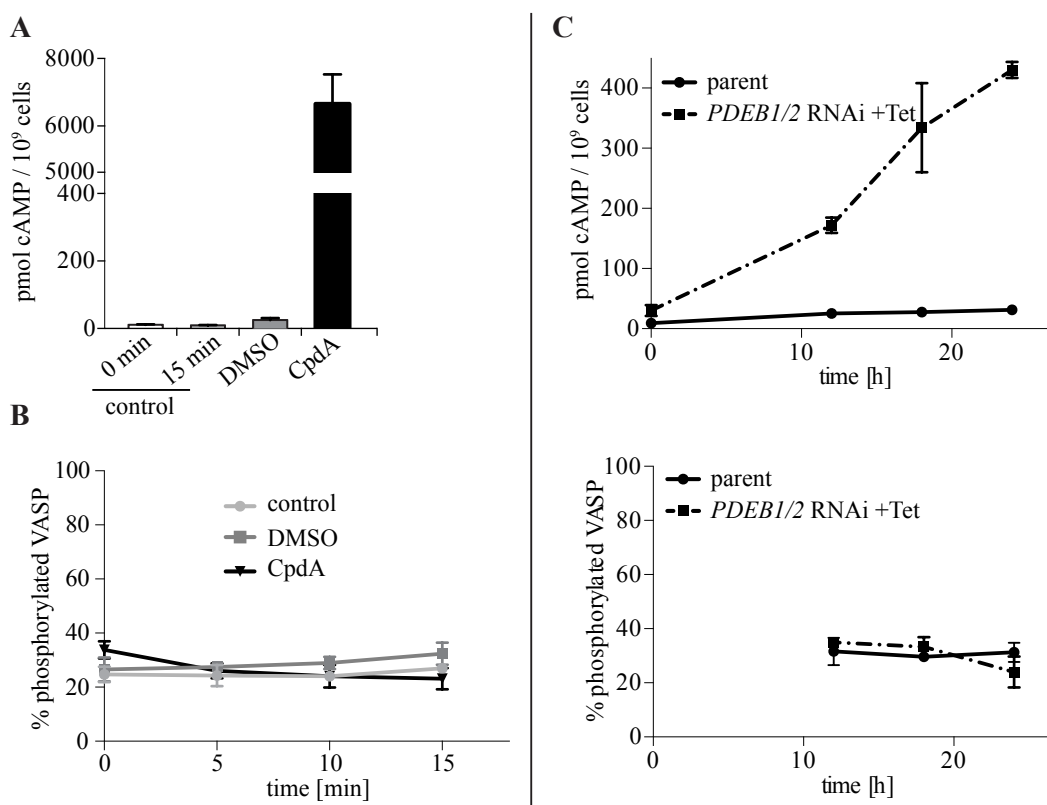


Figure 4: *T. brucei* PKA is not activated by cAMP *in vivo*.

A. Analysis of cAMP levels of trypanosomes treated with 10 μ M Cpda or with the solvent DMSO (1%) for 15 min. Untreated cells were included as control. Results are derived from three independent experiments; error bars represent SD.

B. Analysis of *in vivo* PKA activity in the presence of 10 μ M Cpda or 1% DMSO (solvent control) in a time course over 15 min. Untreated cells were included as control. Results are derived from three independent experiments; error bars represent SD.

C. Determination of cAMP levels (upper panel) and *in vivo* PKA activity (lower panel) upon inducible RNAi against *PDEB1* and *PDEB2* in a time course over 24 h after induction with 1 μ g/ml tetracycline (Tet). Since the PKA substrate VASP was expressed as Tet-inducible version, no VASP phosphorylation could be determined at time point zero. The parental cell line without RNAi against *PDEB1* and *PDEB2* was included as control. Results are derived from three independent experiments; error bars represent SD.

The slight inhibition of VASP phosphorylation at very high cAMP concentrations (Figure 4C, lower panel; S6C) is most likely unphysiological and due to unhealthy and dying cells. Since cAMP levels were determined by boiling lysis, the sum of intracellular and extracellular cAMP was measured. In order to exclude that the >600-fold increase in [cAMP] measured after Cpda treatment was mainly extracellular, excreted or released cAMP, we determined the concentration of the second messenger in the supernatant. Even though in comparison to untreated cells a slight fraction of cAMP was in fact excreted/released, this did not significantly change the calculated intracellular cAMP concentration (data not shown).

4. Activation of *T. brucei* PKA

***T. brucei* PKA is important for growth of bloodstream forms.** Since the *T. brucei* PKA orthologues are not cAMP-responsive, we were interested whether they do have an essential function in the parasite. Hence, several cell lines with genetic manipulation of PKA subunits were generated and analyzed regarding growth and cell cycle phenotypes. Inducible RNAi targeting both, *PKAC1* and *PKAC2*, resulted in a reduction in the PKAC1/2 protein level by 80-90% after 8h of induction with 1 µg/ml tetracycline (Tet) accompanied by a decrease in PKAR protein (by 40-80%, depending on the clone analyzed) (Figure S7A, left). The cells stopped growing within 4 h of RNAi induction with subsequent cell death within 2 days (Figure 5A, left panel; additional clone: Figure S8A, left panel) indicating at least one of the two genes being essential. Western Blot analysis of the cell line Δ pkac1/Ty1-PKAC1 showed that PKAC1 is expressed at a much higher level than PKAC2 in slender BSFs (Figure 1A), even in the presence of only one *PKAC1* allele. In order to find out whether the two subunits are redundant or one or both of them are essential, deletion mutants were generated. Three independent attempts to generate a null mutant of *PKAC1* failed indicating that PKAC1 is likely to be essential. The hemizygous *PKAC1* deletion mutant (Figure S7B), however, only showed a very mild growth phenotype (PDT 6 h) compared to wild type cells (PDT 5.4 h) (Figure 5A, right panel). In contrast to *PKAC1*, it was possible to delete both *PKAC2* alleles (Figure S7C). The *PKAC2* deletion mutant initially showed reduced growth with a PDT of 8.5 h (data not shown), which decreased to 6.8 h after prolonged cultivation (Figure 5A, right panel). Inducible RNAi against *PKAR* resulted in a growth arrest after 8 h of induction (Figure 5A, left panel; additional clone: Figure S8A, right panel). A decrease in PKAR protein by more than 90% with a concomitant decrease in PKAC1/2 levels (by >90%) and PKAC3 levels (by 60-80%) (Figure S7A, right) was observed. The growth phenotype of the *PKAR* RNAi cell line could be either caused by an initial increase in PKA activity due to free C subunits or it could result from a reduction in PKA activity by instability and degradation of free C subunits. The co-regulation of PKAR and PKACs observed in the RNAi cell lines indicates that these subunits interact *in vivo* by formation of a PKA holoenzyme. Co-regulation of PKA subunits has also been reported from mammalian cells, where loss, mutation, or overexpression of one PKA subunit can be partially compensated by co-regulation of the other at the level of protein stability (Amieux et al., 1997; Burton et al., 1997; Duncan et al., 2006; Kirschner et al., 2009). In contrast to the PKAR-PKAC1 co-regulation, which shows a correlation coefficient of $r = 0.91$ ($R^2 = 0.82$) (Figure S7D) and hence represents a nearly perfect correlation, the correlation coefficient for PKAR-PKAC3 is only $r = 0.59$ ($R^2 = 0.35$). This indicates that the amount of PKAC3 is not stoichiometrically co-regulated with the amount of PKAR. Possible explanations are that PKAC3 partially exists as free, inactive catalytic subunit, or that it is bound to an alternative intracellular inhibitor. For the following analyses we hence focused on PKAR and PKAC1/2. In contrast to the *PKAR* RNAi cell line, a homozygous deletion mutant of *PKAR* (Figure S7E) only showed a mild growth phenotype (PDT 7.5 h) (Figure 5A, right panel). The level of PKAC1/2 was reduced to 34% compared to wild type cells (Figure S7E) and hence does not show a perfect correlation with PKAR expression. The generation of a knock out cell line is always accompanied by selection of cells, which are able to survive under the altered conditions, which may be based on secondary adaptations when targeting an essential gene. The level of PKAC1/2 in the *PKAR* knock out cells may correspond to the minimal amount necessary for survival. This could explain why the *PKAR* knock out cells are able to survive in contrast to the *PKAR*

RNAi cell line, in which *PKAC1/2* is reduced to a lower level. To exclude off-target effects of the RNAi fragment targeting *PKAR*, we generated a cell line with inducible RNAi against a non-overlapping fragment covering the C-terminal part of the *PKAR* ORF and part of its 3'UTR. Both *PKAR* RNAi cell lines showed identical results regarding repression efficiency and growth phenotypes upon induction of RNAi (Figure 5A, Figure S7A right, Figure S8A right, Figure S9). The growth defects of *PKAR* and *PKAC1/2* mutants shown in the present study are supported by data from a recent genome-wide RIT-seq screen, in which all three genes have scored essential after 6 days of RNAi induction in BSFs (Alsford et al., 2011). In addition, a recent kinome RNAi screen showed similar phenotypes when targeting *PKAC1* and *PKAC2* (Jones et al., 2014).

Detailed cell cycle analysis revealed pronounced defects of most PKA mutants. By DAPI staining and subsequent determination of kinetoplast/nucleus (K/N) configurations we observed a decrease in the number of 1K1N cells and a concomitant increase in the number of 2K2N and aberrant, multinucleated cells for the *PKAC1* and *PKAC2* deletion mutants and the induced RNAi cell lines in a time course over 10 hours of induction (Figure 5B, Figure S8B). The strongest phenotype was observed for the *PKAC1/2* RNAi cell line, which showed a significant increase in 2K2N and multinucleated cells already after 4h of Tet induction. After 8 hours, nearly 100% of the population consisted of 2K2N and multinucleated cells. The fraction of 2K1N cells decreased to zero. A very similar, but slightly delayed phenotype was observed for the *PKAR* RNAi cell line. As mentioned before, this may be caused by a reduction of total PKA activity, since RNAi against *PKAR* is accompanied by a reduction in *PKAC1/2* levels. The hemizygous deletion mutant of *PKAC1* and the *PKAC2* null mutant showed phenotypes similar to *PKAC1/2* RNAi, but less pronounced, with a doubling of the amount of 2K2N cells and a significant increase in the number of multinucleated cells. These results suggest a block in cytokinesis. In contrast, the *PKAR* null mutant does not show defects in cell division, again stressing the possibility of secondary adaptations in knock out cell lines.

4. Activation of *T. brucei* PKA

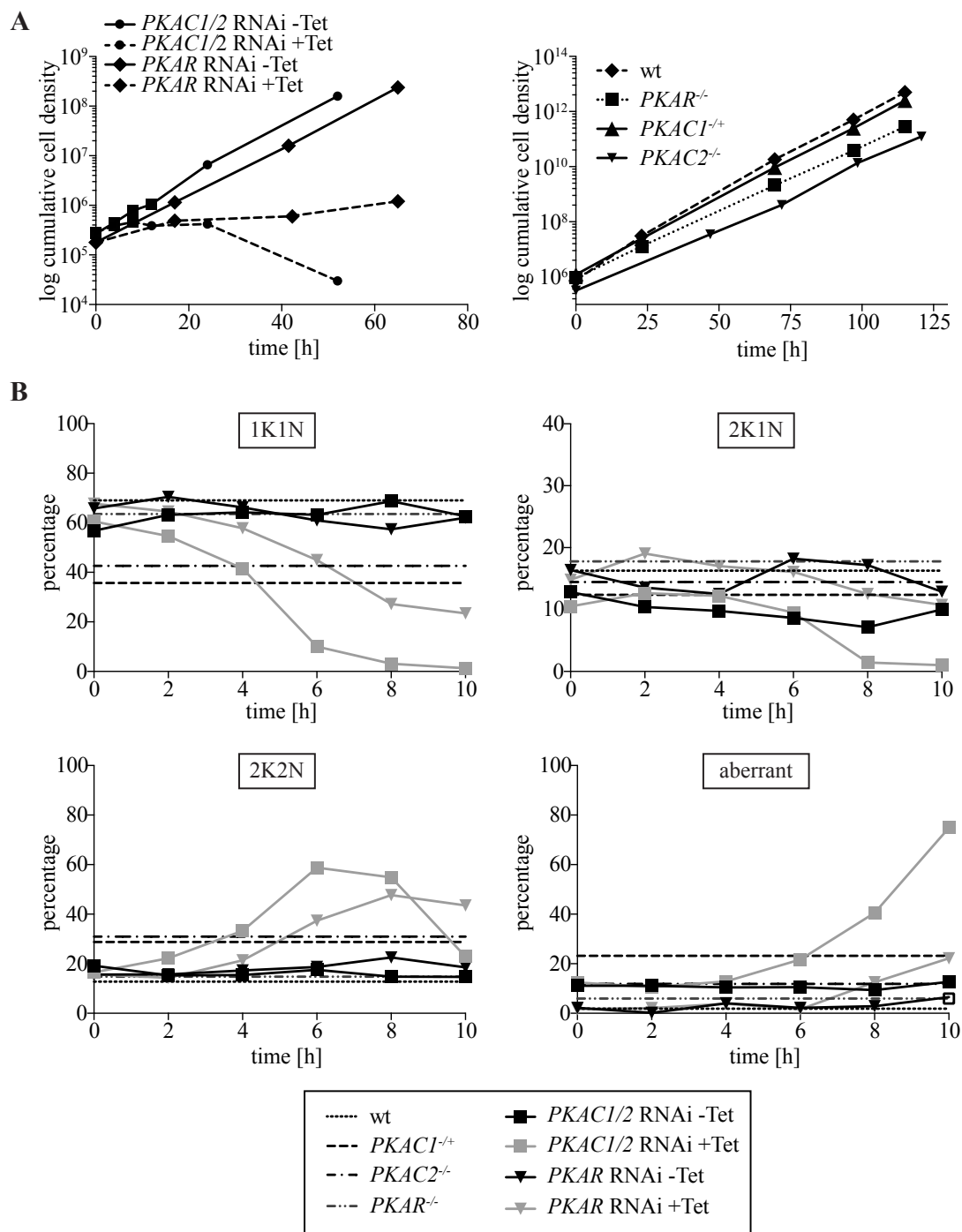


Figure 5: Growth and cell cycle analysis of *T. brucei* PKA mutants.

A. Growth analysis of cell lines with inducible RNAi against *PKAC1/2* or *PKAR* (left panel) grown in the presence (+Tet) or absence (-Tet) of 1 μ g/ml tetracycline as well as of wild type (wt) cells and PKA deletion mutants (*PKAR*^{-/-}, *PKAC1*^{-/+}, *PKAC2*^{-/-}) (right panel). Cells were counted at the indicated time points and diluted if necessary to keep the cell density below 1 \times 10⁶/ml. The y-axes represent the log₁₀ of the cumulative cell densities.

B. Cell cycle analysis by counting the number of kinetoplasts (K) and nuclei (N) per cell of wild type cells (wt), PKA deletion mutants (*PKAR*^{-/-}, *PKAC1*^{-/+}, *PKAC2*^{-/-}) as well as of cell lines with inducible RNAi against *PKAC1/2* or *PKAR* in a time course over 10 h after induction with 1 μ g/ml tetracycline (+Tet). Non-induced cells (-Tet) were included as control. The K/N configurations of wild

type cells and the deletion mutants are represented by dashed lines, since they were analyzed only at one time point. A minimum of 100 cells of each cell line was analyzed at the indicated time points. Note that the y-axis of the 2K1N-analysis was stretched compared to the other analyses in order to be able to distinguish between the single graphs.

***T. brucei* PKA is activated by the PDE inhibitor dipyridamole.** Before CpdA became available, we had used dipyridamole for the experiments shown in Figure 4. Consistent with previous studies (Zoraghi et al., 2001; Laxman et al., 2006), the PDE inhibitor dipyridamole induced a slight increase (2.3-fold compared to treatment with the solvent DMSO in a 15 min assay, $p \leq 0.001$; 2.8-fold in a 90 min assay, $p \leq 0.001$) in the intracellular cAMP level (Figure 6A). Surprisingly, dose- and time-dependent induction of *in vivo* PKA activity was observed upon treatment with dipyridamole (Figure 6B; Figure S10A, B). This activation cannot be due to the slightly increased cAMP levels since no induction was observed upon treatment with the much more potent PDE inhibitor CpdA (Figure 4A, B). The specificity of the dipyridamole-induced PKA activation was proven by treatment with the PKA-specific inhibitor peptide myr-PKI(14-22), which prevented a dipyridamole-induced increase in VASP phosphorylation (Figure S10C). In addition, no activation by dipyridamole was observed in a *PKAR* null mutant (*PKAR*^{-/-}) in comparison to wild type cells and an endogenous *PKAR* rescue cell line (*PKAR*^{-/+}) (Figure S10D) indicating that dipyridamole induces VASP phosphorylation specifically via *PKAR*.

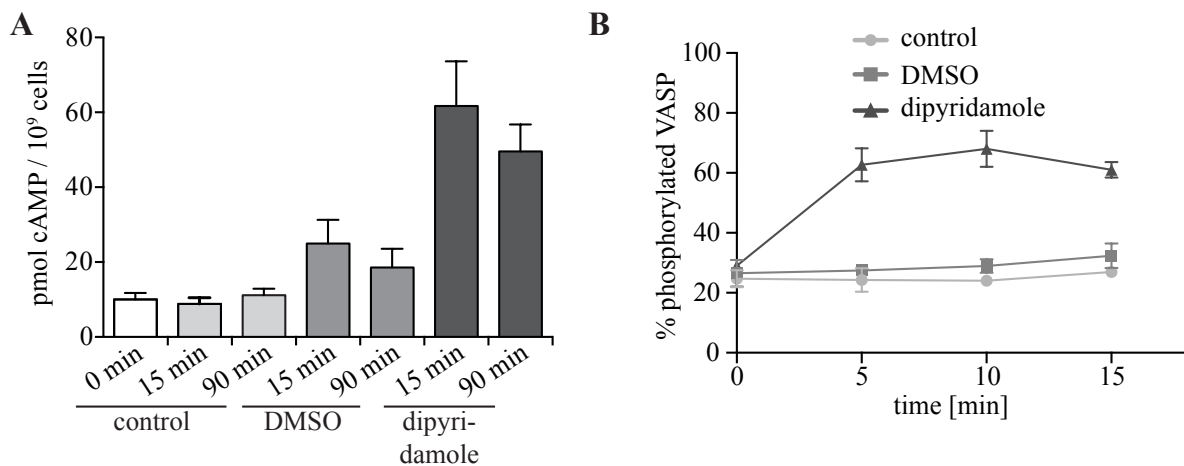


Figure 6: *T. brucei* PKA is activated by dipyridamole *in vivo*.

A. Analysis of cAMP levels upon treatment with 100 μ M dipyridamole or the solvent DMSO (1%) for 15 min or 90 min, respectively. Untreated cells were included as control. Results are derived from three independent experiments; error bars represent SD.

B. Determination of *in vivo* PKA activity upon treatment with 100 μ M dipyridamole or the solvent DMSO (1%) in a time course over 15 min. Untreated cells were included as control. Results are derived from three independent experiments; error bars represent SD.

4. Activation of *T. brucei* PKA

An *in vivo* small-scale screen identifies regulators of *T. brucei* PKA. The unexpected observation that *T. brucei* PKA is activated by dipyrnidamole in a cAMP-independent and PKAR-dependent manner asked for definition of the chemical space of possible activators of the kinase. Among other side effects, dipyrnidamole is known to interfere with adenosine signaling (Pfleger et al., 1969; Klabunde, 1983; Gibbs and Lip, 1998). Hence, we conducted a small-scale chemical screen with a major focus on testing the effect of several different membrane-permeable adenosine analogues on *in vivo* PKA activity as well as on cell proliferation (Table 1, Figure S11). In addition, six membrane-permeable cAMP or cGMP analogues were included in the screen to confirm the absence of cAMP-dependent activation of *T. brucei* PKA and to re-analyze the previously observed activation of the kinase by high concentrations of cGMP (Figure 2; Shalaby et al., 2001). The two adenosine analogues 8-pCPT-adenosine and 8-pCPT-2'O-me-adenosine were identified as inhibitors of *in vivo* PKA activity, although maximal inhibition was only modest (Table 1; Figure S11A). In contrast, 8-pCPT-adenine, a possible intracellular degradation product of 8-pCPT-adenosine, did not show any effect on VASP phosphorylation (Table 1; Figure S11B), additionally serving as a control that the observed effects of 8-pCPT-(2'O-me-)adenosine are not caused by the chlorophenylthio (CPT) group. The nucleoside derivatives 8-pCPT-guanosine, 2-Cl-adenosine, 8-Br-adenosine and 6-Cl-puroribonucleoside as well as six different cAMP or cGMP analogues did not significantly influence kinase activity at physiologically relevant concentrations (Table 1; Figure S11C, D), confirming the absence of cAMP-dependent activation of *T. brucei* PKA. Only at very high concentrations (>1 mM) inhibition by 8-pCPT-cAMP was observed, while high concentrations of 8-pCPT-cGMP caused activation of the kinase (Figure S11E), supporting previous observations (Shalaby et al., 2001). Interestingly, the 7-deaza-adenosine (tubercidin) analogues toyocamycin, 5-I-tubercidin, 5-Br-tubercidin and sangivamycin were identified as *in vivo* activators of *T. brucei* PKA with EC₅₀ values of 87.63 nM, 389.57 nM, 625.07 nM, and 39.26 μM, respectively (Table 1; Figure S11F). In order to prove specificity of PKA activation by toyocamycin, the most potent *in vivo* activator identified in the present study, VASP phosphorylation was analyzed in a null mutant of *PKAR* (Figure S11G) compared to wild type cells in a time course over 30 min. No increase in PKA activity was observed in the *PKAR* deletion mutant indicating that toyocamycin induces VASP phosphorylation specifically via PKAR. In contrast to the 5-substituted tubercidin derivatives, which activate *T. brucei* PKA, no effect was observed upon treatment with tubercidin or 6-Br-tubercidin (Table 1; Figure S11H). Since tubercidin cannot pass membranes by diffusion but has to be taken up via adenosine transporters (de Koning and Jarvis, 1999; Mäser et al., 2001; Geiser et al., 2005), its intracellular concentration may not be sufficient to activate PKA within 15 min. However, the lack of activation by 6-Br-tubercidin indicates that either the electronegative side group at C-5 of tubercidin is essential for activation or that the bromo group at C-6 of tubercidin prevents activation.

Growth analysis by Alamar blue assay revealed that all compounds affecting *in vivo* PKA activity also showed anti-proliferative effects in BSFs (Table 1). 8-pCPT-2'O-me-adenosine, one of the two inhibitors of *T. brucei* PKA, was the most active compound with an IC₅₀ of 122±16 nM. The other inhibitor, 8-pCPT-adenosine, was ~4-fold less potent. Analysis of the growth inhibitory effect in a *PKAR* null mutant showed a significant increase in resistance to 8-pCPT-2'O-me-adenosine and 8-pCPT-adenosine of 2-fold (p≤0.001) and 4-fold (p≤0.001), respectively, indicating that the lethal

effects are at least in part mediated by inhibition of PKA. Similarly, the mutant showed increased resistance to the cAMP derivatives 8-pCPT-2'O-me-cAMP (1.6-fold ($p \geq 0.05$)) and 8-pCPT-cAMP (4-fold ($p \leq 0.05$)), which are likely to be intracellularly degraded to the respective adenosine derivatives. The absence of an effect of these cAMP derivatives in the VASP assay can be easily explained by the short time course of the assay, which is most likely not sufficient for the degradation of the cAMP to the adenosine derivatives. A significant increase in resistance of the *PKAR* null mutant compared to wild type cells was also observed for dipyridamole (1.65-fold; $p \leq 0.01$) and sangivamycin (2.2-fold; $p \leq 0.001$), two of the *in vivo* activators of *T. brucei* PKA identified in the present study. The growth inhibitory effects of the other activators (toyocamycin, 5-I-tubercidin, 5-Br-tubercidin) did not differ between wild type and *PKAR* null mutant, indicating that lethal effects via other targets in the trypanosome cells are dominant. This is not surprising, since these 5-substituted tubercidin analogues are known to have various different intracellular targets in mammalian cells, e.g. inhibition of several kinases (Saffer and Glazer, 1981; Loomis and Bell, 1988; Osada et al., 1989; Palczewski et al., 1990; Bobek and Bloch, 1994) or general inhibition of DNA, RNA and protein synthesis (Cohen and Glazer, 1985).

***T. brucei* PKA is directly activated by 5-substituted tubercidin analogues *in vitro*.** In order to investigate whether the identified *in vivo* regulators of *T. brucei* PKA act directly or indirectly, kinase assays were conducted *in vitro* with recombinantly expressed and purified holoenzyme using kemptide as substrate. Since PKAC1 is more abundant than PKAC2 in BSFs and is essential, it was chosen for inducible co-expression with *T. brucei* PKAR in the *L. tarentolae* expression system (LEXSY) (Figure S12A). Dipyridamole, the initially identified activator of *in vivo* PKA activity in *T. brucei*, did not show any effect on *in vitro* kinase activity indicating an indirect activation mechanism (Table 2, Figure S12B). In contrast, almost all tubercidin derivatives showed activation of the purified holoenzyme *in vitro* with the following order of potency: toyocamycin > 5-I-tubercidin > 5-Br-tubercidin > tubercidin > sangivamycin (Table 2, Figure S12C). This order is almost identical to the *in vivo* observations with the exception that tubercidin did not regulate *in vivo* PKA activity. As mentioned above the most likely reason is that in contrast to all other tubercidin analogues tested in the screen it has to be taken up by adenosine transporters, which is most likely too slow for activation of the kinase within a short incubation time. 8-pCPT-2'O-me-adenosine, one of the two inhibitors of *T. brucei* PKA *in vivo*, did not inhibit PKA activation by toyocamycin *in vitro* suggesting an indirect mechanism (Table 2, Figure S12D). Differences in the EC_{50} values between *in vivo* and *in vitro* experiments can be based e.g. on uptake efficiency or intracellular accumulation.

Toyocamycin does not activate the human PKA holoenzyme. In order to analyze the specificity of activation by toyocamycin for the parasite PKA orthologue, *in vitro* kinase assays were conducted with recombinantly expressed human PKAR1 α -PKAC α holoenzyme. Treatment with toyocamycin did not influence PKA activity up to a concentration of 50 μ M (Figure S12E, left panel), whereas the kinase was activated by treatment with 10 μ M cAMP.

4. Activation of *T. brucei* PKA

Table 1: Influence of different nucleoside/nucleotide derivatives on *in vivo* PKA activity in *T. brucei*.

compound	EC ₅₀ growth wt Alamar blue assay ^{1,2}	EC ₅₀ growth <i>PKAR</i> ^{-/-} Alamar blue assay ^{1,2}	EC ₅₀ VASP phosphorylation wt ^{2,3}	
8-pCPT-adenosine	475 ± 86 nM	1869 ± 292 nM (p ≤ 0.001) ⁵	↓ 369.2 ± 120 nM	PKA inhibitors
8-pCPT-2'O-me-adenosine	122 ± 16 nM	234 ± 20 nM (p ≤ 0.001) ⁵	↓ 110.63 ± 23.5 nM	
8-pCPT-adenine	no effect	no effect	no effect	
8-pCPT-guanosine	20 μM ⁴	n.d.	no effect	
8-Br-adenosine	n.d.	n.d.	no effect	
2-Cl-adenosine	15.82 ± 2.5 μM	17.43 ± 2.3 μM	no effect	
6-Cl-PuR	n.d.	n.d.	no effect	
8-pCPT-cAMP	2.45 ± 0.7 μM	9.95 ± 2.2 μM (p ≤ 0.05) ⁵	no effect	
8-pCPT-2'O-me-cAMP	1.23 ± 0.3 μM	1.98 ± 0.3 μM (p ≥ 0.05) ⁵	no effect	
8-pCPT-cGMP	n.d.	n.d.	no effect	
8-pCPT-2'O-me-cGMP	∞ ⁴	n.d.	no effect	
cAMP-AM	no effect ⁴	n.d.	no effect	
cGMP-AM	no effect ⁴	n.d.	no effect	
dipyridamole	9.93 ± 1 μM	16.3 ± 1.8 μM (p ≤ 0.01) ⁵	↑ 22.35 ± 4.2 μM	PKA activators
toyocamycin	739 ± 59 nM	690 ± 58 nM	↑ 87.63 ± 9.6 nM	
5-I-tubercidin	330 ± 38 nM	346 ± 41 nM	↑ 389.57 ± 20 nM	
5-Br-tubercidin	874 ± 122 nM	1009 ± 95 nM	↑ 625.07 ± 65.5 nM	
sangivamycin	713 ± 40 nM	1548 ± 171 nM (p ≤ 0.001) ⁵	↑ 39.26 ± 5.6 μM	
tubercidin	n.d.	n.d.	no effect	
6-Br-tubercidin	n.d.	n.d.	no effect	

¹ average ± SEM determined from at least six independent replicates

² EC₅₀ determined using GraphPad Prism 6.0

³ average ± SD determined from three independent biological replicates

⁴ determined by manual counting

⁵ p-values indicate the significance of the change in the EC₅₀ of *PKAR*^{-/-} compared to wild type (wt); p-values were determined using the Excel Add-in QI Macros, 2014; F-test for identical or different variances followed by two-tailed T-test
n.d. = not determined; ↑ activation, ↓ inhibition

Table 2: Influence of the identified *in vivo* regulators on *in vitro* *T. brucei* PKA activity.

compound	EC ₅₀ <i>in vitro</i> kinase assay ^{1,2}
dipyridamole	no effect
8-pCPT-2'O-me-adenosine	no effect
toyocamycin	183 ± 70 nM
5-I-tubercidin	227 ± 92 nM
5-Br-tubercidin	2.8 ± 0.9 μM
sangivamycin	≥ 11 μM
6-Br-tubercidin	negligible

PKA activators

¹ average ± SEM determined from at least three independent replicates² EC₅₀ determined using GraphPad Prism 6.0

Toyocamycin as tool to decipher downstream components of the PKA signaling pathway in *T. brucei*. The VASP assay is a useful tool to analyze regulation of PKA *in vivo*. However, nothing is known about endogenous PKA substrates in *T. brucei*. With the identification of toyocamycin as potent activator, the analysis of global changes in phosphorylations and transcript abundance could help identifying further components of this signaling pathway in *T. brucei*. Lysates of BSF wild type and *PKAR* null mutant cells treated or not with toyocamycin were analyzed by Western blot using a Phospho-(Ser/Thr) PKA substrate antibody (Figure 7). Whereas in the wild type sample a strong increase in the number and intensity of the bands recognized by the antibody was observed upon treatment with toyocamycin, no difference between treated and untreated samples was detected for the *PKAR* null mutant. The same result was obtained analyzing a wild type and a *PKAR* null mutant cell line with expression of the reporter substrate VASP (Figure S13). This indicates that toyocamycin can be used as tool to specifically detect proteins phosphorylated by *T. brucei* PKA, which can subsequently be identified by quantitative proteomics.

4. Activation of *T. brucei* PKA

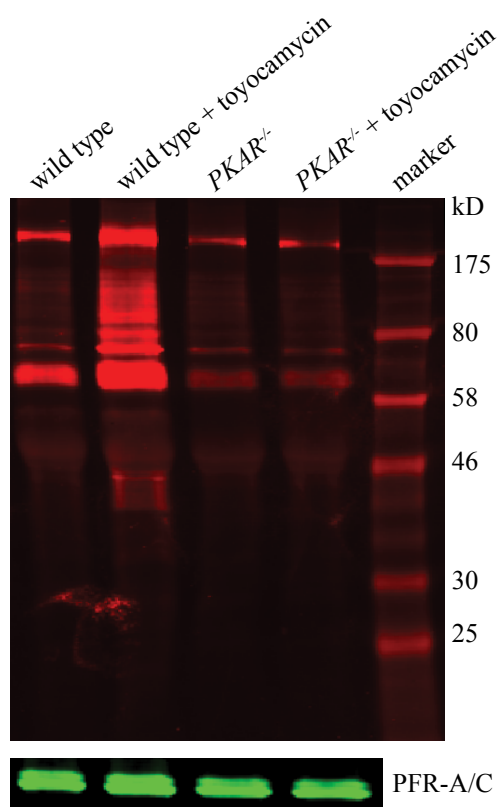


Figure 7: Toyocamycin induces phosphorylation of endogenous PKA substrates.

Western blot analysis with lysates from *T. brucei* wild type or *PKAR*^{-/-} cells treated or not with 2 μ M toyocamycin for 10 min. Proteins phosphorylated at RXXS/T motifs were detected by a Phospho-PKA substrate antibody (anti-RXXS*/T*; * = phosphorylation). The monoclonal antibody L13D6 (Kohl et al., 1999) was used for detection of PFR-A/C as loading control.

In addition, combining activation of PKA by toyocamycin with transcriptome profiling using RNAseq allows the identification of components regulated by PKA at the transcript level. Wild type and *PKAR* null mutant cells were treated with toyocamycin, and RNA samples were taken after 0 h, 0.5 h, 1 h, 4 h, and 8 h. Transcript abundance analyzed by RNAseq revealed significant regulation ($p < 0.05$) of 225 transcripts by toyocamycin in wild type cells without significant regulation in the *PKAR* deletion mutant (Table S1, Figure S14). GO (gene ontology) enrichment analysis using the TriTrypDB database (www.tritrypdb.org) as well as the DAVID bioinformatics database (<http://david.abcc.ncifcrf.gov/>) indicated a major involvement of *T. brucei* PKA in regulation of metabolic processes, translation, protein folding, (ribo-)nucleotide/nucleoside-binding, and transport (Table S2A, B), reminiscent of PKA downstream functions in other organisms (Tash and Means, 1982; Brokaw, 1987; Leclerc et al., 1996; Robertson et al., 2000; Jones et al., 2003; Zhang et al., 2003; Marcus et al., 2004; Hu et al., 2007; Baker, 2011; Wurtz et al., 2011). To validate the RNAseq analysis, the expression of four transcripts (phosphatidic acid phosphatase (Tb927.8.480), procyclin associated gene 1 (Tb927.10.10240), glycerol kinase (cluster of five nearly identical genes: Tb927.9.12550, Tb927.9.12570, Tb927.9.12590, Tb927.9.12610, Tb927.9.12630), and a hypothetical protein (Tb927.8.490)) showing significant toyocamycin-dependent regulation in the wild type but not in the deletion mutant was independently analyzed by qRT-PCR (Figure S15) in wild type and *PKAR* null mutant cells treated or not with toyocamycin for 8 h. The results of the qRT-PCR analysis are fairly in agreement with the RNAseq data.

Discussion

The activation mechanism of Protein Kinase A by cAMP is highly conserved in most eukaryotes ranging from unicellular symbiotic pathogens such as plasmodia over yeast to mammals. Although there are exceptional cases of cAMP-independent regulation (Zhong et al., 1997; Wang et al., 1998; Dulin et al., 2001; Zieger et al., 2001; Yang et al., 2013), all these PKA orthologues can be activated by the cooperative binding of two cAMP molecules to each PKAR subunit. The PKA orthologue of *T. brucei* is the first PKA-related kinase identified, which is completely uncoupled from the second messenger cAMP. Residues mediating specific binding of cAMP to the cyclic nucleotide-binding domains (CNB domains) of PKAR subunits are located within the phosphate binding cassettes (PBCs) (Su et al., 1995; Diller et al., 2001; Berman et al., 2005). Figure 8 shows an alignment of the PBC core sequences of PKARs from the three kinetoplastids *T. brucei*, *T. cruzi* and *L. donovani* with orthologues from other unicellular eukaryotes as well as human PKARI alpha and PKARII alpha. The signature sequence of the PBC domain, which is shown below the alignment, has been determined by Canaves and Taylor (2002) and has been postulated to be characteristic of the PKAR family and sufficient to distinguish it from other cNMP-binding proteins. Although the PBC domains of the kinetoplastid PKAR orthologues show a high overall sequence conservation with PKARs of other organisms, there are a few amino acid deviations (Figure 8). Most importantly, the arginine highlighted in green in Figure 8, which forms specific hydrogen bonds with the O1P phosphate of cAMP (Su et al., 1995; Diller et al., 2001; Berman et al., 2005) and has been shown to be essential for phosphate binding (Bubis et al., 1988; Neitzel et al., 1991), is not conserved, indicating that kinetoplastid PKARs might not be able to specifically bind cNMPs. In contrast, the glutamate highlighted in blue, is responsible for interaction with the 2'OH group of the ribose ring and is conserved in kinetoplastid PKARs, suggesting that nucleoside binding is possible. These structural features are in agreement with the results obtained for *T. brucei* PKA *in vitro* as well as *in vivo*. Since the arginine critical for phosphate binding is not conserved in any of the three kinetoplastid PKARs analyzed (see Figure 8 and TriTrypDB), all orthologues of this ancient, early branching group of eukaryotes are likely to show a similar behavior in terms of cNMP responsiveness.

Dipyridamole, a known inhibitor of mammalian PDEs (Ghosh et al., 2009), weakly inhibits *T. brucei* PDEB1 and PDEB2 (Rascon et al., 2002; Zoraghi and Seebeck, 2002) resulting in a ~2-fold increase in the intracellular cAMP concentration (Zoraghi et al., 2001; Laxman et al., 2006). Since *T. brucei* PKA is not responsive to cAMP, it came as a surprise that dipyridamole activated the kinase *in vivo*. The absence of activation *in vitro* suggests an indirect mechanism. As dipyridamole is known to interfere with adenosine signaling in mammalian cells (Pfleger et al., 1969; Klabunde, 1983; Gibbs and Lip, 1998), it might have similar effects in *T. brucei*. In fact, dipyridamole has been shown to inhibit adenosine uptake in BSFs (James and Born, 1980) and PCFs (Al-Salabi et al., 2007). Hence, perturbation of the parasite's nucleoside metabolism might change the levels of an alternative second messenger-like molecule. This hypothesis is supported by the indirect inhibition of *T. brucei* PKA by the adenosine derivatives 8-pCPT-adenosine and 8-pCPT-2'O-me-adenosine.

4. Activation of *T. brucei* PKA

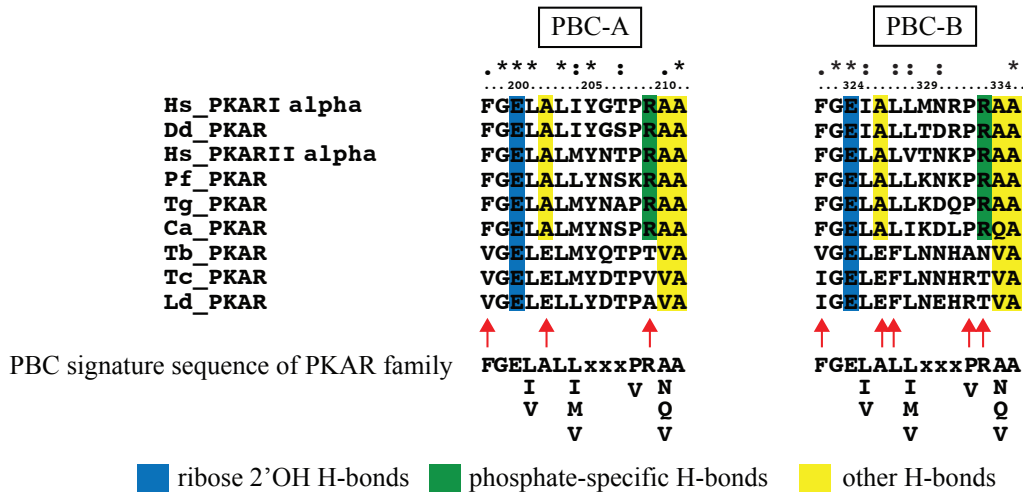


Figure 8: Alignment of PBC core sequences from different PKAR orthologues.

PBC core sequences of PKAR orthologues from *Homo sapiens* (Hs_PKAR alpha, accession P10644; Hs_PKARII alpha, accession P13861), *Dictyostelium discoideum* (Dd_PKAR, accession P05987), *Plasmodium falciparum* (Pf_PKAR, accession Q8T323), *Toxoplasma gondii* (Tg_PKAR, accession Q9BMY7), *Candida albicans* (Ca_PKAR, accession Q9HEW1), *Trypanosoma brucei* (Tb_PKAR, accession Tb427tmp.02.2210), *Trypanosoma cruzi* (Tc_PKAR, accession TcCLB.506227.150) and *Leishmania donovani* (Ld_PKAR, accession LdBPK_130160.1) were obtained from UniProt (www.uniprot.org) or TritypDB (www.tritypdb.org), respectively. Multiple sequence alignment was performed using clustalW2 (<http://www.ebi.ac.uk/Tools/msa/clustalw2/>) with standard settings, and conservation is shown above the alignment according to the clustalW2 standard key. The numbering above the alignment refers to Hs_PKAR α . The signature sequence of PBC domains of the PKAR family determined by Canaves and Taylor (2002) is shown below the alignment. Amino acids of the kinetoplastid PKAR orthologues deviating from the signature motif are marked by red arrows. Residues mediating interaction with the 2'OH group of the ribose ring are highlighted in blue, the arginine important for specific phosphate binding is shown in green, and amino acids forming H-bonds to additional sites are colored in yellow.

In addition to the apparent absence of a cAMP-dependent protein kinase, none of the alternative cAMP effector proteins identified in other organisms like Epac or cyclic nucleotide gated ion channels are encoded by the *T. brucei* genome. However, just recently, an alternative cAMP signaling pathway has been discovered in the parasite: CARP1, a putative cAMP receptor protein, has been identified by a whole genome RNAi library screen selecting for cells resistant to elevated intracellular cAMP levels induced by treatment with CpdA (Gould et al., 2013). Interestingly, CARP1 is kinetoplastid-specific. This fits well into a model in which CARP1 has replaced PKA as primary cAMP acceptor and serves as entry point into a novel, kinetoplastid-specific cAMP-signaling pathway. In contrast to the unconventional upstream signaling pathway of *T. brucei* PKA, a strong overlap of downstream processes regulated by the kinase at the transcriptional level with processes regulated by PKAs of other organisms was observed. Transcriptional profiling revealed a predominant role of the parasite kinase in regulation of metabolic processes, translation, protein folding, and transport, reminiscent of its functions in many other eukaryotes ranging from protozoa over fungi to mammals (Tash and Means, 1982; Brokaw, 1987; Leclerc et al., 1996; Robertson et al., 2000; Jones et al., 2003; Zhang et al., 2003; Harcus et al., 2004; Hu et al., 2007; Baker, 2011; Wurtz et al., 2011).

The compounds 8-pCPT-cAMP as well as 8-pCPT-2'O-me-adenosine/cAMP have been shown to be effective inducers of *in vitro* stumpy formation in *T. brucei* (Vassella et al., 1997; Laxman et al., 2006). In the present study, we could show that 8-pCPT-adenosine and 8-pCPT-2'O-me-adenosine are indirect inhibitors of *in vivo* PKA activity. In addition, their anti-proliferative effects are at least partially mediated by PKA, since the *PKAR* deletion mutant was ~2-fold and ~4-fold, respectively, more resistant compared to wild type cells. A similar increase in resistance was observed upon treatment with 8-pCPT-cAMP and 8-pCPT-2'O-me-cAMP, compounds intracellularly hydrolyzed by PDEs to the respective adenosine derivatives (Laxman et al., 2006). Consistent with this, a recent study has identified PKAR by a whole-genome RNAi library screen selecting for cells resistant to 8-pCPT-cAMP (Mony et al., 2014). Whether *T. brucei* PKAR plays a role in slender to stumpy differentiation is yet an open question.

Toyocamycin and sangivamycin, direct activators of *T. brucei* PKA identified by the current study, are natural antibiotics, produced by certain strains of *Streptomyces*. However, it is highly unlikely that 7-deazapurines are endogenous, natural activators of *T. brucei* PKA since there is no indication for the presence of any enzyme involved in the pathway synthesizing the critical precursor preQ0 in the parasite (McCarty and Bandarian, 2008) (blastp using BLAST+ version 2.2.8 for ToyD, ToyB, ToyC and ToyM sequences from *Streptomyces rimosus*; HMMER search for the profile of ToyB using version 3.1b1; as a reference the proteome of *T. brucei* strain *TREU927*, release 8.0 was downloaded from TriTrypDB).

Most importantly, toyocamycin is an excellent experimental tool for deciphering the PKA downstream signaling pathway in *T. brucei* at the transcriptional and translational level as well as at the level of substrate phosphorylation.

7-deazapurine analogues are known to have pleiotropic targets in various cell types by interfering with cellular processes involving adenine nucleosides and nucleotides, such as inhibition of different kinases (Saffer and Glazer, 1981; Loomis and Bell, 1988; Osada et al., 1989; Palczewski et al., 1990; Bobek and Bloch, 1994) or inhibition of DNA, RNA and protein synthesis (Cohen and Glazer, 1985). Sangivamycin and its derivatives show cytotoxicity against cancer cells (Komi et al., 2007; Lee and Jung, 2007; Cappellini et al., 2009; Kang et al., 2010; Dolloff et al., 2012; Rayala et al., 2014; Wakao et al., 2014) as well as anti-viral activity (Bergstrom et al., 1984; Turk et al., 1987) but do not produce toxicity in humans at maximally tolerated doses (Cavins et al., 1967; Hardesty et al., 1974; Ohno et al., 2001; Komi et al., 2007; Lee and Jung, 2007). Since growth inhibition with EC₅₀ values in the sub-micromolar range was observed upon treatment of *T. brucei* BSF cells with the 7-deazapurine analogues toyocamycin, sangivamycin, 5-I-tubercidin and 5-Br-tubercidin, the potential of 7-deazapurine derivatives for anti-trypanosomal therapy should be exploited in future studies. Yet, the major target of these compounds in *T. brucei* is not PKA, since their anti-proliferative effects were not mediated by the kinase. Only upon treatment with sangivamycin, a two-fold increase in the EC₅₀ for growth inhibition was observed in the *PKAR* deletion mutant compared to wild type cells. Nevertheless, *T. brucei* PKA qualifies as good drug target due to the following aspects: 1) the enzyme is essential; 2) the kinase has ligand-binding domains, which can be exploited in designing specific activators or inhibitors, and which significantly differ from orthologous proteins of the mammalian host; and 3) a compound has been identified, which binds to and activates *T. brucei* PKA in the lower

4. Activation of *T. brucei* PKA

nanomolar range. 7-deazapurine analogues might represent promising leads to design specific activators or inhibitors of *T. brucei* PKA with anti-trypanosomal activity. Due to the sequence conservation of the PBC domains of the kinetoplastid PKAR orthologues, compounds specifically targeting *T. brucei* PKAR are also likely to target the *T. cruzi* and *L. donovani* orthologues. Hence, a drug with the capability to be used against HAT by specifically targeting PKA could potentially also be used for treatment of Chagas disease and Leishmaniasis.

References

- Adams, J.A., McGlone, M.L., Gibson, R., and Taylor, S.S. (1995). Phosphorylation modulates catalytic function and regulation in the cAMP-dependent protein kinase. *Biochemistry* 34, 2447-2454.
- Al-Salabi, M.I., Wallace, L.J., Luscher, A., Maser, P., Candlish, D., Rodenko, B., Gould, M.K., Jabeen, I., Ajith, S.N., and de Koning, H.P. (2007). Molecular interactions underlying the unusually high adenosine affinity of a novel *Trypanosoma brucei* nucleoside transporter. *Mol Pharmacol* 71, 921-929.
- Alibu, V.P., Storm, L., Haile, S., Clayton, C., and Horn, D. (2005). A doubly inducible system for RNA interference and rapid RNAi plasmid construction in *Trypanosoma brucei*. *Mol Biochem Parasitol* 139, 75-82.
- Alsford, S., Turner, D.J., Obado, S.O., Sanchez-Flores, A., Glover, L., Berriman, M., Hertz-Fowler, C., and Horn, D. (2011). High-throughput phenotyping using parallel sequencing of RNA interference targets in the African trypanosome. *Genome Res* 21, 915-924.
- Amieux, P.S., Cummings, D.E., Motamed, K., Brandon, E.P., Wailes, L.A., Le, K., Idzerda, R.L., and McKnight, G.S. (1997). Compensatory regulation of R1alpha protein levels in protein kinase A mutant mice. *J Biol Chem* 272, 3993-3998.
- Anders, S., and Huber, W. (2010). Differential expression analysis for sequence count data. *Genome Biol* 11, R106.
- Bachmaier, S., and Boshart, M. (2013). Kinetoplastid AGC Kinases. In *Protein Phosphorylation in Parasites* (Wiley-VCH Verlag GmbH & Co. KGaA), pp. 99-122.
- Baker, D.A. (2011). Cyclic nucleotide signalling in malaria parasites. *Cell Microbiol* 13, 331-339.
- Bastin, P., Bagherzadeh, Z., Matthews, K.R., and Gull, K. (1996). A novel epitope tag system to study protein targeting and organelle biogenesis in *Trypanosoma brucei*. *Mol Biochem Parasitol* 77, 235-239.
- Benjamini, Y., and Hochberg, Y. (1995). Controlling the False Discovery Rate: A Practical and Powerful Approach to Multiple Testing. *Journal of the Royal Statistical Society Series B (Methodological)* 57, 289-300.
- Bergstrom, D.E., Brattesani, A.J., Ogawa, M.K., Reddy, P.A., Schweickert, M.J., Balzarini, J., and De Clercq, E. (1984). Antiviral activity of C-5 substituted tubercidin analogues. *J Med Chem* 27, 285-292.
- Berman, H.M., Ten Eyck, L.F., Goodsell, D.S., Haste, N.M., Kornev, A., and Taylor, S.S. (2005). The cAMP binding domain: an ancient signaling module. *Proc Natl Acad Sci U S A* 102, 45-50.
- Biebinger, S., Wirtz, L.E., Lorenz, P., and Clayton, C. (1997). Vectors for inducible expression of toxic gene products in bloodstream and procyclic *Trypanosoma brucei*. *Mol Biochem Parasitol* 85, 99-112.
- Bobek, M., and Bloch, A. (1994). Relationship Between the Structure of Sangivamycin-Derived Nucleosides and Their Effect on Leukemic Cell Growth and on Protein Kinase A and C Activity. *Nucleosides and Nucleotides* 13, 429-435.

4. Activation of *T. brucei* PKA

- Bockmuhl, D.P., and Ernst, J.F. (2001). A potential phosphorylation site for an A-type kinase in the Efg1 regulator protein contributes to hyphal morphogenesis of *Candida albicans*. *Genetics* 157, 1523-1530.
- Brenndorfer, M., and Boshart, M. (2010). Selection of reference genes for mRNA quantification in *Trypanosoma brucei*. *Mol Biochem Parasitol* 172, 52-55.
- Bringaud, F., Peris, M., Zen, K.H., and Simpson, L. (1995). Characterization of two nuclear-encoded protein components of mitochondrial ribonucleoprotein complexes from *Leishmania tarentolae*. *Mol Biochem Parasitol* 71, 65-79.
- Brokaw, C.J. (1987). Regulation of sperm flagellar motility by calcium and cAMP-dependent phosphorylation. *Journal of Cellular Biochemistry* 35, 175-184.
- Bubis, J., Neitzel, J.J., Saraswat, L.D., and Taylor, S.S. (1988). A point mutation abolishes binding of cAMP to site A in the regulatory subunit of cAMP-dependent protein kinase. *J Biol Chem* 263, 9668-9673.
- Burton, K.A., Johnson, B.D., Hausken, Z.E., Westenbroek, R.E., Idzerda, R.L., Scheuer, T., Scott, J.D., Catterall, W.A., and McKnight, G.S. (1997). Type II regulatory subunits are not required for the anchoring-dependent modulation of Ca²⁺ channel activity by cAMP-dependent protein kinase. *Proc Natl Acad Sci U S A* 94, 11067-11072.
- Butt, E., Abel, K., Krieger, M., Palm, D., Hoppe, V., Hoppe, J., and Walter, U. (1994). cAMP- and cGMP-dependent protein kinase phosphorylation sites of the focal adhesion vasodilator-stimulated phosphoprotein (VASP) *in vitro* and in intact human platelets. *J Biol Chem* 269, 14509-14517.
- Canaves, J.M., and Taylor, S.S. (2002). Classification and phylogenetic analysis of the cAMP-dependent protein kinase regulatory subunit family. *J Mol Evol* 54, 17-29.
- Cappellini, A., Chiarini, F., Ognibene, A., McCubrey, J.A., and Martelli, A.M. (2009). The cyclin-dependent kinase inhibitor roscovitine and the nucleoside analog sangivamycin induce apoptosis in caspase-3 deficient breast cancer cells independent of caspase mediated P-glycoprotein cleavage: implications for therapy of drug resistant breast cancers. *Cell Cycle* 8, 1421-1425.
- Cavins, J.A., Hall, T.C., Olson, K.B., Khung, C.L., Horton, J., Colsky, J., and Shadduck, R.K. (1967). Initial toxicity study of sangivamycin (NSC-65346). *Cancer Chemother Rep* 51, 197-200.
- Cheek, S., Zhang, H., and Grishin, N.V. (2002). Sequence and structure classification of kinases. *J Mol Biol* 320, 855-881.
- Cohen, M.B., and Glazer, R.I. (1985). Comparison of the cellular and RNA-dependent effects of sangivamycin and toyocamycin in human colon carcinoma cells. *Mol Pharmacol* 27, 349-355.
- Cross, G.A., and Manning, J.C. (1973). Cultivation of *Trypanosoma brucei* spp. in semi-defined and defined media. *Parasitology* 67, 315-331.
- Dalton, G.D., and Dewey, W.L. (2006). Protein kinase inhibitor peptide (PKI): a family of endogenous neuropeptides that modulate neuronal cAMP-dependent protein kinase function. *Neuropeptides* 40, 23-34.

- de Koning, H.P., Gould, M.K., Sterk, G.J., Tenor, H., Kunz, S., Luginbuehl, E., and Seebeck, T. (2012). Pharmacological validation of *Trypanosoma brucei* phosphodiesterases as novel drug targets. *J Infect Dis* 206, 229-237.
- de Koning, H.P., and Jarvis, S.M. (1999). Adenosine transporters in bloodstream forms of *Trypanosoma brucei* brucei: substrate recognition motifs and affinity for trypanocidal drugs. *Mol Pharmacol* 56, 1162-1170.
- Diller, T.C., Madhusudan, Xuong, N.H., and Taylor, S.S. (2001). Molecular basis for regulatory subunit diversity in cAMP-dependent protein kinase: crystal structure of the type II beta regulatory subunit. *Structure* 9, 73-82.
- Dolloff, N.G., Allen, J.E., Dicker, D.T., Aqui, N., Vogl, D., Malysz, J., Talamo, G., and El-Deiry, W.S. (2012). Sangivamycin-like molecule 6 exhibits potent anti-multiple myeloma activity through inhibition of cyclin-dependent kinase-9. *Mol Cancer Ther* 11, 2321-2330.
- Dulin, N.O., Niu, J., Browning, D.D., Ye, R.D., and Voyno-Yasenetskaya, T. (2001). Cyclic AMP-independent activation of protein kinase A by vasoactive peptides. *J Biol Chem* 276, 20827-20830.
- Duncan, F.E., Moss, S.B., and Williams, C.J. (2006). Knockdown of the cAMP-dependent protein kinase (PKA) Type Ialpha regulatory subunit in mouse oocytes disrupts meiotic arrest and results in meiotic spindle defects. *Dev Dyn* 235, 2961-2968.
- Eddy, S.R. (1998). Profile hidden Markov models. *Bioinformatics* 14, 755-763.
- Geiser, F., Luscher, A., de Koning, H.P., Seebeck, T., and Maser, P. (2005). Molecular pharmacology of adenosine transport in *Trypanosoma brucei*: P1/P2 revisited. *Mol Pharmacol* 68, 589-595.
- Gesellchen, F., Bertinetti, O., and Herberg, F.W. (2006). Analysis of posttranslational modifications exemplified using protein kinase A. *Biochim Biophys Acta* 1764, 1788-1800.
- Ghosh, R., Sawant, O., Ganpathy, P., Pitre, S., and Kadam, V.J. (2009). Phosphodiesterase inhibitors; their role and implications. *International Journal of PharmTech Research* 1, 1148-1160.
- Gibbs, C.R., and Lip, G.Y. (1998). Do we still need dipyridamole? *Br J Clin Pharmacol* 45, 323-328.
- Glass, D.B., Cheng, H.C., Mende-Mueller, L., Reed, J., and Walsh, D.A. (1989). Primary structural determinants essential for potent inhibition of cAMP-dependent protein kinase by inhibitory peptides corresponding to the active portion of the heat-stable inhibitor protein. *J Biol Chem* 264, 8802-8810.
- Gould, M.K., Bachmaier, S., Ali, J.A., Alsford, S., Tagoe, D.N., Munday, J.C., Schnauffer, A.C., Horn, D., Boshart, M., and de Koning, H.P. (2013). Cyclic AMP effectors in African trypanosomes revealed by genome-scale RNA interference library screening for resistance to the phosphodiesterase inhibitor CpdA. *Antimicrob Agents Chemother* 57, 4882-4893.
- Haffner, C., Jarchau, T., Reinhard, M., Hoppe, J., Lohmann, S.M., and Walter, U. (1995). Molecular cloning, structural analysis and functional expression of the proline-rich focal adhesion and microfilament-associated protein VASP. *EMBO J* 14, 19-27.
- Halbrugge, M., and Walter, U. (1989). Purification of a vasodilator-regulated phosphoprotein from human platelets. *Eur J Biochem* 185, 41-50.
- Hanks, S.K., Quinn, A.M., and Hunter, T. (1988). The protein kinase family: conserved features and deduced phylogeny of the catalytic domains. *Science* 241, 42-52.

4. Activation of *T. brucei* PKA

- Harcus, D., Nantel, A., Marcil, A., Rigby, T., and Whiteway, M. (2004). Transcription profiling of cyclic AMP signaling in *Candida albicans*. *Mol Biol Cell* 15, 4490-4499.
- Hardesty, C.T., Chaney, N.A., Waravdekar, V.S., and Mead, J.A. (1974). The disposition of the antitumor agent, sangivamycin, in mice. *Cancer Res* 34, 1005-1009.
- Harris, T.E., Persaud, S.J., and Jones, P.M. (1997). Pseudosubstrate inhibition of cyclic AMP-dependent protein kinase in intact pancreatic islets: effects on cyclic AMP-dependent and glucose-dependent insulin secretion. *Biochem Biophys Res Commun* 232, 648-651.
- Hastie, C.J., McLauchlan, H.J., and Cohen, P. (2006). Assay of protein kinases using radiolabeled ATP: a protocol. *Nat Protoc* 1, 968-971.
- Herberg, F.W., Taylor, S.S., and Dostmann, W.R. (1996). Active site mutations define the pathway for the cooperative activation of cAMP-dependent protein kinase. *Biochemistry* 35, 2934-2942.
- Herberg, F.W., Zimmermann, B., McGlone, M., and Taylor, S.S. (1997). Importance of the A-helix of the catalytic subunit of cAMP-dependent protein kinase for stability and for orienting subdomains at the cleft interface. *Protein Sci* 6, 569-579.
- Hochstrasser, M., and Nelson, D.L. (1989). Cyclic AMP-dependent protein kinase in *Paramecium tetraurelia*. Its purification and the production of monoclonal antibodies against both subunits. *J Biol Chem* 264, 14510-14518.
- Hu, G., Steen, B.R., Lian, T., Sham, A.P., Tam, N., Tangen, K.L., and Kronstad, J.W. (2007). Transcriptional regulation by protein kinase A in *Cryptococcus neoformans*. *PLoS Pathog* 3, e42.
- Huang, D., Hubbard, C.J., and Jungmann, R.A. (1995). Lactate dehydrogenase A subunit messenger RNA stability is synergistically regulated via the protein kinase A and C signal transduction pathways. *Mol Endocrinol* 9, 994-1004.
- Huang, D.W., Sherman, B.T., and Lempicki, R.A. (2009a). Bioinformatics enrichment tools: paths toward the comprehensive functional analysis of large gene lists. *Nucleic Acids Res* 37, 1-13.
- Huang, D.W., Sherman, B.T., and Lempicki, R.A. (2009b). Systematic and integrative analysis of large gene lists using DAVID bioinformatics resources. *Nat Protoc* 4, 44-57.
- James, D.M., and Born, G.V. (1980). Uptake of purine bases and nucleosides in African trypanosomes. *Parasitology* 81, 383-393.
- Jones, D.L., Petty, J., Hoyle, D.C., Hayes, A., Ragni, E., Popolo, L., Oliver, S.G., and Stateva, L.I. (2003). Transcriptome profiling of a *Saccharomyces cerevisiae* mutant with a constitutively activated Ras/cAMP pathway. *Physiol Genomics* 16, 107-118.
- Jones, N.G., Thomas, E.B., Brown, E., Dickens, N.J., Hammarton, T.C., and Mottram, J.C. (2014). Regulators of *Trypanosoma brucei* cell cycle progression and differentiation identified using a kinome-wide RNAi screen. *PLoS Pathog* 10, e1003886.
- Kal, A.J., van Zonneveld, A.J., Benes, V., van den Berg, M., Koerkamp, M.G., Albermann, K., Strack, N., Ruijter, J.M., Richter, A., Dujon, B., *et al.* (1999). Dynamics of gene expression revealed by comparison of serial analysis of gene expression transcript profiles from yeast grown on two different carbon sources. *Mol Biol Cell* 10, 1859-1872.

- Kang, J., Lee, D.K., and Lee, C.H. (2010). Cell cycle arrest and cytochrome c-mediated apoptotic induction in human lung cancer A549 cells by MCS-C2, an analogue of sangivamycin. *J Microbiol Biotechnol* 20, 433-437.
- Kemp, B.E., Benjamini, E., and Krebs, E.G. (1976). Synthetic hexapeptide substrates and inhibitors of 3':5'-cyclic AMP-dependent protein kinase. *Proc Natl Acad Sci U S A* 73, 1038-1042.
- Kemp, B.E., Graves, D.J., Benjamini, E., and Krebs, E.G. (1977). Role of multiple basic residues in determining the substrate specificity of cyclic AMP-dependent protein kinase. *J Biol Chem* 252, 4888-4894.
- Kim, C., Xuong, N.H., and Taylor, S.S. (2005). Crystal structure of a complex between the catalytic and regulatory (RIalpha) subunits of PKA. *Science* 307, 690-696.
- Kim, C., Cheng, C.Y., Saldanha, S.A., and Taylor, S.S. (2007). PKA-I holoenzyme structure reveals a mechanism for cAMP-dependent activation. *Cell* 130, 1032-1043.
- Kiriyama, H., Nanmori, T., Hari, K., Matsuoka, D., Fukami, Y., Kikkawa, U., and Yasuda, T. (1999). Identification of the catalytic subunit of cAMP-dependent protein kinase from the photosynthetic flagellate, *Euglena gracilis* Z. *FEBS Lett* 450, 95-100.
- Kirschner, L.S., Yin, Z., Jones, G.N., and Mahoney, E. (2009). Mouse models of altered protein kinase A signaling. *Endocr Relat Cancer* 16, 773-793.
- Klabunde, R.E. (1983). Effects of dipyridamole on postischemic vasodilation and extracellular adenosine. *Am J Physiol* 244, H273-280.
- Kohl, L., Sherwin, T., and Gull, K. (1999). Assembly of the paraflagellar rod and the flagellum attachment zone complex during the *Trypanosoma brucei* cell cycle. *J Eukaryot Microbiol* 46, 105-109.
- Komi, Y., Ohno, O., Suzuki, Y., Shimamura, M., Shimokado, K., Umezawa, K., and Kojima, S. (2007). Inhibition of tumor angiogenesis by targeting endothelial surface ATP synthase with sangivamycin. *Jpn J Clin Oncol* 37, 867-873.
- Kramer, S., Klockner, T., Selmayr, M., and Boshart, M. (2007). Interstrain sequence comparison, transcript map and clonal genomic rearrangement of a 28 kb locus on chromosome 9 of *Trypanosoma brucei*. *Mol Biochem Parasitol* 151, 129-132.
- LaCount, D.J., Barrett, B., and Donelson, J.E. (2002). *Trypanosoma brucei* FLA1 is required for flagellum attachment and cytokinesis. *J Biol Chem* 277, 17580-17588.
- Lastauskiene, E., Zinkeviciene, A., and Citavicius, D. (2014). Ras/PKA signal transduction pathway participates in the regulation of *Saccharomyces cerevisiae* cell apoptosis in an acidic environment. *Biotechnol Appl Biochem* 61, 3-10.
- Laxman, S., and Beavo, J.A. (2007). Cyclic nucleotide signaling mechanisms in trypanosomes: possible targets for therapeutic agents. *Mol Interv* 7, 203-215.
- Laxman, S., Riechers, A., Sadilek, M., Schwede, F., and Beavo, J.A. (2006). Hydrolysis products of cAMP analogs cause transformation of *Trypanosoma brucei* from slender to stumpy-like forms. *Proc Natl Acad Sci U S A* 103, 19194-19199.

4. Activation of *T. brucei* PKA

- Leclerc, P., de Lamirande, E., and Gagnon, C. (1996). Cyclic adenosine 3',5'-monophosphate-dependent regulation of protein tyrosine phosphorylation in relation to human sperm capacitation and motility. *Biol Reprod* *55*, 684-692.
- Lee, S.A., and Jung, M. (2007). The nucleoside analog sangivamycin induces apoptotic cell death in breast carcinoma MCF7/adriamycin-resistant cells via protein kinase Cdelta and JNK activation. *J Biol Chem* *282*, 15271-15283.
- Letunic, I., Copley, R.R., Schmidt, S., Ciccarelli, F.D., Doerks, T., Schultz, J., Ponting, C.P., and Bork, P. (2004). SMART 4.0: towards genomic data integration. *Nucleic Acids Res* *32*, D142-144.
- Loomis, C.R., and Bell, R.M. (1988). Sangivamycin, a nucleoside analogue, is a potent inhibitor of protein kinase C. *J Biol Chem* *263*, 1682-1692.
- Mäser, P., Vogel, D., Schmid, C., Raz, B., and Kaminsky, R. (2001). Identification and characterization of trypanocides by functional expression of an adenosine transporter from *Trypanosoma brucei* in yeast. *J Mol Med (Berl)* *79*, 121-127.
- Matthias, P., Muller, M.M., Schreiber, E., Rusconi, S., and Schaffner, W. (1989). Eukaryotic expression vectors for the analysis of mutant proteins. *Nucleic Acids Res* *17*, 6418.
- McCarty, R.M., and Bandarian, V. (2008). Deciphering deazapurine biosynthesis: pathway for pyrrolopyrimidine nucleosides toyocamycin and sangivamycin. *Chem Biol* *15*, 790-798.
- Mizunuma, M., Tsubakiyama, R., Ogawa, T., Shitamukai, A., Kobayashi, Y., Inai, T., Kume, K., and Hirata, D. (2013). Ras/cAMP-dependent protein kinase (PKA) regulates multiple aspects of cellular events by phosphorylating the Whi3 cell cycle regulator in budding yeast. *J Biol Chem* *288*, 10558-10566.
- Mony, B.M., MacGregor, P., Ivens, A., Rojas, F., Cowton, A., Young, J., Horn, D., and Matthews, K. (2014). Genome-wide dissection of the quorum sensing signalling pathway in *Trypanosoma brucei*. *Nature* *505*, 681-685.
- Mutzel, R., Lacombe, M.L., Simon, M.N., de Gunzburg, J., and Veron, M. (1987). Cloning and cDNA sequence of the regulatory subunit of cAMP-dependent protein kinase from *Dictyostelium discoideum*. *Proc Natl Acad Sci U S A* *84*, 6-10.
- Neitzel, J.J., Dostmann, W.R., and Taylor, S.S. (1991). Role of MgATP in the activation and reassociation of cAMP-dependent protein kinase I: consequences of replacing the essential arginine in cAMP binding site A. *Biochemistry* *30*, 733-739.
- Nett, I.R., Martin, D.M., Miranda-Saavedra, D., Lamont, D., Barber, J.D., Mehlert, A., and Ferguson, M.A. (2009). The phosphoproteome of bloodstream form *Trypanosoma brucei*, causative agent of African sleeping sickness. *Mol Cell Proteomics* *8*, 1527-1538.
- Nilsson, D., Gunasekera, K., Mani, J., Osteras, M., Farinelli, L., Baerlocher, L., Roditi, I., and Ochsenreiter, T. (2010). Spliced leader trapping reveals widespread alternative splicing patterns in the highly dynamic transcriptome of *Trypanosoma brucei*. *PLoS Pathog* *6*, e1001037.
- Oberholzer, M., Marti, G., Baresic, M., Kunz, S., Hemphill, A., and Seebeck, T. (2007). The *Trypanosoma brucei* cAMP phosphodiesterases TbrPDEB1 and TbrPDEB2: flagellar enzymes that are essential for parasite virulence. *FASEB* *21*, 720-731.

- Ogreid, D., and Doskeland, S.O. (1981a). The kinetics of association of cyclic AMP to the two types of binding sites associated with protein kinase II from bovine myocardium. *FEBS Lett* 129, 287-292.
- Ogreid, D., and Doskeland, S.O. (1981b). The kinetics of the interaction between cyclic AMP and the regulatory moiety of protein kinase II. Evidence for interaction between the binding sites for cyclic AMP. *FEBS Lett* 129, 282-286.
- Ohno, O., Shima, Y., Ikeda, Y., Kondo, S.I., Kato, K., Toi, M., and Umezawa, K. (2001). Selective growth inhibition by sangivamycin of human umbilical vein endothelial cells. *Int J Oncol* 18, 1009-1015.
- Olmsted, J.B. (1981). Affinity purification of antibodies from diazotized paper blots of heterogeneous protein samples. *J Biol Chem* 256, 11955-11957.
- Osada, H., Sonoda, T., Tsunoda, K., and Isono, K. (1989). A new biological role of sangivamycin; inhibition of protein kinases. *J Antibiot (Tokyo)* 42, 102-106.
- Palczewski, K., Kahn, N., and Hargrave, P.A. (1990). Nucleoside inhibitors of rhodopsin kinase. *Biochemistry* 29, 6276-6282.
- Pfleger, K., Niederau, D., and Volkmer, I. (1969). Ein Beitrag zum Wirkungsmechanismus von Dipyridamol: Hemmung der Adenosinaufnahme in Erythrocyten durch Dipyridamol. *Naunyn-Schmiedebergs Archiv für Pharmakologie* 265, 118-130.
- Primpke, G., Iassonidou, V., Nellen, W., and Wetterauer, B. (2000). Role of cAMP-dependent protein kinase during growth and early development of *Dictyostelium discoideum*. *Dev Biol* 221, 101-111.
- Rall, T.W., and Sutherland, E.W. (1958). Formation of a cyclic adenine ribonucleotide by tissue particles. *J Biol Chem* 232, 1065-1076.
- Rascon, A., Soderling, S.H., Schaefer, J.B., and Beavo, J.A. (2002). Cloning and characterization of a cAMP-specific phosphodiesterase (TbPDE2B) from *Trypanosoma brucei*. *Proc Natl Acad Sci U S A* 99, 4714-4719.
- Rayala, R., Theard, P., Ortiz, H., Yao, S., Young, J.D., Balzarini, J., Robins, M.J., and Wnuk, S.F. (2014). Synthesis of Purine and 7-Deazapurine Nucleoside Analogues of 6-N-(4-Nitrobenzyl)adenosine; Inhibition of Nucleoside Transport and Proliferation of Cancer Cells. *ChemMedChem*.
- Ringheim, G.E., Saraswat, L.D., Bubis, J., and Taylor, S.S. (1988). Deletion of cAMP-binding site B in the regulatory subunit of cAMP-dependent protein kinase alters the photoaffinity labeling of site A. *J Biol Chem* 263, 18247-18252.
- Robertson, L.S., Causton, H.C., Young, R.A., and Fink, G.R. (2000). The yeast A kinases differentially regulate iron uptake and respiratory function. *Proc Natl Acad Sci U S A* 97, 5984-5988.
- Saffer, J.D., and Glazer, R.I. (1981). Inhibition of histone H1 phosphorylation by sangivamycin and other pyrrolopyrimidine analogues. *Mol Pharmacol* 20, 211-217.
- Salmon, D., Bachmaier, S., Krumbholz, C., Kador, M., Gossmann, J.A., Uzureau, P., Pays, E., and Boshart, M. (2012a). Cytokinesis of *Trypanosoma brucei* bloodstream forms depends on

4. Activation of *T. brucei* PKA

- expression of adenylyl cyclases of the ESAG4 or ESAG4-like subfamily. *Mol Microbiol* *84*, 225-242.
- Salmon, D., Vanwalleghem, G., Morias, Y., Denoëud, J., Krumbholz, C., Lhomme, F., Bachmaier, S., Kador, M., Gossmann, J., Dias, F.B., *et al.* (2012b). Adenylate cyclases of *Trypanosoma brucei* inhibit the innate immune response of the host. *Science* *337*, 463-466.
- Saran, S., Meima, M.E., Alvarez-Curto, E., Weening, K.E., Rozen, D.E., and Schaap, P. (2002). cAMP signaling in *Dictyostelium*. Complexity of cAMP synthesis, degradation and detection. *J Muscle Res Cell Motil* *23*, 793-802.
- Schimanski, B., Nguyen, T.N., and Gunzl, A. (2005). Highly efficient tandem affinity purification of trypanosome protein complexes based on a novel epitope combination. *Eukaryot Cell* *4*, 1942-1950.
- Scholten, A., Aye, T.T., and Heck, A.J. (2008). A multi-angular mass spectrometric view at cyclic nucleotide dependent protein kinases: *in vivo* characterization and structure/function relationships. *Mass Spectrom Rev* *27*, 331-353.
- Schultz, J., Milpetz, F., Bork, P., and Ponting, C.P. (1998). SMART, a simple modular architecture research tool: identification of signaling domains. *Proc Natl Acad Sci U S A* *95*, 5857-5864.
- Schumann Burkard, G., Jutzi, P., and Roditi, I. (2011). Genome-wide RNAi screens in bloodstream form trypanosomes identify drug transporters. *Mol Biochem Parasitol* *175*, 91-94.
- Sechi, A.S., and Wehland, J. (2004). ENA/VASP proteins: multifunctional regulators of actin cytoskeleton dynamics. *Front Biosci* *9*, 1294-1310.
- Seebeck, T., Gong, K., Kunz, S., Schaub, R., Shalaby, T., and Zoraghi, R. (2001). cAMP signalling in *Trypanosoma brucei*. *Int J Parasitol* *31*, 491-498.
- Seebeck, T., Schaub, R., and Johnner, A. (2004). cAMP signalling in the kinetoplastid protozoa. *Curr Mol Med* *4*, 585-599.
- Seidler, J., Adal, M., Kubler, D., Bossemeyer, D., and Lehmann, W.D. (2009). Analysis of autophosphorylation sites in the recombinant catalytic subunit alpha of cAMP-dependent kinase by nano-UPLC-ESI-MS/MS. *Anal Bioanal Chem* *395*, 1713-1720.
- Seipel, K., Georgiev, O., and Schaffner, W. (1992). Different activation domains stimulate transcription from remote ('enhancer') and proximal ('promoter') positions. *EMBO J* *11*, 4961-4968.
- Shabb, J.B. (2001). Physiological substrates of cAMP-dependent protein kinase. *Chem Rev* *101*, 2381-2411.
- Shalaby, T., Liniger, M., and Seebeck, T. (2001). The regulatory subunit of a cGMP-regulated protein kinase A of *Trypanosoma brucei*. *Eur J Biochem* *268*, 6197-6206.
- Siman-Tov, M.M., Aly, R., Shapira, M., and Jaffe, C.L. (1996). Cloning from *Leishmania major* of a developmentally regulated gene, c-lpk2, for the catalytic subunit of the cAMP-dependent protein kinase. *Mol Biochem Parasitol* *77*, 201-215.
- Skalhegg, B.S., and Tasken, K. (2000). Specificity in the cAMP/PKA signaling pathway. Differential expression, regulation, and subcellular localization of subunits of PKA. *Front Biosci* *5*, D678-693.

- Sonneborn, A., Bockmuhl, D.P., Gerads, M., Kurpanek, K., Sanglard, D., and Ernst, J.F. (2000). Protein kinase A encoded by TPK2 regulates dimorphism of *Candida albicans*. *Mol Microbiol* 35, 386-396.
- Steichen, J.M., Iyer, G.H., Li, S., Saldanha, S.A., Deal, M.S., Woods, V.L., Jr., and Taylor, S.S. (2010). Global consequences of activation loop phosphorylation on protein kinase A. *J Biol Chem* 285, 3825-3832.
- Steinberg, R.A., Cauthron, R.D., Symcox, M.M., and Shuntoh, H. (1993). Autoactivation of catalytic (C alpha) subunit of cyclic AMP-dependent protein kinase by phosphorylation of threonine 197. *Mol Cell Biol* 13, 2332-2341.
- Stouffer, S.A. (1949). *The American soldier*. Vol. 1: Adjustment during army life (Princeton University Press).
- Su, Y., Dostmann, W.R., Herberg, F.W., Durick, K., Xuong, N.H., Ten Eyck, L., Taylor, S.S., and Varughese, K.I. (1995). Regulatory subunit of protein kinase A: structure of deletion mutant with cAMP binding domains. *Science* 269, 807-813.
- Tamanai, F. (2011). Ras signaling in yeast. *Genes Cancer* 2, 210-215.
- Tash, J.S., and Means, A.R. (1982). Regulation of protein phosphorylation and motility of sperm by cyclic adenosine monophosphate and calcium. *Biol Reprod* 26, 745-763.
- Taylor, S.S., Yang, J., Wu, J., Haste, N.M., Radzio-Andzelm, E., and Anand, G. (2004). PKA: a portrait of protein kinase dynamics. *Biochim Biophys Acta* 1697, 259-269.
- Turk, S.R., Shipman, C., Jr., Nassiri, R., Genzlinger, G., Krawczyk, S.H., Townsend, L.B., and Drach, J.C. (1987). Pyrrolo[2,3-d]pyrimidine nucleosides as inhibitors of human cytomegalovirus. *Antimicrob Agents Chemother* 31, 544-550.
- Urbaniak, M.D., Martin, D.M., and Ferguson, M.A. (2013). Global quantitative SILAC phosphoproteomics reveals differential phosphorylation is widespread between the procyclic and bloodstream form lifecycle stages of *Trypanosoma brucei*. *J Proteome Res* 12, 2233-2244.
- Vaidyanathan, P.P., Zinshteyn, B., Thompson, M.K., and Gilbert, W.V. (2014). Protein kinase A regulates gene-specific translational adaptation in differentiating yeast. *RNA*.
- Vassella, E., Kramer, R., Turner, C.M., Wankell, M., Modes, C., van den Bogaard, M., and Boshart, M. (2001). Deletion of a novel protein kinase with PX and FYVE-related domains increases the rate of differentiation of *Trypanosoma brucei*. *Mol Microbiol* 41, 33-46.
- Vassella, E., Reuner, B., Yutzy, B., and Boshart, M. (1997). Differentiation of African trypanosomes is controlled by a density sensing mechanism which signals cell cycle arrest via the cAMP pathway. *J Cell Sci* 110 (Pt 21), 2661-2671.
- Wakao, K., Watanabe, T., Takadama, T., Ui, S., Shigemi, Z., Kagawa, H., Higashi, C., Ohga, R., Taira, T., and Fujimuro, M. (2014). Sangivamycin induces apoptosis by suppressing Erk signaling in primary effusion lymphoma cells. *Biochem Biophys Res Commun* 444, 135-140.
- Walsh, D.A., Ashby, C.D., Gonzalez, C., Calkins, D., and Fischer, E.H. (1971). Purification and characterization of a protein inhibitor of adenosine 3',5'-monophosphate-dependent protein kinases. *J Biol Chem* 246, 1977-1985.
- Walsh, D.A., Perkins, J.P., and Krebs, E.G. (1968). An adenosine 3',5'-monophosphate-dependant protein kinase from rabbit skeletal muscle. *J Biol Chem* 243, 3763-3765.

4. Activation of *T. brucei* PKA

- Wang, L., Zhu, Y., and Sharma, K. (1998). Transforming growth factor-beta1 stimulates protein kinase A in mesangial cells. *J Biol Chem* 273, 8522-8527.
- Wilson, W.A., Roach, P.J., Montero, M., Baroja-Fernandez, E., Munoz, F.J., Eydallin, G., Viale, A.M., and Pozueta-Romero, J. (2010). Regulation of glycogen metabolism in yeast and bacteria. *FEMS Microbiol Rev* 34, 952-985.
- Wirtz, E., Leal, S., Ochatt, C., and Cross, G.A. (1999). A tightly regulated inducible expression system for conditional gene knock-outs and dominant-negative genetics in *Trypanosoma brucei*. *Mol Biochem Parasitol* 99, 89-101.
- Witt, J.J., and Roskoski, R., Jr. (1975). Rapid protein kinase assay using phosphocellulose-paper absorption. *Anal Biochem* 66, 253-258.
- Wurtz, N., Chapus, C., Desplans, J., and Parzy, D. (2011). cAMP-dependent protein kinase from *Plasmodium falciparum*: an update. *Parasitology* 138, 1-25.
- Xong, H.V., Vanhamme, L., Chamekh, M., Chimfwembe, C.E., Van Den Abbeele, J., Pays, A., Van Meirvenne, N., Hamers, R., De Baetselier, P., and Pays, E. (1998). A VSG expression site-associated gene confers resistance to human serum in *Trypanosoma rhodesiense*. *Cell* 95, 839-846.
- Yang, H., Li, G., Wu, J.J., Wang, L., Uhler, M., and Simeone, D.M. (2013). Protein kinase A modulates transforming growth factor-beta signaling through a direct interaction with Smad4 protein. *J Biol Chem* 288, 8737-8749.
- Yonemoto, W., Garrod, S.M., Bell, S.M., and Taylor, S.S. (1993). Identification of phosphorylation sites in the recombinant catalytic subunit of cAMP-dependent protein kinase. *J Biol Chem* 268, 18626-18632.
- Zhang, H., Heid, P.J., Wessels, D., Daniels, K.J., Pham, T., Loomis, W.F., and Soll, D.R. (2003). Constitutively active protein kinase A disrupts motility and chemotaxis in *Dictyostelium discoideum*. *Eukaryot Cell* 2, 62-75.
- Zhong, H., SuYang, H., Erdjument-Bromage, H., Tempst, P., and Ghosh, S. (1997). The transcriptional activity of NF-kappaB is regulated by the IkappaB-associated PKAc subunit through a cyclic AMP-independent mechanism. *Cell* 89, 413-424.
- Zieger, M., Tausch, S., Henklein, P., Nowak, G., and Kaufmann, R. (2001). A novel PAR-1-type thrombin receptor signaling pathway: cyclic AMP-independent activation of PKA in SNB-19 glioblastoma cells. *Biochem Biophys Res Commun* 282, 952-957.
- Zoraghi, R., Kunz, S., Gong, K., and Seebeck, T. (2001). Characterization of TbPDE2A, a novel cyclic nucleotide-specific phosphodiesterase from the protozoan parasite *Trypanosoma brucei*. *J Biol Chem* 276, 11559-11566.
- Zoraghi, R., and Seebeck, T. (2002). The cAMP-specific phosphodiesterase TbPDE2C is an essential enzyme in bloodstream form *Trypanosoma brucei*. *Proc Natl Acad Sci U S A* 99, 4343-4348.

Acknowledgements

We thank U. Walter (University of Würzburg) for the plasmid p14/1 (bearing the VASP cDNA) and A. Bindereif (University of Gießen) for the plasmid pC-PTP-NEO. Moreover, we acknowledge E. Pays for the anonymous cDNA P2 and P. Bastin and K. Gull for the anti-PFR-A/C and the anti-Ty1 hybridoma.

This work was supported by the University of Munich and grants DFG 1100/7 and BELSPO PAI 6/15 to MB.

4.2 A cold-inducible protein kinase A regulates stage differentiation of trypanosomes.

Sabine Bachmaier¹, Susanne Kramer^{1*}, Julia Pepper^{1§}, George Githure¹, Lars Israel², Axel Imhof², Michael Boshart^{1#}

¹ *Biocenter, Section Genetics, Ludwig-Maximilians-Universität München, D-82152 Martinsried, Germany*

² *Adolf-Butenandt-Institute, Medical Faculty, Molecular Biology, Ludwig-Maximilians-Universität München, D-80336 München, Germany*

* *present address: Biozentrum der Universität Würzburg, Theodor-Boveri-Institut für Lebenswissenschaften*

§ *present address: Institute of Molecular Life Sciences, University of Zürich, Zürich, Switzerland*

Manuscript

To whom correspondence should be addressed:

Prof. Dr. Michael Boshart
boshart@lmu.de
Tel.: 49-89-2180-74600

Abstract

The cyclic AMP-dependent protein kinase PKA is one of the best-studied protein kinases. The enzyme is conserved in most eukaryotes and is responsible for regulation of a variety of cellular processes such as energy metabolism, differentiation, transcription, or transport. In *Trypanosoma brucei*, a unicellular, eukaryotic parasite with a complex life cycle involving a host switch between a mammal and an arthropod vector, the cAMP and PKA signal transduction pathways have been retooled. The conserved parasite PKA is not regulated by the second messenger cAMP but by a drop in temperature, an important trigger of life cycle stage differentiation. The kinase is activated by low temperature thereby sensitizing short stumpy bloodstream form trypanosomes to low, physiological concentrations of citrate/*cis*-aconitate, an essential stimulus for differentiation to insect stage procyclic trypanosomes. Identification of endogenous substrates of *T. brucei* PKA revealed partial conservation of processes regulated by PKA from trypanosomes over yeast to humans. However, one third of the identified proteins phosphorylated by the parasite kinase, are kinetoplastid- or *Trypanosoma*-specific with largely unknown function, supporting the unique role of this ubiquitous and in other organisms highly conserved signal transduction pathway in the evolutionary early branching eukaryote *T. brucei*.

Introduction

The parasitic protozoan *Trypanosoma brucei*, the causative agent of human African sleeping sickness (HAT) and Nagana in cattle (Brun et al., 2010), has a complex life cycle with a host switch between an arthropod vector, the tsetse fly, and a mammalian host. Hence, the parasite faces highly variable environmental conditions, and the ability to quickly adapt to a new environment is crucial for survival and transmission efficiency. Changes in temperature, nutrient availability, pH or osmolarity, as well as attack by proteases or the immune system are conditions trypanosomes have to cope with. In both the mammalian host as well as the arthropod vector, dividing stages as well as cell cycle arrested stages exist with the latter being pre-adapted to the life in the next host (Fenn and Matthews, 2007). In the mammalian bloodstream, the dividing long slender (LS) and the cell cycle arrested short stumpy (SS) bloodstream forms (BSFs) live in an environment with plenty of glucose as energy source (Bringaud et al., 2006) and a constant temperature of 37°C. LS cells differentiate in a density-dependent, quorum sensing-like mechanism into SS cells (Reuner et al., 1997; MacGregor et al., 2011), which differ in characteristic features from LS cells: procyclin, the major surface protein of insect-stage, procyclic form (PCF) trypanosomes, is expressed and routed to the cell surface (Fenn and Matthews, 2007). Furthermore, enzymes crucial for utilization of alternative energy sources in the fly are expressed. Upon a blood meal on an infected mammal, tsetse flies take up LS and SS trypanosomes. The latter, pre-adapted to the life in the insect vector, differentiate within a few days into the dividing PCF form. LS cells, however, are attacked and killed by proteases in the fly midgut. *In vitro*, the differentiation process from SS to PCF can be induced by treatment with citrate/*cis*-aconitate (CCA) (Ziegelbauer et al., 1990), mild acid stress (Rolin et al., 1998) or proteases (Hunt et al., 1994; Sbicego et al., 1999; Szöör et al., 2013). In addition, a temperature drop of >15°C (cold shock) sensitizes stumpy trypanosomes to low concentrations of CCA (Engstler and Boshart, 2004). The molecular mechanisms and signaling pathways underlying these differentiation processes are only partially uncovered. A family of putative citrate transporters, the PAD proteins, is required for perception of the CCA stimulus at the surface of SS cells (Dean et al., 2009). PAD proteins are encoded by an array of eight genes, and simultaneous knockdown of all members results in reduced ability to differentiate to the insect form and eliminates CCA hypersensitivity under cold shock conditions. Although all *PAD* genes encode closely related proteins, they might fulfill distinct functions: whereas PAD1 serves as molecular marker for defining the short stumpy stage (Dean et al., 2009; MacGregor et al., 2011), exposure of SS trypanosomes to cold shock induces expression and surface routing of PAD2, which might act as CCA receptor (Dean et al., 2009). Moreover, a phosphatase cascade involving the protein phosphatases PTP1 and PIP39 controls differentiation from SS to PCF (Szöör et al., 2006; Szöör et al., 2010) with PTP1 being a negative and PIP39 a positive regulator. Phosphorylation of PIP39 at Y278 is a prerequisite for differentiation to the insect stage. As long as SS forms reside in the mammalian bloodstream, PTP1 inactivates PIP39 by dephosphorylation at Y278 and thereby prevents differentiation. PIP39 activates PTP1 and thereby promotes its own inhibition. Szöör et al. (2013) propose a model in which the feedback inhibition of PIP39 by PTP1 is blocked by a CCA-dependent mechanism upon uptake of SS cells by a tsetse fly: CCA entering the cells via transporters of the PAD family localized at the surface of SS cells promotes interaction between PIP39 and PTP1 and

independently blocks the ability of PIP39 to enhance PTP1 activity. In addition, expression of PIP39 in SS is induced by cold shock (Szöör et al., 2010). These combined events eventually result in increased amounts of phosphorylated PIP39, which localizes to the glycosomes and consequently promotes efficient differentiation into PCFs. So far, the kinase responsible for phosphorylation of PIP39 at Y278 as well as the downstream pathway ultimately resulting in differentiation to the PCF stage is unknown. By a global kinome RNAi library screen, Jones et al. (2014) have recently discovered two kinases, RDK1 and RDK2, which negatively regulate SS to PCF differentiation. RDK1 has been shown to act in conjunction with the TbPTP1/TbPIP39 pathway blocking uncontrolled BSF to PCF differentiation, whereas RDK2 might act upstream of RDK1 and TbPTP1.

In many organisms, the cAMP-PKA-signaling pathway is involved in sensing and/or response to environmental changes (Smith et al., 1998; Taminato et al., 2002; Hoffman, 2005; Busti et al., 2010; Fuller and Rhodes, 2012) and regulation of differentiation processes (Loomis, 1998; Yao et al., 1998; Blaschke et al., 2000; Busti et al., 2010; Fuller and Rhodes, 2012; Yamamizu et al., 2012). The *T. brucei* genome encodes one orthologue of a regulatory and three isoforms of catalytic subunits of a PKA-related kinase. In contrast to its orthologues from other organisms, the enzyme is not regulated by the second messenger cAMP but potentially by an alternative endogenous, purine nucleoside-related ligand (Bachmaier et al., manuscript, see chapter 4.1). The present study extends the peculiarity of the *T. brucei* PKA signaling pathway upstream as well as downstream: instead of activation by cAMP, the kinase is specifically activated by a drop in temperature and is responsible for cold shock-mediated sensitization of stumpy trypanosomes to low CCA concentrations promoting efficient differentiation to the PCF stage. Putative substrates identified by a phosphoproteome approach reveal partial conservation of the PKA signaling pathway from the ancient eukaryote *T. brucei* over yeast to humans. One third of the identified substrates, however, represent kinetoplastid- or even *Trypanosoma*-specific proteins with largely unknown function, stressing the partial re-tooling of this ubiquitous and in other organisms highly conserved signaling pathway.

Material and Methods

Trypanosome strains, culture conditions and *in vitro* differentiation.

Bloodstream forms of the monomorphic strain Lister 427, variant MiTat 1.2 (Cross and Manning, 1973), of *Trypanosoma brucei brucei* were cultivated at 37°C in a 5% CO₂ atmosphere in modified HMI-9 medium (Vassella et al., 1997) supplemented with 10% (v/v) heat-inactivated fetal bovine serum (FBS). Slender bloodstream forms of the pleomorphic *T. b. brucei* strain AnTat 1.1 (Delauw et al., 1985) were harvested from immunosuppressed Wistar rats (Charles River Laboratories; intraperitoneal injection of 200 mg cyclophosphamide per kg body weight 16-24 h before infection) at a parasitemia below 8×10⁷/ml blood three to five days after infection with 1×10⁶ trypanosomes per animal. The blood was collected in 2 ml trypanosome dilution buffer (TDB; 5 mM KCl, 80 mM NaCl, 1 mM MgSO₄, 20 mM Na₂HPO₄, 2 mM NaH₂PO₄, 20 mM glucose [pH 7.4]) with 5000 i.U. heparin (Applichem). The parasites were separated from red blood cells by two centrifugation steps (10 min, 300×g, RT; 10 min, 1400×g, RT) followed by a buffy coat preparation and frozen in HMI-9 medium supplemented with 20% FBS and 10% glycerol. Slender trypanosomes were thawed and plated on agarose plates (Vassella and Boshart, 1996) with cell numbers between 5×10⁴ and 1.5×10⁶ parasites per plate. After 3-6 days, pure populations of stumpy trypanosomes were harvested from the plates and transferred into modified DTM medium (Overath et al., 1986; modified by Vassella and Boshart (1996)) complemented with 15% (v/v) heat-inactivated FBS at a density of 2×10⁶/ml. The cells were incubated for 16 h either at 20°C to induce sensitization to low *cis*-aconitate concentrations (Engstler and Boshart, 2004) or at 27°C. Differentiation to the procyclic stage was subsequently induced by addition of different concentrations of *cis*-aconitate (0, 0.06, 0.4, 6 mM; Sigma-Aldrich) and cultivation at 27°C. Procyclic forms of AnTat 1.1 were grown at 27°C in SDM-79 medium (Brun and Schonenberger, 1979) supplemented with 10% (v/v) heat-inactivated FBS.

Cloning and generation of transgenic trypanosomes. A cell line with deletion of both alleles of *PKAC3* (Tb427.10.13010) was generated by transfection of Lister 427, variant MiTat 1.2, with the plasmids pBΔPKAC3NEO and pBΔPKAC3HYGRO. These constructs contained the *PKAC3* UTRs and a neomycin or hygromycin resistance cassette flanked by actin UTRs. Linearization for transfection was done using DraIII and PvuI (pBΔPKAC3NEO) or HindIII (pBΔPKAC3HYGRO), respectively. Selection was performed with 2 μg/ml G418 and 2.5 μg/ml hygromycin B.

Monomorphic and pleomorphic trypanosome cell lines expressing a double tetracycline repressor were generated by transfection of monomorphic MiTat 1.2 Lister 427 or pleomorphic AnTat 1.1 cells with the plasmid pHD1313 (Alibu et al., 2005). The plasmid was linearized with NotI before transfection, and cells were grown in the presence of 10 μg/ml phleomycin.

PKAC1 and *PKAC2* were simultaneously targeted by a hairpin RNAi construct based on pHD615 (Biebinger et al., 1997). Sense (ORF pos. 136-469) and antisense (ORF pos. 28-520) fragments of *PKAC1/2* were amplified by PCR from genomic DNA of MiTat 1.2 Lister 427. After digestion of the sense fragment with HindIII and XhoI and the antisense fragment with XhoI and BamHI, the hairpin RNAi vector pHD615[PAC]PKAC1/2 RNAi was generated by a three-component ligation with pHD615[PAC] (derivative of pHD615 with puromycin instead of hygromycin resistance cassette) digested with BamHI and HindIII. To exclusively target *PKAC1* but not *PKAC2* a hairpin RNAi

vector based on pHD615[PAC] was generated targeting part of the *PKAC1* 3'UTR (sense fragment pos. Tb427_09_v4 1700775-1701234, antisense fragment pos. Tb927_09_v4 1700692-1701234). The pHD615[PAC] plasmids were linearized with NotI for transfection, and antibiotic selection was performed in the presence of 0.1 µg/ml puromycin. Details on primer sequences and cloning strategies are available upon request. All transfections were performed as described previously (Schumann Burkard et al., 2011).

Northern Blot. Total RNA (5 µg) was isolated from AnTat 1.1 parasites from infected irradiated rats (described in Reuner et al., 1997) 2.5 days post infection (long slender, LS), 5-6 days post infection (short stumpy, SS, 90% diaphorase-positiv), from culture two days after *in vitro* differentiation (procyclic form, PCF1), or from an established procyclic culture (PCF2). RNA separation and blotting was performed as previously described (Boshart et al., 1991). Antisense RNA probes were synthesized from nt position 923 to 1938 relative to the start codon of *PKAC3*, from nt position 26 to 1524 downstream of the stop codon for *PKAC1*, and from nt position 60 to 885 downstream of the stop codon for *PKAC2*. Random prime labeled DNA probes serving as loading controls were synthesized from the actin gene (SallI fragment; (Ben Amar et al., 1988)) or the anonymous cDNA *P2* (EcoRI/KpnI fragment, provided by E. Pays).

Western blot. Western blot analyses of PKA subunits, of proteins containing phospho-RXXS*/T* sites and of the PKA reporter substrate VASP were done as described previously (Bachmaier et al., manuscript, see chapter 4.1). Detection of the stumpy marker PAD1 was performed according to Dean et al. (2009).

2D gel electrophoresis. 2D gel electrophoresis was essentially carried out as described previously (van Deursen et al., 2003). Isoelectric focusing was done with lysates of 1×10^8 trypanosomes using ReadyStrip™ IPG strips pH 3-10NL (BioRad).

Staining of proteins in polyacrylamide gels. Proteins separated in polyacrylamide gels were visualized by staining with Coomassie Brilliant Blue (Candiano et al., 2004) or by silver staining (Blum et al., 1987; Chevallet et al., 2006).

VASP assay. Trypanosomes were harvested (10 min, 1400×g, 37°C (BSF) or 10 min, 900×g, 27°C (PCF)) and resuspended in fresh HMI-9 (BSF) or SDM-79 (PCF) medium at a density of 5×10^7 cells/ml. After a 5-10 minute recovery at 37°C (BSF) or 27°C (PCF) while slightly shaking, the cells were transferred to the indicated temperature (37°C, 27°C, 20°C, 4°C) for a fixed time period or over a defined time course. Care was taken that the temperature in each single experiment was constant and that cells were not cold shocked if not intended. All tubes, media and centrifuges were preheated to 37°C (BSF) or 27°C (PCF) and the temperature of all heating blocks was constantly checked with a thermometer. Cells were lysed with 6× Laemmli sample buffer preheated to 95°C and incubated for 5 minutes at 95°C.

FACS analysis. $1-2 \times 10^7$ trypanosomes were fixed overnight in 2% paraformaldehyde in PBS at 4°C. The repeat portion of EP procyclin on the parasite surface was detected by a monoclonal mouse anti-EP antibody (1:500; Cedar Lane Laboratories). Alexa 488 donkey anti-mouse IgG (H+L) antibody (Molecular Probes; 1:2000) was used as secondary antibody. Quantitative analysis was

4. Activation of *T. brucei* PKA

performed with a FACS-Calibur Flow Cytometer (Beckton Dickinson) using the software CellQuest (Becton Dickinson) and FlowJo (TreeStar).

Immunoprecipitation. For immunoprecipitation of proteins with a phosphorylated RXXS*/T* motif, 5×10^7 trypanosomes were harvested ($1400 \times g$, 10 min, $4^\circ C$), resuspended in RIPA buffer ($4^\circ C$) supplemented with protease and phosphatase inhibitors (complete EDTA-free, Roche; 25 $\mu g/ml$ pepstatin A; PhosSTOP, Roche) and incubated on ice for 15 min. After centrifugation ($20000 \times g$, 20 min, $4^\circ C$), the soluble fraction was incubated overnight with the Phospho-(Ser/Thr) PKA Substrate Antibody (Cell Signaling Technologies, catalogue number 9621) covalently coupled to magnetic protein A beads (Invitrogen) using DMP (Thermo Scientific) for crosslinking according to the manufacturer's instructions. The beads were washed three times with RIPA buffer, followed by a final wash with PBS. Elution was performed by incubation with Laemmli sample buffer for 10 min at $70^\circ C$. For identification of phospho-RXXS*/T* containing proteins by mass spectrometry, a lysate of 4×10^8 trypanosomes was used for immunoprecipitation.

Identification of phospho-RXXS/T proteins by mass spectrometry. The immunoprecipitated proteins were separated in an SDS gel and visualized by silver staining (Blum et al., 1987; Chevallet et al., 2006). The whole lane was cut into 27 slices, followed by reduction of the proteins by treatment with 1 mM dithiothreitol, alkylation with 5.5 mM iodoacetamide and digestion with an excess of endoproteinase Lys-C (1:100 w/w) and modified sequencing grade trypsin (1:100 w/w) after 4-fold dilution in deionized water, as described previously (Olsen et al., 2006). The resulting peptides were separated on a reversed-phase Sep-Pak C18 peptide purification cartridge via an acetonitrile gradient. Spectra were recorded on a QSTAR XL mass spectrometer (Applied Biosystems), followed by analysis of the resulting MS/MS data set using the Mascot search engine (Matrix Science Ltd.; Perkins et al., 1999) and the total proteome of *T. brucei* TREU927 (TriTrypDB release 3.3).

Bioinformatics. Detailed analysis of mass spectrometry data was performed using the proteome software Scaffold 2 (Proteome Software, Inc.; Searle, 2010) with the following settings: a protein threshold of 90% and a minimum of three peptides with a peptide threshold of 95%. Bioinformatic data about the identified genes were retrieved from TriTrypDB (<http://tritrypdb.org/>), GeneDB (<http://www.genedb.org>), and OrthoMCL (<http://www.orthomcl.org/>). Putative PKA phosphorylation sites were predicted using NetPhosK 1.0 (<http://www.cbs.dtu.dk/services/NetPhosK/>).

Immunofluorescence. For immunofluorescence analysis, 2×10^6 trypanosomes were fixed in 2% formaldehyde. Phospho-RXXS*/T* containing proteins were detected by the Phospho-(Ser/Thr) PKA Substrate Antibody (1:2000; Cell Signaling Technologies, catalogue number 9621) and visualized using the Alexa Fluor 594-conjugated goat anti-rabbit IgG (H+L) secondary antibody (1:2000; Life Technologies, Thermo Fisher Scientific). Cellular DNA was stained with 4',6-diamidino-2-phenylindole (DAPI; 1 $\mu g/ml$). Vertical stacks (0.2 μm steps) were captured using personal DV (Applied Precision) deconvolution (softWoRx Software) microscopy. The average Z-projection of nine images is shown.

Results

Developmental regulation of PKA subunit expression and phosphorylation. Expression analysis of *T. brucei* PKA subunits in fully differentiation competent, pleomorphic AnTat 1.1 cells revealed inverse regulation of *PKAC1* and *PKAC2* mRNAs in the different life cycle stages with *PKAC1* being predominantly expressed in BSF and *PKAC2* in PCF stages (Figure 1A). In contrast, the *PKAC3* transcript was detectable at approximately equal amounts in all stages with a slight decrease in PCFs. The PKAC3 protein followed a similar expression pattern (Figure 1B). Due to their high sequence similarity and nearly identical molecular weight the isoforms PKAC1 and PKAC2 are not distinguishable by the PKAC1/2 antibody on a Western blot (Bachmaier et al., manuscript, see chapter 4.1). PKAC1/2 expression is not significantly regulated between slender and stumpy BSFs but is down-regulated in the procyclic stage (Figure 1B). Analysis of PKA subunit expression in slender and stumpy-like stages of the monomorphic strain MiTat 1.2 Lister 427 (Figure S1) showed comparable results to expression in pleomorphic cells. To be able to discriminate between PKAC1 and PKAC2, the monomorphic cell line Δ pkac1/PKAC1-Ty1 (Bachmaier et al., manuscript, see chapter 4.1) was used for expression analysis. In this cell line, one allele of *PKAC1* has been deleted and the other allele has been tagged with a Ty1-epitope resulting in an electrophoretic mobility shift thereby allowing the distinction between the two isoforms. A Western blot with lysates of the different developmental stages of this cell line showed that PKAC1 is almost exclusively expressed in BSFs, while PKAC2 is more abundant in PCFs (Figure 1C), which is fairly in agreement with their transcript levels in the different stages. As one *PKAC1* allele has been deleted in this cell line, the actual expression of PKAC1 in wild type cells might be higher. In addition, PKAC1 shows two bands with the upper one being more prominent in the stumpy-like stage. Although PKAC1 and PKAC2 share 94% sequence identity, this modification is absent from PKAC2. Since the few amino acid differences, which are located at the very N- and C-terminal ends of these two isoforms, encompass several phosphorylation sites (Nett et al., 2009; Urbaniak et al., 2013), a PKAC1-specific phosphorylation might be responsible for the observed mobility shift. The *PKAR* transcript was expressed at approximately equal amounts in LS and SS and lowered in PCF cells (data not shown), which is in agreement with the data from Shalaby et al. (2001). This regulation is as well reflected at the protein level (Figure 1B). The expression of PKA subunits in *T. brucei* is therefore most likely regulated at the level of mRNA stability.

4. Activation of *T. brucei* PKA

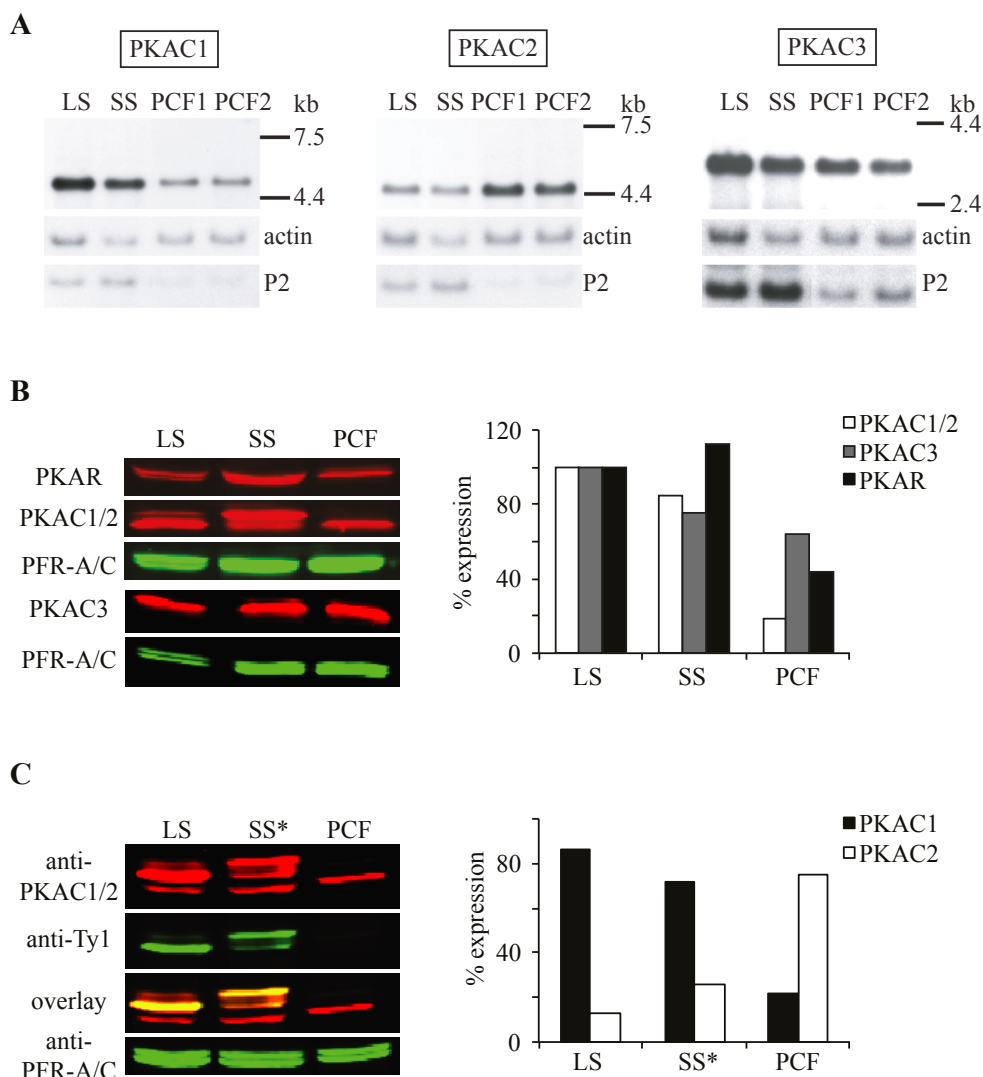


Figure 1: Developmental regulation of PKA subunit expression at the transcript (A) or protein level (B, C).

A. Northern blot analysis of total RNA (5 μ g) isolated from AnTat 1.1 parasites at different life cycle stages. *PKAC1*, *PKAC2* and *PKAC3* transcripts were detected by gene-specific probes. Actin and the anonymous cDNA *P2* (provided by E. Pays) served as internal controls. Actin is equally expressed in slender (LS) and procyclic (PCF) cells but reduced in stumpy (SS) cells (Ben Amar et al., 1988). *P2* is equally expressed in LS and SS cells but reduced in PCF cells. PCF1: procyclic cells after 2 days of *in vitro* differentiation; PCF2: established procyclic cells.

B. Protein expression of PKA subunits in slender (LS), stumpy (SS) and established procyclic (PCF) pleomorphic AnTat 1.1 cells was analyzed by Western blotting using specific antibodies against PKAC1/2, PKAC3 (Bachmaier et al., manuscript, see chapter 4.1) and PKAR (Bachmaier et al., 2015, submitted manuscript, see chapter 5). PFR-A/C detected by the monoclonal antibody L13D6 (Kohl et al., 1999) was used for normalization. The diagram shows the percentage of PKAR, PKAC1/2 and PKAC3 in the different life cycle stages (LS was set to 100%).

C. Western blot analysis of PKAC1 and PKAC2 expression in slender (LS), stumpy-like (SS*) and established procyclic (PCF) stages of the monomorphic cell line MiTat 1.2 Δ *pkac1*/Ty1-*PKAC1*, which allows discrimination between PKAC1 and PKAC2 due to deletion of one *PKAC1* allele and fusion of the other one to Ty1-tag. PFR-A/C detected by the monoclonal antibody L13D6 (Kohl et al., 1999) was used for normalization. The diagram shows the percentage of PKAC1 and PKAC2 on the total amount of PKAC1/2 (set to 100%) in the different life cycle stages.

***T. brucei* PKAR-C1 is rapidly and reversibly activated by temperatures below 37°C in BSFs.** The developmental regulation of PKA subunit expression prompted us to examine the effect of developmental triggers on *in vivo* PKA activity. We have recently established an *in vivo* PKA reporter assay in *T. brucei* that is based on phosphorylation of the transgenically expressed PKA reporter substrate VASP and can be used as a specific measure for endogenous PKA activity (Bachmaier et al., manuscript, see chapter 4.1). Reporter substrate phosphorylation in a monomorphic BSF cell line was not dependent on cell density or treatment with *cis*-aconitate (Figure S2A, B), both of which are important triggers for life cycle stage differentiation of the parasite. However, exposure to low temperature, an important trigger for BSF to PCF differentiation *in vitro* (Engstler and Boshart, 2004), caused rapid and reversible increase in VASP phosphorylation (Figure 2A). Temperatures below 37°C induced a rapid phosphorylation of the reporter substrate with a maximum after 5-10 minutes, which was completely reversible when transferred back to 37°C. Lower temperatures resulted in stronger phosphorylation. Cold shock is known to act as an inducer of life cycle stage differentiation in *T. brucei in vitro* by sensitizing stumpy cells to low citrate/*cis*-aconitate concentrations inducing differentiation to the procyclic stage (Engstler and Boshart, 2004). Investigation of temperature-dependent PKA activation in different developmental stages revealed that cold activation is specific for the bloodstream stage (Figure 2B; Figure S2C). Since the regulatory subunit of *T. brucei* PKA can form a heterodimeric holoenzyme with any of the three different catalytic subunits (Bachmaier et al., manuscript, see chapter 4.1), cold inducibility was analyzed in a number of PKA mutants. Upon deletion of both alleles of *PKAR*, cold shock activation of PKA was lost, but was restored by add-back of a *PKAR* wild type copy (Figure 2C) in the endogenous locus. Inhibition of cold shock-induced VASP phosphorylation was also obtained by knock down of *PKAC1/2* by RNAi or by specifically targeting *PKAC1* by RNAi against its 3'UTR (Figure 2C; Figure S3B, C). In contrast, homozygous deletion mutants of *PKAC2* (Bachmaier et al., manuscript, see chapter 4.1) or *PKAC3* (Figure S3A) showed induction by cold shock comparable to wild type cells (Figure 2C). We conclude that the PKAR-PKAC1 holoenzyme is specifically activated by cold shock, although cold-dependent activation of PKAR-PKAC2 cannot be completely ruled out due to the low expression of PKAC2 in BSF cells. All attempts to knock out both alleles of *PKAC1* or to replace them by *PKAC2* were unsuccessful indicating that *PKAC1* might be essential. All deletion mutants and RNAi cell lines were viable with several cell lines showing slight growth phenotypes (PDT wild type: 5.6h; PDT *PKAR*^{-/-}: 7.5h; PDT *PKAC2*^{-/-}: 6.8h; PDT *PKAC3*^{-/-}: 9.2h; PDT *PKAC1/2* RNAi +/- Tet: 5.9/6.1h; PDT *PKAC1* UTR RNAi +/- Tet: 5.7/5.8h). Note that we have previously published a *PKAC1/2* RNAi cell line with a severe growth and cytokinesis phenotype upon induction of RNAi, which eventually resulted in cell death (Bachmaier et al., 2014, manuscript, see chapter 4.1). While in the cell line of the previous study the RNAi strategy was based on a p2t7 plasmid (Wickstead et al., 2002; RNAi driven by T7 polymerase from two opposing T7 promoters), in the present study we used a hairpin-based RNAi strategy (using the vector pHD615 (Biebinger et al., 1997), RNAi regulated by Tet operator only). The efficiency of the RNAi-mediated repression of *PKAC1/2* was identical between the two cell lines. The different phenotypes might depend on the kinetics of the RNAi.

4. Activation of *T. brucei* PKA

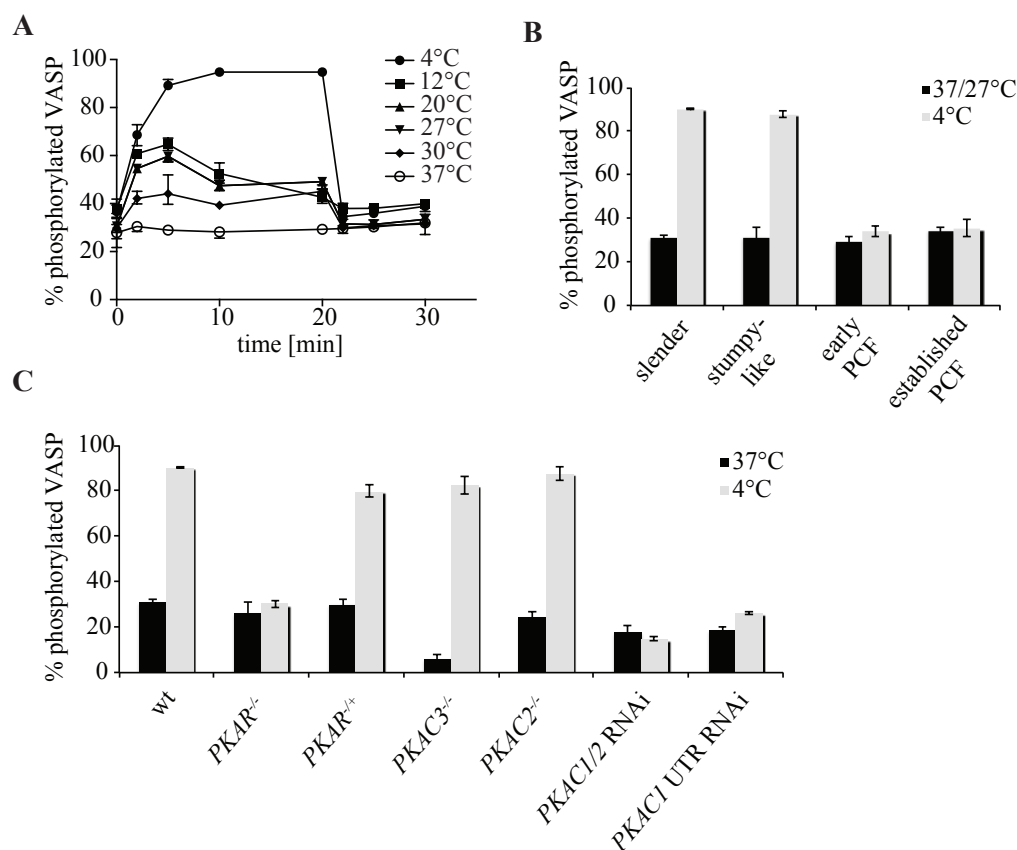


Figure 2: Specific activation of *T. brucei* PKA by cold shock.

A. Rapid and reversible increase in VASP phosphorylation by temperatures below 37°C. VASP phosphorylation was analyzed over 20 min at 37°C, 27°C, 20°C, 12°C or 4°C. After 20 min incubation at the respective temperature, the trypanosomes were transferred to 37°C, and VASP phosphorylation was analyzed over 10 min. Data points represent means of triplicate determinations; error bars indicate SD.

B. Cold shock-induced VASP phosphorylation is specific for BSFs. VASP phosphorylation was analyzed in wild type BSF slender and stumpy-like trypanosomes and in early (2 days after induction of differentiation) and established procyclic cells after 10 min incubation at 37°C (BSFs) or 27°C (PCFs), respectively, and at 4°C. Data points represent means of triplicate determinations; error bars indicate SD.

C. Cold shock induced VASP phosphorylation is mediated by PKAR-C1. VASP phosphorylation was analyzed in different mutants of PKA subunits and isoforms and in wild type (wt) cells expressing VASP after 10 min incubation at 37°C or 4°C, respectively. Data points represent means of triplicate determinations; error bars indicate SD.

PKAR^{-/-}: homozygous deletion mutant of *PKAR*; *PKAR*^{+/+}: endogenous *PKAR* rescue; *PKAC3*^{-/-}: homozygous deletion mutant of *PKAC3*; *PKAC2*^{-/-}: homozygous deletion mutant of *PKAC2*; *PKAC1/2* RNAi: cell line with inducible RNAi against *PKAC1/2*; *PKAC1* UTR RNAi: cell line with inducible RNAi against the *PKAC1* UTR.

***T. brucei* PKA mediates cold shock-induced sensitization to low CCA concentrations in SS cells promoting differentiation to the PCF stage.** Since cold shock is a known differentiation trigger in the *T. brucei* life cycle by sensitizing SS trypanosomes to low CCA concentrations and thereby promoting differentiation to the PCF stage (Engstler and Boshart, 2004), the observed stage-specific activation of the parasite PKA by low temperatures suggested a putative role of the kinase in this differentiation process. To analyze this hypothesis, a pleomorphic and hence fully differentiation-competent cell line with inducible RNAi against *PKAC1/2* was generated. Expression analysis of the stumpy marker PAD1 in pleomorphic AnTat 1.1 wild type cells grown on agarose plates showed that maximal expression was observed after three days of cultivation (Figure S4A). Stumpy stage AnTat 1.1 wild type as well as *PKAC1/2* RNAi cells grown in the presence or absence of 10 µg/ml tetracycline were harvested from agarose plates followed by expression analysis of PKAC1/2 and PAD1 (Figure 3A). While PAD1 expression was at the same level in all cell lines, PKAC1/2 was efficiently repressed in the *PKAC1/2* RNAi cell line induced with tetracycline. Another marker for a population with a high proportion of stumpy cells is surface expression of EP procyclin after exposure to 6 mM *cis*-aconitate. EP surface expression was analyzed by flow cytometry in AnTat 1.1 wild type and *PKAC1/2* RNAi cells induced or not with 10 µg/ml tetracycline (Figure S4B). Stumpy cells harvested from agarose plates were transferred into DTM, and samples for flow cytometry were taken after exposure to the following conditions: immediately after transfer into DTM (0 h), after 16 h cultivation at 27°C, or after 16 h cultivation at 27°C in the presence of 6 mM *cis*-aconitate. All cell lines showed efficient induction of EP surface expression upon incubation with 6 mM *cis*-aconitate, characteristic for populations with a high proportion of stumpy cells. To analyze whether PKAC1/2 plays a role in cold shock-mediated sensitization to low *cis*-aconitate concentrations, SS cells were transferred into DTM medium and subjected to a cold shock at 20°C for 16 h. To induce differentiation to the PCF stage, different concentrations of *cis*-aconitate were added (0, 0.06, 0.4 or 6 mM, respectively), and differentiation efficiency was analyzed by outgrowth of procyclic cells (Figure 3B). Whereas all cell lines showed efficient differentiation at 6 mM *cis*-aconitate, at 0.4 mM or 0.06 mM *cis*-aconitate only the wild type and the non-induced *PKAC1/2* RNAi cells differentiated.

4. Activation of *T. brucei* PKA

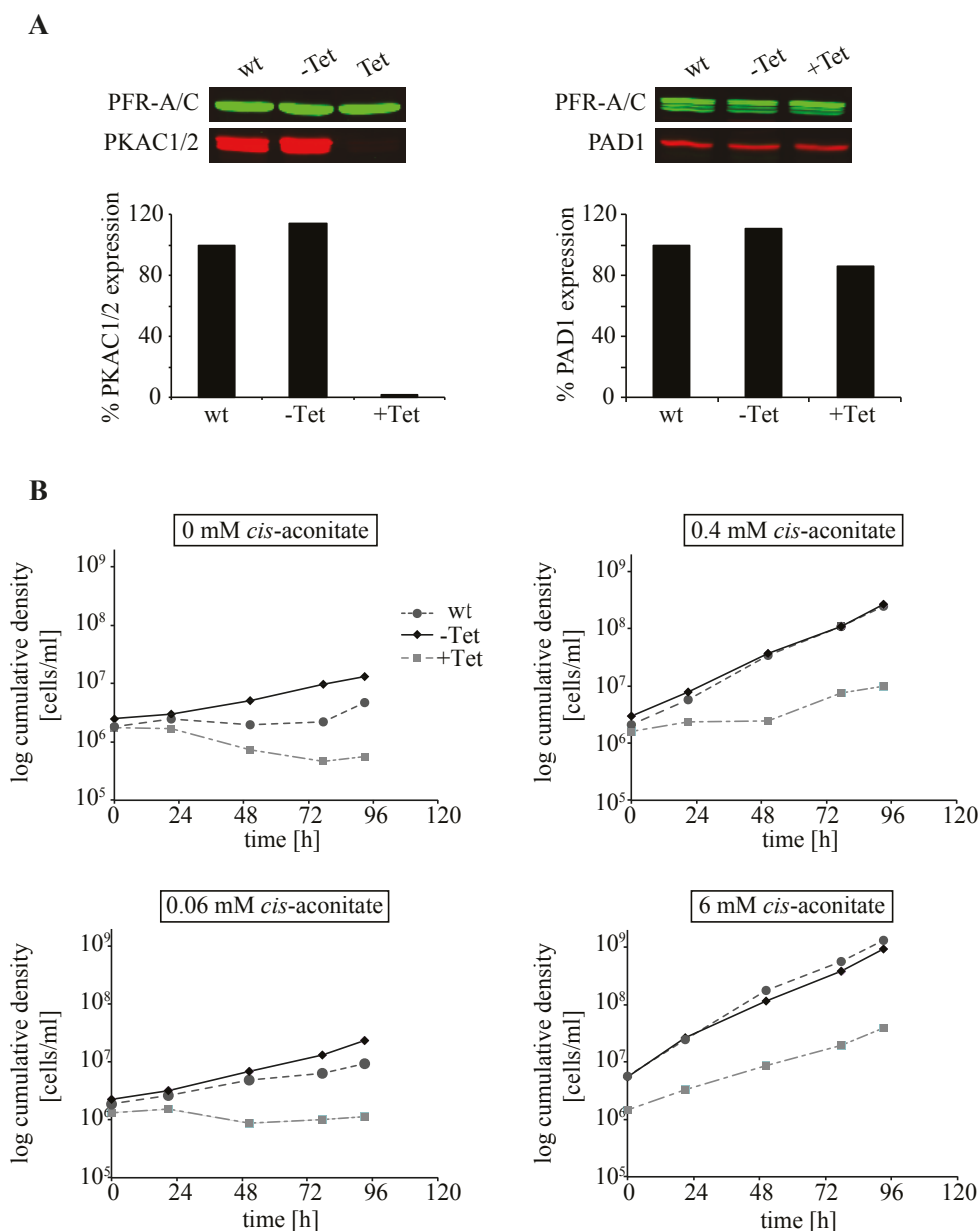


Figure 3: Role of *T. brucei* PKA for *in vitro* differentiation of pleomorphic trypanosomes.

A. Western blot analysis of PKAC1/2 (left) or PADI1 (right) expression in pleomorphic AnTat 1.1 cells (wt) and derived AnTat 1.1 1313 *PKAC1/2* RNAi cells in the presence (+Tet) or absence (-Tet) of 10 µg/ml tetracycline. Slender cells derived from infected rats were plated on agarose plates and grown for 4 days until the population showed a clear stumpy morphology. Required selection antibiotics as well as tetracycline were included in the plates. PFR-A/C detected by the monoclonal antibody L13D6 (Kohl et al., 1999) was used for normalization. The normalized signal for PKAC1/2 or PADI1, respectively, in the parental AnTat 1.1 cell line was set to 100%.

B. Differentiation of pleomorphic AnTat 1.1 and derived AnTat 1.1 1313 *PKAC1/2* RNAi cells to the procyclic stage in the presence (+Tet) or absence (-Tet) of 10 µg/ml tetracycline. Stumpy cells harvested from agarose plates were subjected to differentiation by transfer into differentiation medium (DTM) and incubation at 20°C for 16 h, followed by addition of the indicated concentrations of *cis*-aconitate and subsequent incubation at 27°C. Cell growth was determined daily using a Casy® automated cell counter, and cells were diluted if required to keep the cell density between 2×10^6 and 1×10^7 cells/ml.

Upon differentiation from SS to PCF, the cells re-enter the cell cycle accompanied by a change in the distances between nucleus, kinetoplast and posterior end of the cell (Matthews et al., 1995). Upon treatment with 6 mM *cis*-aconitate for 24 h, all cell lines showed a high fraction of cells with a subterminal kinetoplast, characteristic for PCF cells, indicating that differentiation is complete (Figure S4C, D). However, the time course analysis of kinetoplast repositioning revealed a differentiation delay in the induced *PKAC1/2* RNAi cell line. In contrast, upon treatment with 0.4 mM *cis*-aconitate, only the wild type and non-induced *PKAC1/2* RNAi cell lines showed a significant increase in the fraction of cells with subterminal kinetoplast, while the majority of the induced *PKAC1/2* RNAi cells had a kinetoplast, which was positioned at the very posterior end of the cell, a typical feature of SS cells. Hence, we conclude that repression of *PKAC1/2* prevents cold shock-induced sensitization to low *cis*-aconitate concentrations, suggesting that the kinase is involved in transduction of the cold shock stimulus to the CCA sensing pathway.

Specific phosphorylation of endogenous PKA substrates upon cold shock. We have previously shown that *T. brucei* PKA substrates can be effectively and specifically detected by a phospho-PKA substrate antibody (Bachmaier et al., manuscript, see chapter 4.1). Western blot analysis of lysates from MiTat 1.2 wild type cells incubated for 10 min at 37°C or 4°C, respectively, showed a strong increase in the number and intensity of bands detected by the Phospho-(Ser/Thr) PKA Substrate antibody upon cold shock (Figure 4A). As control, lysates from VASP expressing MiTat 1.2 cells were analyzed, and phosphorylation of the band corresponding to the size of the reporter substrate increased significantly upon cold shock. Consistent with the results of the PKA reporter assay (Figure 2), no increase in PKA-specific phosphorylations was observed in PCFs or in the homozygous *PKAR* deletion mutant (Figure 4A). Moreover, upon treatment with the myristoylated peptide myr-PKI(14-22) derived from the PKA-specific inhibitor PKI (Walsh et al., 1971; Glass et al., 1989; Harris et al., 1997; Dalton and Dewey, 2006), no bands could be detected with the phospho-PKA substrate antibody in VASP expressing wild type or *PKAR* knock out cells at 37°C or 4°C, respectively, further supporting the high specificity of the antibody for detection of PKA-dependent phosphorylations in *T. brucei*. The motif RXXS/T is also a well-known consensus phosphorylation sequence for a few other kinases, e.g. calmodulin-dependent kinase II (CaMKII) or ribosomal S6 kinase (RSK) (Ubersax and Ferrell Jr, 2007; Salazar and Hofer, 2009; Pearce et al., 2010), both of which are present in the *T. brucei* kinome (Parsons et al., 2005). However, the disappearance of all bands detected by the anti-RXXS*/T* antibody after treatment with the PKA-specific inhibitor myr-PKI(14-22) suggests a higher abundance of RXXS/T sites phosphorylated by PKA than by any other kinase in *T. brucei*. Alternatively, the other parasite kinases might show different substrate specificities.

4. Activation of *T. brucei* PKA

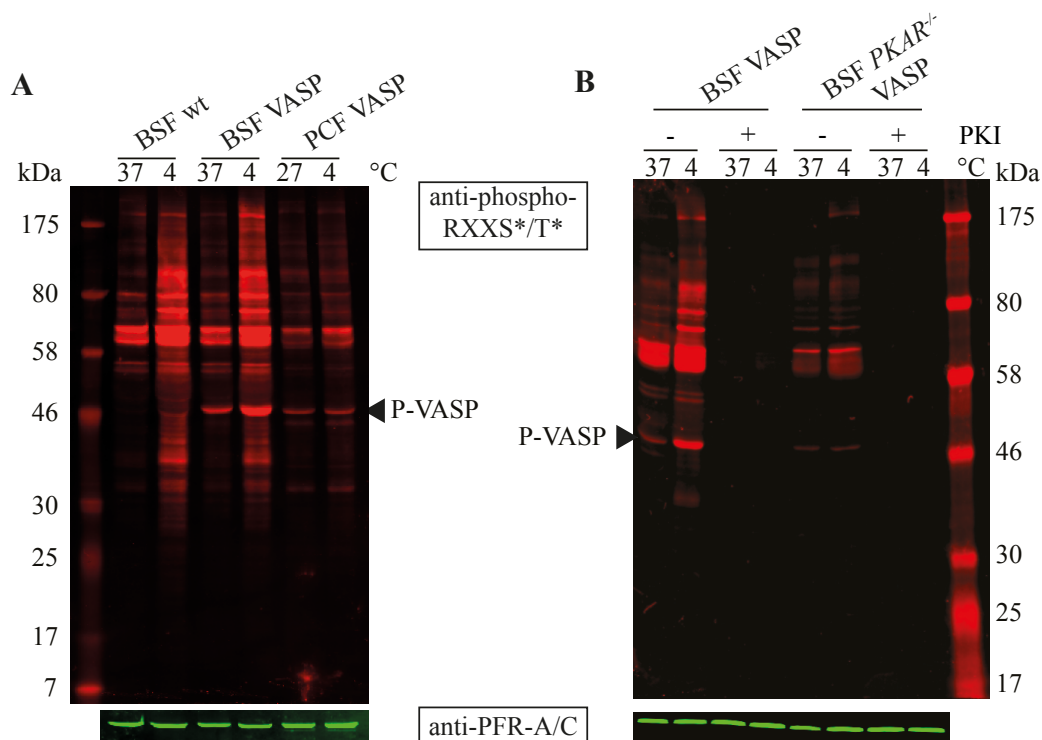


Figure 4: Detection of Phospho-PKA substrates in *T. brucei*. The antibodies used for all Western blots are Phospho-(Ser/Thr) PKA Substrate antibody (anti-RXXS*/T*) and anti-PFR-A/C (Kohl et al., 1999).

A. Western blot analysis of proteins phosphorylated at the motif RXXS*/T* in *T. brucei* BSF wild type cells (BSF wt) or VASP expressing BSF (BSF VASP) or procyclic trypanosomes (PCF VASP) incubated for 10 min at 4°C compared to incubation at 37°C (BSF) or 27°C (PCF), respectively.

B. Western blot analysis of proteins phosphorylated at the motif RXXS*/T* in a VASP expressing *T. brucei* BSF cell line (BSF VASP) compared to a VASP expressing BSF cell line with deletion of both alleles of *PKAR* (BSF *PKAR*^{-/-} VASP) in the presence (+PKI) or absence (-PKI) of the membrane-permeable, PKA-specific inhibitor peptide myr-PKI(14-22) combined with cold shock (4°C) or normal temperature (37°C).

Identification of *T. brucei* PKA substrates by a phosphoproteomics approach.

Phosphorylation of the transgenically expressed reporter substrate VASP serves as useful assay for analysis of regulation of *in vivo* PKA activity. However, the endogenous substrates of the kinase are completely unknown so far. In a first approach, lysates of VASP expressing MiTat 1.2 cells incubated for 10 min at 4°C or 37°C, respectively, were separated by 2D gel electrophoresis (Figure S5) and analyzed by Western blotting using the Phospho-(Ser/Thr) PKA Substrate antibody. Consistent with the results of the 1D Western blot analysis (Figure 4), the number and intensity of the spots detected by the antibody increased significantly upon cold shock (Figure S5). In order to validate the usefulness of the Phospho-(Ser/Thr) PKA Substrate antibody in detecting and identifying PKA substrates from *T. brucei* lysates, two of the spots, which showed a significant cold-dependent increase in signal intensity for PKA-dependent phosphorylation and correspond to the molecular weight of phosphorylated VASP, were cut from the corresponding Coomassie-stained gel and confirmed by MS/MS analysis. However, in other spots cut from the gel a complex mixture of proteins was detected by MS, indicating the requirement for reduction in sample complexity. Hence, in a second approach, proteins

containing phosphorylated RXXS*/T* sites were enriched by immunoprecipitation using the Phospho-(Ser/Thr) PKA Substrate antibody. Although phosphorylation of RXXS/T sites seems to be predominantly mediated by PKA in *T. brucei* (Figure 4), we cannot exclude that our approach identifies substrates of other kinases, like CaMKII or RSK, with an overlapping consensus phosphorylation motif (Ubersax and Ferrell Jr, 2007; Salazar and Hofer, 2009; Pearce et al., 2010). The elution fraction was separated by SDS PAGE and the whole lane was cut into slices and analyzed by MS/MS (Figure 5). 178 proteins were identified (Table S1), out of which 171 proteins contain RXXS/T motifs within their primary amino acid sequence (Figure 6A). The seven proteins without RXXS/T motif might either be false positives or co-immunoprecipitated proteins, with five of these seven proteins being putative ribosomal proteins. Phosphorylated RXXS*/T* sites were identified for twelve of the 171 proteins, with eight of these proteins having an unknown function. Since the IP with the phospho-PKA substrate antibody pulls down phospho-RXXS*/T*-containing proteins, which are subsequently digested into peptides before they are analyzed by MS/MS, the probability of identifying a phosphorylated RXXS*/T* by MS/MS is very low. Functional analysis by bioinformatics revealed a high abundance of proteins involved regulation of processes like ribosome biogenesis/translation, metabolism, RNA association, protein folding or motility (Figure 6B) as putative substrates of *T. brucei* PKA, which is reminiscent of the situation in other organisms (Skalhegg and Tasken, 2000; Shabb, 2001; Santangelo, 2006; Livas et al., 2011; Vaidyanathan et al., 2014). Evolutionary analysis via OrthoMCL showed that 112 out of the 171 identified putative PKA substrates are conserved beyond kinetoplastids, whereas one third is kinetoplastid- (41 proteins) or *Trypanosoma*-specific (14 proteins), (Figure 6C; Table S1) with largely unknown functions, supporting a partially unique role of the kinase in *T. brucei*. According to available proteome data (Broadhead et al., 2006; Bridges et al., 2008; Zhou et al., 2010; Oberholzer et al., 2011; Subota et al., 2014), *T. brucei* PKA substrates are strongly enriched in the plasma membrane, cytoskeleton and flagellar fractions (Figure 6D; Table S1), which was confirmed by immunofluorescence analysis using the Phospho-(Ser/Thr) PKA Substrate antibody in BSF and PCF trypanosomes (Figure 6E).

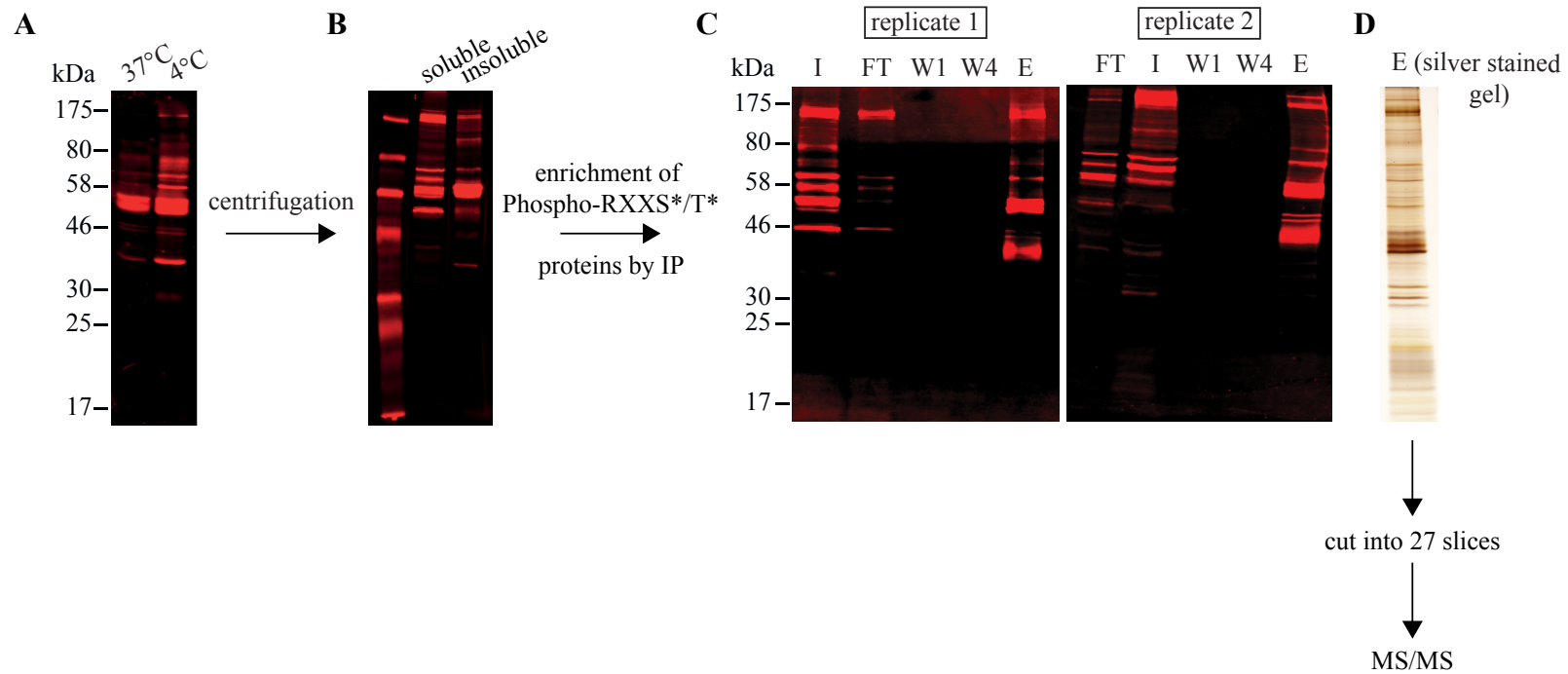


Figure 5: Identification of *T. brucei* PKA substrates by a phosphoproteome approach.

Upon cold shock, the number and intensity of bands detected by the Phospho-(Ser/Thr) PKA Substrate antibody (anti-RXXS*/T*) increases significantly (Western blot A). The cold shocked sample was centrifuged to separate soluble from insoluble proteins (Western blot B). Pull down of proteins with a phosphorylated RXXS*/T* motif from the soluble fraction of the cold shocked sample was achieved by immunoprecipitation using the Phospho-(Ser/Thr) PKA Substrate antibody (anti-RXXS*/T*) (Western blots C; two independent biological replicates). I = input fraction; FT = flow through; W1, W4 = wash fractions; E = elution. Enriched proteins from the elution fraction were cut from a silver-stained polyacrylamide gel (D) and identified by MS/MS.

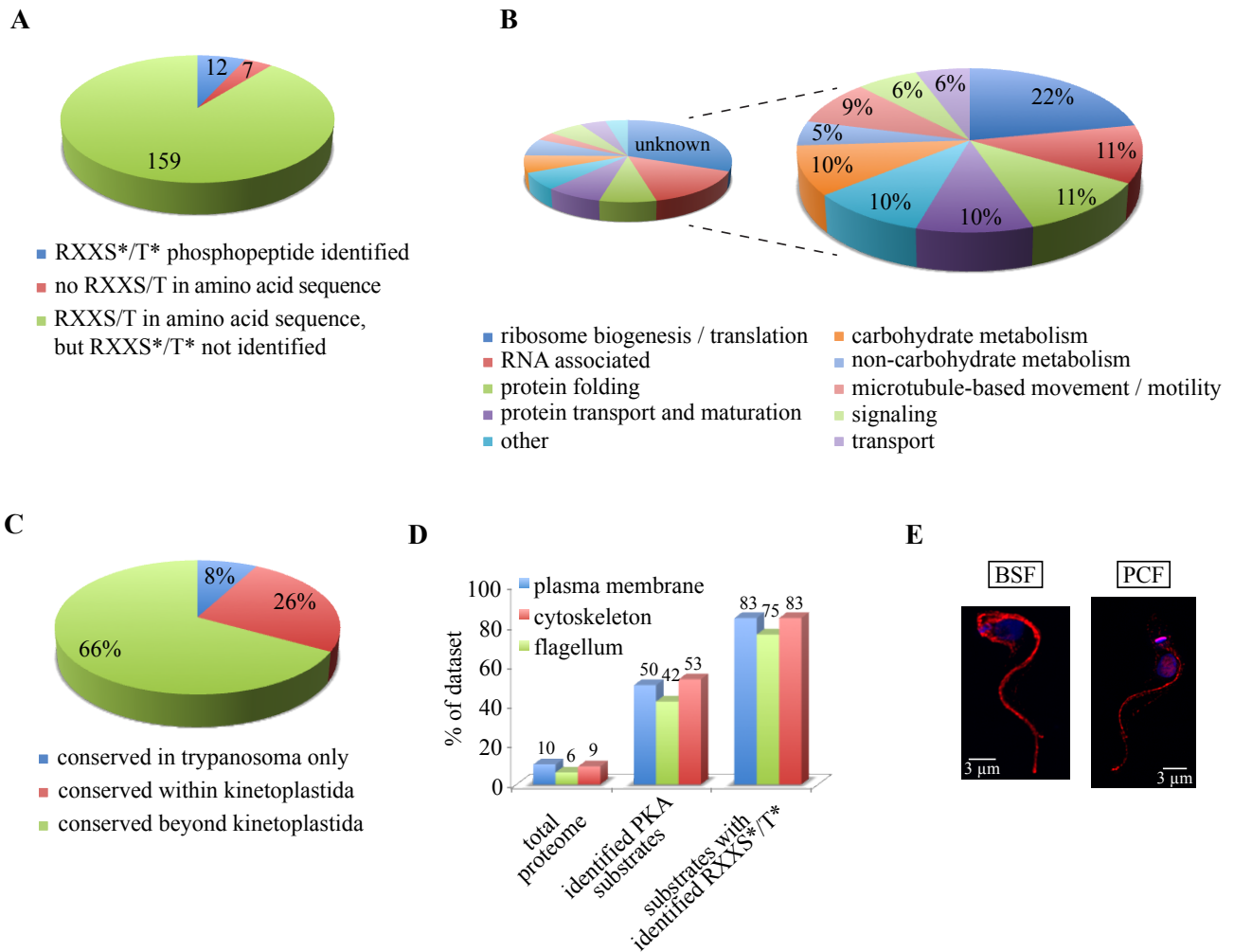


Figure 6: Bioinformatics analyses of *T. brucei* PKA substrates.

A. Sequence analysis of the 178 identified putative *T. brucei* PKA substrates regarding the presence of RXXS/T motifs. The proteins fall into three categories: 1) RXXS*/T* phosphopeptide identified: phosphorylated RXXS*/T* motifs were identified in 12 proteins; 2) no RXXS/T in primary amino acid sequence: 7 identified proteins do not contain an RXXS/T motif; 3) RXXS/T motif in primary amino acid sequence but RXXS*/T* phosphopeptide not identified. 159 proteins contain an RXXS/T motif in their amino acid sequence but phosphorylated RXXS*/T* peptides were not identified.

B. Functional analysis of the identified, putative *T. brucei* PKA substrates by bioinformatics. The proteins were classified into ten categories (carbohydrate and non-carbohydrate metabolism, microtubule-based movement, other, protein folding, protein transport and maturation, ribosome biogenesis/translation, RNA associated, signaling, transport) according to their GO term annotation.

C. Conservation analysis of the identified, putative *T. brucei* PKA substrates using the OrthoMCL database. Whereas 66% (112 out of 171) of the identified proteins with RXXS/T motif are conserved beyond kinetoplastids, 26% (41 out of 171) are conserved within kinetoplastids and 8% (14 out of 171) are *Trypanosoma*-specific.

D. Subcellular localization of the identified putative *T. brucei* PKA substrates compared to the total proteome. Comparison of identified PKA substrates with the published plasma membrane, cytoskeleton and flagellar proteomes (Bridges et al., 2008; Broahdead et al., 2006; Zhou et al., 2010; Oberholzer et al., 2011; Subota et al., 2014) shows a strong enrichment in these fractions.

E. Immunofluorescence analysis of *T. brucei* PKA substrates with the anti-RXXS*/T* antibody in BSF and PCF trypanosomes. Red = phospho-PKA substrates; blue = DAPI. The scale bar represents 3 μm.

Discussion

Role of *T. brucei* PKA in cold shock-induced SS to PCF differentiation. A signaling cascade including the phosphatases TbPTP1 (Szöör et al., 2006) and TbPIP39 (Szöör et al., 2010) as well as CCA transporters of the PAD family (Dean et al., 2009) has been shown to be involved in regulation of SS to PCF differentiation. Phosphorylation of the serine/threonine phosphatase TbPIP39 at Y278 by a so far unknown kinase is a prerequisite for this differentiation process. Depletion of *PKAC1/2* by RNAi prevents cold shock-induced sensitization to low CCA concentrations, resembling the phenotype observed upon depletion of *TbPIP39* (Szöör et al., 2010). In LS cells, PKA and TbPTP1 are expressed (Figure 7A). Since TbPIP39 is not expressed in LS, the cells cannot differentiate to the PCF stage. In SS cells, all known components of the differentiation pathway are expressed: PAD, PKA, TbPTP1, TbPIP39. However, differentiation is prevented by TbPTP1, which negatively regulates TbPIP39 by dephosphorylation. TbPIP39 positively regulates TbPTP1 thereby enhancing its own inhibition. In the tsetse environment, CCA (or an alternative, as yet unknown signal) is taken up by a carboxylate transporter of the PAD family expressed at the surface of stumpy cells and inhibits the feedback activation of TbPTP1 by TbPIP39 (Szöör et al., 2010). In turn, phosphorylated TbPIP39 promotes differentiation by a so far unknown downstream pathway. Yet, for sufficient inhibition of TbPTP1 unphysiologically high concentrations of CCA are required. Here we observe that activation of the parasite PKA by cold shock sensitizes the cells to physiological CCA concentrations. There are several models of how PKA could be involved in regulation of temperature-dependent differentiation (Figure 7B). One possible scenario is that upon cold shock PKA directly inhibits TbPTP1 by phosphorylation at Thr238 (model 1, Figure 7B), a site with an RXXT PKA consensus phosphorylation motif, which according to NetPhosK is predicted to be a PKA phosphorylation site with a probability of 0.58. PKA-dependent inhibition of human tyrosine phosphatases, including PTP1B, has been reported by several studies (Garton and Tonks, 1994; Tao et al., 2001; Howe, 2004). However, TbPTP1 has not been identified as PKA substrate in *T. brucei* by our phosphoproteome screen, rather supporting an indirect mechanism of regulation. Human PTP1B can be phosphorylated and thereby activated by kinases of the cdc2-like kinase (CLK) family (Moeslein et al., 1999). Since a CLK family kinase (Tb11.01.4230) has been identified as putative substrate of *T. brucei* PKA (Table S1, S2), the following pathway would be possible (model 2, Figure 7B): TbPTP1 is phosphorylated and activated by the CLK kinase in BSF cells in the mammalian bloodstream and keeps TbPIP39 in an inactive state. Upon uptake of SS cells by a tsetse fly, PKA is activated by cold shock and phosphorylates the CLK kinase thereby inactivating it. Inactive CLK kinase can no longer phosphorylate and activate TbPTP1 resulting in increased amounts of phosphorylated TbPIP39 that promotes differentiation. Apart from phosphorylation, human PTP1B can be regulated by oxidation, sumoylation or proteolysis (Bourdeau et al., 2005; Dadke et al., 2007; Yip et al., 2010). Several studies report activation of human PTP1B by cleavage mediated by the protease calpain (Frangioni et al., 1993; Franco and Huttenlocher, 2005; Cortesio et al., 2008; Yip et al., 2010). Calpain, which has been suggested by several studies to be negatively regulated by direct phosphorylation by PKA in humans (Jay et al., 2000; Shiraha et al., 2002; Smith et al., 2003; Franco and Huttenlocher, 2005), has been identified as PKA substrate in *T. brucei* by our phosphoproteome

study with a mapped PKA consensus phosphorylation site at S261 (Tb927.8.8330; NetPhosK 0.81), determined by mass spectrometry (Table S1). Assuming that cold shock-activated PKA phosphorylates and thereby inhibits calpain in SS cells, cleavage and hence activation of TbPTP1 would be prevented (model 3, Figure 7B). In turn, phosphorylated, active TbPIP39 would promote differentiation. According to recent SILAC proteome data, calpain expression is strongly downregulated in PCFs (Urbaniak et al., 2012; Butter et al., 2013), supporting a BSF-specific function. Regulation of PTP1 activity by sumoylation could also be dependent on phosphorylation by PKA. Just recently, it has been shown that human PKA is able to promote protein sumoylation by phosphorylation (Su et al., 2012; Lee et al., 2014). Combined inhibition of TbPTP1 by CCA and cold shock-activated PKA (either directly or indirectly) upon uptake of SS trypanosomes by a tsetse fly could result in a larger amount of phosphorylated TbPIP39 eventually causing efficient differentiation to the PCF stage. However, if PKA would directly or indirectly inhibit TbPTP1, cold shock alone should be sufficient to induce differentiation at least to some extent. Yet, it has been shown that CCA but not cold shock alone can induce differentiation (Engstler and Boshart, 2004). An alternative model of action for the parasite PKA in the differentiation process would be regulation of the kinase, which is responsible for phosphorylation of TbPIP39 at Y278 (model 4, Figure 7B). Since phosphorylation of TbPIP39 is essential to promote SS to PCF differentiation, activation of the upstream kinase by a cold shock-induced pathway e.g. upon phosphorylation by cold-induced PKA would be a conceivable scenario. Cold shock alone would not be sufficient to induce differentiation, since active TbPTP1 would immediately dephosphorylate TbPIP39 thereby inactivating it. Only in the tsetse midgut or upon addition of CCA for *in vitro* differentiation, TbPTP1 gets inactivated and SS cells differentiate into PCFs. Due to the absence of conventional tyrosine kinases in most protozoans including *T. brucei*, tyrosine residues are phosphorylated by dual specificity kinases, which are able to phosphorylate substrates at serine, threonine and tyrosine residues (Parsons et al., 2005; Nett et al., 2009). Our phosphoproteome analysis revealed seven protein kinases as putative PKA substrates with mapped, phosphorylated RXXS*/T* sites for two of the kinases, determined by mass spectrometry (Table S2): mitogen-activated protein kinase 2 (MAPK2, Tb927.10.5140), casein kinase I isoform 2 (CK1.2, Tb927.5.800, mapped phosphorylation site S186(p)), glycogen synthase kinase 3 (GSK3, Tb927.10.13780), a protein kinase belonging CLK family of CMGC kinases (Tb11.01.4230), a kinase of the PEK (pancreatic eIF-2 α kinase) kinase family (Tb11.02.5050), and two unique, kinetoplastid-specific kinases (Tb11.01.1050; Tb927.2.2720, phosphorylation sites S492(p), S1427(p)). Dual specificity of orthologous kinases in other organisms has been reported for CLK (Ben-David et al., 1991; Howell et al., 1991; Myers et al., 1994; Lee et al., 1996), CK1 (Ali et al., 1994; Hoekstra et al., 1994; Klimczak et al., 1995; Pulgar et al., 1996; Kametani et al., 2009) and GSK3 (Wang et al., 1994), albeit most of these studies showed only intramolecular autophosphorylation at tyrosine residues and/or were conducted *in vitro* with recombinantly expressed and purified kinase and/or synthetic substrate(s). Dual specificity regarding phosphorylation of downstream substrates is only known from a small group of kinases, e.g. MAPKKs (Dhanasekaran and Premkumar Reddy, 1998) or casein kinase 2 (CK2) (Litchfield, 2003). Although genes encoding these kinases are found in the *T. brucei* genome (Parsons et al., 2005), none of these kinases has been identified as putative PKA substrate. Phosphorylation of tyrosine residues can also be accomplished by atypical tyrosine kinases like Wee1

4. Activation of *T. brucei* PKA

(Squire et al., 2005). Interestingly, although Wee1 is functionally a tyrosine kinase, it most closely resembles serine/threonine kinases such as Chk1 or PKA in structure and sequence. Hence, the large number of unique, kinetoplastid-specific kinases in the *T. brucei* kinome, which cannot be placed into typical groups or families of eukaryotic protein kinases (Parsons et al., 2005), could represent a reservoir of atypical tyrosine or dual specificity kinases. Domain analysis using Pfam 27.0 predicted that the kinetoplastid-specific kinase Tb11.01.1050, which has been identified as putative substrate of *T. brucei* PKA, contains an N-terminal protein tyrosine kinase domain (pos. 32-199) with an E-value of $6.3e^{-08}$. Whether this kinase is able to phosphorylate Y278 of TbPIP39 or tyrosine residues of other trypanosomal proteins is yet an open question. Although highly unlikely, *T. brucei* PKAC1/2 itself could show dual specificity and directly phosphorylate TbPIP39 upon activation by cold shock.

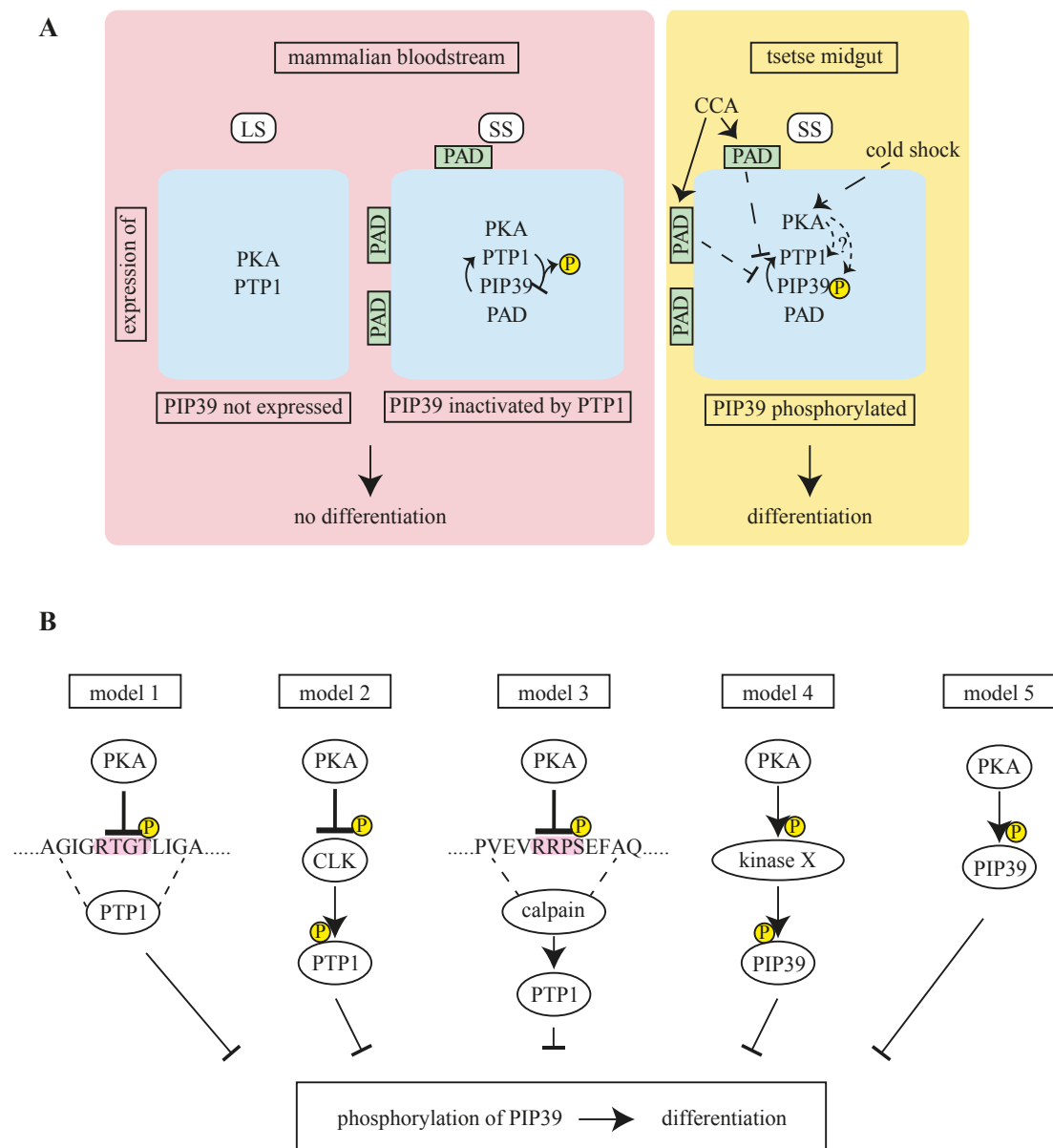


Figure 7: Possible roles of *T. brucei* PKA in SS to PCF differentiation.

A. Expression and regulation of known components of the BSF to PCF differentiation pathway in slender (LS) and stumpy (SS) trypanosomes. In LS cells, PKA and PTP1 are expressed, whereas

PIP39 and PAD proteins are not. Since the presence of phosphorylated PIP39 is a prerequisite of differentiation to the PCF stage, LS cells are unable to differentiate. In the SS stage, all known components of the BSF to PCF differentiation pathway are expressed. However, PTP1 dephosphorylates and inactivates PIP39, thereby preventing differentiation of SS cells in the mammalian bloodstream. PIP39 activates PTP1 and thus enhances its own inhibition. In the tsetse midgut, CCA is taken up by transporters of the PAD family expressed at the surface of SS cells and inhibits the feedback activation of PTP1 by PIP39. For efficient differentiation, additional stimulation by cold shock is required. Cold shock activates the parasite PKA thereby sensitizing the cells to low, physiological concentrations of CCA.

B. Possible modes of action of PKA in BSF to PCF differentiation. The presence of phosphorylated PIP39 is a prerequisite of this differentiation step. In the mammalian bloodstream, PTP1 inhibits PIP39 by dephosphorylation. Upon uptake by a tsetse fly, the trypanosome encounters a cold shock resulting in activation of the parasite PKA, which in turn:

Model 1: directly inhibits PTP1 by phosphorylation at T238.

Model 2: inhibits PTP1 by an inhibitory phosphorylation of its upstream activating CLK kinase Tb11.01.4230.

Model 3: inhibits PTP1 by an inhibitory phosphorylation of its upstream activating protease calpain.

Model 4: activates the kinase, which phosphorylates and thereby activates PIP39.

Model 5: directly phosphorylates and activates PIP39.

Activation of *T. brucei* PKA by low temperature. Usually, the rate of an enzyme-catalyzed reaction increases as the temperature is raised. In addition, each enzyme has a specific temperature optimum. Hence, the observation that low temperature induces the activity of the *T. brucei* PKA orthologue raised the question about the mechanism of activation. In several freeze-tolerant or hibernating animals, purified PKA catalytic subunit showed a higher activity at low temperatures *in vitro*, most likely induced by a temperature-dependent conformational change (Holden and Storey, 1998; MacDonald and Storey, 1998; Holden and Storey, 2000). However, in *T. brucei*, analysis of *in vivo* PKA activity by a specific reporter assay revealed that cold shock activation is dependent on PKAR. If both alleles of *PKAR* were deleted, no temperature-dependent increase in PKA activity was observed excluding a role of the catalytic subunit alone in the activation mechanism. Changes in PKA subunit expression upon a temperature drop as observed in *S. cerevisiae* and human hepatoblastoma cells (Ohsaka et al., 2001; Sahara et al., 2002) cannot account for the increased kinase activity in *T. brucei*, since maximal activation was observed within minutes. Direct or indirect activation mechanisms of *T. brucei* PKA are conceivable. Direct activation by low temperature could be an intrinsic property of the parasite PKA holoenzyme, resulting in a conformational change of PKAR with subsequent release of an active catalytic subunit. We have previously reported that *T. brucei* PKA is indirectly activated *in vivo* by dipyrindamole, an adenosine antimetabolite, suggesting the presence of an endogenous ligand (Bachmaier et al., manuscript, see chapter 4.1). In addition, the kinase can be activated by direct binding of 5-substituted tubercidin analogues to the cryptic cNMP-binding sites of PKAR resulting in holoenzyme dissociation and release of an active catalytic subunit. Hence, it is possible that the cold shock-induced conformational change does not alone induce dissociation of the holoenzyme but sensitizes it to the local concentration of a putative endogenous ligand. Chaperones like the heat shock protein Hsp90, whose expression is up-regulated in response to temperature changes or other cellular stresses in pro- and eukaryotes (Liu et al., 1994; Martinez et al., 2002;

4. Activation of *T. brucei* PKA

Sonoda et al., 2006) thereby assisting the folding of a specific subset of proteins (Young et al., 2001; Delogu et al., 2002; Li et al., 2012), could support a conformational change of PKAR upon a temperature shift. Alternatively, cold shock could induce the production of a putative endogenous ligand, which binds to PKAR resulting in a conformational change and eventually in release of an active catalytic subunit. Reduction in membrane fluidity, inefficient folding of some proteins, or changes in DNA and RNA secondary structure impairing transcriptional and translational efficiency are among the immediate general cellular consequences of a temperature drop (Phadtare, 2004; Phadtare and Severinov, 2010). In bacteria, membranes have been shown to be able to sense temperature changes by alterations in their membrane phase state and microdomain organization, resulting in activation of a two-component signal transduction pathway involving a sensor kinase and a response regulator (Weber and Marahiel, 2003). Interestingly, major changes in the *T. brucei* BSF plasma membrane upon a temperature drop below 26°C have been reported (Ter Kuile et al., 1992). Although several kinases have been described in plants, which are activated in the early response to cold shock (Jonak et al., 1996; Li and Komatsu, 2000; Sangwan et al., 2002), nothing is known about the underlying activation mechanism.

Evolutionary conservation of the PKA downstream signaling pathway? By a phosphoproteomics approach using an anti-Phospho-(SerThr) PKA Substrate antibody, which recognizes the phosphorylated motif RXXS*/T*, for immunoprecipitation, we identified 171 putative substrates of *T. brucei* PKA. Although other kinases like Akt/PKB, RSK or CaMKII are known to have highly similar consensus phosphorylation motifs, treatment with the myristoylated peptide myr-PKI(14-22) derived from the PKA-specific inhibitor PKI (Walsh et al., 1971; Glass et al., 1989; Harris et al., 1997; Dalton and Dewey, 2006) resulted in disappearance of all visible bands detected by the anti-RXXS*/T* antibody, suggesting that the majority of proteins with phosphorylated RXXS*/T* sites were substrates of the parasite PKA. Bioinformatics analysis revealed a role of the kinase in regulation of diverse cellular processes with a high abundance of substrates involved in metabolism and ribosome biogenesis/translation as well as in RNA-binding. This strongly resembles PKA functions known from many other organisms, in which the kinase has pleiotropic functions including regulation of energy metabolism and transcription (Skalhegg and Tasken, 2000; Shabb, 2001; Ptacek et al., 2005; Santangelo, 2006; Livas et al., 2011; <http://www.phosphosite.org> (Hornbeck et al., 2012), www.phospho.elm.eu.org/ (Dinkel et al., 2011)). Interestingly, one third of the identified proteins, comprise kinetoplastid- or *Trypanosoma*-specific proteins with largely unknown function, highlighting the partially unique role of PKA in the evolutionary early branching eukaryote *T. brucei*. The special features of trypanosomal transcription, i.e. transcription in polycistronic units, co-transcriptional trans-splicing and the absence of transcription factors prevent regulation of transcription by PKA at the level of transcription factors. Posttranscriptional regulation in trypanosomes is mainly based on RNA stability and translational efficiency. RNA-associated proteins phosphorylated by *T. brucei* PKA might be important regulators of downstream processes regulated by the kinase. This is consistent with our recent transcriptome study, which showed that PKA regulates processes like translation, transport or metabolism at the posttranscriptional level (Bachmaier et al., manuscript, see chapter 4.1).

References

- Ali, N., Halfter, U., and Chua, N.H. (1994). Cloning and biochemical characterization of a plant protein kinase that phosphorylates serine, threonine, and tyrosine. *J Biol Chem* 269, 31626-31629.
- Alibu, V.P., Storm, L., Haile, S., Clayton, C., and Horn, D. (2005). A doubly inducible system for RNA interference and rapid RNAi plasmid construction in *Trypanosoma brucei*. *Mol Biochem Parasitol* 139, 75-82.
- Ben Amar, M.F., Pays, A., Tebabi, P., Dero, B., Seebeck, T., Steinert, M., and Pays, E. (1988). Structure and transcription of the actin gene of *Trypanosoma brucei*. *Mol Cell Biol* 8, 2166-2176.
- Ben-David, Y., Letwin, K., Tannock, L., Bernstein, A., and Pawson, T. (1991). A mammalian protein kinase with potential for serine/threonine and tyrosine phosphorylation is related to cell cycle regulators. *EMBO J* 10, 317-325.
- Biebinger, S., Wirtz, L.E., Lorenz, P., and Clayton, C. (1997). Vectors for inducible expression of toxic gene products in bloodstream and procyclic *Trypanosoma brucei*. *Mol Biochem Parasitol* 85, 99-112.
- Blaschke, R.J., Monaghan, A.P., Bock, D., and Rappold, G.A. (2000). A novel murine PKA-related protein kinase involved in neuronal differentiation. *Genomics* 64, 187-194.
- Blum, H., Beier, H., and Gross, H.J. (1987). Improved silver staining of plant proteins, RNA and DNA in polyacrylamide gels. *ELECTROPHORESIS* 8, 93-99.
- Boshart, M., Weih, F., Nichols, M., and Schutz, G. (1991). The tissue-specific extinguisher locus TSE1 encodes a regulatory subunit of cAMP-dependent protein kinase. *Cell* 66, 849-859.
- Bourdeau, A., Dube, N., and Tremblay, M.L. (2005). Cytoplasmic protein tyrosine phosphatases, regulation and function: the roles of PTP1B and TC-PTP. *Curr Opin Cell Biol* 17, 203-209.
- Bridges, D.J., Pitt, A.R., Hanrahan, O., Brennan, K., Voorheis, H.P., Herzyk, P., de Koning, H.P., and Burchmore, R.J. (2008). Characterisation of the plasma membrane subproteome of bloodstream form *Trypanosoma brucei*. *Proteomics* 8, 83-99.
- Bringaud, F., Riviere, L., and Coustou, V. (2006). Energy metabolism of trypanosomatids: adaptation to available carbon sources. *Mol Biochem Parasitol* 149, 1-9.
- Broadhead, R., Dawe, H.R., Farr, H., Griffiths, S., Hart, S.R., Portman, N., Shaw, M.K., Ginger, M.L., Gaskell, S.J., McKean, P.G., *et al.* (2006). Flagellar motility is required for the viability of the bloodstream trypanosome. *Nature* 440, 224-227.
- Brun, R., Blum, J., Chappuis, F., and Burri, C. (2010). Human African trypanosomiasis. *Lancet* 375, 148-159.
- Brun, R., and Schonenberger (1979). Cultivation and *in vitro* cloning or procyclic culture forms of *Trypanosoma brucei* in a semi-defined medium. Short communication. *Acta Trop* 36, 289-292.
- Busti, S., Coccetti, P., Alberghina, L., and Vanoni, M. (2010). Glucose signaling-mediated coordination of cell growth and cell cycle in *Saccharomyces cerevisiae*. *Sensors (Basel)* 10, 6195-6240.

4. Activation of *T. brucei* PKA

- Butter, F., Bucerius, F., Michel, M., Cicova, Z., Mann, M., and Janzen, C.J. (2013). Comparative proteomics of two life cycle stages of stable isotope-labeled *Trypanosoma brucei* reveals novel components of the parasite's host adaptation machinery. *Mol Cell Proteomics* 12, 172-179.
- Candiano, G., Bruschi, M., Musante, L., Santucci, L., Ghiggeri, G.M., Carnemolla, B., Orecchia, P., Zardi, L., and Righetti, P.G. (2004). Blue silver: a very sensitive colloidal Coomassie G-250 staining for proteome analysis. *Electrophoresis* 25, 1327-1333.
- Chevallet, M., Luche, S., and Rabilloud, T. (2006). Silver staining of proteins in polyacrylamide gels. *Nat Protoc* 1, 1852-1858.
- Colasante, C., Ellis, M., Ruppert, T., and Voncken, F. (2006). Comparative proteomics of glycosomes from bloodstream form and procyclic culture form *Trypanosoma brucei brucei*. *Proteomics* 6, 3275-3293.
- Cortesio, C.L., Chan, K.T., Perrin, B.J., Burton, N.O., Zhang, S., Zhang, Z.Y., and Huttenlocher, A. (2008). Calpain 2 and PTP1B function in a novel pathway with Src to regulate invadopodia dynamics and breast cancer cell invasion. *J Cell Biol* 180, 957-971.
- Cross, G.A., and Manning, J.C. (1973). Cultivation of *Trypanosoma brucei* spp. in semi-defined and defined media. *Parasitology* 67, 315-331.
- Dadke, S., Cotteret, S., Yip, S.C., Jaffer, Z.M., Haj, F., Ivanov, A., Rauscher, F., 3rd, Shuai, K., Ng, T., Neel, B.G., *et al.* (2007). Regulation of protein tyrosine phosphatase 1B by sumoylation. *Nat Cell Biol* 9, 80-85.
- Dalton, G.D., and Dewey, W.L. (2006). Protein kinase inhibitor peptide (PKI): a family of endogenous neuropeptides that modulate neuronal cAMP-dependent protein kinase function. *Neuropeptides* 40, 23-34.
- Dean, S., Marchetti, R., Kirk, K., and Matthews, K.R. (2009). A surface transporter family conveys the trypanosome differentiation signal. *Nature* 459, 213-217.
- Delauw, M.F., Pays, E., Steinert, M., Aerts, D., Van Meirvenne, N., and Le Ray, D. (1985). Inactivation and reactivation of a variant-specific antigen gene in cyclically transmitted *Trypanosoma brucei*. *EMBO J* 4, 989-993.
- Delogu, G., Signore, M., Mechelli, A., and Famularo, G. (2002). Heat shock proteins and their role in heart injury. *Curr Opin Crit Care* 8, 411-416.
- Dhanasekaran, N., and Premkumar Reddy, E. (1998). Signaling by dual specificity kinases. *Oncogene* 17, 1447-1455.
- Dinkel, H., Chica, C., Via, A., Gould, C.M., Jensen, L.J., Gibson, T.J., and Diella, F. (2011). Phospho.ELM: a database of phosphorylation sites--update 2011. *Nucleic Acids Res* 39, D261-267.
- Engstler, M., and Boshart, M. (2004). Cold shock and regulation of surface protein trafficking convey sensitization to inducers of stage differentiation in *Trypanosoma brucei*. *Genes Dev* 18, 2798-2811.
- Fenn, K., and Matthews, K.R. (2007). The cell biology of *Trypanosoma brucei* differentiation. *Curr Opin Microbiol* 10, 539-546.

- Franco, S.J., and Huttenlocher, A. (2005). Regulating cell migration: calpains make the cut. *J Cell Sci* *118*, 3829-3838.
- Frangioni, J.V., Oda, A., Smith, M., Salzman, E.W., and Neel, B.G. (1993). Calpain-catalyzed cleavage and subcellular relocation of protein phosphotyrosine phosphatase 1B (PTP-1B) in human platelets. *EMBO J* *12*, 4843-4856.
- Fuller, K.K., and Rhodes, J.C. (2012). Protein kinase A and fungal virulence: a sinister side to a conserved nutrient sensing pathway. *Virulence* *3*, 109-121.
- Garton, A.J., and Tonks, N.K. (1994). PTP-PEST: a protein tyrosine phosphatase regulated by serine phosphorylation. *EMBO J* *13*, 3763-3771.
- Glass, D.B., Cheng, H.C., Mende-Mueller, L., Reed, J., and Walsh, D.A. (1989). Primary structural determinants essential for potent inhibition of cAMP-dependent protein kinase by inhibitory peptides corresponding to the active portion of the heat-stable inhibitor protein. *J Biol Chem* *264*, 8802-8810.
- Güther, M.L., Urbaniak, M.D., Tavendale, A., Prescott, A., and Ferguson, M.A. (2014). High-confidence glycosome proteome for procyclic form *Trypanosoma brucei* by epitope-tag organelle enrichment and SILAC proteomics. *J Proteome Res* *13*, 2796-2806.
- Harris, T.E., Persaud, S.J., and Jones, P.M. (1997). Pseudosubstrate inhibition of cyclic AMP-dependent protein kinase in intact pancreatic islets: effects on cyclic AMP-dependent and glucose-dependent insulin secretion. *Biochem Biophys Res Commun* *232*, 648-651.
- Hoekstra, M.F., Dhillon, N., Carmel, G., DeMaggio, A.J., Lindberg, R.A., Hunter, T., and Kuret, J. (1994). Budding and fission yeast casein kinase I isoforms have dual-specificity protein kinase activity. *Mol Biol Cell* *5*, 877-886.
- Hoffman, C.S. (2005). Glucose sensing via the protein kinase A pathway in *Schizosaccharomyces pombe*. *Biochem Soc Trans* *33*, 257-260.
- Holden, C.P., and Storey, K.B. (1998). Protein kinase A from bat skeletal muscle: a kinetic study of the enzyme from a hibernating mammal. *Arch Biochem Biophys* *358*, 243-250.
- Holden, C.P., and Storey, K.B. (2000). Purification and characterization of protein kinase A from liver of the freeze-tolerant wood frog: role in glycogenolysis during freezing. *Cryobiology* *40*, 323-331.
- Hornbeck, P.V., Kornhauser, J.M., Tkachev, S., Zhang, B., Skrzypek, E., Murray, B., Latham, V., and Sullivan, M. (2012). PhosphoSitePlus: a comprehensive resource for investigating the structure and function of experimentally determined post-translational modifications in man and mouse. *Nucleic Acids Res* *40*, D261-270.
- Howe, A.K. (2004). Regulation of actin-based cell migration by cAMP/PKA. *Biochim Biophys Acta* *1692*, 159-174.
- Howell, B.W., Afar, D.E., Lew, J., Douville, E.M., Icely, P.L., Gray, D.A., and Bell, J.C. (1991). STY, a tyrosine-phosphorylating enzyme with sequence homology to serine/threonine kinases. *Mol Cell Biol* *11*, 568-572.
- Hunt, M., Brun, R., and Kohler, P. (1994). Studies on compounds promoting the *in vitro* transformation of *Trypanosoma brucei* from bloodstream to procyclic forms. *Parasitol Res* *80*, 600-606.

4. Activation of *T. brucei* PKA

- Jay, D., Garcia, E.J., Lara, J.E., Medina, M.A., and de la Luz Ibarra, M. (2000). Determination of a cAMP-dependent protein kinase phosphorylation site in the C-terminal region of human endothelial actin-binding protein. *Arch Biochem Biophys* 377, 80-84.
- Jonak, C., Kiegerl, S., Ligterink, W., Barker, P.J., Huskisson, N.S., and Hirt, H. (1996). Stress signaling in plants: a mitogen-activated protein kinase pathway is activated by cold and drought. *Proc Natl Acad Sci U S A* 93, 11274-11279.
- Jones, N.G., Thomas, E.B., Brown, E., Dickens, N.J., Hammarton, T.C., and Mottram, J.C. (2014). Regulators of *Trypanosoma brucei* cell cycle progression and differentiation identified using a kinome-wide RNAi screen. *PLoS Pathog* 10, e1003886.
- Kametani, F., Nonaka, T., Suzuki, T., Arai, T., Dohmae, N., Akiyama, H., and Hasegawa, M. (2009). Identification of casein kinase-1 phosphorylation sites on TDP-43. *Biochem Biophys Res Commun* 382, 405-409.
- Klimeczak, L.J., Farini, D., Lin, C., Ponti, D., Cashmore, A.R., and Giuliano, G. (1995). Multiple isoforms of *Arabidopsis* casein kinase I combine conserved catalytic domains with variable carboxyl-terminal extensions. *Plant Physiol* 109, 687-696.
- Lee, G.Y., Jang, H., Lee, J.H., Huh, J.Y., Choi, S., Chung, J., and Kim, J.B. (2014). PIASy-mediated sumoylation of SREBP1c regulates hepatic lipid metabolism upon fasting signaling. *Mol Cell Biol* 34, 926-938.
- Lee, K., Du, C., Horn, M., and Rabinow, L. (1996). Activity and autophosphorylation of LAMMER protein kinases. *J Biol Chem* 271, 27299-27303.
- Li, J., Soroka, J., and Buchner, J. (2012). The Hsp90 chaperone machinery: Conformational dynamics and regulation by co-chaperones. *Biochimica et Biophysica Acta (BBA) - Molecular Cell Research* 1823, 624-635.
- Li, W.G., and Komatsu, S. (2000). Cold stress-induced calcium-dependent protein kinase(s) in rice (*Oryza sativa* L.) seedling stem tissues. *Theoretical and Applied Genetics* 101, 355-363.
- Litchfield, D.W. (2003). Protein kinase CK2: structure, regulation and role in cellular decisions of life and death. *Biochem J* 369, 1-15.
- Liu, A.Y., Bian, H., Huang, L.E., and Lee, Y.K. (1994). Transient cold shock induces the heat shock response upon recovery at 37 degrees C in human cells. *J Biol Chem* 269, 14768-14775.
- Livas, D., Almering, M.J., Daran, J.M., Pronk, J.T., and Gancedo, J.M. (2011). Transcriptional responses to glucose in *Saccharomyces cerevisiae* strains lacking a functional protein kinase A. *BMC Genomics* 12, 405.
- Loomis, W.F. (1998). Role of PKA in the timing of developmental events in *Dictyostelium* cells. *Microbiol Mol Biol Rev* 62, 684-694.
- MacDonald, J.A., and Storey, K.B. (1998). cAMP-dependent protein kinase from brown adipose tissue: temperature effects on kinetic properties and enzyme role in hibernating ground squirrels. *J Comp Physiol B* 168, 513-525.
- MacGregor, P., Savill, N.J., Hall, D., and Matthews, K.R. (2011). Transmission stages dominate trypanosome within-host dynamics during chronic infections. *Cell Host Microbe* 9, 310-318.

- Martinez, J., Perez-Serrano, J., Bernadina, W.E., and Rodriguez-Caabeiro, F. (2002). Oxidative and cold shock cause enhanced induction of a 50 kDa stress protein in *Trichinella spiralis*. *Parasitol Res* 88, 427-430.
- Matthews, K.R., Sherwin, T., and Gull, K. (1995). Mitochondrial genome repositioning during the differentiation of the African trypanosome between life cycle forms is microtubule mediated. *J Cell Sci* 108 (Pt 6), 2231-2239.
- Moeslein, F.M., Myers, M.P., and Landreth, G.E. (1999). The CLK family kinases, CLK1 and CLK2, phosphorylate and activate the tyrosine phosphatase, PTP-1B. *J Biol Chem* 274, 26697-26704.
- Myers, M.P., Murphy, M.B., and Landreth, G. (1994). The dual-specificity CLK kinase induces neuronal differentiation of PC12 cells. *Mol Cell Biol* 14, 6954-6961.
- Nett, I.R., Martin, D.M., Miranda-Saavedra, D., Lamont, D., Barber, J.D., Mehlert, A., and Ferguson, M.A. (2009). The phosphoproteome of bloodstream form *Trypanosoma brucei*, causative agent of African sleeping sickness. *Mol Cell Proteomics* 8, 1527-1538.
- Oberholzer, M., Langousis, G., Nguyen, H.T., Saada, E.A., Shimogawa, M.M., Jonsson, Z.O., Nguyen, S.M., Wohlschlegel, J.A., and Hill, K.L. (2011). Independent analysis of the flagellum surface and matrix proteomes provides insight into flagellum signaling in mammalian-infectious *Trypanosoma brucei*. *Mol Cell Proteomics* 10, M111 010538.
- Ohsaka, Y., Ohgiya, S., Hoshino, T., and Ishizaki, K. (2001). Cold-stimulated increase in a regulatory subunit of cAMP-dependent protein kinase in human hepatoblastoma cells. *DNA Cell Biol* 20, 667-673.
- Olsen, J.V., Blagoev, B., Gnad, F., Macek, B., Kumar, C., Mortensen, P., and Mann, M. (2006). Global, in vivo, and site-specific phosphorylation dynamics in signaling networks. *Cell* 127, 635-648.
- Overath, P., Czichos, J., and Haas, C. (1986). The effect of citrate/cis-aconitate on oxidative metabolism during transformation of *Trypanosoma brucei*. *Eur J Biochem* 160, 175-182.
- Parsons, M., Worthey, E.A., Ward, P.N., and Mottram, J.C. (2005). Comparative analysis of the kinomes of three pathogenic trypanosomatids: *Leishmania major*, *Trypanosoma brucei* and *Trypanosoma cruzi*. *BMC Genomics* 6, 127.
- Pearce, L.R., Komander, D., and Alessi, D.R. (2010). The nuts and bolts of AGC protein kinases. *Nat Rev Mol Cell Biol* 11, 9-22.
- Perkins, D.N., Pappin, D.J.C., Creasy, D.M., and Cottrell, J.S. (1999). Probability-based protein identification by searching sequence databases using mass spectrometry data. *ELECTROPHORESIS* 20, 3551-3567.
- Phadtare, S. (2004). Recent developments in bacterial cold-shock response. *Curr Issues Mol Biol* 6, 125-136.
- Phadtare, S., and Severinov, K. (2010). RNA remodeling and gene regulation by cold shock proteins. *RNA Biology* 7, 788-795.
- Ptacek, J., Devgan, G., Michaud, G., Zhu, H., Zhu, X., Fasolo, J., Guo, H., Jona, G., Breitkreutz, A., Sopko, R., et al. (2005). Global analysis of protein phosphorylation in yeast. *Nature* 438, 679-684.

4. Activation of *T. brucei* PKA

- Pulgar, V., Tapia, C., Vignolo, P., Santos, J., Sunkel, C.E., Allende, C.C., and Allende, J.E. (1996). The recombinant alpha isoform of protein kinase CK1 from *Xenopus laevis* can phosphorylate tyrosine in synthetic substrates. *Eur J Biochem* 242, 519-528.
- Reuner, B., Vassella, E., Yutzy, B., and Boshart, M. (1997). Cell density triggers slender to stumpy differentiation of *Trypanosoma brucei* bloodstream forms in culture. *Mol Biochem Parasitol* 90, 269-280.
- Rolin, S., Hancocq-Quertier, J., Paturiaux-Hanocq, F., Nolan, D.P., and Pays, E. (1998). Mild acid stress as a differentiation trigger in *Trypanosoma brucei*. *Mol Biochem Parasitol* 93, 251-262.
- Sahara, T., Goda, T., and Ohgiya, S. (2002). Comprehensive expression analysis of time-dependent genetic responses in yeast cells to low temperature. *J Biol Chem* 277, 50015-50021.
- Salazar, C., and Hofer, T. (2009). Multisite protein phosphorylation-from molecular mechanisms to kinetic models. *FEBS J* 276, 3177-3198.
- Sangwan, V., Orvar, B.L., Beyerly, J., Hirt, H., and Dhindsa, R.S. (2002). Opposite changes in membrane fluidity mimic cold and heat stress activation of distinct plant MAP kinase pathways. *Plant J* 31, 629-638.
- Santangelo, G.M. (2006). Glucose signaling in *Saccharomyces cerevisiae*. *Microbiol Mol Biol Rev* 70, 253-282.
- Sbicego, S., Vassella, E., Kurath, U., Blum, B., and Roditi, I. (1999). The use of transgenic *Trypanosoma brucei* to identify compounds inducing the differentiation of bloodstream forms to procyclic forms. *Mol Biochem Parasitol* 104, 311-322.
- Schumann Burkard, G., Jutzi, P., and Roditi, I. (2011). Genome-wide RNAi screens in bloodstream form trypanosomes identify drug transporters. *Mol Biochem Parasitol* 175, 91-94.
- Searle, B.C. (2010). Scaffold: A bioinformatic tool for validating MS/MS-based proteomic studies. *PROTEOMICS* 10, 1265-1269.
- Shabb, J.B. (2001). Physiological substrates of cAMP-dependent protein kinase. *Chem Rev* 101, 2381-2411.
- Shalaby, T., Liniger, M., and Seebeck, T. (2001). The regulatory subunit of a cGMP-regulated protein kinase A of *Trypanosoma brucei*. *Eur J Biochem* 268, 6197-6206.
- Shiraha, H., Glading, A., Chou, J., Jia, Z., and Wells, A. (2002). Activation of m-calpain (calpain II) by epidermal growth factor is limited by protein kinase A phosphorylation of m-calpain. *Mol Cell Biol* 22, 2716-2727.
- Skalhegg, B.S., and Tasken, K. (2000). Specificity in the cAMP/PKA signaling pathway. Differential expression, regulation, and subcellular localization of subunits of PKA. *Front Biosci* 5, D678-693.
- Smith, S.D., Jia, Z., Huynh, K.K., Wells, A., and Elce, J.S. (2003). Glutamate substitutions at a PKA consensus site are consistent with inactivation of calpain by phosphorylation. *FEBS Lett* 542, 115-118.
- Smith, A., Ward, M.P., and Garrett, S. (1998). Yeast PKA represses Msn2p/Msn4p-dependent gene expression to regulate growth, stress response and glycogen accumulation. *EMBO J* 17, 3556-3564.

- Sonoda, S., Fukumoto, K., Izumi, Y., Yoshida, H., and Tsumuki, H. (2006). Cloning of heat shock protein genes (hsp90 and hsc70) and their expression during larval diapause and cold tolerance acquisition in the rice stem borer, *Chilo suppressalis* Walker. *Arch Insect Biochem Physiol* 63, 36-47.
- Squire, C.J., Dickson, J.M., Ivanovic, I., and Baker, E.N. (2005). Structure and inhibition of the human cell cycle checkpoint kinase, Wee1A kinase: an atypical tyrosine kinase with a key role in CDK1 regulation. *Structure* 13, 541-550.
- Su, Y.F., Shyu, Y.C., Shen, C.K., and Hwang, J. (2012). Phosphorylation-dependent SUMOylation of the transcription factor NF-E2. *PLoS One* 7, e44608.
- Subota, I., Julkowska, D., Vincensini, L., Reeg, N., Buisson, J., Blisnick, T., Huet, D., Perrot, S., Santi-Rocca, J., Duchateau, M., *et al.* (2014). Proteomic analysis of intact flagella of procyclic *Trypanosoma brucei* cells identifies novel flagellar proteins with unique sub-localization and dynamics. *Mol Cell Proteomics* 13, 1769-1786.
- Szöör, B., Dyer, N.A., Ruberto, I., Acosta-Serrano, A., and Matthews, K.R. (2013). Independent Pathways Can Transduce the Life-Cycle Differentiation Signal in *Trypanosoma brucei*. *PLoS Pathog* 9, e1003689.
- Szöör, B., Ruberto, I., Burchmore, R., and Matthews, K.R. (2010). A novel phosphatase cascade regulates differentiation in *Trypanosoma brucei* via a glycosomal signaling pathway. *Genes Dev* 24, 1306-1316.
- Szöör, B., Wilson, J., McElhinney, H., Taberner, L., and Matthews, K.R. (2006). Protein tyrosine phosphatase TbPTP1: A molecular switch controlling life cycle differentiation in trypanosomes. *J Cell Biol* 175, 293-303.
- Taminato, A., Bagattini, R., Gorjao, R., Chen, G., Kuspa, A., and Souza, G.M. (2002). Role for YAKA, cAMP, and protein kinase A in regulation of stress responses of *Dictyostelium discoideum* cells. *Mol Biol Cell* 13, 2266-2275.
- Tao, J., Malbon, C.C., and Wang, H.Y. (2001). Insulin stimulates tyrosine phosphorylation and inactivation of protein-tyrosine phosphatase 1B in vivo. *J Biol Chem* 276, 29520-29525.
- Ter Kuile, B.H., Wiemer, E.A., Michels, P.A., and Opperdoes, F.R. (1992). The electrochemical proton gradient in the bloodstream form of *Trypanosoma brucei* is dependent on the temperature. *Mol Biochem Parasitol* 55, 21-27.
- Ubersax, J.A., and Ferrell Jr, J.E. (2007). Mechanisms of specificity in protein phosphorylation. *Nat Rev Mol Cell Biol* 8, 530-541.
- Urbaniak, M.D., Martin, D.M., Ferguson, M.A., 2013. Global quantitative SILAC phosphoproteomics reveals differential phosphorylation is widespread between the procyclic and bloodstream form lifecycle stages of *Trypanosoma brucei*. *Journal of proteome research* 12, 2233-2244.
- Urbaniak, M.D., Guther, M.L., and Ferguson, M.A. (2012). Comparative SILAC proteomic analysis of *Trypanosoma brucei* bloodstream and procyclic lifecycle stages. *PLoS One* 7, e36619.
- Vaidyanathan, P.P., Zinshteyn, B., Thompson, M.K., and Gilbert, W.V. (2014). Protein kinase A regulates gene-specific translational adaptation in differentiating yeast. *RNA* 20, 912-922.

4. Activation of *T. brucei* PKA

- van Deursen, F.J., Thornton, D.J., and Matthews, K.R. (2003). A reproducible protocol for analysis of the proteome of *Trypanosoma brucei* by 2-dimensional gel electrophoresis. *Molecular and Biochemical Parasitology* 128, 107-110.
- Vassella, E., and Boshart, M. (1996). High molecular mass agarose matrix supports growth of bloodstream forms of pleomorphic *Trypanosoma brucei* strains in axenic culture. *Mol Biochem Parasitol* 82, 91-105.
- Vassella, E., Reuner, B., Yutzy, B., and Boshart, M. (1997). Differentiation of African trypanosomes is controlled by a density sensing mechanism which signals cell cycle arrest via the cAMP pathway. *J Cell Sci* 110 (Pt 21), 2661-2671.
- Vertommen, D., Van Roy, J., Szikora, J.P., Rider, M.H., Michels, P.A., and Opperdoes, F.R. (2008). Differential expression of glycosomal and mitochondrial proteins in the two major life-cycle stages of *Trypanosoma brucei*. *Mol Biochem Parasitol* 158, 189-201.
- Walsh, D.A., Ashby, C.D., Gonzalez, C., Calkins, D., and Fischer, E.H. (1971). Purification and characterization of a protein inhibitor of adenosine 3',5'-monophosphate-dependent protein kinases. *J Biol Chem* 246, 1977-1985.
- Wang, Q.M., Fiol, C.J., DePaoli-Roach, A.A., and Roach, P.J. (1994). Glycogen synthase kinase-3 beta is a dual specificity kinase differentially regulated by tyrosine and serine/threonine phosphorylation. *J Biol Chem* 269, 14566-14574.
- Weber, M.H., and Marahiel, M.A. (2003). Bacterial cold shock responses. *Sci Prog* 86, 9-75.
- Wickstead, B., Ersfeld, K., Gull, K. (2002). Targeting of a tetracycline-inducible expression system to the transcriptionally silent minichromosomes of *Trypanosoma brucei*. *Mol Biochem Parasitol* 125, 211-216.
- Yamamizu, K., Fujihara, M., Tachibana, M., Katayama, S., Takahashi, A., Hara, E., Imai, H., Shinkai, Y., and Yamashita, J.K. (2012). Protein kinase A determines timing of early differentiation through epigenetic regulation with G9a. *Cell Stem Cell* 10, 759-770.
- Yao, H., York, R.D., Misra-Press, A., Carr, D.W., and Stork, P.J.S. (1998). The Cyclic Adenosine Monophosphate-dependent Protein Kinase (PKA) Is Required for the Sustained Activation of Mitogen-activated Kinases and Gene Expression by Nerve Growth Factor. *Journal of Biological Chemistry* 273, 8240-8247.
- Yip, S.C., Saha, S., and Chernoff, J. (2010). PTP1B: a double agent in metabolism and oncogenesis. *Trends Biochem Sci* 35, 442-449.
- Young, J.C., Moarefi, I., and Hartl, F.U. (2001). Hsp90: a specialized but essential protein-folding tool. *J Cell Biol* 154, 267-273.
- Zhou, Q., Gheiratmand, L., Chen, Y., Lim, T.K., Zhang, J., Li, S., Xia, N., Liu, B., Lin, Q., and He, C.Y. (2010). A comparative proteomic analysis reveals a new bi-lobe protein required for bi-lobe duplication and cell division in *Trypanosoma brucei*. *PLoS One* 5, e9660.
- Ziegelbauer, K., Quinten, M., Schwarz, H., Pearson, T.W., and Overath, P. (1990). Synchronous differentiation of *Trypanosoma brucei* from bloodstream to procyclic forms *in vitro*. *Eur J Biochem* 192, 373-378.

Acknowledgements

We are grateful to Larissa Ivanova (Munich) for competent technical support. We thank E. Pays for the anonymous cDNA P2 and P. Bastin and K. Gull for the anti-PFR-A/C and the anti-Ty1 hybridoma. This work was supported by the University of Munich and grants DFG 1100/7, BELSPO PAI 6/15, and 1065-86.13/2008 from the German-Israeli Foundation for Scientific Research and Development (GIF) to MB.

5. Bidirectional axenic differentiation of *Leishmania* implicates changes in protein kinase A signaling.

Sabine Bachmaier^{1*}, Ronit Witztum^{2*}, Polina Tsigankov², Roni Koren², Dan Zilberstein², Michael Boshart^{1#}

¹ *Biocenter, Section Genetics, Ludwig-Maximilians-Universität München, 82152 Martinsried, Germany*

² *Faculty of Biology, Technion-Israel Institute of Technology, Haifa 32000, Israel*

* these authors contributed equally to this manuscript.

Manuscript

To whom correspondence should be addressed:

Prof. Dr. Michael Boshart

boshart@lmu.de

Tel.: 49-89-2180-74600

Abstract

Parasitic protozoa of the genus *Leishmania* are obligatory intracellular parasites that cycle between the phagolysosome of mammalian macrophages, where they grow as intracellular amastigotes, and the midgut of female sand flies, where they proliferate as extracellular promastigotes. Shifting between the two environments induces signaling pathway-mediated developmental processes that enable adaptation to both host and vector. Developmentally regulated expression and phosphorylation of protein kinase A (PKA) subunits in *Leishmania* and in *T. brucei* point to an involvement of PKA in parasite development. To assess this hypothesis in *L. donovani*, we determined proteome-wide changes in phosphorylation of PKA substrates. Using a phospho-specific antibody for detection of the conserved PKA phosphorylation motifs RXXS and RXXT, rapid dephosphorylation of PKA substrates was observed upon initiation of promastigote to amastigote differentiation in culture. No phosphorylated substrates were detected in axenic amastigotes. To analyze the kinetics of substrate (re)phosphorylation during axenic reverse differentiation from *L. donovani* amastigotes to promastigotes, we first established a map of this process with morphological and molecular markers. Upon initiation, the parasites rest for 6-12 hours before proliferation of an asynchronous population resumes. After early changes in cell shape, the major changes in molecular marker expression and flagella biogenesis occurred between 24 and 33 hours after initiation. PKA substrate rephosphorylation and expression of the regulatory subunit PKAR1 correlated with promastigote maturation, indicating a promastigote-specific function of PKA signaling. This is supported by the localization of PKAR1 to the flagellum, an organelle absent from amastigote forms. A significant increase in PKA-mediated phosphorylation is part of the ordered changes that characterize the amastigote to promastigote differentiation.

Introduction

Leishmania donovani are intracellular parasitic protozoa that cause kala azar, a fatal form of visceral leishmaniasis in humans. During their life cycle, the parasites shuttle between the midgut of female sand flies, where they proliferate as extracellular flagellated promastigotes, and the phagolysosomes of human macrophages, where they live as aflagellated amastigotes (Herwaldt, 1999). Upon a blood meal of an infected sand fly, virulent metacyclic promastigotes are transmitted to the host and phagocytosed by resident macrophages near the bite (Chang and Dwyer, 1976). Following infection, the parasites encounter a temperature increase of $>10^{\circ}\text{C}$ (from 26 to 37°C) followed by a significant pH shift, from pH 7 in the vector to around pH 5 in the phagolysosome (Zilberstein, 2008).

Development of host-free systems using axenic culture conditions has enabled a better understanding of the molecular mechanism of *Leishmania* intracellular differentiation. *L. donovani* differentiation can be induced by exposing promastigotes to the high temperature and acidity (37°C , pH5.5, 5% CO_2) typically found in the phagolysosome (Saar et al., 1998; Burchmore and Barrett, 2001; Zilberstein, 2008). The axenic amastigotes of both old and new world species have been shown to resemble real animal-derived amastigotes using biochemical and molecular markers (Bates, 1994; Saar et al., 1998; Goyard et al., 2003; Debrabant et al., 2004). Based on morphological criteria, axenic *L. donovani* differentiation consists of four phases (Barak et al., 2005): signal perception with no morphological change (phase I, 0-5 hours); movement cessation and aggregation (phase II, 5-10 hours); morphological transformation to amastigote-shaped cells (phase III, 10-25 hours); and amastigote maturation (phase IV, 25-144 hours). Analyses using high-coverage transcriptomic and proteomic approaches showed that *L. donovani* differentiation is well-regulated with ordered and coordinated changes in mRNA and protein abundance (Saxena et al., 2007; Rosenzweig et al., 2008b) that result in the parasites retooling their metabolic pathways for life in the new host environment. We recently described stage-specific protein phosphorylation patterns (Tsigankov et al., 2013) and have now completed an extensive examination of phosphorylation changes during promastigote-to-amastigote differentiation (Tsigankov et al., 2014).

When amastigote parasites residing in host macrophages are ingested by the vector during a blood meal, sensing of a colder and more alkaline environment in the fly gut induces development into the promastigote insect stage. Temperature and pH are also well-known triggers of life cycle stage differentiation in the related kinetoplastid parasite *Trypanosoma brucei*, the causative agent of Human African sleeping sickness (Czichos et al., 1986; Overath et al., 1986; Rolin et al., 1998; Engstler and Boshart, 2004; Szöör et al., 2013). In *T. brucei*, the regulatory pathway that controls differentiation from the mammalian to the fly stage in a culture model of differentiation involves a cascade of the protein phosphatases PTP1B and PIP39 (Szöör et al., 2006; Szöör et al., 2010) and protein kinases RDK1 and RDK2 (Jones et al., 2014), indicating the dominant role of protein phosphorylation in the process. The high phosphorylation dynamics during promastigote to amastigote differentiation (Tsigankov et al., 2014) also suggests that protein phosphorylation cascades are involved in the developmental regulation of *Leishmania* parasites.

Several observations suggest an involvement of PKA signaling in regulation of the differentiation process in *Leishmania*: (1) a catalytic subunit of PKA termed c-Lpk2 (the orthologue of *T. brucei*

PKAC3 (Bachmaier and Boshart, 2013)) is differentially expressed in the promastigote and the amastigote stage at the mRNA level and undergoes temperature-dependent regulation at the level of mRNA stability (Siman-Tov et al., 1996); (2) an orthologue of the regulatory subunit of PKA is regulated during promastigote to amastigote differentiation and has been suggested to be important for metacyclogenesis based on reverse genetic analysis (Bhattacharya et al., 2012); (3) the abundance of consensus PKA phosphorylation motifs (RRXS, RXXS) shows stage-specific regulation (Tsigankov et al., 2013) and (4) a *Leishmania*-specific protein with similarity to the PKA regulatory subunit contains 12 sites that are differentially phosphorylated during promastigote to amastigote differentiation (Tsigankov et al., 2014). These observations prompted us to study the kinetics of PKA-specific phosphorylation during differentiation in more detail.

Using antibodies recognizing the PKA-specific substrate phosphorylation motif RXXS*/T* (* phosphorylation), we investigated changes in PKA phosphorylation activity during the complete life cycle of *L. donovani*, i.e. during bidirectional axenic differentiation from promastigote to amastigote as well as from amastigote to promastigote forms. Interestingly, we observed that PKA-mediated phosphorylation faded completely and rapidly at the end of phase I of promastigote differentiation to amastigotes. During the reverse differentiation process from the amastigote to the promastigote stage, PKA-dependent phosphorylations reappeared more gradually and peaked during terminal promastigote maturation. This study provides direct evidence that PKA substrate phosphorylation is correlated with stage differentiation and is particularly important for promastigote-specific functions.

Materials and Methods

Cell culture and differentiation of *L. donovani*. A cloned line of *L. donovani* 1SR cells was used in all experiments (Saar et al., 1998). Promastigotes were grown at 26°C in medium 199 (Sigma, St. Louis, MO, USA) supplemented with 10% fetal calf serum (FCS). Differentiation of promastigotes to amastigotes in axenic culture was carried out as in Barak et al. (2005). To initiate differentiation of axenic amastigotes to promastigotes, log phase axenic amastigotes ($0.5-1 \times 10^7$ cells/ml) were centrifuged using a table swing out centrifuge at $1244 \times g$ for 10 minutes at room temperature (22-25°C). Subsequently, the cell pellet was resuspended in promastigote medium (M199 at pH 7 + 10% FCS) to a density of 0.5×10^6 cells/ml and incubated at 26°C. Aliquots were taken after 3, 6, 10, 16, 20, 24, 30, 33, 48 and 96 hours. At each time point, parasites were collected, washed in phosphate buffered saline (PBS) and used for microscopy and lysate sampling.

Cultivation of *Trypanosoma b. brucei* and generation of transgenic lines. Bloodstream forms of the monomorphic strain Lister 427, variant MiTat1.2 (Cross and Manning, 1973) were cultivated at 37°C in a 5% CO₂ atmosphere in modified HMI-9 medium (Vassella et al., 1997) supplemented with 10% (v/v) heat-inactivated fetal bovine serum. A homozygous deletion mutant of the regulatory subunit of protein kinase A (*PKAR*) (Tb427tmp.02.2210) was generated by transfection of MiTat1.2 with the plasmids pBSK.PKARko.puro and pBSK.PKARko.hygro. These constructs contained a puromycin or hygromycin resistance cassette, respectively, flanked by actin UTRs and the *PKAR* UTRs. The constructs were digested with KpnI and XmnI for transfection, and *PKAR* knock out cells were grown in the presence of 0.05 µg/ml puromycin and 1 µg/ml hygromycin B. The *L. donovani* *PKAR* ORF (LdBPK_130160.1) was amplified from genomic DNA of *L. donovani* strain Lo8 and cloned into the pBSK.phleo backbone containing the phleomycin resistance cassette flanked by actin UTRs and *T. brucei* *PKAR* UTRs. The construct was digested with KpnI and XmnI for transfection, and antibiotic selection was performed by addition of 2.5 µg/ml phleomycin to the culture medium.

Antibodies. The gene encoding the *L. donovani* 2,3-trans-enoyl CoA isomerase precursor (LdteCi1, LdBPK_312400.1) was cloned into pGEX4T-1 and expressed in *E. coli*-E151. Bacteria formed inclusion bodies of expressed LdteCi1 were extracted according to Sambrook and Russell (2001), and 0.5 mg of recombinant LdteCi1 protein was injected into rabbits with five consecutive boosts. Injections and bleedings were carried out as a contracted service by Sigma-Aldrich. Antiserum was used at a dilution of 1:1000. For production of a polyclonal antibody against *T. brucei* PKAR, the full-length protein was expressed as C-terminal hexahistidine fusion protein in *E. coli* M15 and purified under denaturing conditions using Ni-NTA columns (Qiagen). After separation of the concentrated protein fractions on a 10% SDS gel, rabbits were immunized with Coomassie-stained PKAR containing gel slices according to a standard immunization protocol (BioScience, Göttingen). Affinity purification of the antibody was performed according to the method of Olmsted (1981). A dilution of 1:250-1:500 was used for Western blot analysis. Other antibodies used were: anti-Hsp90 and anti-Hsp100 (Hubel et al., 1997; kindly provided by Dr. Joachim Clos, Bernhart Nocht Institute, Hamburg), L13D6 monoclonal antibodies against *Leishmania* paraflagellar rod 2C (LinJ.16.1510 and LinJ.16.1520) and *T. brucei* PFR-A/C (Kohl et al., 1999; kindly provided by Dr. Philippe Bastin,

Institute Pasteur, Paris) and Phospho-(Ser/Thr) PKA substrate antibody (1:1000; Cell Signaling Technologies, catalog number 9621).

Western blot analyses. Western blot analyses of *L. donovani* and *T. brucei* lysates were performed as previously reported (Barak et al., 2005; Salmon et al., 2012) using either luminol reagent for detection of peroxidase-conjugated secondary antibodies, or fluorescently labeled secondary antibodies (IRDye 680LT goat anti-rabbit IgG (H+L), 1:50000; IRDye 800CW goat anti-mouse IgG (H+L), 1:5000; IRDye 800 donkey anti-chicken; 1:5000; all from LI-COR) and the Odyssey™ IR fluorescence scanning system (LI-COR). For quantification, signals were normalized to the Hsp90 internal control after automatic subtraction of the background values (median left/right method) using the Odyssey software (LI-COR).

Growth and cell cycle analyses. Radiolabeled thymidine (³H-thymidine, Perkin-Elmer Inc.) incorporation into differentiating axenic *L. donovani* was used to determine the rate of cell proliferation as previously described (Shaked-Mishan et al., 2001). At different time points of amastigote to promastigote differentiation, cell aliquots were collected and subjected to flow cytometry as described previously (Barak et al., 2005). For each assay, 5 ml of cell culture ($0.5\text{--}1\times 10^7$ cells/ml) were collected, washed twice with PBS and suspended in 70% ice-cold methanol for fixation. These cells were kept at -20°C for further use. Prior to analysis, the cells were treated with 20 mg/ml RNase A for one hour at 37°C . Subsequently, DNA was stained using propidium iodide and 20,000 cells were analyzed for DNA content using the BD LSR-II flow cytometer (Becton Dickinson). The distribution of G1, S and G2/M phases was calculated from each histogram using FCS Express 4 flow cytometry (Denovo Software Inc.).

Scanning electron microscopy. At each time point, 1×10^8 cells were washed once ($1244\times g$, 10 min, room temperature) in PBS and subsequently settled on poly-L-lysine coated silicon discs. Cells were fixed using 2.5% glutaraldehyde, washed three times in PBS and dehydrated in increasing concentrations of ethanol, from 30 to 100%, followed by critical point drying (CPD, Baltek Inc.). Finally, cells were viewed in a FEI E-SEM Quanta-200 scanning electron microscope.

Fluorescence microscopy. For immunofluorescence, mid-log *L. donovani* axenic promastigotes and amastigotes (1×10^8 cells) were fixed in 1% formaldehyde/PBS on a slide for 10 min, followed by permeabilization with 0.2% Triton X-100/PBS for 10 min. Blocking in 10% (v/v) non-fat dried skimmed milk powder/PBST for 30 minutes was followed by incubation with anti-TbPKAR antiserum (1:50 dilution) for 1 h (all at room temperature). Polyclonal goat anti-rabbit IgG conjugated to Cy3 (1:500 dilution; Jackson Inc.) was used as secondary antibody. For counterstaining, rabbit anti *L. donovani* membranes IgG (1:2000 dilution; Saar et al., 1998) and polyclonal goat anti-rabbit IgG conjugated to Alexa 488 (1:500 dilution; Jackson Inc.) were used. Cellular DNA was stained with DAPI (4',6-diamidino-2-phenylindole; Fluka; $0.25\ \mu\text{g/ml}$), and cells were imaged with a Zeiss LSM 700 Inverted confocal laser scanning microscope.

Results

Protein kinase A (PKA)-mediated signaling was investigated as candidate pathway implicated in stage differentiation in *Leishmania*, mainly motivated by the observed stage-specific expression and phosphorylation of PKA subunits (Siman-Tov et al., 1996; Rosenzweig et al., 2008a; Bhattacharya et al., 2012; Tsigankov et al., 2013; Tsigankov et al., 2014). Global patterns of PKA substrate phosphorylation can be probed by phospho-specific antibodies specifically detecting the RXXS*/T* peptide motif that characterizes a large fraction of all known PKA phosphorylation sites in a broad range of organisms and substrates (Shabb, 2001). We have used this tool to probe the degree of proteome-wide PKA substrate phosphorylation during axenic promastigote to amastigote differentiation using the established differentiation protocol of Barak et al. (2005). In promastigotes (Fig. 1A, t=0), many proteins, most prominently visible as a cluster of bands in the 50-60 kDa range, were detected by the phospho-specific antibody. Interestingly, the abundance of these RXXS*/T* phospho-sites decreased ~5-fold within 6 h of differentiation, i.e. the end of phase I (Barak et al., 2005). This lower level of phosphorylation remained unchanged through subsequent phases of differentiation and in mature amastigotes. Remarkably, exposure of promastigotes to amastigote growth conditions for only 10 minutes resulted in complete loss of PKA-dependent phosphorylations (Fig. 1B), excluding the possibility that changes in the expression level of PKA substrates account for the altered phosphorylation pattern. Furthermore, we show that the RXXS*/T*-specific antibody detects PKA-specific phosphorylation. In the related organism *T. brucei*, RXXS/T phosphorylation is completely abolished upon incubation with the cell-permeable, myristoylated derivative of the PKI (14-22) peptide inhibitor (Supplementary Fig. S1). PKI is the gold standard PKA-specific inhibitor (Walsh et al., 1971; Glass et al., 1989; Harris et al., 1997; Dalton and Dewey, 2006). Moreover, in a mutant cell line with homozygous deletion of the *T. brucei* gene encoding the regulatory subunit of PKA (lane $\Delta pkar/\Delta pkar$ in Supplementary Fig. S1 and Fig. S2), RXXS/T phosphorylation is strongly reduced. Since PKA is a complex of catalytic and regulatory subunits, the $\Delta pkar/\Delta pkar$ mutant still expresses low amounts of catalytic subunits (data not shown) and therefore is not expected to abolish substrate phosphorylation completely (Supplementary Fig. S1, lane $\Delta pkar/\Delta pkar$).

We then asked whether PKA substrates or PKA substrate phosphorylation reappeared upon differentiation of amastigotes back to promastigotes in culture. To initiate differentiation, logarithmic phase axenic amastigotes grown in amastigote medium were shifted to promastigote growth conditions (see Materials and Methods, section 2.1). Subsequently, parasite aliquots were collected at the indicated time points after initiation of differentiation and probed for RXXS/T phospho-sites (Fig. 1C). Phosphorylated RXXS/T sites became detectable 24 hours after initiation of differentiation and reached the maximum level at 48 hours.

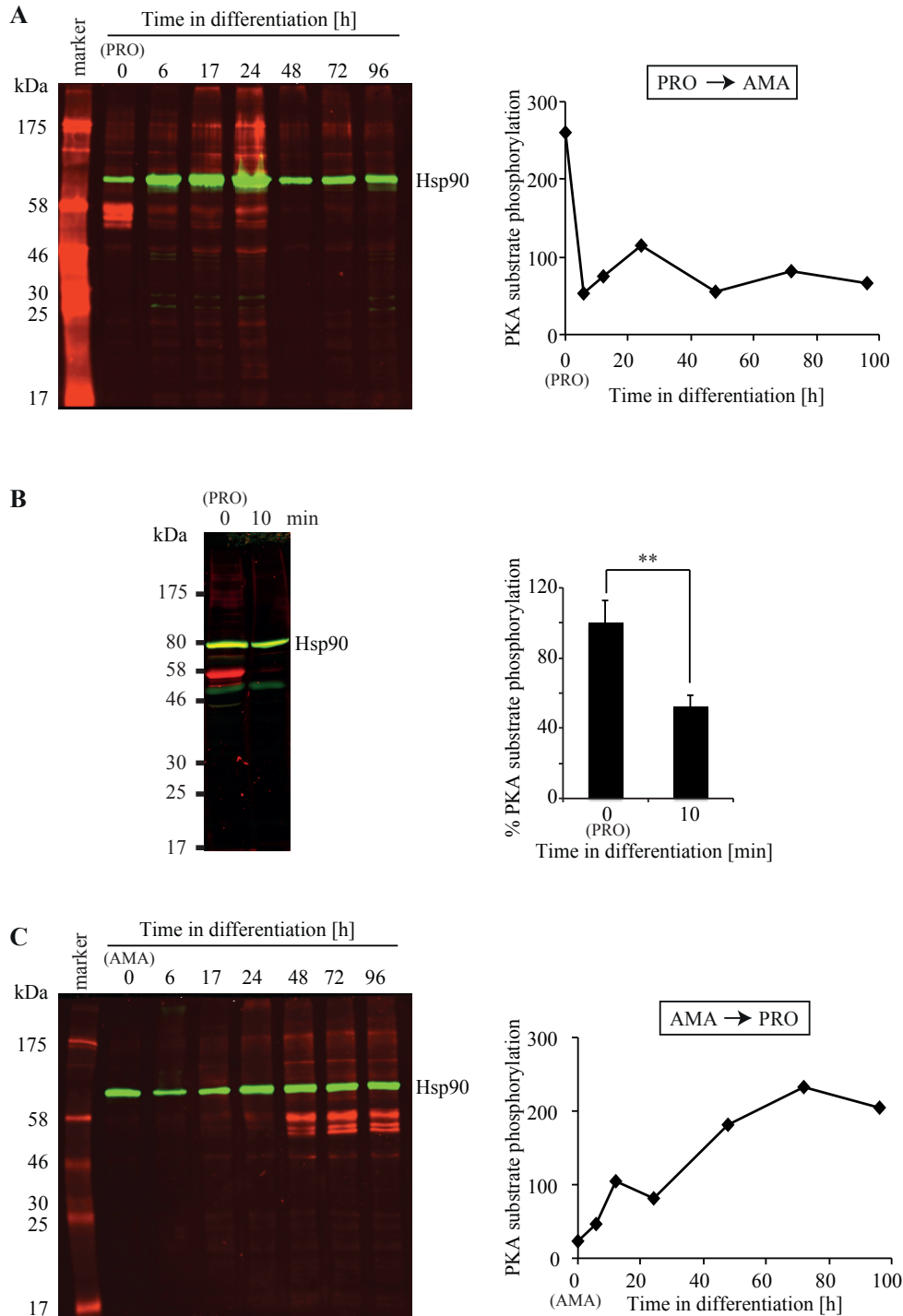


Figure 1: Regulation of phosphorylated PKA substrates during differentiation of *L. donovani*. Lysates were prepared at the indicated time points after initiation of differentiation. Western blot analysis during promastigote to amastigote (A) or amastigote to promastigote (C) differentiation was performed using antibodies specifically detecting Phospho-(Ser/Thr) RXXS/T sites, mainly representing phosphorylated PKA substrates. The abundance of these phospho-sites was quantified by fluorescence imaging and normalized to Hsp90 as loading control (graphs adjacent to the Western blots; y-axes represent normalized intensity counts). A minor and transient upregulation of Hsp90 in amastigotes has been reported (Krobitch et al., 1998), which may lead to maximally 1.5-fold overestimation of regulation at some time points. (B) Regulation of PKA substrate phosphorylation upon exposure of *L. donovani* promastigotes to differentiation conditions for 10 min.

5. *Leishmania donovani* PKA

The quantification shows the mean of six independent biological replicates; error bars represent SEM; significance was determined using the Excel Add-in QI Macros, 2014, with a two-tailed T-test assuming equal variances (determined by F-test). Note that in (B) less material has been loaded compared to (A) and (C).

As the time course of axenic amastigote to promastigote differentiation has not been described in detail, we were unable to correlate the reappearance of phosphorylated PKA sites (Fig. 1C) with a particular process during differentiation. Therefore, the morphology was recorded in a time course of *L. donovani* amastigote to promastigote differentiation (Fig. 2). Samples were collected at 0, 3, 6, 8, 16, 24, 33, 40, 48 and 96 hours after shift to promastigote growth conditions for morphologic analysis using scanning electron microscopy. No change in amastigote morphology was observed during the first 3 hours (Fig. 2A-B). At 6 hours, one third of the parasite population started to elongate, but with no sign of flagella biogenesis (C). The proportion of elongated cells increased to 44% at 8 hours, and at 16 hours two thirds were elongated almost to the length of mature promastigotes but still had no visible flagella (D-E). First signs of flagellar emergence were observed at 24 hours after initiation of differentiation. At this time point, all cells in culture were elongated, 19% of them had developed short flagella (F). At 33 hours, most cells had visible flagella (G), and at 40 hours, the culture contained predominantly mature promastigotes as judged by morphology and motility (H-J). Thus, as displayed in Fig. 1C, the PKA-specific phospho-sites first became visible at 24 hours, when flagella emerged.

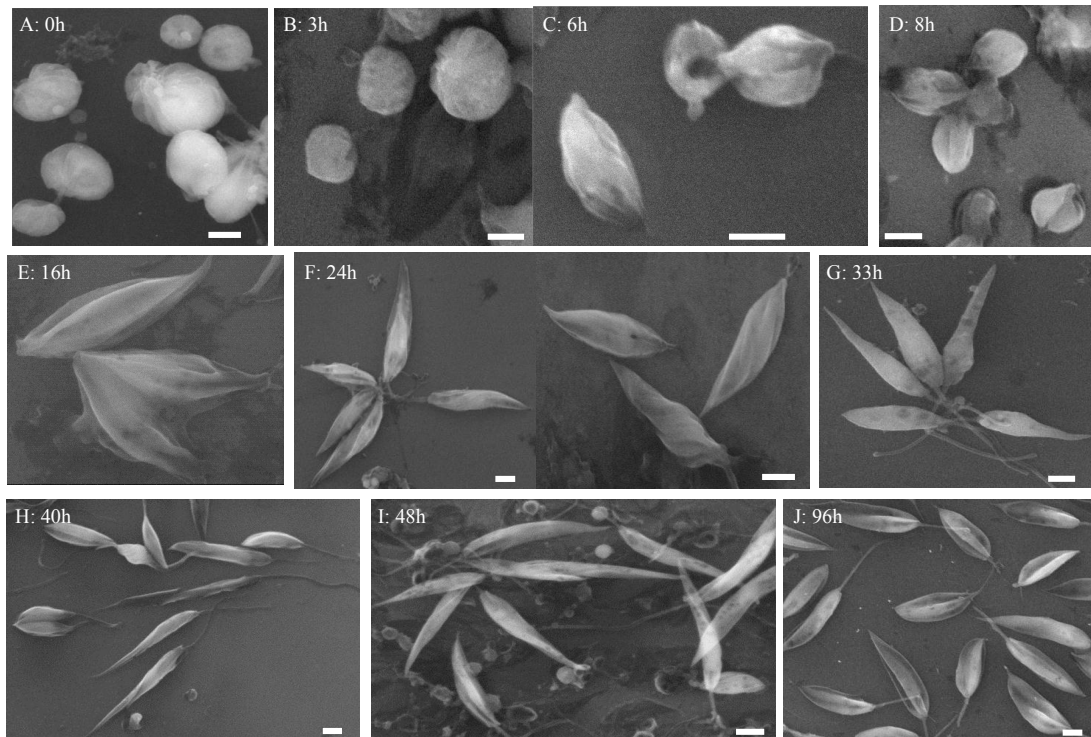


Figure 2: Time course of axenic amastigote morphogenesis to promastigotes during differentiation in vector-free culture. Axenic amastigotes were subjected to promastigote growth medium as described in Materials and Methods (section 2.1), and aliquots were collected at the indicated time points after initiation of differentiation for scanning electron microscopy (see Materials and Methods, section 2.6). Cell body elongation is detected as early as 6 hours after medium change. Flagellated promastigote-like cells first appeared at 24 hours after differentiation was initiated. Bars represent 2 μ m.

The growth curve of a representative differentiation experiment (Fig. 3A) suggests that upon initiation of differentiation, amastigotes rest for about 12 h before they reinitiate proliferation as elongated cells and show signs of flagellar outgrowth. This is reminiscent of promastigote to amastigote differentiation, which is initiated by growth arrest and synchronization of cells in the G1 phase of the cell cycle (Barak et al., 2005). We therefore determined thymidine incorporation in a time course of differentiation. As shown in Fig. 3B (grey squares), the rate of thymidine incorporation dropped within the first 6 hours after transferring amastigotes to promastigote growth conditions and then steeply increased 8-fold within the following 27 hours. At later time points, the rate of thymidine incorporation returned to the level of promastigotes (about 2.5 times higher than that of amastigotes). The fraction of cells in S-phase was also determined by DNA content analysis using flow cytometry (Fig. 3B, black diamonds). The S-phase fraction initially dropped to a minimum value during the first 6 hours of differentiation and then peaked at ~16 hours and ~32 hours. As the population doubling time of the differentiating population is around 16 hours (Fig. 3A), the double peak might reflect transient synchronization when cells reenter the cell cycle. Thymidine incorporation does not show this double peak, probably due to the length of the labeling pulse. The consistent results of both thymidine incorporation and flow cytometry confirmed an initial cell cycle arrest prior to differentiation of amastigotes to promastigotes. After the lag, a constant growth rate (population doubling time of 16 h) indicates that differentiation in culture is an efficient process (Fig. 3A). The possible transient synchronization is not maintained (not shown).

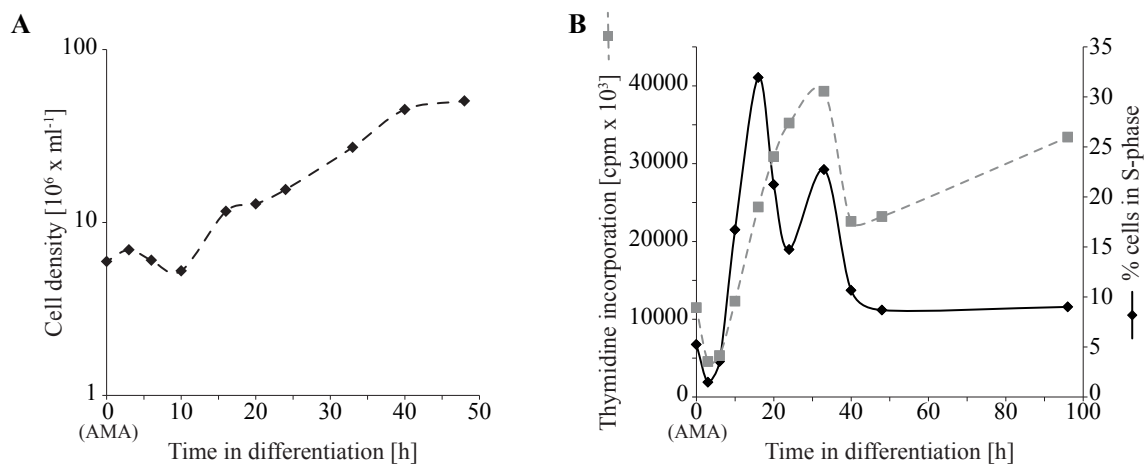


Figure 3: Growth arrest during *L. donovani* amastigote to promastigote differentiation. Aliquots of amastigote cells inoculated in promastigote culture medium were collected at the indicated time points. (A) Growth curve. From the linear regression of values between 10 and 50 hours after initiation of differentiation, a population doubling time of 16 hours is estimated. (B) Cell cycle analysis: aliquots of cells were pulse labeled for 1 hour with [^3H]-thymidine, nuclei were purified, and radioactivity was determined by scintillation counting (\blacksquare). Values represent the average of two independent biological replicates. Additional aliquots were subjected to RNase A treatment followed by propidium iodide staining and flow cytometry to quantify DNA content and determine the relative number of S phase cells (\blacklozenge). Data points represent the average of three biological replicates.

We also have used protein markers to relate the abundance of PKA-specific phospho-sites to the kinetics of amastigote to promastigote differentiation. The first marker is a putative 2,3-trans-enoyl CoA isomerase precursor (LdteCi1, LdBPK_312400.1) whose protein abundance increases 7-fold at late stages of promastigote to amastigote differentiation (Saxena et al., 2007; Rosenzweig et al., 2008a). The *L. donovani* genome contains encodes a second isoforms of this protein: LdteCi2 (LdBPK_312320.1) is 89% identical to LdteCi1, but lacks 7 amino acids near its N-terminus and has a divergent C-terminal region. Antibodies raised against LdteCi1 detect both isoforms with LdteCi1 showing a slightly higher molecular weight (data not shown). As shown in Fig. 4A, axenic amastigotes express predominantly LdteCi1. This level of expression remains unchanged during the first 24 hours of amastigote to promastigote differentiation, when the parasites complete elongation but still lack flagella. Later the level decreases. LdteCi2 is expressed in amastigotes at a low level, and its abundance increases from 24 hours on. The second marker is the paraflagellar rod 2C protein (PFR2C; LdBPK_161520.1). Previous proteomic analysis indicated that this protein is hardly expressed in amastigotes (Rosenzweig et al., 2008a). This was further confirmed using monoclonal antibodies against PFR2C (Fig. 4A, middle row). Amastigotes also do not express *PFR2C* mRNA (Lahav et al., 2011). The PFR2C protein appeared on the Western blot at 33 hours after differentiation initiation. This perfectly corresponds to the time when flagella have emerged in most differentiating cells (33 h in Fig. 2G), as expected for a protein that has been associated with flagellar motility in promastigotes (Santrich et al., 1997). The third marker is Hsp100, whose expression is induced by elevated temperature and thus is expressed at higher level in amastigotes (Hubel et al., 1997; Krobitch et al., 1998). As shown in the lower row of Fig. 4A and in agreement with Rosenzweig et al. (2008a), Hsp100 abundance dropped 24 hours after differentiation initiation. Important changes in marker protein expression thus occur between 24 and 33 h after initiation of differentiation, i.e. at least 12 h after the onset of proliferation. Comparing the differentiation marker kinetics with the kinetics in Fig. 1C, we conclude that the change of PKA phospho-site abundance is not an early event in amastigote to promastigote differentiation, but correlated with promastigote maturation. This suggests stage-specific roles of PKA signaling. Expression of the regulatory subunit of PKA (LdPKAR1) was also quantified during differentiation. The antibody used was raised against *T. brucei* PKAR and cross-reacts sensitively and specifically with the transgenically expressed *L. donovani* protein (Supplementary Fig. S2). Fig. 4B shows stage-specific regulation of LdPKAR1 expression. A low level in amastigotes contrasts with a 3- and 5-fold increase after 24 and 48 hours, respectively, post initiation of differentiation. The regulatory subunit binds and inhibits the catalytic subunit, and its amount correlates with maximally stimulatable PKA activity, as PKA R and C subunits are co-regulated due to instability of free catalytic subunits in most cells including *T. brucei* (see Supplementary Fig. S1, lane $\Delta pkar/\Delta pkar$). Interestingly, LdPKAR1 was predominantly localized to the flagellum of promastigotes as seen by immunofluorescence microscopy (Fig. 4C), but was undetectable in amastigotes that do not have a flagellum. This is in agreement with stage-specific expression of LdPKAR1 shown in Fig. 4B. In summary, PKA-specific phosphorylation of many substrates increases during amastigote to promastigote differentiation, implicating this kinase in a regulatory process important for promastigote maturation, function or promastigote adaptation to environmental conditions.

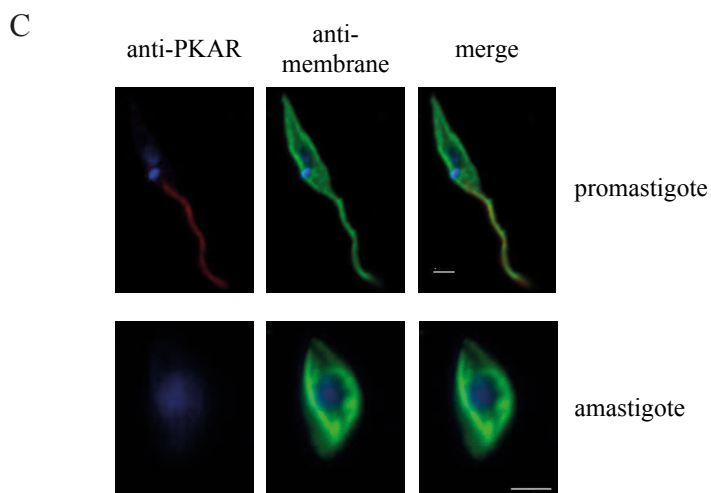
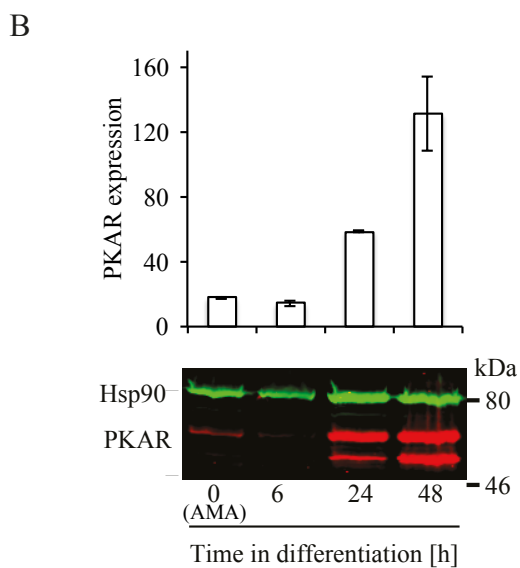
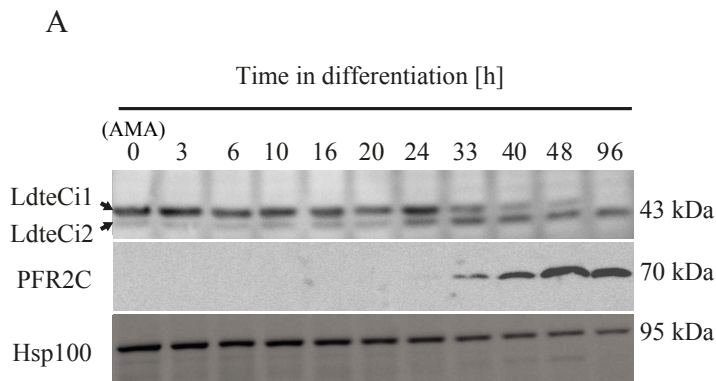


Figure 4: Expression of marker proteins and PKAR during axenic differentiation of amastigotes into promastigotes. (A) Lysates were prepared from parasites at the indicated time points after differentiation was initiated. Western blot analysis was performed with: rabbit anti-2,3-trans-enoyl CoA isomerase precursor (LdteCi1, LdBPK_312400.1), mouse anti-paraflagellar rod protein 2C (PFR2C), and chicken anti-Hsp100. Secondary antibodies coupled to horseradish peroxidase were used for chemiluminescence detection. Equal cell numbers were loaded. (B) Lysates were prepared from parasites at the indicated time points after differentiation was initiated. LdPKAR1 was quantified by fluorescence detection on Western blots with a cross-reacting anti-TbPKAR antiserum and anti-Hsp90 as internal reference for normalization. Anti-PKAR antibody specificity is documented in Supplementary Fig. S2. The graph gives the mean and the range of LdPKAR1 abundance from two independent biological replicates, one of which is shown as Western blot. The y-axis represents normalized intensity counts. (C) Subcellular localization of LdPKAR1 by confocal fluorescence microscopy of promastigotes and amastigotes stained with the PKAR-specific antibody (red channel). The cell surface is counterstained with anti *L. donovani* membranes IgG (green channel), and DNA is stained with DAPI. The size bar corresponds to 2 μ m. Fluorescence was monitored using a Zeiss LSM 700 Inverted confocal laser scanning microscope.

Discussion

This study uses an established protocol for axenic differentiation of *Leishmania* promastigotes to amastigotes (Barak et al., 2005) and axenic reverse differentiation of amastigotes to promastigotes to generate a complete life cycle profile of PKA substrate phosphorylation.

In vitro systems that simulate parasite development are essential tools for the discovery of host and vector signals that enable parasites to identify their host environment and subsequently activate the signaling pathways that stimulate their transformation from one developmental stage to the other.

The axenic reverse amastigote to promastigote differentiation has been reported previously (Duncan et al., 2001) but has not been correlated to defined morphological events. Analyzing the kinetics of this developmental process, we detected a transient growth and cell cycle arrest that precedes the changes in marker expression and morphology. This arrest may be important for reprogramming of gene expression. Resetting the cell cycle may also be required to enable cytoskeletal changes associated with morphogenesis and flagellar biogenesis. A transient cell cycle arrest is a defining feature of kinetoplastid differentiation, as described in detail for promastigote to amastigote differentiation in *Leishmania* (Barak et al., 2005) and bloodstream to procyclic differentiation in *T. brucei* where a well-defined arrested life cycle stage, the stumpy bloodstream form, exists (Vickerman, 1985; Vassella et al., 1997; MacGregor et al., 2011; MacGregor et al., 2012).

In *T. brucei*, bloodstream to procyclic stage differentiation is co-stimulated by a temperature shift of > 10°C, termed cold shock (Engstler and Boshart, 2004; Dean et al., 2009; Szöör et al., 2010). Similarly, shifting *L. donovani* amastigotes from body temperature (37°C) to insect temperature (26°C) together with a change in pH was sufficient to induce differentiation of axenic amastigotes into promastigotes within 24-30 hours.

The global detection of PKA substrate phosphorylation in *L. donovani* showed strong developmental regulation. The rapid and almost complete loss of phosphorylated PKA substrates upon initiation of promastigote to amastigote differentiation within minutes can only be explained by a change in the balance between the kinase and counteracting protein phosphatases. A very fast proteolysis of all of these substrates with a similar time course is highly unlikely. Inactivation of the kinase is the most likely event initially triggered. In fact, this is followed by a second phase of down-regulation of the mRNA encoding a catalytic subunit of PKA (*c-Lpk2*; Siman-Tov et al., 1996; Duncan et al., 2001) and of the regulatory subunit LdPKAR1 (LdBPK_130160.1) (Fig. 4B). During the reverse differentiation of amastigotes to promastigotes, phosphorylated PKA substrates and, by inference, PKA activity rose only later and gradually after the initial growth arrest phase and reached high levels during maturation of promastigotes. This again corresponds perfectly to the profile of *c-lpk2* mRNA expression during amastigote to promastigote differentiation (Duncan et al., 2001). The rapid loss of PKA substrate phosphorylation upon promastigote to amastigote differentiation suggests that PKA activity and signaling are dispensable in amastigotes but required for promastigote-specific functions. In agreement with this argument, LdPKAR1 is specifically localized in the flagellum, a structure essentially absent from amastigotes. A flagellar localization has also been observed for the *T. brucei* PKAR orthologue (Krumbholz C. and Boshart M., unpublished), consistent with its identification in the soluble flagellar proteome (Oberholzer et al., 2011; Subota et al., 2014). Reverse genetic depletion

in *T. brucei* has furthermore established a role for PKAR in flagellar motility (Oberholzer et al., 2011; Krumbholz and Boshart, unpublished). Yet, the role of PKA seems not to be limited to flagellar motility as overexpression of LdPKAR1 in *L. donovani* accelerates autophagy, a starvation-induced cytological event necessary for metacyclogenesis (Bhattacharya et al., 2012). Surprisingly, the protein detected by the anti-PKAR1 antibody used in Bhattacharya et al. (2012) is distributed evenly in the cell body but excluded from the flagellum. Moreover, the developmental expression profile of LdPKAR1 deviates significantly from the profile shown here (Fig. 4B). Since the specificity of our anti-PKAR antibody has been proven by a gene knock out and a genetic rescue (Supplementary Fig. S2), it remains possible that Bhattacharya et al. (2012) do not detect the same protein (LdBPK_130160.1) in *L. donovani* cells. The phosphorylation kinetics suggests that *in vivo* PKA activity is regulated at multiple levels, including kinase inactivation/activation and expression of PKA subunits, during bidirectional axenic differentiation. We cannot separate the obvious promastigote-specific functions suggested by differential activity and localization of PKA subunits from a possible direct involvement of this kinase in signaling environmental conditions that trigger differentiation. However, the bidirectional differentiation system will be very valuable in addressing these questions directly by genetic analysis.

References

- Bachmaier, S., Boshart, M., 2013. Kinetoplastid AGC Kinases, Protein Phosphorylation in Parasites. Wiley-VCH Verlag GmbH & Co. KGaA, pp. 99-122.
- Barak, E., Amin-Spector, S., Gerliak, E., Goyard, S., Holland, N., Zilberstein, D., 2005. Differentiation of *Leishmania donovani* in host-free system: analysis of signal perception and response. *Molecular and biochemical parasitology* 141, 99-108.
- Bates, P.A., 1994. The developmental biology of *Leishmania* promastigotes. *Experimental parasitology* 79, 215-218.
- Bhattacharya, A., Biswas, A., Das, P.K., 2012. Identification of a protein kinase A regulatory subunit from *Leishmania* having importance in metacyclogenesis through induction of autophagy. *Molecular microbiology* 83, 548-564.
- Burchmore, R.J., Barrett, M.P., 2001. Life in vacuoles--nutrient acquisition by *Leishmania* amastigotes. *International journal for parasitology* 31, 1311-1320.
- Chang, K.P., Dwyer, D.M., 1976. Multiplication of a human parasite (*Leishmania donovani*) in phagolysosomes of hamster macrophages *in vitro*. *Science* 193, 678-680.
- Cross, G.A., Manning, J.C., 1973. Cultivation of *Trypanosoma brucei* spp. in semi-defined and defined media. *Parasitology* 67, 315-331.
- Czichos, J., Nonnengaesser, C., Overath, P., 1986. *Trypanosoma brucei*: cis-aconitate and temperature reduction as triggers of synchronous transformation of bloodstream to procyclic trypomastigotes *in vitro*. *Experimental parasitology* 62, 283-291.
- Dalton, G.D., Dewey, W.L., 2006. Protein kinase inhibitor peptide (PKI): a family of endogenous neuropeptides that modulate neuronal cAMP-dependent protein kinase function. *Neuropeptides* 40, 23-34.
- Dean, S., Marchetti, R., Kirk, K., Matthews, K.R., 2009. A surface transporter family conveys the trypanosome differentiation signal. *Nature* 459, 213-217.
- Debrabant, A., Joshi, M.B., Pimenta, P.F., Dwyer, D.M., 2004. Generation of *Leishmania donovani* axenic amastigotes: their growth and biological characteristics. *International journal for parasitology* 34, 205-217.
- Duncan, R., Alvarez, R., Jaffe, C.L., Wiese, M., Klutch, M., Shakarian, A., Dwyer, D., Nakhasi, H.L., 2001. Early response gene expression during differentiation of cultured *Leishmania donovani*. *Parasitology research* 87, 897-906.
- Engstler, M., Boshart, M., 2004. Cold shock and regulation of surface protein trafficking convey sensitization to inducers of stage differentiation in *Trypanosoma brucei*. *Genes & development* 18, 2798-2811.
- Glass, D.B., Cheng, H.C., Mende-Mueller, L., Reed, J., Walsh, D.A., 1989. Primary structural determinants essential for potent inhibition of cAMP-dependent protein kinase by inhibitory peptides corresponding to the active portion of the heat-stable inhibitor protein. *The Journal of biological chemistry* 264, 8802-8810.

- Goyard, S., Segawa, H., Gordon, J., Showalter, M., Duncan, R., Turco, S.J., Beverley, S.M., 2003. An *in vitro* system for developmental and genetic studies of *Leishmania donovani* phosphoglycans. *Molecular and biochemical parasitology* 130, 31-42.
- Harris, T.E., Persaud, S.J., Jones, P.M., 1997. Pseudosubstrate inhibition of cyclic AMP-dependent protein kinase in intact pancreatic islets: effects on cyclic AMP-dependent and glucose-dependent insulin secretion. *Biochemical and biophysical research communications* 232, 648-651.
- Herwaldt, B.L., 1999. Leishmaniasis. *Lancet* 354, 1191-1199.
- Hubel, A., Krobitsch, S., Horauf, A., Clos, J., 1997. *Leishmania major* Hsp100 is required chiefly in the mammalian stage of the parasite. *Molecular and cellular biology* 17, 5987-5995.
- Jones, N.G., Thomas, E.B., Brown, E., Dickens, N.J., Hammarton, T.C., Mottram, J.C., 2014. Regulators of *Trypanosoma brucei* cell cycle progression and differentiation identified using a kinome-wide RNAi screen. *PLoS pathogens* 10, e1003886.
- Kohl, L., Sherwin, T., Gull, K., 1999. Assembly of the paraflagellar rod and the flagellum attachment zone complex during the *Trypanosoma brucei* cell cycle. *The Journal of eukaryotic microbiology* 46, 105-109.
- Krobitsch, S., Brandau, S., Hoyer, C., Schmetz, C., Hubel, A., Clos, J., 1998. *Leishmania donovani* heat shock protein 100. Characterization and function in amastigote stage differentiation. *The Journal of biological chemistry* 273, 6488-6494.
- Lahay, T., Sivam, D., Volpin, H., Ronen, M., Tsigankov, P., Green, A., Holland, N., Kuzyk, M., Borchers, C., Zilberstein, D., Myler, P.J., 2011. Multiple levels of gene regulation mediate differentiation of the intracellular pathogen *Leishmania*. *FASEB journal : official publication of the Federation of American Societies for Experimental Biology* 25, 515-525.
- MacGregor, P., Savill, N.J., Hall, D., Matthews, K.R., 2011. Transmission stages dominate trypanosome within-host dynamics during chronic infections. *Cell host & microbe* 9, 310-318.
- MacGregor, P., Szoor, B., Savill, N.J., Matthews, K.R., 2012. Trypanosomal immune evasion, chronicity and transmission: an elegant balancing act. *Nature reviews. Microbiology* 10, 431-438.
- Oberholzer, M., Langousis, G., Nguyen, H.T., Saada, E.A., Shimogawa, M.M., Jonsson, Z.O., Nguyen, S.M., Wohlschlegel, J.A., Hill, K.L., 2011. Independent analysis of the flagellum surface and matrix proteomes provides insight into flagellum signaling in mammalian-infectious *Trypanosoma brucei*. *Molecular & cellular proteomics : MCP* 10, M111 010538.
- Olmsted, J.B., 1981. Affinity purification of antibodies from diazotized paper blots of heterogeneous protein samples. *The Journal of biological chemistry* 256, 11955-11957.
- Overath, P., Czichos, J., Haas, C., 1986. The effect of citrate/cis-aconitate on oxidative metabolism during transformation of *Trypanosoma brucei*. *European journal of biochemistry / FEBS* 160, 175-182.
- Rolin, S., Hancocq-Quertier, J., Paturiaux-Hanocq, F., Nolan, D.P., Pays, E., 1998. Mild acid stress as a differentiation trigger in *Trypanosoma brucei*. *Molecular and biochemical parasitology* 93, 251-262.

- Rosenzweig, D., Smith, D., Myler, P.J., Olafson, R.W., Zilberstein, D., 2008a. Post-translational modification of cellular proteins during *Leishmania donovani* differentiation. *Proteomics* 8, 1843-1850.
- Rosenzweig, D., Smith, D., Opperdoes, F., Stern, S., Olafson, R.W., Zilberstein, D., 2008b. Retooling *Leishmania* metabolism: from sand fly gut to human macrophage. *FASEB journal : official publication of the Federation of American Societies for Experimental Biology* 22, 590-602.
- Saar, Y., Ransford, A., Waldman, E., Mazareb, S., Amin-Spector, S., Plumblee, J., Turco, S.J., Zilberstein, D., 1998. Characterization of developmentally-regulated activities in axenic amastigotes of *Leishmania donovani*. *Molecular and biochemical parasitology* 95, 9-20.
- Salmon, D., Bachmaier, S., Krumbholz, C., Kador, M., Gossmann, J.A., Uzureau, P., Pays, E., Boshart, M., 2012. Cytokinesis of *Trypanosoma brucei* bloodstream forms depends on expression of adenylyl cyclases of the ESAG4 or ESAG4-like subfamily. *Molecular microbiology* 84, 225-242.
- Sambrook, J., Russell, D.W., 2001. *Molecular Cloning: A Laboratory Manual*. Cold Spring Harbor Laboratory Press.
- Santrich, C., Moore, L., Sherwin, T., Bastin, P., Brokaw, C., Gull, K., LeBowitz, J.H., 1997. A motility function for the paraflagellar rod of *Leishmania* parasites revealed by PFR-2 gene knockouts. *Molecular and biochemical parasitology* 90, 95-109.
- Saxena, A., Lahav, T., Holland, N., Aggarwal, G., Anupama, A., Huang, Y., Volpin, H., Myler, P.J., Zilberstein, D., 2007. Analysis of the *Leishmania donovani* transcriptome reveals an ordered progression of transient and permanent changes in gene expression during differentiation. *Molecular and biochemical parasitology* 152, 53-65.
- Shabb, J.B., 2001. Physiological substrates of cAMP-dependent protein kinase. *Chemical reviews* 101, 2381-2411.
- Shaked-Mishan, P., Ulrich, N., Ephros, M., Zilberstein, D., 2001. Novel Intracellular SbV reducing activity correlates with antimony susceptibility in *Leishmania donovani*. *The Journal of biological chemistry* 276, 3971-3976.
- Siman-Tov, M.M., Aly, R., Shapira, M., Jaffe, C.L., 1996. Cloning from *Leishmania major* of a developmentally regulated gene, c-lpk2, for the catalytic subunit of the cAMP-dependent protein kinase. *Molecular and biochemical parasitology* 77, 201-215.
- Subota, I., Julkowska, D., Vincensini, L., Reeg, N., Buisson, J., Blisnick, T., Huet, D., Perrot, S., Santi-Rocca, J., Duchateau, M., Hourdel, V., Rousselle, J.C., Cayet, N., Namane, A., Chamot-Rooke, J., Bastin, P., 2014. Proteomic analysis of intact flagella of procyclic *Trypanosoma brucei* cells identifies novel flagellar proteins with unique sub-localization and dynamics. *Molecular & cellular proteomics : MCP* 13, 1769-1786.
- Szöör, B., Dyer, N.A., Ruberto, I., Acosta-Serrano, A., Matthews, K.R., 2013. Independent pathways can transduce the life-cycle differentiation signal in *Trypanosoma brucei*. *PLoS pathogens* 9, e1003689.
- Szöör, B., Ruberto, I., Burchmore, R., Matthews, K.R., 2010. A novel phosphatase cascade regulates differentiation in *Trypanosoma brucei* via a glycosomal signaling pathway. *Genes & development* 24, 1306-1316.

- Szöör, B., Wilson, J., McElhinney, H., Taberner, L., Matthews, K.R., 2006. Protein tyrosine phosphatase TbPTP1: A molecular switch controlling life cycle differentiation in trypanosomes. *The Journal of cell biology* 175, 293-303.
- Tsigankov, P., Gherardini, P.F., Helmer-Citterich, M., Spath, G.F., Myler, P.J., Zilberstein, D., 2014. Regulation dynamics of *Leishmania* differentiation: deconvoluting signals and identifying phosphorylation trends. *Molecular & cellular proteomics : MCP* 13, 1787-1799.
- Tsigankov, P., Gherardini, P.F., Helmer-Citterich, M., Spath, G.F., Zilberstein, D., 2013. Phosphoproteomic analysis of differentiating *Leishmania* parasites reveals a unique stage-specific phosphorylation motif. *Journal of proteome research* 12, 3405-3412.
- Vassella, E., Reuner, B., Yutzy, B., Boshart, M., 1997. Differentiation of African trypanosomes is controlled by a density sensing mechanism which signals cell cycle arrest via the cAMP pathway. *J Cell Sci* 110 (Pt 21), 2661-2671.
- Vickerman, K., 1985. Developmental cycles and biology of pathogenic trypanosomes. *British Medical Bulletin* 41, 105-114.
- Walsh, D.A., Ashby, C.D., Gonzalez, C., Calkins, D., Fischer, E.H., 1971. Krebs EG: Purification and characterization of a protein inhibitor of adenosine 3',5'-monophosphate-dependent protein kinases. *The Journal of biological chemistry* 246, 1977-1985.
- Zilberstein, D., 2008. Physiological and biochemical aspects of *Leishmania* development., in: Myler, P.J., Fasel, N. (Eds.), *Leishmania after the genome: biology and control*. Horizon Scientific Press and Caister Academic Press, New York, pp. 107-122

Acknowledgements

We are grateful to Joachim Clos, Hamburg and Philippe Bastin, Paris for providing antibody reagents. We thank Prof. Moshe Ephros and Dr. Gerald Spaeth for critical comments on some experiments. This work was supported by grant number 1065-86.13/2008 from the German-Israeli Foundation for Scientific Research and Development (GIF) to M. B. and D. Z.

6. Concluding Discussion

The cAMP/PKA signaling pathway, which is highly conserved in most eukaryotes, is significantly different in the evolutionary early branching protozoan parasite *T. brucei* (Figure 6.1): A large family of receptor-type adenylate cyclases with atypical sequence and structural features (Figure 1.2 (Introduction)) may replace the receptor function of GPCRs, which are apparently absent from trypanosomal genomes. Cyclic AMP produced by ACs does not activate the parasite PKA orthologue, nor does the trypanosomal genome encode any proteins with similarity to known alternative cAMP effectors from other organisms (such as CRP, Epac or cyclic nucleotide regulated ion channels). Instead, CARP1, a protein exclusively found in kinetoplastids, acts as putative cAMP acceptor and might represent the entry point into a novel, kinetoplastid-specific cAMP signaling pathway. Apart from its involvement in regulation of cell division, cAMP plays an important extracellular role by modulation of the host innate immune response thereby ensuring high parasite transmission. The PKA orthologue of *T. brucei* is the first example of a PKA not regulated by cAMP. In *T. brucei*, we discovered regulation by low temperature and presumably by an alternative endogenous ligand. The kinase is involved in regulation of parasite differentiation, motility, carbohydrate metabolism, ribosome biogenesis, translation, transport, and protein folding, reminiscent of PKA downstream functions in other organisms (Skalhegg and Tasken, 2000; Shabb, 2001; Ptacek et al., 2005; Vaidyanathan et al., 2014). One third of the putative substrates of *T. brucei* PKA, however, are kinetoplastid- or even *Trypanosoma*-specific proteins with mostly unknown function and hence might indicate partially unique PKA downstream signaling.

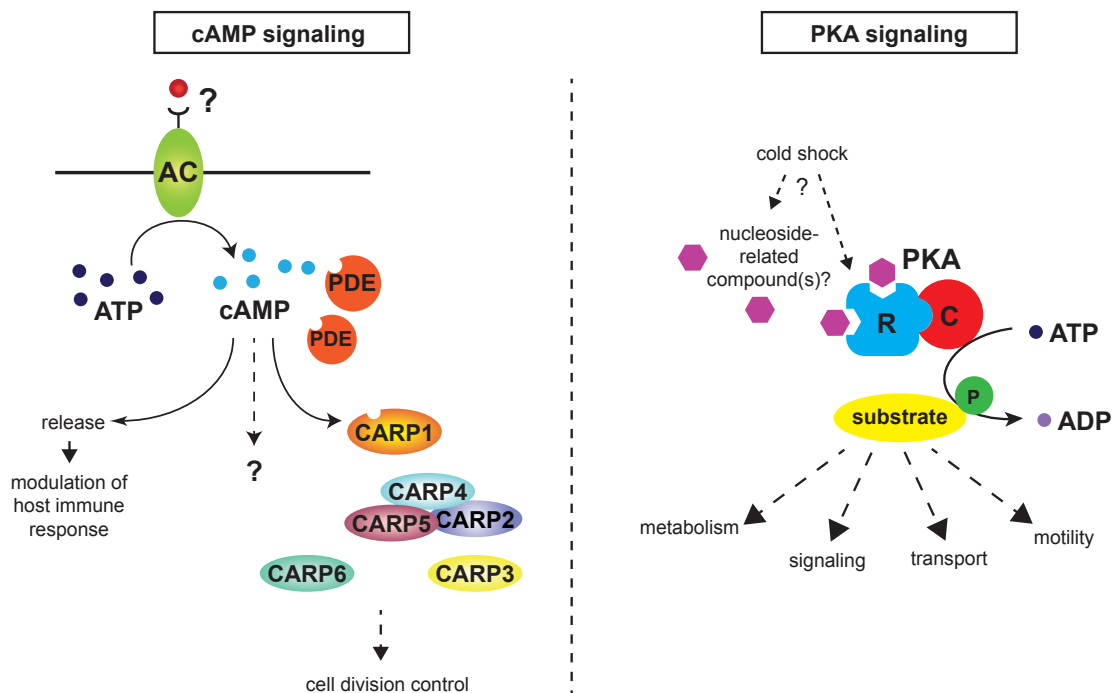


Figure 6.1: *T. brucei* cAMP (left) and PKA signaling (right) pathways.

6.1 Why is there such a diversity of ACs in *T. brucei*?

The surprisingly high number of AC isoforms encoded by the *T. brucei* genome (>80 isoforms; www.tritrypdb.org; Salmon et al., 2012a; Salmon et al., 2012b) compared to the human genome (9 isoforms; Ludwig and Seuwen, 2002) raises the question: why do trypanosomes need such a high number of diverse ACs? To be able to answer this question, a better understanding of the function of the variable extracellular domain will be required. This domain is discussed to serve as receptor domain for extracellular ligands replacing the receptor function of GPCRs (Gould and de Koning, 2011). The architectural similarity of trypanosomal ACs to receptor-type GCs (Seebeck et al., 2004), their localization at the flagellar surface (Paindavoine et al., 1992; Salmon et al., 2012b; Saada et al., 2014) as well as the reported enrichment of sites of positive selection in the variable, extracellular region compared to the catalytic domain (Emes and Yang, 2008) are facts supporting the receptor hypothesis. Moreover, the extracellular domain displays homology to the superfamily of ‘Periplasmic binding protein-like I’ domains (analyzed by <http://supfam.cs.bris.ac.uk/SUPERFAMILY/index.html>). Interestingly, periplasmic binding proteins (PBP) function as primary receptors for a variety of ligands implicated in regulation of signal transduction, chemotaxis and metabolite transport systems in archaea, bacteria and eukaryotes (Munshi et al., 2013). Yet, no ligand binding to kinetoplastid ACs has been identified to date. The remarkable expansion of the AC family in extracellular African trypanosomes (*T. brucei*, *T. congolense*, *T. vivax*) in contrast to intracellularly developing related kinetoplastids (*T. cruzi*, *Leishmania major*) (Salmon et al., 2012b) indicates a link between AC diversity and exposure to the host immune system and hence points to a role for ACs in host-parasite interaction. Moreover, the large variety of ACs at the trypanosomal surface could be important for binding of diverse ligands in the different life cycle stages and host environments. This idea is supported by life cycle stage specific expression of several AC isoforms: whereas some ACs are predominantly expressed in BSFs, a recent study identified AC isoforms strongly up-regulated in PCFs (Saada et al., 2014). Interestingly, isoform-specific localization to distinct flagellar subdomains (along the flagellum or at the distal tip of the flagellum) has been observed for insect stage-specific ACs, thus enabling compartmentalization of cAMP signaling by initiation of independent downstream pathways. Since the flagellum and particularly the flagellar tip play an important role in the differentiation from epimastigote to infectious, metacyclic forms in the fly (Vickerman et al., 1988), microdomains of cAMP signaling involving specific AC isoforms might play a role in these differentiation processes. A putative role for specific AC isoforms in interaction of the parasite with defined tsetse fly environments is furthermore supported by the observed variation of the AC family expansion among tsetse-transmitted parasites: the complexity of development as well as the tissue distribution in the insect vector correlate with the size of the AC gene family, with *T. vivax* (developing in the fly mouthparts and foregut) showing the lowest, *T. congolense* (developing in the fly mouthparts, foregut and midgut) an intermediate and *T. brucei* (developing in the fly mouthparts, foregut, midgut and salivary glands) showing the largest number of AC genes (Saada et al., 2014). Perception of an extracellular ligand is also important for the density-dependent differentiation from the LS to the SS stage within the mammalian bloodstream (Reuner et al., 1997; Vassella et al., 1997) (see Introduction, chapter 1.2.3.1). Increase in the extracellular concentration of SIF, a molecule

thought to be excreted by the trypanosomes, is perceived by a quorum sensing-like mechanism (Reuner et al., 1997; MacGregor et al., 2011). Interestingly, a PBP domain is also found in the quorum sensing signal binding protein LuxP of *Vibrio harveyi* (Pappas et al., 2004). Could specific AC isoforms act as SIF receptors at the surface of *T. brucei* LS cells? The observed transient increase in the intracellular cAMP concentration by treatment of LS trypanosomes with conditioned medium containing SIF (Vassella et al., 1997) would support this hypothesis. Whether specific AC isoforms could indeed act as SIF receptors and whether trypanosomal ACs are able to bind ligands at all is yet an open question and should be subject of extensive future studies.

Activation of trypanosomal ACs has so far only been observed upon membrane stress e.g. by acid treatment, osmotic lysis or attack by the host immune system (Voorheis and Martin, 1980; Rolin et al., 1996; Nolan et al., 2000; Salmon et al., 2012b). Hence, trypanosomal ACs might act as sensors of general disturbances within the cell surface membrane, maybe via sensing the density of the VSG coat. This hypothesis fits well to the proposed involvement of ACs in regulation of cytokinesis (Salmon et al., 2012a).

6.2 Unconventional upstream activation mechanism(s) of *T. brucei* PKA

The activation mechanism of PKA by the second messenger cAMP is highly conserved in organisms ranging from primitive protozoa to humans. Hence, the discovery of a PKA orthologue in *T. brucei* with strong sequence conservation but complete insensitivity to cAMP came as an unexpected surprise. Intriguingly, there is evidence for the presence of an endogenous, nucleoside-related ligand, which may activate the parasite kinase via a mechanism similar to the conserved cAMP-dependent activation of other PKA orthologues. Moreover, *in vivo* kinase activity is induced upon exposure to low temperature by an as yet unknown mechanism. In this chapter, potential mechanisms of *T. brucei* PKA activation as well as a possible connection between cold shock and ligand-mediated activation will be discussed.

6.2.1 No activation by cAMP – predictable from the primary amino acid sequence of *T. brucei* PKAR?

All cAMP-binding proteins are characterized by the presence of a highly conserved cyclic nucleotide-binding domain (CNB) harboring the phosphate-binding cassette (PBC), a module providing the key residues for cAMP interaction. Based on sequence comparison of PKAR orthologues from a large and evolutionary divergent set of eukaryotes ranging from protozoa such as *Paramecium tetraurelia* to humans, Canaves and Taylor (2002) derived a signature sequence capable of unequivocally identifying members of the PKAR family (F-G-E-[LIV]-A-L-[LIMV]-x(3)-[PV]-R-[ANQV]-A; x represents any amino acid) and distinguishing them from other cAMP-binding proteins. However, although the strong overall sequence conservation undoubtedly classifies the *T. brucei* PKAR orthologue as a member of the PKAR family, there are deviations from the proposed signature sequence of the PBC (G. Githure PhD thesis, 2014; chapter 4.1; *T. brucei* PBC-A: V-G-E-L-E-L-M-Y-Q-T-P-T-V-A; PBC-B: V-G-E-L-E-F-L-N-N-H-A-N-V-A; residues shown in red deviate from the consensus signature sequence shown above). Most importantly, these deviations include an arginine,

suggested to be invariant and required for interaction with the phosphate moiety of cAMP. Was the cAMP-insensitivity of *T. brucei* PKA predictable? Mutation of the conserved arginine in human PKAR or in the cyclic nucleotide regulated channels MlotiK1 (bacterial) and HCN2 (mammalian) results in significant reduction in cAMP affinity (Bubis et al., 1988; Tibbs et al., 1998; Kannan et al., 2007; Zhou and Siegelbaum, 2007; Altieri et al., 2008). Thus, at most it could have been predicted that *T. brucei* PKAR might have a somewhat lower affinity to cAMP compared to PKAR orthologues from other organisms. Moreover, activation by cAMP is **the** identifying feature of a cAMP-dependent protein kinase. Proving the existence of a conserved PKA devoid of cAMP sensitivity necessitated several complementary, independent approaches. Strikingly, rendering the PBCs of *T. brucei* PKAR more similar to the proposed signature sequence by introducing only three mutations within each cassette (PBC-A: E311A, T318R, V319A; PBC-B: E435A, N442R, V443A) guided by structural modeling was sufficient to restore some cAMP sensitivity of the parasite PKA (G. Githure PhD thesis, 2014). This mutated PKAR was not only recombinantly expressed for *in vitro* kinase assays but was also endogenously expressed in *T. brucei*. Several characteristics of this cell line (designated PKAR PBCmut) will be of great importance for the discussion of putative activation mechanisms of *T. brucei* PKA.

6.2.2 Possible mechanisms of cold shock-induced PKA activation

According to the Arrhenius equation, there is a positive correlation between the rate of an enzymatic reaction and the reaction temperature within a certain temperature range. In addition, each enzyme has a specific temperature optimum. Unexpectedly, in contrast to any other PKA orthologue characterized to date, *T. brucei* PKA is activated upon exposure to low temperature (see chapter 4.2), an important trigger in the parasite's life cycle. In the absence of experimental data regarding the mechanism of cold shock activation of *T. brucei* PKA, only speculations can be drawn, mainly deduced from known mechanisms of cold shock perception and transduction in other organisms. The temperature-dependent activation of *T. brucei* PKA can either be based on the intrinsic property of the enzyme, i.e. temperature-dependent structural rearrangements influencing enzymatic activity, or on temperature-dependent changes of upstream components of PKA signaling in *T. brucei*. In other words: is *T. brucei* PKA itself a temperature sensor? Or are there alternative temperature sensors, which mediate kinase activation upon exposure to low temperature? Most examples of cold-activated enzymes are found in plants, hibernating animals and cold-adapted psychrophilic and psychrotolerant (micro-)organisms. The higher enzymatic activity under cold conditions is an intrinsic property of many of these enzymes and is based on temperature-dependent structural rearrangements. Cold-induced conformational changes in *T. brucei* PKAC resulting in increased enzymatic activity, as observed for purified PKAC orthologues from several hibernating animals (Holden and Storey, 1998; MacDonald and Storey, 1998; Holden and Storey, 2000), can be excluded, since in the absence of PKAR, no cold shock activation was observed *in vivo* (see chapter 4.2). However, structural changes in PKAR or the PKA holoenzyme upon exposure to cold conditions resulting in increased enzymatic activity would be a possible scenario. Biophysical methods for studying the thermal stability of proteins such as circular

dichroism, fluorescence spectroscopy or differential scanning calorimetry (He et al., 2013) will be used in future experiments to address this question.

Assuming that *T. brucei* PKA itself is not a temperature sensor, a temperature-dependent upstream mechanism must be responsible for regulation of kinase activity. In plants, an increase in the cytoplasmic calcium concentration has been reported as an immediate (<1 minute) consequence of a temperature drop, presumably via cold-induced changes in membrane fluidity resulting in activation of calcium channels (Knight et al., 1991; Knight et al., 1996; Plieth et al., 1999; Martin and Busconi, 2001). This observation has led to the hypothesis that calcium might act as second messenger in response to chilling and cold acclimation. The manifold, well-known examples of crosstalk between calcium and cAMP/PKA signaling (Bugrim, 1999; Bruce et al., 2003; Borodinsky and Spitzer, 2006; Howe, 2011) might also provide a link between cold shock, calcium and PKA activation in *T. brucei*. The high abundance of putative components of cAMP/PKA (e.g. ACs, PDEs, PKAR, PKAC and other putative cAMP-binding proteins) and calcium signaling (e.g. calflagins, calmodiluns, Ca²⁺-binding proteins, calpains, calcium channels) inside the trypanosomal flagellum (Broadhead et al., 2006; Oberholzer et al., 2007; Saada et al., 2014; Subota et al., 2014) suggests close proximity of at least parts of these signaling pathways. Moreover, the identification of several proteins with possible involvement in calcium signaling as putative substrates of *T. brucei* PKA (see Supplemental Material - Chapter 4.2, Table S1) supports the idea of crosstalk between these signaling pathways in trypanosomes. Adenylate cyclases are considered to be centers of highly organized microdomains of cAMP and calcium and hence represent a major interface for these two signaling pathways (Cooper and Tabbasum, 2014). As observed for many AC isoforms from a variety of organisms, *T. brucei* AC activity is induced by calcium (Voorheis and Martin, 1980, 1981). However, given the uncoupling of the parasite PKA from cAMP, an increase in the concentration of the second messenger will not result in direct PKA activation. Moreover, treatment of BSF trypanosomes with 300 μ M CaCl₂ did not affect *in vivo* PKA activity over a time course of 20 minutes at 37°C or 4°C (data not shown). Nevertheless, there could be alternative ways of crosstalk between calcium and PKA signaling. An approach involving measurement of intracellular calcium levels and simultaneous analysis of *in vivo* PKA activity upon exposure to low temperature will be appropriate to answer this open question.

A temperature-dependent increase in the intracellular concentration of certain cations is also known to be mediated by receptors of the TRP (transient receptor potential) superfamily of cation channels, which are responsible for sensing a huge variety of environmental signals such as temperature or osmolarity in many evolutionary divergent organisms ranging from bacteria over unicellular eukaryotes such as *Euglena gracilis* or *Chlamydomonas reinhardtii* to mammals (Huang et al., 2007; Venkatachalam and Montell, 2007; Häder et al., 2009; Fujii et al., 2011; Nilius and Owsianik, 2011). TRPs are characterized by six transmembrane domains (TMDs), which connect the intracellular N- and C-termini and form a pore between TMD5 and TMD6. In mammals, six different temperature-activated TRP channels have been identified four of which are activated by heat (TRPV1-4) and two by cold (TRPM8 and TRPA1) (Dhaka et al., 2006). While their intrinsic thermodynamic properties are discussed to be directly responsible for gating, channel activity after the initial stimulation can be regulated by several other mechanisms e.g. by phosphorylation, as observed for the cold-stimulated mammalian TRPM8 receptor, which is regulated by PKA-mediated phosphorylation (De Petrocellis et

al., 2007; Bavencoffe et al., 2010). While two putative TRP homologues have recently been identified in kinetoplastids (Chenik et al., 2005) with one of them having a putative role in iron transport from the lysosome to the cytosol in *T. brucei* (Taylor et al., 2013), genes with significant similarity to the known mammalian temperature-activated TRP receptors are apparently absent from kinetoplastid genomes. However, due to the diversity between subfamilies of the large TRP superfamily as well as the diversity between TRP receptors of evolutionary divergent species, the presence of cold-activated TRP-like channels in trypanosomes is not excluded.

Proteins bearing cold shock domains (CSDs) constitute a protein family involved in temperature sensing of many organisms. CSD-containing proteins, also called cold shock proteins (CSPs), have first been identified in bacteria (Horn et al., 2007) and are now being discovered in a growing number of eukaryotes ranging from yeast to humans (Mihailovich et al., 2010). The CSD represents a highly conserved nucleic acid-binding domain capable of interaction with DNA and RNA thereby enabling CSPs to regulate transcription, translation and RNA turnover. A BLAST search for sequences with homology to the CSD domain (Pfam PF00313) revealed four proteins encoded by the *T. brucei* TREU927 genome (www.tritrypdb.org) (TriTrypDB entries: Tb927.11.7900, Tb927.8.7820, Tb927.4.4520, Tb927.7.3810). However, an increase in PKA activity due to temperature-dependent transcriptional changes as shown for yeast and human PKA in hepatoblastoma cells (Ohsaka et al., 2001; Sahara et al., 2002) can be excluded since maximal activation of *T. brucei* PKA is observed within minutes.

6.2.3 Ligand-dependent activation of *T. brucei* PKA.

6.2.3.1 Activation by a/several purine nucleoside-related endogenous ligand/s?

The observation that *T. brucei* PKA was activated by dipyridamole *in vivo* via an indirect mechanism provided strong evidence for the presence of an endogenous, nucleoside-related ligand. Dipyridamole, a potent inhibitor of mammalian PDEs (Ghosh et al., 2009) with poor activity against trypanosomal PDEs (Rascon et al., 2002; Zoraghi and Seebeck, 2002), is known to significantly interfere with mammalian adenosine metabolism via several independent mechanisms (Pfleger et al., 1969; Klabunde, 1983; Gibbs and Lip, 1998) and has been shown to similarly block adenosine uptake in trypanosomes (James and Born, 1980; Al-Salabi et al., 2007). This raises that question whether purine nucleosides could be endogenous regulators of the parasite kinase. Trypanosomes, as most other protozoan parasites, are devoid of de novo purine synthesis and hence rely on salvage of purines from the mammalian host (Hammond and Gutteridge, 1984; de Koning et al., 2005). Notably, proteins with putative functions in nucleoside metabolism are significantly enriched in the proteome of the *T. brucei* flagellum (Broadhead et al., 2006; Zhou et al., 2010; Oberholzer et al., 2011; Subota et al., 2014), the predominant localization of the parasite PKA (C. Krumbholz PhD thesis, 2006; Oberholzer et al., 2011; Subota et al., 2014). Moreover, we have identified adenosine derivatives (8-pCPT-adenosine, 8-pCPT-2'O-me-adenosine), which block PKA activation via an as yet unknown, indirect mechanism (this study, data not shown; J. Pepperl Diploma thesis, 2007; G. Githure PhD thesis, 2014), possibly having an impact on nucleoside metabolism, thereby supporting the idea of an endogenous,

nucleoside-related ligand. Another interesting finding in this context is provided by the PBC mutant of *T. brucei* PKAR, which bears mutations in the PBC domains (see chapter 6.2.1): while the recombinantly expressed protein has gained some cAMP sensitivity *in vitro* (EC_{50} 20 μ M) (G. Githure PhD thesis, 2014), the corresponding *T. brucei* cell line has lost activation by toyocamycin or dipyrindamole *in vivo* (G. Githure PhD thesis, 2014 and data not shown). A small-scale chemical screen aiming to define the chemical space of putative ligands resulted in identification of several activating 7-substituted adenosine derivatives with toyocamycin (7-cyano-7-deaza-adenosine) being the most potent compound *in vivo* (EC_{50} 78 nM) (see chapter 4.1) and *in vitro* (EC_{50} 183 nM) (G. Githure PhD thesis, 2014). A possible effect of the common nucleosides adenosine, guanosine and inosine on PKA activity was tested *in vitro* due to the poor membrane permeability of these molecules. The *in vitro* kinase assay showed that all three nucleosides directly activate the *T. brucei* R-C1 holoenzyme with different affinities (G. Githure PhD thesis, 2014). Taken together, these results indicate regulation of *T. brucei* PKA via binding of an intracellular purine nucleoside-related compound to PKAR. The very few amino acid deviations within the PBCs of *T. brucei* PKAR from orthologues of other organisms account for the replacement of cAMP as upstream activator by a purine nucleoside-related ligand.

6.2.3.2 What could be the physiological relevance of the proposed nucleoside-dependent regulation of *T. brucei* PKA?

The essential uptake of nucleosides and nucleobases from the environment is mediated by nucleoside/nucleobase transporters of the ENT (equilibrative nucleoside transporter) family some of which show life cycle stage-specific expression (de Koning et al., 2005; Jensen et al., 2009; Kabani et al., 2009; Ortiz et al., 2009; Queiroz et al., 2009; Urbaniak et al., 2012; Butter et al., 2013; Capewell et al., 2013; Jensen et al., 2014; Telleria et al., 2014; Vasquez et al., 2014). This may indicate stage-specific availability of nucleosides/nucleobases and/or stage-specific requirements. Assuming that the parasite PKA, according to the *in vitro* observations, can also be regulated *in vivo* by several purine nucleosides (inosine, adenosine and guanosine) with different affinities, regulation of kinase activity dependent on nucleoside availability would be possible. Interestingly, as shown in Table 6.1, despite a comparable level of basal kinase activity in BSF and PCF trypanosomes, activation by cold shock, toyocamycin or dipyrindamole is restricted to BSFs. This might be dependent on the presence of different R-C holoenzymes with distinct affinities to putative ligands in the specific life cycle stages.

Table 6.1: Stage-specific characteristics of *T. brucei* PKA activity *in vivo*

	BSF	PCF
basal activity	20-30%	20-30%
activation by cold shock	✓	✗
activation by 7-deazapurines	✓	✗
activation by dipyrindamole	✓	✗

6. Discussion

C1 expression level	high	no expression
C2 expression level	low	high

R-C1 is exclusively present in BSFs and is regulated by the aforementioned stimuli *in vivo* and *in vitro*. Lack of detectable kinase activation in PCFs, which show a high relative expression level of PKAC2, as well as in a BSF cell line with RNAi-mediated depletion of *PKAC1*, indicates that the R-C2 holoenzyme might be refractory to the identified activators. These findings may indicate that R-C1 and R-C2 indeed exhibit distinct characteristics not only in terms of expression during the parasite's life cycle but also regarding their response to putative upstream regulators. Yet, the high sequence identity between C1 and C2 (94% at the protein level) with only few amino acid differences at the very N- and C-terminal ends (Bachmaier and Boshart, 2013) rather argues against an activation mechanism specific for R-C1. The low abundance of R-C2 holoenzymes in BSFs could well explain the lack of a visible increase in cold-induced substrate phosphorylation in *PKAC1*-depleted cells *in vivo*. Moreover, other putative life cycle stage-specific differences such as a stage-specific posttranslational modification of the regulatory and/or catalytic subunits could influence kinase inducibility. In fact, a recent study has shown that PKA subunit phosphorylation is strongly regulated between BSFs and PCFs (Urbaniak et al., 2013). Moreover, C1 but not C2 undergoes stumpy-specific phosphorylation (see chapter 4.2; S. Kramer PhD thesis, 2004) (albeit no functional role of this modification could be established yet). The question whether the observed differences in sensitivity to the identified regulators reflect distinct intrinsic properties of the R-C1 and R-C2 holoenzymes can be addressed by two complementary genetic approaches:

- 1) generation of a *T. brucei* BSF cell line expressing C2 instead of C1;
- 2) expression of C1 in procyclic stage trypanosomes.

Several attempts to replace *C1* by *C2* in BSFs (in the *C1* locus with *C1* UTRs) have failed either indicating an essential C1-specific function or toxicity of higher levels of C2 in this life cycle stage, most likely dependent on the few amino acid differences between these two isoforms. Inducible expression of C1 in PCFs followed by analysis of sensitivity to the identified regulators of *in vivo* PKA activity will be the next step in this project. *In vitro* kinase assays with recombinantly expressed PKAR-C2 holoenzyme will complement the *in vivo* studies.

It is well possible that sensitivity to the identified regulators might be dependent on both, holoenzyme composition and life cycle stage. In any case, the stage-specific properties of *T. brucei* PKA point towards distinct functions of the enzyme presumably at various stages of the parasite's life cycle. The strong upregulation of C2 expression in PCFs combined with the significantly increased phosphorylation at four sites (which are unique to C2, i.e. not present in C1) compared to BSFs (Urbaniak et al., 2013) suggests an insect stage-specific, as yet unknown function of C2. Interestingly, two independent studies have recently identified C2 in the glycosomal proteome of PCFs (Güther et al., 2014; F. Bringaud, Bordeaux, personal communication). Glycosomes are peroxisome-like organelles mainly occupying metabolic enzymes and detoxification pathways. An additional role of this organelle in signal transduction is displayed by the presence of putative signaling proteins

including the protein serine/threonine phosphatase PIP39. Glycosomal localization of PIP39 has been shown to be essential for BSF to PCF differentiation (Szöör et al., 2010).

6.2.3.3 Does *T. brucei* PKAR play a role in LS to SS differentiation?

An interesting observation that supports the idea of a nucleoside-dependent regulation of *T. brucei* PKA is the putative involvement of PKAR in slender to stumpy differentiation. The hydrolysable cAMP derivatives 8-pCPT-(2'O-me)-cAMP as well as degradation products thereof, namely the respective 5'AMP and adenosine derivatives, can mimic the effect of SIF by inducing LS to SS differentiation (Vassella et al., 1997; Laxman et al., 2006) (see Introduction, chapter 1.2.3.1). Interestingly, a cell line with deletion of both alleles of *PKAR* showed increased resistance to 8-pCPT-cAMP and 8-pCPT-(2'O-me)-adenosine compared to wild type cells (see chapter 4.1). Consistent with this, a recent whole-genome RNAi library screen selecting for cells resistant to these compounds and hence defective in stumpy formation, identified PKAR among several other proteins (Mony et al., 2014). Although proof for a role of PKAR in this differentiation process is still missing, preliminary experiments showed that LS to SS differentiation was strongly impaired in a pleomorphic *PKAR* knock out mutant compared to wild type cells (data not shown). Even at high cell densities, several independent clones of the mutant cell line showed slender morphology and were devoid of PAD1 expression (marker for stumpy stage; Dean et al., 2009). These experiments were however complicated by the reversion of this phenotype after a prolonged cultivation period, most likely due to secondary adaptations. Follow-up experiments to confirm the putative role of PKAR in LS to SS differentiation will be conducted with freshly transfected *PKAR* knock out cells as well as with *PKAR* RNAi cells. The putative involvement of PKA in LS to SS differentiation cannot (yet) be unambiguously assigned to one specific R-C holoenzyme. However, the low abundance of R-C2 in BSFs and the insensitivity of R-C3 to the stumpy-inducing compound 8-pCPT-adenosine (data not shown) render a role of these holoenzymes in LS to SS differentiation rather unlikely. Moreover, a pleomorphic cell line with inducible RNAi against *C1/2* shows normal LS to SS differentiation at maximal *C1/2* repression (no difference in the expression level of the stumpy marker PAD1 between wild type, uninduced and induced RNAi cell line; see chapter 4.2). These findings rather point to a C-independent function of R in the signaling mechanism involved in regulation of LS to SS differentiation. Identification of putative PKAR-interacting proteins might be very useful for the discovery of other signaling components putatively involved in regulation of this differentiation step.

6.2.4 Is there a physiological connection between cold shock- and purine nucleoside-dependent PKA activation?

T. brucei PKA activity is regulated by temperature and by purine nucleoside derivatives *in vivo*. Although there might be independent upstream signaling pathways eventually resulting in kinase induction, the perfect correlation between the results obtained from the *in vivo* PKA assays upon exposure to cold shock with the ones involving toyocamycin as regulator point to a connection between cold shock- and nucleoside-dependent activation (Table 6.2).

Table 6.2 Regulation of *in vivo* PKA activity in different *T. brucei* cell lines

	activation by:		
	cold shock	toyocamycin	dipyridamole
BSF wt	✓	✓	✓
BSF Rko	✗	✗	✗
BSF PKAR_PBCmut	✗	✗	✗
BSF C1/2 RNAi -Tet	✓	✓	n.d.
BSF C1/2 RNAi +Tet	✗	✗	n.d.
BSF C1_UTR_RNAi -Tet	✓	✓	n.d.
BSF C1_UTR_RNAi +Tet	✗	✗	n.d.
BSF C2ko	✓	✓	n.d.
BSF C3ko	✓	✓	n.d.
PCF wt	✗	✗	✗

One possibility for interconnection between the two upstream activating pathways would be temperature-dependent availability of the putative endogenous, nucleoside-related ligand(s), e.g. via a cold-sensitive enzyme producing the ligand(s) or via a cold-sensitive transporter responsible for uptake of a precursor of the ligand(s). Alternatively, cold shock might induce conformational changes in PKAR or the PKA holoenzyme resulting in altered affinity to the local concentration of the nucleoside-related ligand(s). The kinetics of PKA activation by cold shock with maximal activation after only two minutes rather argues for the latter hypothesis. Moreover, a preliminary experiment showed temperature-dependent changes in the affinity of recombinantly expressed and purified R-C1 holoenzyme to adenosine *in vitro* (G. Githure PhD thesis, 2014).

6.3 The special properties of the catalytic PKA isoform C3

The catalytic isoform C3 differs in several aspects from C1 and C2: while C1 and C2 share 94% sequence identity and show inversely regulated expression during the trypanosomal life cycle, C3 is more divergent (only 59% and 58% identity to C1 and C2, respectively) and is expressed at comparable levels between slender, stumpy and procyclic trypanosomes. Moreover, the R-C3 holoenzyme is refractory to any of the identified *in vivo* regulators (inducers as well as inhibitors!) of PKA activity (see chapter 4.2, figure 2; and unpublished observations). C3 accounts for ~75% of the basal *in vivo* PKA activity in BSFs (see chapter 4.2, figure 2), suggesting the presence of ‘free’ C3 (i.e. not interacting with R). It is well known from several mammalian cell types as well as from other eukaryotes that free catalytic (as well as free regulatory) PKA subunits are more susceptible to proteolytic degradation than PKA subunits in the holoenzyme complex, consequently resulting in a rather tight co-regulation of R and C protein levels e.g. upon genetic perturbations (Amieux et al., 1997; Burton et al., 1997; Park et al., 2000; Duncan et al., 2006; Kirschner et al., 2009). Consistent with the suggested occurrence of ‘free’ C3 in *T. brucei*, we observed co-regulation between R and

C1/2 but not between R and C3 in RNAi and knock out cell lines (see Supplemental Material - Chapter 4.1, figure S7D). Two additional observations point to the association of a fraction of C3 with an alternative binding partner (hereinafter referred to as 'X'): knock out of *PKAR* resulted in complete loss of flagellar localization of C1/2, whereas a fraction of C3 remained localized to the flagellum. Moreover, detergent treatment resulted in complete solubilization of R and C1/2, but only in partial solubilization of C3 (C. Krumbholz, unpublished). Although it is completely open, whether the suggested alternative interaction partner of C3 exhibits PKAR-like properties regarding structure and function (i.e. regulator of C3), the putative X-C3 complex is certainly not responsive to cAMP nor to any of the identified regulators of *in vivo* PKA activity in *T. brucei*. Unfortunately, protein-protein-interaction analysis based on tandem affinity purification (TAP) followed by mass spectrometry has so far only identified PKAR as interaction partner of C3 (G. Githure PhD thesis, 2014), possibly due to the apparent detergent resistance of X. BioID (proximity-dependent biotin identification), a recently established method for identification of proximal and interacting proteins (Roux et al., 2012), might be a particularly promising approach to identify rather insoluble interacting partners. This technique is based on inducible expression of a targeting protein fused to a promiscuous *E. coli* biotin protein ligase, which biotinylates proteins that are in close proximity to the fusion protein. Biotinylated proteins are affinity purified using a streptavidin matrix and subsequently analyzed by MS. Since biotinylation of nearby proteins occurs before solubilization, this method is equally well applicable for soluble and insoluble proteins. Detergents such as SDS and Triton-X100 can be added to the lysis buffer to ensure high solubilization efficiency. This method has already successfully been used for identification of novel protein-protein-interactions in *T. brucei* (Morriswood et al., 2013) and is currently being optimized and expanded in our laboratory with the aim to identify interacting partners of *T. brucei* cAMP response proteins (CARPs) (see discussion chapter 6.5).

6.4 Downstream signaling of *T. brucei* PKA

In mammalian cells, PKA regulates a number of different cellular processes such as metabolism, transcription, differentiation, and motility (Shabb, 2001). An involvement of PKA in control of differentiation (BSF to PCF, see chapter 4.2) and motility (C. Krumbholz PhD thesis, 2006; (Oberholzer et al., 2011)) was as well observed in *T. brucei*, yet the downstream components of the pathway involved in regulation of these processes are unknown. In order to identify downstream targets of PKA signaling in *T. brucei* as well as to determine additional physiological functions of the kinase, we applied transcriptome profiling (see chapter 4.1) and MS-based phosphoproteomics (see chapter 4.2). These studies revealed putative involvement in regulation of a number of cellular processes with a major focus on carbohydrate metabolism, transport, ribosome biogenesis and translation, and motility. Moreover, RNA-binding proteins were highly represented within the putative substrates directly phosphorylated by PKA. RNA-binding proteins play a major role in trypanosomal gene expression control (recent review: (Clayton, 2013)), which occurs exclusively at the posttranscriptional level (i.e. transcript stability, transcript processing and transport, and translational efficiency) owing to the virtual absence of regulation at the transcriptional level (Clayton, 2002; Haile and Papadopoulou, 2007). Phosphorylation of RNA-binding proteins by *T. brucei* PKA might also

6. Discussion

account for the changes observed by RNAseq analysis upon activation of the kinase. Several of the putative physiological functions of *T. brucei* PKA are conserved in *S. cerevisiae* and humans such as regulation of carbohydrate metabolism, transport, or differentiation (Tash and Means, 1982; Brokaw, 1987; Leclerc et al., 1996; Robertson et al., 2000; Shabb, 2001; Jones et al., 2003; Ptacek et al., 2005). However, a considerable number of putative downstream targets are kinetoplastid- or *Trypanosoma*-specific with mostly unknown function and largely devoid of conserved functional domains, likely representing partially unique functions of the kinase in the evolutionary early branching kinetoplastid parasite.

Candidate substrates acting as possible PKA downstream effectors in regulation of cold shock-induced BSF to PCF differentiation have already been discussed in chapter 4.2. The present chapter will focus on PKA substrates with a possible link to regulation of flagellar motility. A role of the parasite PKA in regulation of BSF motility has been first discovered in a *PKAR* knock out cell line (C. Krumbholz PhD thesis, 2006) and subsequently described in a cell line with down-regulation of *PKAR* by RNAi (Oberholzer et al., 2011). Since the same motility phenotype is found upon RNAi-mediated down-regulation of *PKAC1/2* (targeting both catalytic subunits simultaneously) or *PKAC1* (targeting specifically the *PKAC1* 3'UTR) in BSFs and is absent from BSF *PKAC2* or *PKAC3* deletion mutants and from procyclic *PKAR* knock out cells (personal observations, not shown), the R-C1 holoenzyme is likely to be involved in motility control. An essential role of PKA in motility has also been observed in several other ciliated or flagellated eukaryotes: in addition to the well-established role of human PKA in regulation of sperm motility (Tash and Means, 1982; Brokaw, 1987; Leclerc et al., 1996), the kinase has been implicated in controlling locomotion of several protozoa including the slime mold *Dictyostelium discoideum* (Zhang et al., 2003) and the malaria parasite *Plasmodium falciparum* (Lasonder et al., 2012a; Lasonder et al., 2012b). *T. brucei* PKA substrate candidates with a putative or experimentally verified role in parasite motility are listed in Table S1 (Supplemental Material – Discussion, Table S1), and several interesting candidates are discussed in detail in the following.

The axoneme, a bundle of microtubules (MTs) with nine outer doublet MTs surrounding a central pair of singlet MTs, represents a conserved structure of nearly all eukaryotic motile cilia and flagella. ATP-dependent axonemal dynein heavy chains trigger flagellar bending by driving the sliding of the outer doublet MTs against one another eventually resulting in generation of the flagellar beat (Satir, 1995; Cosson, 1996). Mutation or deregulation of axonemal dyneins is linked to ciliary disease in humans, and consistently, a number of previous studies in *T. brucei* revealed motility defects upon down-regulation or mutation of dyneins in BSFs and PCFs (Branche et al., 2006; Baron et al., 2007a; Baron et al., 2007b; Monnerat et al., 2009; Ralston et al., 2011; Springer et al., 2011; Zukas et al., 2012; Kisalu et al., 2014; Rotureau et al., 2014). The three dyneins (Tb11.02.0760; Tb927.3.930; Tb11.02.0030) identified as putative PKA substrates (Table S1) hence represent promising downstream candidates for regulation of motility. Interestingly, PKA-dependent regulation of axonemal dyneins has also been proposed in *Paramecium* (Walczak and Nelson, 1993) and in *Chlamydomonas* (Howard et al., 1994). The transport of components into and out of the flagellum is mainly accomplished by specific kinesins and dyneins, responsible for anterograde and retrograde transport, respectively, and intraflagellar transport proteins (IFTs). Since impairment of the transport

of proteins essential for flagellar motility is likely to result in motility defects, the three kinesins (Tb927.10.890; Tb927.10.12490; Tb927.10.14890) and the three IFTs (IFT172 (Tb927.10.1170); IFT88 (Tb11.55.0006); PIFTF6 (Tb11.03.0880)) identified as putative PKA substrates (Table S1) are candidates to be tested for a role in PKA-mediated motility control. Recently, members of the kinesin 9 family have been shown to be important for proper motility in *T. brucei* BSFs (Demonchy et al., 2009) and in *Chlamydomonas* (Yokoyama et al., 2004).

Flagella of kinetoplastids, euglenoids and dinoflagellates differ from other eukaryotic flagella and cilia by the presence of the so-called paraflagellar rod (PFR), a lattice-like structure proximal to the axoneme (Cachon et al., 1988). The PFR is mainly composed of the two proteins PFR1 and PFR2 and is essential for parasite motility (Bastin et al., 1998; Bastin et al., 1999; Durand-Dubief et al., 2003). Moreover, several other proteins, designated paraflagellar rod components (PFCs) localize to this structure in *T. brucei*. PKA-dependent phosphorylation of PFR components represents a possible way of motility control. PFR1 and PFC1 have been identified as putative PKA substrates (Table S1), and future experiments will aim to analyze a role of these proteins in PKA-dependent motility control.

The kinetoplastid-specific protein TbLRRP, whose depletion causes severe motility defects in PCFs, is putatively phosphorylated by PKA at three sites (Table S1), all of them predicted to be PKA phosphorylation sites (PTM prediction software NetPhosK; <http://www.cbs.dtu.dk/services/NetPhosK/>). TbLRRP has recently been shown to form a complex with Ran and RanBP (Brasseur et al., 2014) thereby possibly acting as RanGAP (Ran GTPase activating protein). Interestingly, Ran is known to be involved in regulation of ciliary protein targeting in various eukaryotes (Dishinger et al., 2010; Fan et al., 2011; Ludington et al., 2013). Intriguingly, the only Ran homologue of *T. brucei* (Tb927.3.1120) has also been identified by the PKA phosphoproteome screen (see Supplemental Material - Chapter 4.2, Table S1). It could either be directly phosphorylated by PKA (two RXXT sites in the primary amino acid sequence) or it could be co-precipitated with TbLRRP by the phospho-PKA substrate antibody. Co-precipitation is also one possible explanation for identification of proteins lacking RXXS/T sites in their primary amino acid sequence by immunoprecipitation with the anti-RXXS*/T* antibody. An alternative explanation may be provided by the findings of a recent study (Duarte et al., 2014), which revealed that phosphorylation motifs could also be formed by the secondary structure of a protein, hence adding even more complexity to the nature of signal transduction pathways.

Further interesting candidate substrates of *T. brucei* PKA are homologues of calpain, casein kinase 1 (CK1) and 14-3-3 protein, all of which are well-known substrates of human PKA (Table S1). Human calpain homologues function as MT-stabilizing proteins (calpain-6) (Tonami et al., 2007; Tonami et al., 2011) and are suggested to control cell motility (Wells et al., 2005). Casein kinase 1 (CK1) homologues are important for proper motility in the flagellated eukaryotes *C. reinhardtii* and *Paramecium* (Walczak and Nelson, 1993; Gokhale et al., 2009; Boesger et al., 2012). Down-regulation of *T. brucei* 14-3-3 homologues results in motility defects of procyclic trypanosomes, and mammalian homologues play as well a role in regulation of cell motility.

All these PKA substrate candidates with putative or experimentally verified functions in regulation of trypanosomal motility will be analyzed by reverse genetic approaches, i.e. RNAi-mediated down-regulation and generation of phosphomutants, followed by detailed motility analyses.

6.5 A kinetoplastid-specific cAMP downstream pathway

Initially, the discovery of a PKA completely uncoupled from cAMP came as an unexpected surprise, especially in the absence of any other known alternative cAMP downstream effectors in *T. brucei*. The identification of the putative, kinetoplastid-specific cAMP receptor protein CARP1 provided the missing piece in the puzzle (see chapter 3). Recent pull-down experiments with BSF lysates have indeed confirmed that CARP1 is able to bind cAMP coupled to agarose beads (Radoslaw Omelianczyk, Master thesis, 2014). CARP1 might represent a promising drug target due to the following aspects: 1) CARP1 is a kinetoplastid-specific protein without orthologues in any other known clade; 2) all attempts to generate homozygous deletion mutants of *CARP1* failed indicating that it is essential for *T. brucei* (note that upon RNAi-mediated repression of *CARP1*, the expression level was reduced by only two-fold (see chapter 3) and hence might correlate with the amount required for parasite survival); 3) CARP1 bears known ligand-binding domains, the cNMP-binding domains, which differ significantly from mammalian cNMP-binding domain-containing proteins and hence provide an excellent target structure for designing and developing specific inhibitors. Since genes encoding CARP1 orthologues are found in all kinetoplastid genomes sequenced to date, a drug with the potential of curing HAT by specifically interfering with *T. brucei* CARP1 might also be effective against Chagas disease and Leishmaniasis caused by *T. cruzi* and *Leishmania spp.*, respectively.

Interaction studies by yeast two-hybrid (Y2H) analysis revealed direct interaction of CARP2 with CARP4 and CARP5, as well as interaction of CARP4 with CARP2 and CARP6 in a complex (unpublished observations, Ana Brennand, this lab). (Note that CARP5 (Tb927.10.12390) and CARP6 (Tb927.10.1740) are not published yet; these proteins were identified by RITseq analysis of the cell line resistant to elevated levels of CpdA (see chapter 3) after publication of CARP1-4 in Gould et al., 2013). Interestingly, no significant interaction of the primary cAMP receptor CARP1 with CARP2-6 has been detected by the Y2H analysis. However, technical limitations of Y2H assays resulting in false-negative results cannot be excluded. Since the whole genome RNAi library screen conducted to identify *T. brucei* CARPs is limited to identification of proteins, which are non-essential at the level of induced RNAi-mediated repression, the existence of additional primary cAMP receptor proteins in *T. brucei* is well possible. CARP1-6 have been identified as putative cAMP downstream signaling components in BSFs, but with the recent discovery of PCF-specific adenylate cyclases (Saada et al., 2014) and the essential role of a subset of these ACs for social motility (Lopez et al., 2014) additional, insect stage-specific cAMP receptors become possible. It will be highly interesting to find out whether CARP1 also functions as cAMP receptor protein in insect stages and whether it might be required for development within the tsetse vector. This hypothesis will be addressed by generation of procyclic cAMP-binding site mutants of CARP1 and *CARP1* RNAi cell lines, which will be fed to tsetse flies followed by analysis of their ability to differentiate into subsequent life cycle stages. In parallel, cAMP binding of CARP1 will be analyzed by pull-down assays with cAMP coupled to agarose beads.

6.6 Evolutionary conservation of the unconventional cAMP and PKA signal transduction pathways within kinetoplastids?

Most of the discovered peculiarities of the cAMP and PKA signal transduction pathways in *T. brucei* seem to be conserved in other kinetoplastids. The existence of unconventional ACs and the absence of GPCRs and heterotrimeric G-proteins are common kinetoplastid characteristics. The sequence deviations of the CNB domains of *T. brucei* PKAR from the highly conserved signature sequence are also found in PKAR orthologues of *T. cruzi* and *L. donovani* (see chapter 4.1) indicating that uncoupling of PKA from cAMP might be conserved within kinetoplastids. This fits perfectly into a model in which the kinetoplastid-specific protein CARP1 has replaced the cAMP receptor function of PKA within the evolutionary early branching kinetoplastid order. Like CARP1, PKA represents an ideal drug target due to its essentiality and its cNMP-binding domains that significantly differ from mammalian cNMP-binding domain-containing proteins. Moreover, the discovery of toyocamycin as high-affinity ligand that activates the kinase in the lower nanomolar range *in vivo* offers a good starting point for anti-trypanosomal drug development.

6.7 References for discussion

- Al-Salabi, M.I., Wallace, L.J., Luscher, A., Maser, P., Candlish, D., Rodenko, B., Gould, M.K., Jabeen, I., Ajith, S.N., and de Koning, H.P. (2007). Molecular interactions underlying the unusually high adenosine affinity of a novel *Trypanosoma brucei* nucleoside transporter. *Mol Pharmacol* 71, 921-929.
- Altieri, S.L., Clayton, G.M., Silverman, W.R., Olivares, A.O., De la Cruz, E.M., Thomas, L.R., and Morais-Cabral, J.H. (2008). Structural and energetic analysis of activation by a cyclic nucleotide binding domain. *J Mol Biol* 381, 655-669.
- Amieux, P.S., Cummings, D.E., Motamed, K., Brandon, E.P., Wailes, L.A., Le, K., Idzerda, R.L., and McKnight, G.S. (1997). Compensatory regulation of RIalpha protein levels in protein kinase A mutant mice. *J Biol Chem* 272, 3993-3998.
- Bachmaier, S., and Boshart, M. (2013). Kinetoplastid AGC Kinases. In *Protein Phosphorylation in Parasites* (Wiley-VCH Verlag GmbH & Co. KGaA), pp. 99-122.
- Baron, D.M., Kabututu, Z.P., and Hill, K.L. (2007a). Stuck in reverse: loss of LC1 in *Trypanosoma brucei* disrupts outer dynein arms and leads to reverse flagellar beat and backward movement. *J Cell Sci* 120, 1513-1520.
- Baron, D.M., Ralston, K.S., Kabututu, Z.P., and Hill, K.L. (2007b). Functional genomics in *Trypanosoma brucei* identifies evolutionarily conserved components of motile flagella. *J Cell Sci* 120, 478-491.
- Bastin, P., Pullen, T.J., Sherwin, T., and Gull, K. (1999). Protein transport and flagellum assembly dynamics revealed by analysis of the paralysed trypanosome mutant *snl-1*. *J Cell Sci* 112 (Pt 21), 3769-3777.
- Bastin, P., Sherwin, T., and Gull, K. (1998). Paraflagellar rod is vital for trypanosome motility. *Nature* 391, 548-548.

6. Discussion

- Bavencoffe, A., Gkika, D., Kondratskyi, A., Beck, B., Borowiec, A.-S., Bidaux, G., Busserolles, J., Eschalier, A., Shuba, Y., Skryma, R., *et al.* (2010). The Transient Receptor Potential Channel TRPM8 Is Inhibited via the α 2A Adrenoreceptor Signaling Pathway. *Journal of Biological Chemistry* 285, 9410-9419.
- Berbari, N.F., Kin, N.W., Sharma, N., Michaud, E.J., Kesterson, R.A., Yoder, B.K. (2011). Mutations in Traf3ip1 reveal defects in ciliogenesis, embryonic development, and altered cell size regulation. *Developmental biology* 360, 66-76.
- Boesger, J., Wagner, V., Weisheit, W., and Mittag, M. (2012). Application of Phosphoproteomics to Find Targets of Casein Kinase 1 in the Flagellum of *Chlamydomonas*. *International Journal of Plant Genomics* 2012, 9.
- Borodinsky, L.N., and Spitzer, N.C. (2006). Second messenger pas de deux: the coordinated dance between calcium and cAMP. *Sci STKE* 2006, pe22.
- Boudreau, A.C., Ferrario, C.R., Glucksman, M.J., Wolf, M.E. (2009). Signaling pathway adaptations and novel protein kinase A substrates related to behavioral sensitization to cocaine. *Journal of neurochemistry* 110, 363-377.
- Branche, C., Kohl, L., Toutirais, G., Buisson, J., Cosson, J., and Bastin, P. (2006). Conserved and specific functions of axoneme components in trypanosome motility. *J Cell Sci* 119, 3443-3455.
- Brasseur, A., Bayat, S., Chua, X.L., Zhang, Y., Zhou, Q., Low, B.C., and He, C.Y. (2014). The bilobe-associated LRRP1 regulates Ran activity in *Trypanosoma brucei*. *J Cell Sci* 127, 4846-4856.
- Broadhead, R., Dawe, H.R., Farr, H., Griffiths, S., Hart, S.R., Portman, N., Shaw, M.K., Ginger, M.L., Gaskell, S.J., McKean, P.G., *et al.* (2006). Flagellar motility is required for the viability of the bloodstream trypanosome. *Nature* 440, 224-227.
- Brokaw, C.J. (1987). Regulation of sperm flagellar motility by calcium and cAMP-dependent phosphorylation. *Journal of Cellular Biochemistry* 35, 175-184.
- Bruce, J.I., Straub, S.V., and Yule, D.I. (2003). Crosstalk between cAMP and Ca²⁺ signaling in non-excitable cells. *Cell Calcium* 34, 431-444.
- Bubis, J., Neitzel, J.J., Saraswat, L.D., and Taylor, S.S. (1988). A point mutation abolishes binding of cAMP to site A in the regulatory subunit of cAMP-dependent protein kinase. *J Biol Chem* 263, 9668-9673.
- Bugrim, A.E. (1999). Regulation of Ca²⁺ release by cAMP-dependent protein kinase. A mechanism for agonist-specific calcium signaling? *Cell Calcium* 25, 219-226.
- Burton, K.A., Johnson, B.D., Hausken, Z.E., Westenbroek, R.E., Idzerda, R.L., Scheuer, T., Scott, J.D., Catterall, W.A., and McKnight, G.S. (1997). Type II regulatory subunits are not required for the anchoring-dependent modulation of Ca²⁺ channel activity by cAMP-dependent protein kinase. *Proc Natl Acad Sci U S A* 94, 11067-11072.
- Butter, F., Bucerius, F., Michel, M., Cicova, Z., Mann, M., and Janzen, C.J. (2013). Comparative proteomics of two life cycle stages of stable isotope-labeled *Trypanosoma brucei* reveals novel components of the parasite's host adaptation machinery. *Mol Cell Proteomics* 12, 172-179.

- Cachon, J., Cachon, M., Cosson, M.-P., and Cosson, J. (1988). The paraflagellar rod: a structure in search of a function. *Biology of the Cell* 63, 169-181.
- Canaves, J.M., and Taylor, S.S. (2002). Classification and phylogenetic analysis of the cAMP-dependent protein kinase regulatory subunit family. *J Mol Evol* 54, 17-29.
- Capewell, P., Monk, S., Ivens, A., MacGregor, P., Fenn, K., Walrad, P., Bringaud, F., Smith, T.K., and Matthews, K.R. (2013). Regulation of *Trypanosoma brucei* Total and Polysomal mRNA during Development within Its Mammalian Host. *PLoS ONE* 8, e67069.
- Chenik, M., Douagi, F., Ben Achour, Y., Khalef, N.B., Ouakad, M., Louzir, H., and Dellagi, K. (2005). Characterization of two different mucolipin-like genes from *Leishmania major*. *Parasitol Res* 98, 5-13.
- Clayton, C. (2013). The regulation of trypanosome gene expression by RNA-binding proteins. *PLoS Pathog* 9, e1003680.
- Clayton, C.E. (2002). Life without transcriptional control? From fly to man and back again. *Embo j* 21, 1881-1888.
- Cooper, D.M., and Tabbasum, V.G. (2014). Adenylate cyclase-centred microdomains. *Biochem J* 462, 199-213.
- Cosson, J. (1996). A moving image of flagella: news and views on the mechanisms involved in axonemal beating. *Cell Biol Int* 20, 83-94.
- de Koning, H.P., Bridges, D.J., and Burchmore, R.J. (2005). Purine and pyrimidine transport in pathogenic protozoa: from biology to therapy. *FEMS Microbiol Rev* 29, 987-1020.
- De Petrocellis, L., Starowicz, K., Moriello, A.S., Vivese, M., Orlando, P., and Di Marzo, V. (2007). Regulation of transient receptor potential channels of melastatin type 8 (TRPM8): effect of cAMP, cannabinoid CB(1) receptors and endovanilloids. *Exp Cell Res* 313, 1911-1920.
- Dean, S., Marchetti, R., Kirk, K., and Matthews, K.R. (2009). A surface transporter family conveys the trypanosome differentiation signal. *Nature* 459, 213-217.
- Demonchy, R., Blisnick, T., Deprez, C., Toutirais, G., Loussert, C., Marande, W., Grellier, P., Bastin, P., and Kohl, L. (2009). Kinesin 9 family members perform separate functions in the trypanosome flagellum. *The Journal of Cell Biology* 187, 615-622.
- Dhaka, A., Viswanath, V., and Patapoutian, A. (2006). Trp ion channels and temperature sensation. *Annu Rev Neurosci* 29, 135-161.
- Dishinger, J.F., Kee, H.L., Jenkins, P.M., Fan, S., Hurd, T.W., Hammond, J.W., Truong, Y.N., Margolis, B., Martens, J.R., and Verhey, K.J. (2010). Ciliary entry of the kinesin-2 motor KIF17 is regulated by importin-beta2 and RanGTP. *Nat Cell Biol* 12, 703-710.
- Duarte, M.L., Pena, D.A., Nunes Ferraz, F.A., Berti, D.A., Paschoal Sobreira, T.J., Costa-Junior, H.M., Abdel Baqui, M.M., Disatnik, M.H., Xavier-Neto, J., Lopes de Oliveira, P.S., *et al.* (2014). Protein folding creates structure-based, noncontiguous consensus phosphorylation motifs recognized by kinases. *Sci Signal* 7, ra105.
- Duncan, F.E., Moss, S.B., and Williams, C.J. (2006). Knockdown of the cAMP-dependent protein kinase (PKA) Type Ialpha regulatory subunit in mouse oocytes disrupts meiotic arrest and results in meiotic spindle defects. *Dev Dyn* 235, 2961-2968.

6. Discussion

- Durand-Dubief, M., Kohl, L., and Bastin, P. (2003). Efficiency and specificity of RNA interference generated by intra- and intermolecular double stranded RNA in *Trypanosoma brucei*. *Molecular and Biochemical Parasitology* *129*, 11-21.
- Emes, R.D., and Yang, Z. (2008). Duplicated Paralogous Genes Subject to Positive Selection in the Genome of *Trypanosoma brucei*. *PLoS ONE* *3*, e2295.
- Fan, S., Whiteman, E.L., Hurd, T.W., McIntyre, J.C., Dishinger, J.F., Liu, C.J., Martens, J.R., Verhey, K.J., Sajjan, U., and Margolis, B. (2011). Induction of Ran GTP drives ciliogenesis. *Mol Biol Cell* *22*, 4539-4548.
- Fujiu, K., Nakayama, Y., Iida, H., Sokabe, M., and Yoshimura, K. (2011). Mechanoreception in motile flagella of *Chlamydomonas*. *Nat Cell Biol* *13*, 630-632.
- Ghosh, R., Sawant, O., Ganpathy, P., Pitre, S., and Kadam, V.J. (2009). Phosphodiesterase inhibitors; their role and implications. *International Journal of PharmTech Research* *1*, 1148-1160.
- Gibbs, C.R., and Lip, G.Y. (1998). Do we still need dipyridamole? *Br J Clin Pharmacol* *45*, 323-328.
- Goc, A., Abdalla, M., Al-Azayzih, A., Somanath, P.R. (2012). Rac1 Activation Driven by 14-3-3 ζ Dimerization Promotes Prostate Cancer Cell-Matrix Interactions, Motility and Transendothelial Migration. *PLoS ONE* *7*, e40594.
- Gokhale, A., Wirschell, M., and Sale, W.S. (2009). Regulation of dynein-driven microtubule sliding by the axonemal protein kinase CK1 in *Chlamydomonas* flagella. *The Journal of Cell Biology* *186*, 817-824.
- Gould, M.K., and de Koning, H.P. (2011). Cyclic-nucleotide signalling in protozoa. *FEMS Microbiol Rev* *35*, 515-541.
- Güther, M.L., Urbaniak, M.D., Tavendale, A., Prescott, A., and Ferguson, M.A. (2014). High-confidence glycosome proteome for procyclic form *Trypanosoma brucei* by epitope-tag organelle enrichment and SILAC proteomics. *J Proteome Res* *13*, 2796-2806.
- Häder, D.-P., Richter, P.R., Schuster, M., Daiker, V., and Lebert, M. (2009). Molecular analysis of the graviperception signal transduction in the flagellate *Euglena gracilis*: Involvement of a transient receptor potential-like channel and a calmodulin. *Advances in Space Research* *43*, 1179-1184.
- Haile, S., and Papadopoulou, B. (2007). Developmental regulation of gene expression in trypanosomatid parasitic protozoa. *Current Opinion in Microbiology* *10*, 569-577.
- Hammond, D.J., and Gutteridge, W.E. (1984). Purine and pyrimidine metabolism in the trypanosomatidae. *Molecular and Biochemical Parasitology* *13*, 243-261.
- He, F., Razinkov, V., Middaugh, C.R., and Becker, G. (2013). High-Throughput Biophysical Approaches to Therapeutic Protein Development. In *Biophysics for Therapeutic Protein Development*, L.O. Narhi, ed. (Springer New York), pp. 7-31.
- Holden, C.P., and Storey, K.B. (1998). Protein kinase A from bat skeletal muscle: a kinetic study of the enzyme from a hibernating mammal. *Arch Biochem Biophys* *358*, 243-250.
- Holden, C.P., and Storey, K.B. (2000). Purification and characterization of protein kinase A from liver of the freeze-tolerant wood frog: role in glycogenolysis during freezing. *Cryobiology* *40*, 323-331.

- Horn, G., Hofweber, R., Kremer, W., and Kalbitzer, H.R. (2007). Structure and function of bacterial cold shock proteins. *Cellular and Molecular Life Sciences* 64, 1457-1470.
- Howard, D.R., Habermacher, G., Glass, D.B., Smith, E.F., and Sale, W.S. (1994). Regulation of *Chlamydomonas* flagellar dynein by an axonemal protein kinase. *J Cell Biol* 127, 1683-1692.
- Howe, A.K. (2011). Cross-talk between calcium and protein kinase A in the regulation of cell migration. *Curr Opin Cell Biol* 23, 554-561.
- Huang, K., Diener, D.R., Mitchell, A., Pazour, G.J., Witman, G.B., and Rosenbaum, J.L. (2007). Function and dynamics of PKD2 in *Chlamydomonas reinhardtii* flagella. *The Journal of Cell Biology* 179, 501-514.
- James, D.M., and Born, G.V. (1980). Uptake of purine bases and nucleosides in African trypanosomes. *Parasitology* 81, 383-393.
- Jensen, B.C., Ramasamy, G., Vasconcelos, E.J., Ingolia, N.T., Myler, P.J., and Parsons, M. (2014). Extensive stage-regulation of translation revealed by ribosome profiling of *Trypanosoma brucei*. *BMC Genomics* 15, 911.
- Jensen, B.C., Sivam, D., Kifer, C.T., Myler, P.J., and Parsons, M. (2009). Widespread variation in transcript abundance within and across developmental stages of *Trypanosoma brucei*. *BMC Genomics* 10, 482.
- Jones, D.L., Petty, J., Hoyle, D.C., Hayes, A., Ragni, E., Popolo, L., Oliver, S.G., and Stateva, L.I. (2003). Transcriptome profiling of a *Saccharomyces cerevisiae* mutant with a constitutively activated Ras/cAMP pathway. *Physiol Genomics* 16, 107-118.
- Kabani, S., Fenn, K., Ross, A., Ivens, A., Smith, T.K., Ghazal, P., and Matthews, K. (2009). Genome-wide expression profiling of *in vivo*-derived bloodstream parasite stages and dynamic analysis of mRNA alterations during synchronous differentiation in *Trypanosoma brucei*. *BMC Genomics* 10, 427.
- Kannan, N., Wu, J., Anand, G.S., Yooseph, S., Neuwald, A.F., Venter, J.C., and Taylor, S.S. (2007). Evolution of allostery in the cyclic nucleotide binding module. *Genome Biol* 8, R264.
- Kirschner, L.S., Yin, Z., Jones, G.N., and Mahoney, E. (2009). Mouse models of altered protein kinase A signaling. *Endocr Relat Cancer* 16, 773-793.
- Kisalu, N.K., Langousis, G., Bentolila, L.A., Ralston, K.S., and Hill, K.L. (2014). Mouse infection and pathogenesis by *Trypanosoma brucei* motility mutants. *Cell Microbiol* 16, 912-924.
- Klabunde, R.E. (1983). Effects of dipyridamole on postischemic vasodilation and extracellular adenosine. *Am J Physiol* 244, H273-280.
- Knight, H., Trewavas, A.J., and Knight, M.R. (1996). Cold calcium signaling in *Arabidopsis* involves two cellular pools and a change in calcium signature after acclimation. *Plant Cell* 8, 489-503.
- Knight, M.R., Campbell, A.K., Smith, S.M., and Trewavas, A.J. (1991). Transgenic plant aequorin reports the effects of touch and cold-shock and elicitors on cytoplasmic calcium. *Nature* 352, 524-526.
- Kunitomo, H., Iino, Y. (2008). *Caenorhabditis elegans* DYF-11, an orthologue of mammalian Traf3ip1/MIP-T3, is required for sensory cilia formation. *Genes to cells : devoted to molecular & cellular mechanisms* 13, 13-25.

6. Discussion

- Lasonder, E., Green, J.L., Camarda, G., Talabani, H., Holder, A.A., Langsley, G., and Alano, P. (2012a). The *Plasmodium falciparum* Schizont Phosphoproteome Reveals Extensive Phosphatidylinositol and cAMP-Protein Kinase A Signaling. *Journal of Proteome Research* *11*, 5323-5337.
- Lasonder, E., Treeck, M., Alam, M., and Tobin, A.B. (2012b). Insights into the *Plasmodium falciparum* schizont phospho-proteome. *Microbes Infect* *14*, 811-819.
- Laxman, S., Riechers, A., Sadilek, M., Schwede, F., and Beavo, J.A. (2006). Hydrolysis products of cAMP analogs cause transformation of *Trypanosoma brucei* from slender to stumpy-like forms. *Proc Natl Acad Sci U S A* *103*, 19194-19199.
- Leclerc, P., de Lamirande, E., and Gagnon, C. (1996). Cyclic adenosine 3',5'-monophosphate-dependent regulation of protein tyrosine phosphorylation in relation to human sperm capacitation and motility. *Biol Reprod* *55*, 684-692.
- Li, C., Inglis, P.N., Leitch, C.C., Efimenko, E., Zaghloul, N.A., Mok, C.A., Davis, E.E., Bialas, N.J., Healey, M.P., Héon, E., Zhen, M., Swoboda, P., Katsanis, N., Leroux, M.R. (2008). An Essential Role for DYF-11/MIP-T3 in Assembling Functional Intraflagellar Transport Complexes. *PLoS Genetics* *4*, e1000044.
- Lopez, M.A., Saada, E.A., and Hill, K.L. (2014). Insect stage-specific adenylate cyclases regulate social motility in African trypanosomes. *Eukaryot Cell*.
- Loza-Huerta, A., Vera-Estrella, R., Darszon, A., and Beltran, C. (2013). Certain *Strongylocentrotus purpuratus* sperm mitochondrial proteins co-purify with low density detergent-insoluble membranes and are PKA or PKC-substrates possibly involved in sperm motility regulation. *Biochim Biophys Acta* *1830*, 5305-5315.
- Ludington, W.B., Wemmer, K.A., Lechtreck, K.F., Witman, G.B., and Marshall, W.F. (2013). Avalanche-like behavior in ciliary import. *Proc Natl Acad Sci U S A* *110*, 3925-3930.
- Ludwig, M.G., and Seuwen, K. (2002). Characterization of the human adenylyl cyclase gene family: cDNA, gene structure, and tissue distribution of the nine isoforms. *J Recept Signal Transduct Res* *22*, 79-110.
- MacDonald, J.A., and Storey, K.B. (1998). cAMP-dependent protein kinase from brown adipose tissue: temperature effects on kinetic properties and enzyme role in hibernating ground squirrels. *J Comp Physiol B* *168*, 513-525.
- MacGregor, P., Savill, N.J., Hall, D., and Matthews, K.R. (2011). Transmission stages dominate trypanosome within-host dynamics during chronic infections. *Cell Host Microbe* *9*, 310-318.
- Martin, M.L., and Busconi, L. (2001). A rice membrane-bound calcium-dependent protein kinase is activated in response to low temperature. *Plant Physiol* *125*, 1442-1449.
- Mihailovich, M., Militti, C., Gabaldon, T., and Gebauer, F. (2010). Eukaryotic cold shock domain proteins: highly versatile regulators of gene expression. *Bioessays* *32*, 109-118.
- Monnerat, S., Clucas, C., Brown, E., Mottram, J.C., and Hammarton, T.C. (2009). Searching for novel cell cycle regulators in *Trypanosoma brucei* with an RNA interference screen. *BMC Res Notes* *2*, 46.

- Mony, B.M., MacGregor, P., Ivens, A., Rojas, F., Cowton, A., Young, J., Horn, D., and Matthews, K. (2014). Genome-wide dissection of the quorum sensing signalling pathway in *Trypanosoma brucei*. *Nature* *505*, 681-685.
- Morriswood, B., Havlicek, K., Demmel, L., Yavuz, S., Sealey-Cardona, M., Vidilaseris, K., Anrather, D., Kostan, J., Djinovic-Carugo, K., Roux, K.J., *et al.* (2013). Novel bilobe components in *Trypanosoma brucei* identified using proximity-dependent biotinylation. *Eukaryot Cell* *12*, 356-367.
- Munshi, P., Stanley, C.B., Ghimire-Rijal, S., Lu, X., Myles, D.A., and Cuneo, M.J. (2013). Molecular details of ligand selectivity determinants in a promiscuous beta-glucan periplasmic binding protein. *BMC Struct Biol* *13*, 18.
- Nilius, B., and Owsianik, G. (2011). The transient receptor potential family of ion channels. *Genome Biol* *12*, 218.
- Nolan, D.P., Rolin, S., Rodriguez, J.R., Van Den Abbeele, J., and Pays, E. (2000). Slender and stumpy bloodstream forms of *Trypanosoma brucei* display a differential response to extracellular acidic and proteolytic stress. *Eur J Biochem* *267*, 18-27.
- Oberholzer, M., Langousis, G., Nguyen, H.T., Saada, E.A., Shimogawa, M.M., Jonsson, Z.O., Nguyen, S.M., Wohlschlegel, J.A., and Hill, K.L. (2011). Independent analysis of the flagellum surface and matrix proteomes provides insight into flagellum signaling in mammalian-infectious *Trypanosoma brucei*. *Mol Cell Proteomics* *10*, M111 010538.
- Oberholzer, M., Marti, G., Baresic, M., Kunz, S., Hemphill, A., and Seebeck, T. (2007). The *Trypanosoma brucei* cAMP phosphodiesterases TbrPDEB1 and TbrPDEB2: flagellar enzymes that are essential for parasite virulence. *FASEB* *21*, 720-731.
- Ohsaka, Y., Ohgiya, S., Hoshino, T., and Ishizaki, K. (2001). Cold-stimulated increase in a regulatory subunit of cAMP-dependent protein kinase in human hepatoblastoma cells. *DNA Cell Biol* *20*, 667-673.
- Omori, Y., Zhao, C., Saras, A., Mukhopadhyay, S., Kim, W., Furukawa, T., Sengupta, P., Veraksa, A., Malicki, J. (2008). Elipsa is an early determinant of ciliogenesis that links the IFT particle to membrane-associated small GTPase Rab8. *Nature cell biology* *10*, 437-444.
- Ortiz, D., Sanchez, M.A., Quecke, P., and Landfear, S.M. (2009). Two novel nucleobase/pentamidine transporters from *Trypanosoma brucei*. *Mol Biochem Parasitol* *163*, 67-76.
- Paindavoine, P., Rolin, S., Van Assel, S., Geuskens, M., Jauniaux, J.C., Dinsart, C., Huet, G., and Pays, E. (1992). A gene from the variant surface glycoprotein expression site encodes one of several transmembrane adenylate cyclases located on the flagellum of *Trypanosoma brucei*. *Mol Cell Biol* *12*, 1218-1225.
- Pappas, K.M., Weingart, C.L., and Winans, S.C. (2004). Chemical communication in proteobacteria: biochemical and structural studies of signal synthases and receptors required for intercellular signalling. *Molecular Microbiology* *53*, 755-769.
- Park, S.K., Sedore, S.A., Cronmiller, C., and Hirsh, J. (2000). Type II cAMP-dependent Protein Kinase-deficient *Drosophila* Are Viable but Show Developmental, Circadian, and Drug Response Phenotypes. *Journal of Biological Chemistry* *275*, 20588-20596.

6. Discussion

- Pfleger, K., Niederau, D., and Volkmer, I. (1969). Ein Beitrag zum Wirkungsmechanismus von Dipyridamol: Hemmung der Adenosinaufnahme in Erythrocyten durch Dipyridamol. *Naunyn-Schmiedebergs Archiv für Pharmakologie* 265, 118-130.
- Plieth, C., Hansen, U.P., Knight, H., and Knight, M.R. (1999). Temperature sensing by plants: the primary characteristics of signal perception and calcium response. *Plant J* 18, 491-497.
- Ptacek, J., Devgan, G., Michaud, G., Zhu, H., Zhu, X., Fasolo, J., Guo, H., Jona, G., Bretkreutz, A., Sopko, R., *et al.* (2005). Global analysis of protein phosphorylation in yeast. *Nature* 438, 679-684.
- Queiroz, R., Benz, C., Fellenberg, K., Hoheisel, J.D., and Clayton, C. (2009). Transcriptome analysis of differentiating trypanosomes reveals the existence of multiple post-transcriptional regulons. *BMC Genomics* 10, 495.
- Ralston, K.S., Kisalu, N.K., and Hill, K.L. (2011). Structure-function analysis of dynein light chain 1 identifies viable motility mutants in bloodstream-form *Trypanosoma brucei*. *Eukaryot Cell* 10, 884-894.
- Rascon, A., Soderling, S.H., Schaefer, J.B., and Beavo, J.A. (2002). Cloning and characterization of a cAMP-specific phosphodiesterase (TbPDE2B) from *Trypanosoma brucei*. *Proc Natl Acad Sci U S A* 99, 4714-4719.
- Reuner, B., Vassella, E., Yutzy, B., and Boshart, M. (1997). Cell density triggers slender to stumpy differentiation of *Trypanosoma brucei* bloodstream forms in culture. *Mol Biochem Parasitol* 90, 269-280.
- Robertson, L.S., Causton, H.C., Young, R.A., and Fink, G.R. (2000). The yeast A kinases differentially regulate iron uptake and respiratory function. *Proceedings of the National Academy of Sciences* 97, 5984-5988.
- Rolin, S., Hanocq-Quertier, J., Paturiaux-Hanocq, F., Nolan, D., Salmon, D., Webb, H., Carrington, M., Voorheis, P., and Pays, E. (1996). Simultaneous but independent activation of adenylate cyclase and glycosylphosphatidylinositol-phospholipase C under stress conditions in *Trypanosoma brucei*. *J Biol Chem* 271, 10844-10852.
- Rotureau, B., Ooi, C.P., Huet, D., Perrot, S., and Bastin, P. (2014). Forward motility is essential for trypanosome infection in the tsetse fly. *Cell Microbiol* 16, 425-433.
- Roux, K.J., Kim, D.I., Raida, M., and Burke, B. (2012). A promiscuous biotin ligase fusion protein identifies proximal and interacting proteins in mammalian cells. *The Journal of Cell Biology* 196, 801-810.
- Saada, E.A., Kabututu, Z.P., Lopez, M., Shimogawa, M.M., Langousis, G., Oberholzer, M., Riestra, A., Jonsson, Z.O., Wohlschlegel, J.A., and Hill, K.L. (2014). Insect stage-specific receptor adenylate cyclases are localized to distinct subdomains of the *Trypanosoma brucei* flagellar membrane. *Eukaryot Cell* 13, 1064-1076.
- Sahara, T., Goda, T., and Ohgiya, S. (2002). Comprehensive expression analysis of time-dependent genetic responses in yeast cells to low temperature. *J Biol Chem* 277, 50015-50021.
- Salmon, D., Bachmaier, S., Krumbholz, C., Kador, M., Gossmann, J.A., Uzureau, P., Pays, E., and Boshart, M. (2012a). Cytokinesis of *Trypanosoma brucei* bloodstream forms depends on

- expression of adenylyl cyclases of the ESAG4 or ESAG4-like subfamily. *Mol Microbiol* *84*, 225-242.
- Salmon, D., Vanwalleghem, G., Morias, Y., Denoed, J., Krumbholz, C., Lhomme, F., Bachmaier, S., Kador, M., Gossmann, J., Dias, F.B., *et al.* (2012b). Adenylate cyclases of *Trypanosoma brucei* inhibit the innate immune response of the host. *Science* *337*, 463-466.
- Satir, P. (1995). Landmarks in cilia research from leeuwenhoek to US. *Cell Motility and the Cytoskeleton* *32*, 90-94.
- Seebeck, T., Schaub, R., and Johner, A. (2004). cAMP signalling in the kinetoplastid protozoa. *Curr Mol Med* *4*, 585-599.
- Shabb, J.B. (2001). Physiological substrates of cAMP-dependent protein kinase. *Chem Rev* *101*, 2381-2411.
- Skalhegg, B.S., and Tasken, K. (2000). Specificity in the cAMP/PKA signaling pathway. Differential expression, regulation, and subcellular localization of subunits of PKA. *Front Biosci* *5*, D678-693.
- Springer, A.L., Bruhn, D.F., Kinzel, K.W., Rosenthal, N.F., Zukas, R., and Klingbeil, M.M. (2011). Silencing of a putative inner arm dynein heavy chain results in flagellar immotility in *Trypanosoma brucei*. *Mol Biochem Parasitol* *175*, 68-75.
- Subota, I., Julkowska, D., Vincensini, L., Reeg, N., Buisson, J., Blisnick, T., Huet, D., Perrot, S., Santi-Rocca, J., Duchateau, M., *et al.* (2014). Proteomic analysis of intact flagella of procyclic *Trypanosoma brucei* cells identifies novel flagellar proteins with unique sub-localization and dynamics. *Mol Cell Proteomics* *13*, 1769-1786.
- Szöör, B., Ruberto, I., Burchmore, R., and Matthews, K.R. (2010). A novel phosphatase cascade regulates differentiation in *Trypanosoma brucei* via a glycosomal signaling pathway. *Genes Dev* *24*, 1306-1316.
- Tash, J.S., and Means, A.R. (1982). Regulation of protein phosphorylation and motility of sperm by cyclic adenosine monophosphate and calcium. *Biol Reprod* *26*, 745-763.
- Taylor, M.C., McLatchie, A.P., and Kelly, J.M. (2013). Evidence that transport of iron from the lysosome to the cytosol in African trypanosomes is mediated by a mucolipin orthologue. *Mol Microbiol* *89*, 420-432.
- Telleria, E.L., Benoit, J.B., Zhao, X., Savage, A.F., Regmi, S., Alves e Silva, T.L., O'Neill, M., and Aksoy, S. (2014). Insights into the trypanosome-host interactions revealed through transcriptomic analysis of parasitized tsetse fly salivary glands. *PLoS Negl Trop Dis* *8*, e2649.
- Tibbs, G.R., Liu, D.T., Leypold, B.G., and Siegelbaum, S.A. (1998). A state-independent interaction between ligand and a conserved arginine residue in cyclic nucleotide-gated channels reveals a functional polarity of the cyclic nucleotide binding site. *J Biol Chem* *273*, 4497-4505.
- Tonami, K., Kurihara, Y., Aburatani, H., Uchijima, Y., Asano, T., and Kurihara, H. (2007). Calpain 6 Is Involved in Microtubule Stabilization and Cytoskeletal Organization. *Molecular and Cellular Biology* *27*, 2548-2561.
- Tonami, K., Kurihara, Y., Arima, S., Nishiyama, K., Uchijima, Y., Asano, T., Sorimachi, H., and Kurihara, H. (2011). Calpain-6, a microtubule-stabilizing protein, regulates Rac1 activity and cell motility through interaction with GEF-H1. *J Cell Sci* *124*, 1214-1223.

6. Discussion

- Urbaniak, M.D., Guther, M.L., and Ferguson, M.A. (2012). Comparative SILAC proteomic analysis of *Trypanosoma brucei* bloodstream and procyclic lifecycle stages. *PLoS One* 7, e36619.
- Urbaniak, M.D., Martin, D.M., and Ferguson, M.A. (2013). Global quantitative SILAC phosphoproteomics reveals differential phosphorylation is widespread between the procyclic and bloodstream form lifecycle stages of *Trypanosoma brucei*. *J Proteome Res* 12, 2233-2244.
- Vaidyanathan, P.P., Zinshteyn, B., Thompson, M.K., and Gilbert, W.V. (2014). Protein kinase A regulates gene-specific translational adaptation in differentiating yeast. *RNA*.
- Vasquez, J.-J., Hon, C.-C., Vanselow, J.T., Schlosser, A., and Siegel, T.N. (2014). Comparative ribosome profiling reveals extensive translational complexity in different *Trypanosoma brucei* life cycle stages. *Nucleic Acids Research* 42, 3623-3637.
- Vassella, E., Reuner, B., Yutzy, B., and Boshart, M. (1997). Differentiation of African trypanosomes is controlled by a density sensing mechanism which signals cell cycle arrest via the cAMP pathway. *J Cell Sci* 110 (Pt 21), 2661-2671.
- Venkatachalam, K., and Montell, C. (2007). TRP channels. *Annu Rev Biochem* 76, 387-417.
- Vickerman, K., Tetley, L., Hendry, K.A., and Turner, C.M. (1988). Biology of African trypanosomes in the tsetse fly. *Biol Cell* 64, 109-119.
- Voorheis, H.P., and Martin, B.R. (1980). 'Swell dialysis' demonstrates that adenylate cyclase in *Trypanosoma brucei* is regulated by calcium ions. *Eur J Biochem* 113, 223-227.
- Voorheis, H.P., and Martin, B.R. (1981). Characteristics of the calcium-mediated mechanism activating adenylate cyclase in *Trypanosoma brucei*. *Eur J Biochem* 116, 471-477.
- Walczak, C.E., and Nelson, D.L. (1993). *In vitro* phosphorylation of ciliary dyneins by protein kinases from *Paramecium*. *J Cell Sci* 106 (Pt 4), 1369-1376.
- Wells, A., Huttenlocher, A., and Lauffenburger, D.A. (2005). Calpain Proteases in Cell Adhesion and Motility. In *International Review of Cytology*, W.J. Kwang, ed. (Academic Press), pp. 1-16.
- Yokoyama, R., O'Toole, E., Ghosh, S., and Mitchell, D.R. (2004). Regulation of flagellar dynein activity by a central pair kinesin. *Proceedings of the National Academy of Sciences of the United States of America* 101, 17398-17403.
- Zhang, H., Heid, P.J., Wessels, D., Daniels, K.J., Pham, T., Loomis, W.F., and Soll, D.R. (2003). Constitutively active protein kinase A disrupts motility and chemotaxis in *Dictyostelium discoideum*. *Eukaryot Cell* 2, 62-75.
- Zhou, L., and Siegelbaum, S.A. (2007). Gating of HCN channels by cyclic nucleotides: residue contacts that underlie ligand binding, selectivity, and efficacy. *Structure* 15, 655-670.
- Zhou, Q., Gheiratmand, L., Chen, Y., Lim, T.K., Zhang, J., Li, S., Xia, N., Liu, B., Lin, Q., and He, C.Y. (2010). A comparative proteomic analysis reveals a new bi-lobe protein required for bi-lobe duplication and cell division in *Trypanosoma brucei*. *PLoS One* 5, e9660.
- Zoraghi, R., and Seebeck, T. (2002). The cAMP-specific phosphodiesterase TbPDE2C is an essential enzyme in bloodstream form *Trypanosoma brucei*. *Proc Natl Acad Sci U S A* 99, 4343-4348.
- Zukas, R., Chang, A.J., Rice, M., and Springer, A.L. (2012). Structural analysis of flagellar axonemes from inner arm dynein knockdown strains of *Trypanosoma brucei*. *Biocell* 36, 133-141.

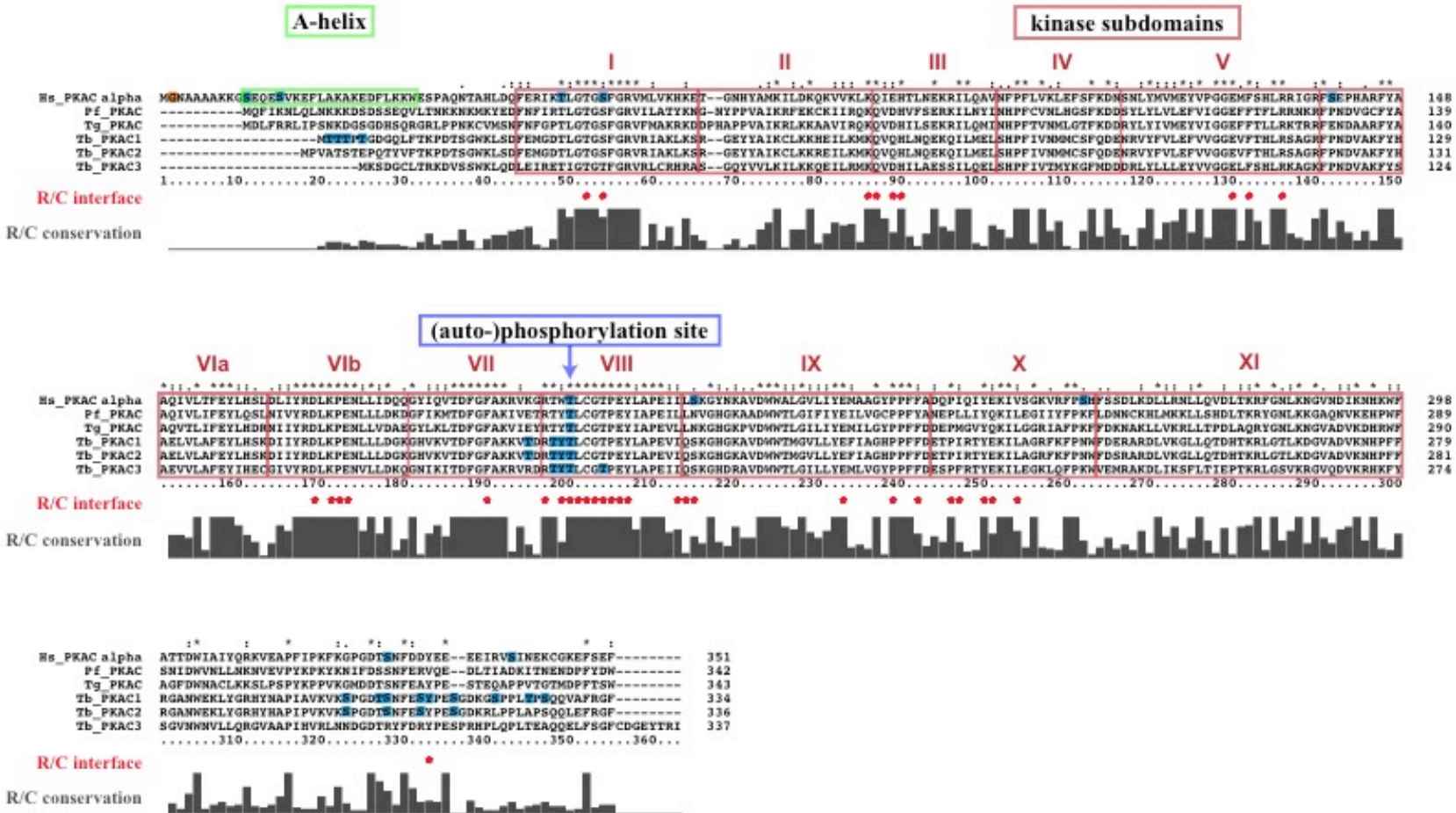


Figure S1A: Sequence comparison of PKAC orthologues. *Homo sapiens* (Hs_PKACalpha, accession P17612), *Plasmodium falciparum* (Pf_PKAC, accession Q7K6A0), *Toxoplasma gondii* (Tg_PKAC, accession S7UXF9) and *Trypanosoma brucei* (Tb_PKAC1, accession Tb427tmp.211.2410; Tb_PKAC2, accession Tb427tmp.211.2360; Tb_PKAC3, accession Tb427.10.13010) PKAC sequences were obtained

from Uniprot (www.uniprot.org) or TriTrypDB (www.tritrypdb.org), respectively. Multiple sequence alignment was performed using clustalW (www.ebi.ac.uk/Tools/msa/clustalW2/) with standard settings. Important domains are boxed by different colors. The A-helix, which is conserved in PKAs of higher eukaryotes, is boxed in green. The 11 canonical kinase subdomains are boxed in red. The highly conserved (auto-)phosphorylation site in the kinase activation loop is indicated by a blue arrow. Phosphorylation sites identified by mass spectrometry (Seidler et al., 2009 for the mammalian C α ; Nett et al., 2009 and Urbaniak et al., 2013 for TbPKACs) are highlighted in light blue, the N-terminal myristoylation site of human PKAC α is shown in orange. Residues important for R-C interaction (Kim et al., 2005; Kim et al., 2007) are marked by red asterisks.





Figure S1B: Sequence comparison of PKAR orthologues. *Homo sapiens* (Hs_PKARI alpha, accession P10644; Hs_PKARII alpha, accession P13861), *Dictyostelium discoideum* (Dd_PKAR, accession P05987), *Plasmodium falciparum* (Pf_PKAR, accession Q8T323), *Toxoplasma gondii* (Tg_PKAR, accession Q9BMY7), *Candida albicans* (Ca_PKAR, accession Q9HEW1), *Trypanosoma brucei* (Tb_PKAR, accession Tb427tmp.02.2210), *Trypanosoma cruzi* (Tc_PKAR, accession TcCLB.506227.150) and *Leishmania donovani* (Ld_PKAR, accession LdBPK_130160.1) PKAR sequences were obtained from UniProt (www.uniprot.org) or TriTrypDB (www.tritrypdb.org), respectively. Multiple sequence alignment was performed using clustalW2 (www.ebi.ac.uk/Tools/msa/clustalw2/) with standard settings. Important domains are highlighted by different colors. The elongated N-terminus of kinetoplastid PKAR proteins is highlighted in blue, the leucin-rich repeat (LRR) region in yellow. The dimerization / docking (DD) domain of PKAR proteins of higher eukaryotes, which is responsible for PKAR dimerization and for interaction with anchoring proteins, is colored in orange. The inhibitor site, which enables discrimination between type I and type II PKAR proteins in mammalian cells, is shown in green. The cyclic nucleotide binding (CNB) domains A and B including their phosphate binding cassettes (PBC) are highlighted in red.

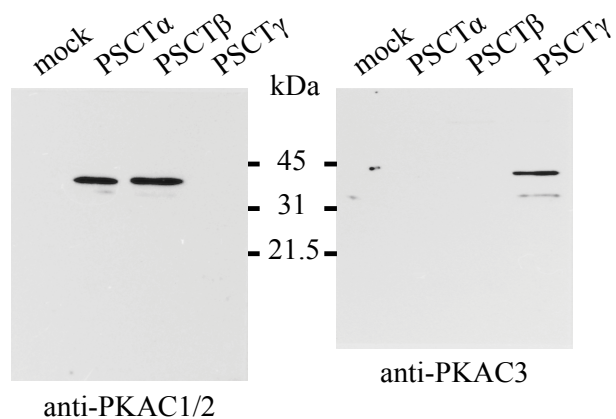
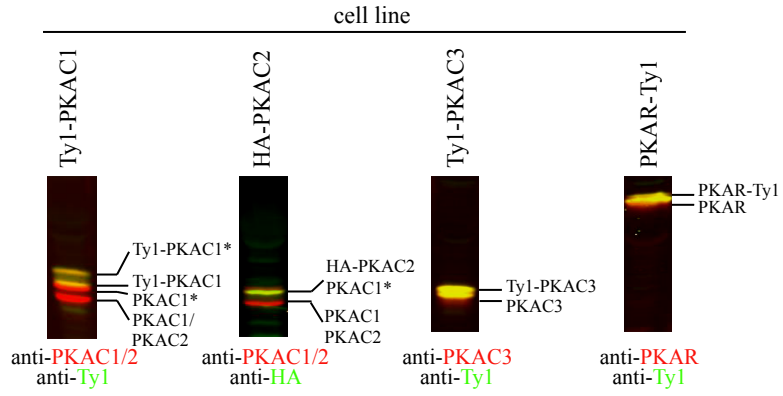


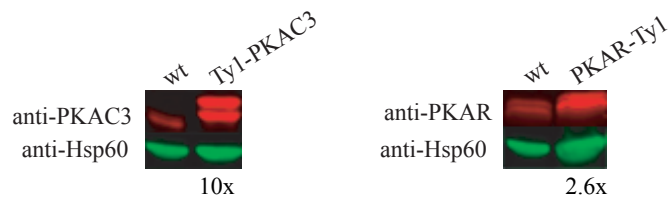
Figure S2: Specificity of the *T. brucei* anti-PKAC antibodies.

The anti-PKAC1/2 and anti-PKAC3 antibodies specifically recognize the respective *T. brucei* PKA catalytic subunits. *T. brucei* PKAC1, PKAC2 or PKAC3 were transiently expressed in human 293 cells as GST-tagged fusion proteins. 10 μ g of soluble protein was separated by SDS PAGE, transferred to a nitrocellulose membrane and detected with the anti-PKAC1/2 (left) or anti-PKAC3 antibodies (right). Cells transfected with the empty vector (PSCTEV3s) were included as control.

A



B



C

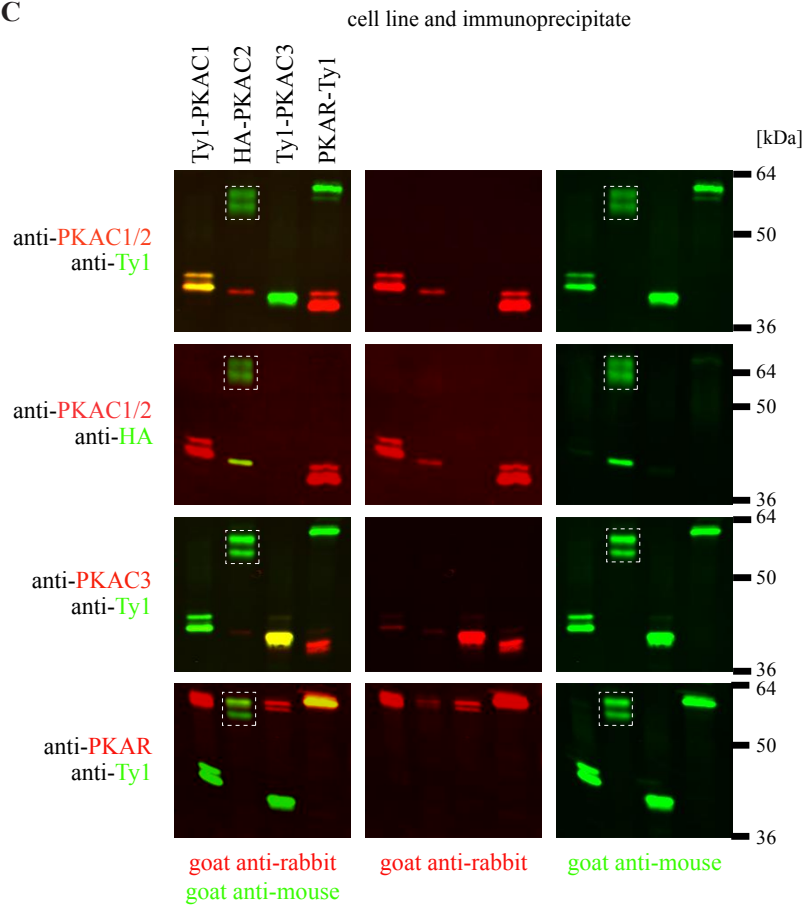


Figure S3: *T. brucei* PKAR interacts with all three different catalytic isoforms in cell lines with independently tagged PKA subunits.

A. Western blot analysis of *T. brucei* cell lines with expression of epitope-tagged PKA subunits. PKAC1 and PKAC2 were *in situ* tagged with a Ty1- or HA-epitope tag, respectively, whereas PKAC3 and PKAR were ectopically overexpressed as Ty1-tag fusions. The Western blots were probed with the respective PKA subunit antibody (anti-PKAR: Bachmaier et al., submitted manuscript; see chapter 5) as well as with anti-Ty1 (Ty1-PKAC1, Ty1-PKAC3, PKAR-Ty1) or anti-HA (HA-PKAC2), respectively. Epitope tagged PKA subunits appear yellow in the merged image due to color blending. Note that the band shift due to the Ty1-epitope tag merges with the upper band of PKAC1, which is marked by an asterisk (*).

B. Western blot analysis of *T. brucei* cell lines with overexpression of Ty1-PKAC3 or PKAR-Ty1, respectively. Immunodetection was performed with anti-PKAC3 or anti-PKAR (Bachmaier et al., submitted manuscript; see chapter 5), respectively, as well as with anti-HSP60 (Bringaud et al., 1995) for normalization. The quantification after normalization is given as fold increase compared to wild type cells (wt) (set to 1).

C. Ty1-PKAC1, HA-PKAC2, Ty1-PKAC3 and PKAR-Ty1 were immunoprecipitated with the epitope tag antibodies anti-Ty1 or anti-HA. The precipitates were analyzed on four parallel blots, and each blot was probed with a different PKA antibody together with the respective epitope tag antibody, as indicated. Each Western blot is shown three times, with both secondary antibodies (left), with Alexa Fluor® 680 goat anti-rabbit (red, center), and with IRDye 800CW goat anti-mouse (green, right). Note that the latter antibody also recognizes the heavy chain of anti-HA IgG (white dashed square), since anti-HA was not cross-linked to the sepharose beads.

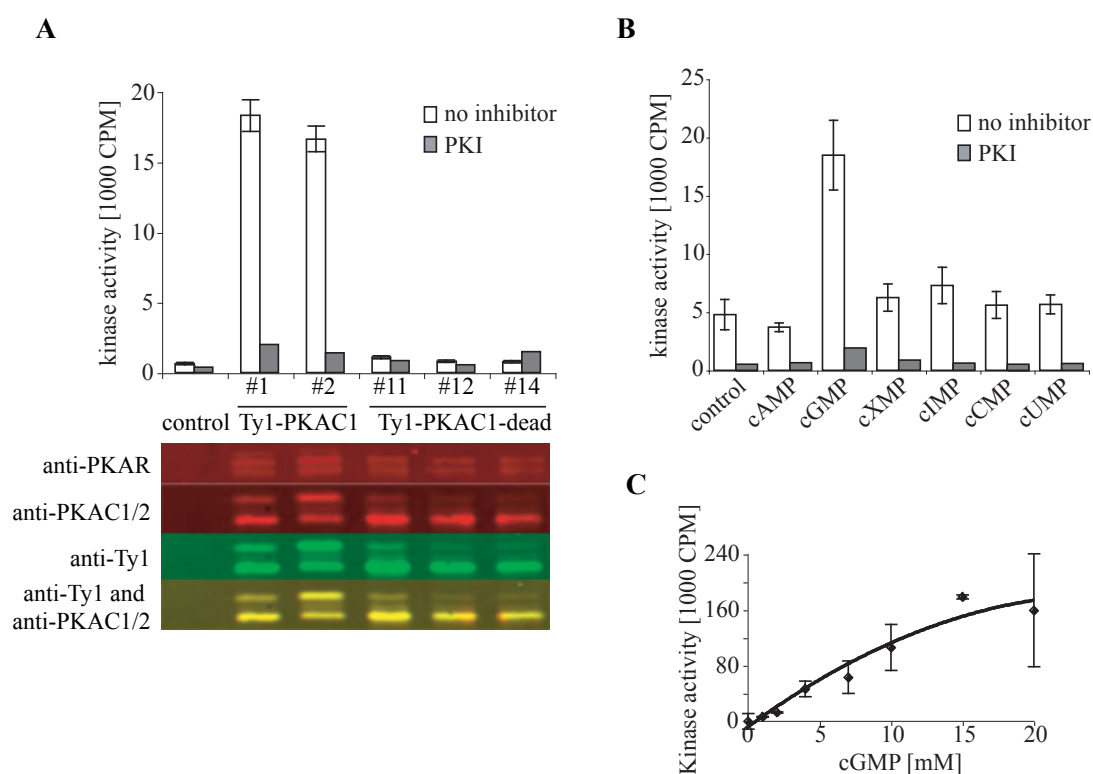


Figure S4: Kinase activity in response to cyclic nucleotides.

A. *In vitro* kinase assays analyzing phosphorylation of the PKA-specific substrate kemptide by immunoprecipitated Ty1-PKAC1 (two independent clones (#1, #2)) or a kinase dead mutant (Ty1-PKAC1-dead; N165->A; three independent clones (#11, #12, #14)) in the presence or absence of 5 μ M PKI(5-24). Immunoprecipitate from wild type cells was included as negative control (control). Each assay (except the ones with PKI) was performed in triplicate. Standard deviations are indicated by error bars. The Western blot shows the precipitated amount of PKAR and PKAC1 of the clones analyzed in the kinase assay. It was probed with anti-PKAR (Bachmaier et al., submitted manuscript; see chapter 5), anti-PKAC1/2 and anti-Ty1 (Bastin et al., 1996).

B. *In vitro* kinase assays analyzing kemptide phosphorylation by the PKA holoenzyme immunoprecipitated via Ty1-PKAC1 in the presence or absence of different cyclic nucleotides (1 mM). Each assay (except the ones with PKI) was performed in triplicate. Standard deviations are indicated by error bars. (cXMP: xanthosine-3',5'-cyclic monophosphate; cIMP: inosine-3',5'-cyclic monophosphate; cCMP: cytidine-3',5'-cyclic monophosphate; cUMP: uridine -3',5'-cyclic monophosphate).

C. *In vitro* kinase assay analyzing the EC_{50} of cGMP for kemptide phosphorylation by immunoprecipitated PKA. Immunoprecipitation was done via PKAR-Ty1 using the anti-Ty1 antibody coupled to sepharose beads. Each assay was performed in triplicate. Standard deviations are indicated by error bars.

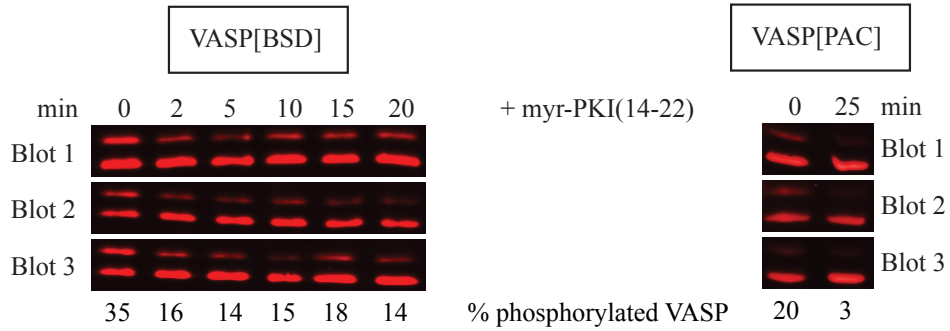


Figure S5: VASP phosphorylation is independent of the selectable marker.

VASP phosphorylation was analyzed in the cell lines VASP[BSD] and VASP[PAC] in the presence or absence of myr-PKI(14-22). In the cell line VASP[BSD], reporter substrate phosphorylation was analyzed in a time course over 20 min after addition of 100 μ M myr-PKI(14-22), whereas in the cell line VASP[PAC], substrate phosphorylation was only analyzed at time points zero and 25 min after addition of 200 μ M myr-PKI(14-22). The values of VASP phosphorylation given in percentage indicate the mean of three independent biological replicates represented by the Western blots.

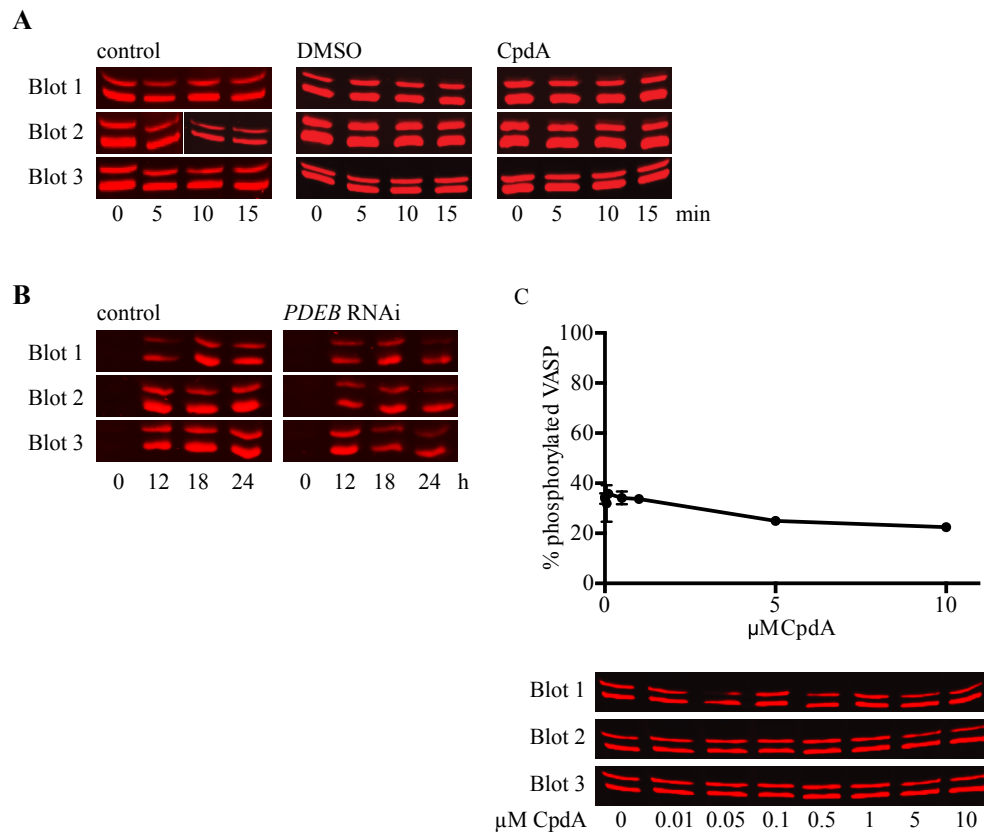
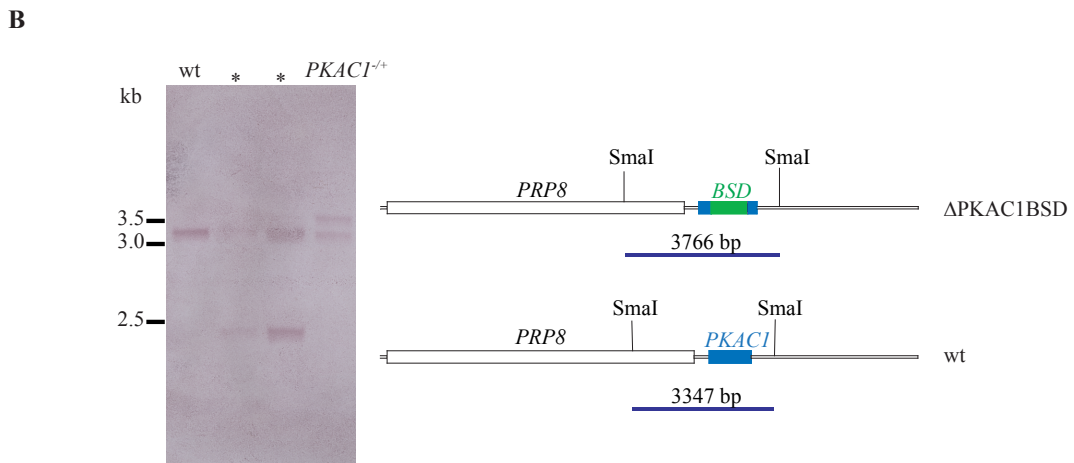
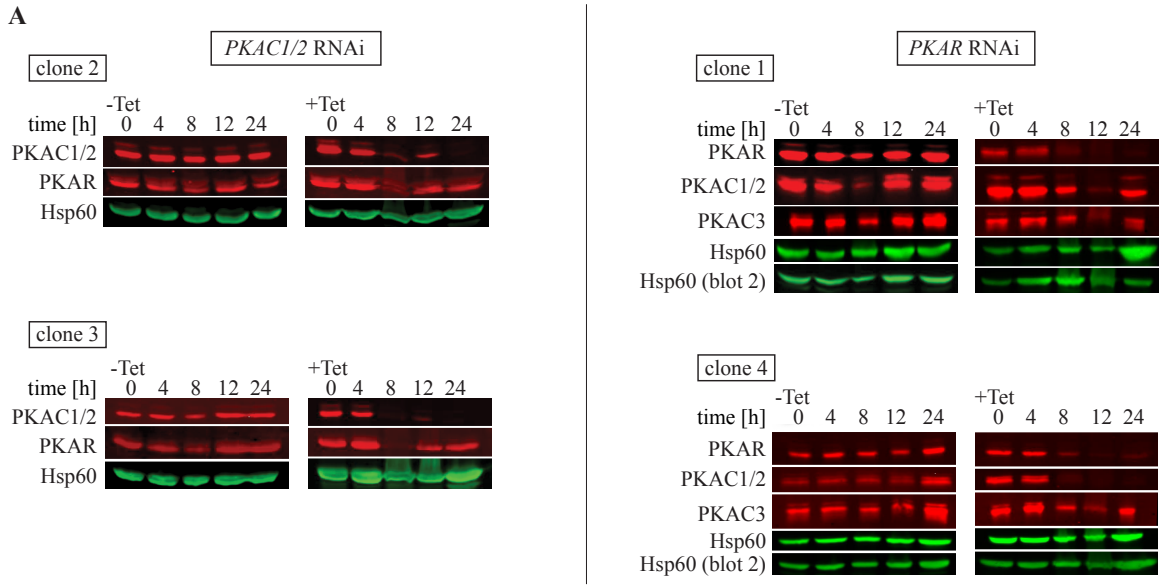


Figure S6: *T. brucei* PKA is not activated by cAMP *in vivo*.

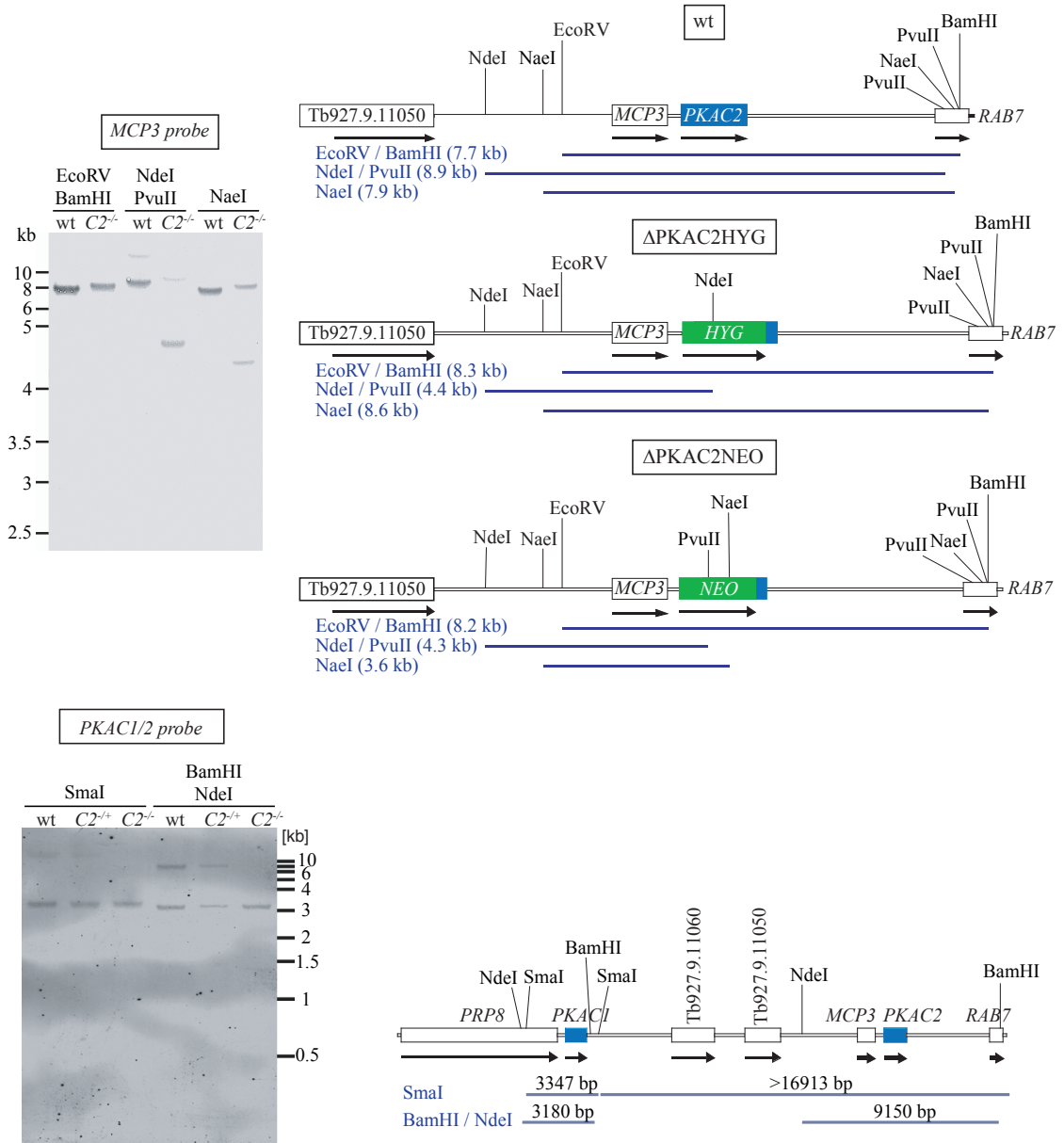
A. Western blots corresponding to the quantification shown in Figure 4B. VASP phosphorylation was analyzed in the presence of 10 μM CpdA or the solvent DMSO (1%) over 15 min. Untreated cells were included as control. The three Western blots (blot 1-3) represent three independent biological replicates.

B. Western blots corresponding to the quantification shown in Figure 4C, lower panel. VASP phosphorylation was investigated in a cell line with inducible RNAi targeting *PDEB1* and *PDEB2* in a time course over 24 h. Since the reporter substrate was expressed as Tet-inducible version, no signal was detected at time point zero. The parental cell line without RNAi against *PDEB1* and *PDEB2* was included as control. The three Western blots (blot 1-3) represent three independent biological replicates.

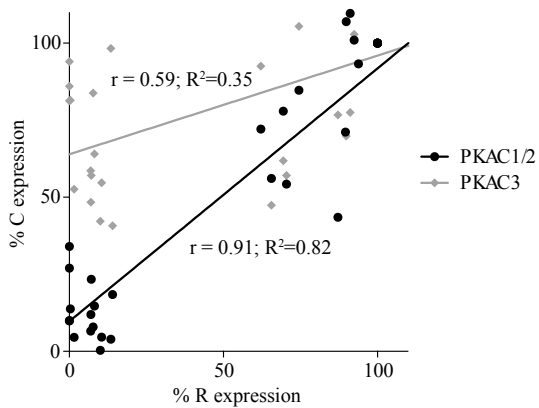
C. Dose-response analysis of VASP phosphorylation upon incubation with the PDE inhibitor CpdA for 15 min. The three Western blots (blot 1-3) represent three independent biological replicates and were used for the quantification shown in the chart; error bars represent SD.



C



D



E

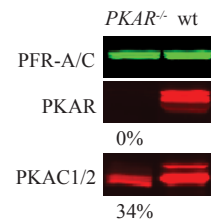


Figure S7: Western and Southern blot analyses of PKA mutants.

A. Expression of PKAR and PKAC1/2 in cell lines with inducible RNAi against *PKAC1/2* (left) or *PKAR* (right). Two clones of each RNAi cell line were analyzed. Samples were taken at time points 0, 4, 8, 12 and 24 h from the non-induced control (-Tet) or after induction of RNAi by addition of 1 $\mu\text{g/ml}$ tetracycline (+Tet). Detection of Hsp60 served as normalization control.

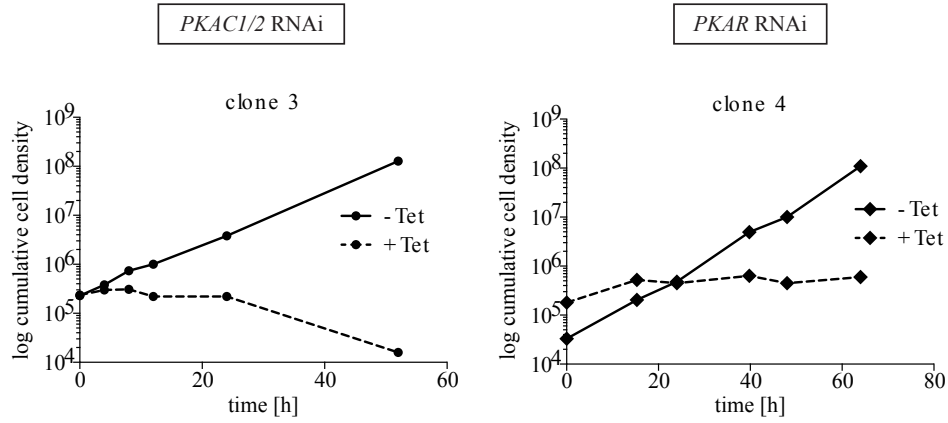
B. Southern blot confirming the replacement of one *PKAC1* allele by a blasticidin resistance cassette. Genomic DNA of wild type cells (wt) or a hemizygous deletion mutant of *PKAC1* (*PKAC1*^{-/+}) was digested with SmaI, separated on an agarose gel, transferred to a nylon membrane and probed with a digoxigenine labeled probe against the C-terminus of *PRP8*, the gene upstream of *PKAC1*. The expected DNA fragment sizes are: 3347 bp for wt and 3766 bp for *PKAC1*^{-/+}. Restriction maps are shown for the wt and the $\Delta\text{PKAC1BSD}$ locus. The two lanes marked with an asterisk (*) correspond to samples not related to this work.

C. Southern blot analyses of hemizygous and homozygous deletion mutants of *PKAC2*. Genomic DNA of wild type cells (wt) and *PKAC2* deletion mutants (*C2*^{-/+}, *C2*^{-/-}) was digested with the indicated enzymes, separated on agarose gels and blotted to nylon membranes. The blots were probed with digoxigenine labeled *MCP3* (upper blot) or *PKAC1/2* (lower blot) probes. *MCP3* is the gene upstream of *PKAC2*. It was used to enable the detection of the *PKAC2* replacement fragments. The *PKAC1/2* probe detects both *PKAC1* and *PKAC2* but not the deleted *PKAC2* allele. It was used to prove absence of additional *PKAC2* alleles. Restriction maps are shown for the wt, $\Delta\text{PKAC2HYG}$ and $\Delta\text{PKAC2NEO}$ locus. Sizes of the expected DNA fragments are indicated.

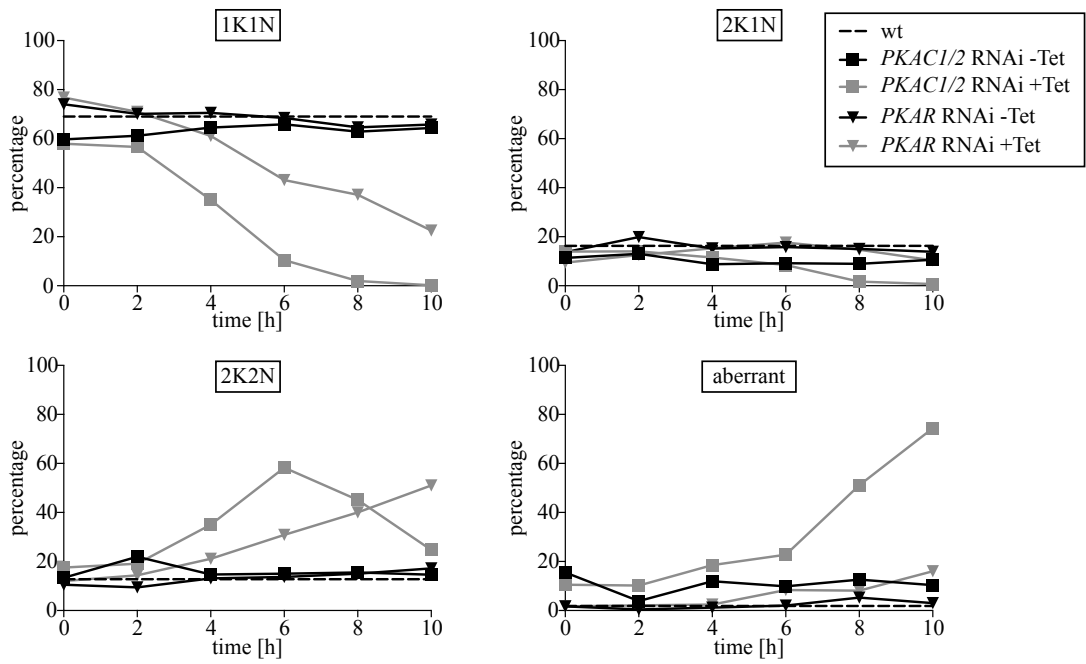
D. Co-regulation of PKA subunit expression. Signals corresponding to PKAR, PKAC1/2 and PKAC3 were quantified from Western blots of *PKAR* RNAi clones (Western blots shown in S7A and Western blots from additional clones not shown) and the *PKAR* deletion mutant (Western blot shown in S7C and additional Western blots not shown). The correlation between PKAR expression (x-axis; given in percentage) and PKAC1/2 or PKAC3 expression (y-axis; given in percentage), respectively, is depicted in the diagram. The correlation coefficient (r) and the coefficient of determination (R^2) are given for each graph.

E. Western blot showing the expression of PKAR and PKAC1/2 in a homozygous deletion mutant of *PKAR* (*PKAR*^{-/-}) compared to wild type cells (wt). Expression levels normalized on PFR-A/C detected by the monoclonal antibody L13D6 (Kohl et al., 1999) are given as percentage of wild type (wt) levels.

A



B



C

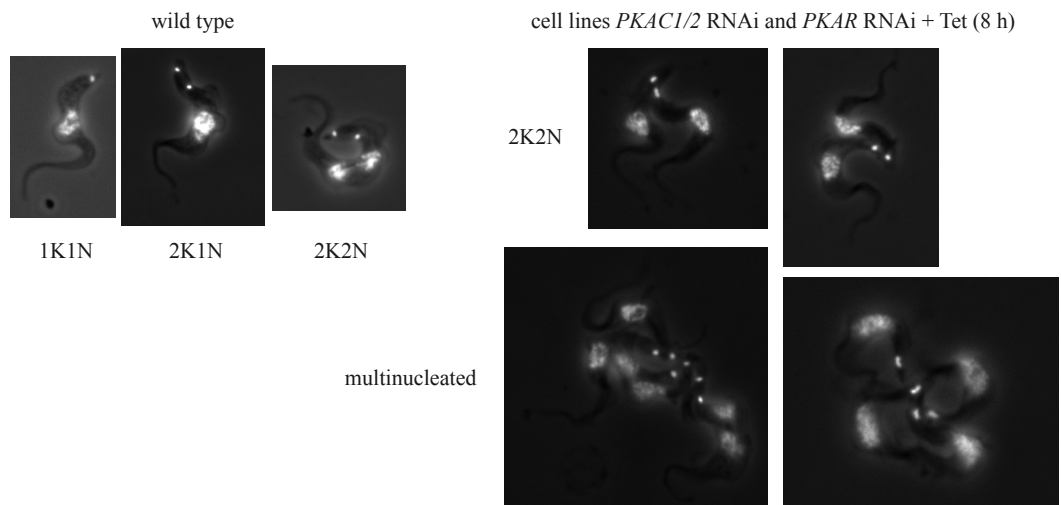
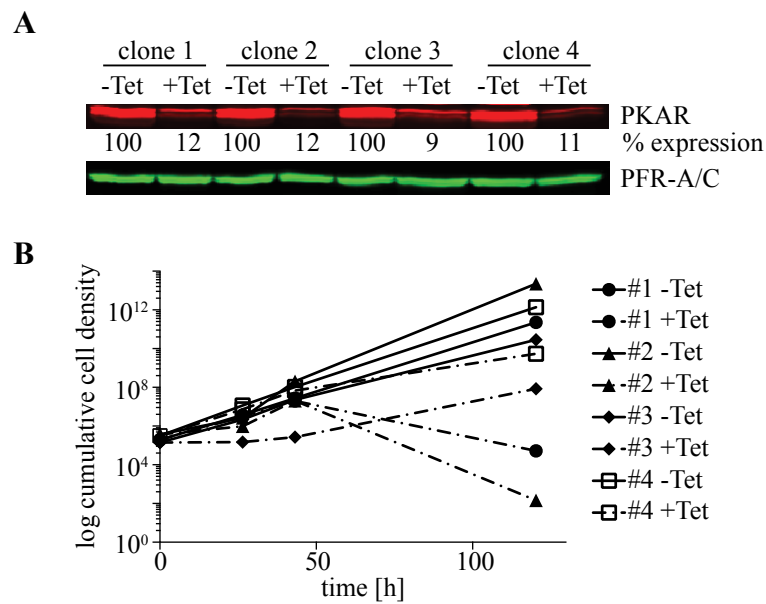


Figure S8: Growth and cell cycle analysis of additional clones of the cell lines *PKACI/2* RNAi and *PKAR* RNAi.

A. Growth analysis of cell lines with inducible RNAi against *PKACI/2* or *PKAR* in the presence or absence of 1 $\mu\text{g/ml}$ tetracycline (Tet). Cells were counted at the indicated time points and diluted if necessary to keep the cell density below $1 \times 10^6/\text{ml}$. The y-axes represent the \log_{10} of the cumulative cell densities.

B. Cell cycle analysis by counting the number of kinetoplasts (K) and nuclei (N) per cell in wild type cells (wt) and cell lines with inducible RNAi against *PKACI/2* or *PKAR* in a time course of 10 hours after induction with 1 $\mu\text{g/ml}$ tetracycline (Tet). The K/N configurations of wild type cells are represented by dashed lines, since they were analyzed only at one time point. A minimum of 100 cells of each cell line was analyzed at the indicated time points.

C. Representative microscopic images showing typical 1K1N, 2K1N, and 2K2N configurations in wild type cells as well as typical 2K2N and multinucleated cells of the cell lines *PKACI/2* RNAi and *PKAR* RNAi after induction with 1 $\mu\text{g/ml}$ tetracycline for 8 h.

**Figure S9: Non-overlapping RNAi against *T. brucei* *PKAR* targeting a C-terminal fragment of the ORF and part of the 3'UTR.**

A. Western blot analysis of a cell line with inducible RNAi against *PKAR* revealed efficient repression of the *PKAR* protein (given in percentage) after 24 h of induction with 1 $\mu\text{g/ml}$ tetracycline (+Tet) compared to non-induced cells (-Tet). Four independent clones (clones 1-4) were analyzed, and detection of PFR-A/C by the monoclonal antibody L13D6 (Kohl et al., 1999) served as normalization control.

B. Growth of four independent clones (#1, #2, #3, #4) of a cell line with inducible RNAi against *PKAR* was analyzed over a time course of 120 h in the presence (+Tet) or absence (-Tet) of 1 $\mu\text{g/ml}$ tetracycline. The y-axis represents the \log_{10} of the cumulative cell density.

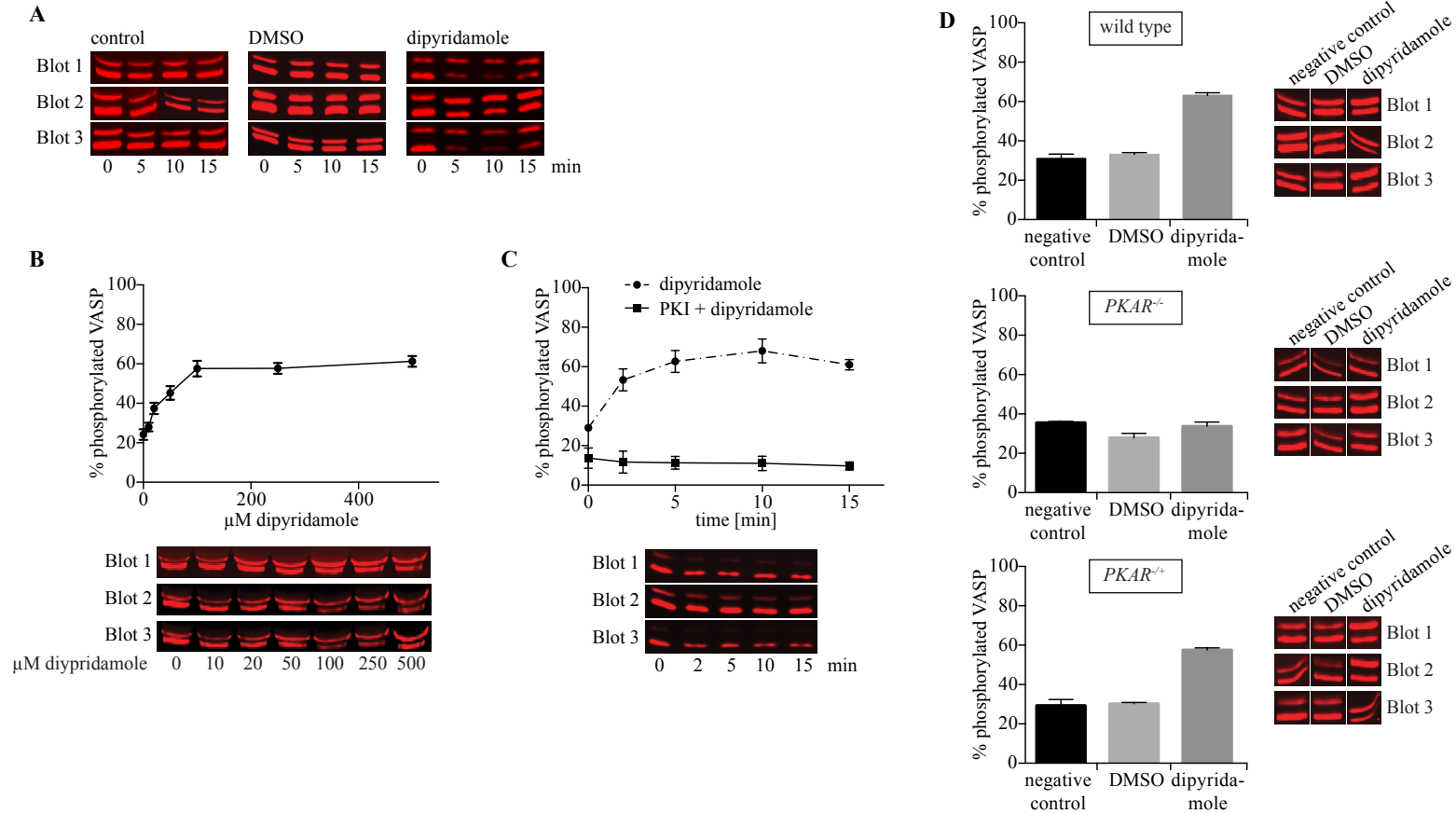


Figure S10: Specific activation of *T. brucei* PKA by dipyridamole *in vivo*.

A. Western blots corresponding to the quantification shown in Figure 6B. VASP phosphorylation was analyzed over 15 min in the presence of 100 μM dipyridamole or 1% DMSO (solvent control). Untreated cells were included as control. The three Western blots (blot 1-3) represent three independent biological replicates.

B. Dose-Response analysis of VASP phosphorylation upon incubation with dipyridamole for 15 min. The three Western blots (blot 1-3) represent three independent biological replicates and were used for the quantification shown in the chart; error bars represent SD.

C. Inhibition of dipyridamole-induced PKA activation by treatment with 100 μ M myr-PKI(14-22). VASP phosphorylation was determined upon incubation with or without 100 μ M myr-PKI(14-22) for 10 min followed by addition of 100 μ M dipyridamole. Samples were taken at the indicated time points. The three Western blots (blot 1-3) shown below the graph represent three independent biological replicates of cells treated with myr-PKI(14-22) and dipyridamole. The Western blots with the samples of the cells treated with dipyridamole only are shown in (A) (the samples taken after 2 min are not shown). Error bars represent SD.

D. Dipyridamole-induced PKA activation is dependent on PKAR. VASP phosphorylation was investigated in wild type, *PKAR*^{-/-} and *PKAR*^{-/+} (endogenous rescue) cells in the presence of 100 μ M dipyridamole or 1% DMSO (solvent control) or without treatment (negative control). Samples were taken after 10 min of incubation. Error bars represent SD of three independent biological replicates corresponding to the three Western blots shown.

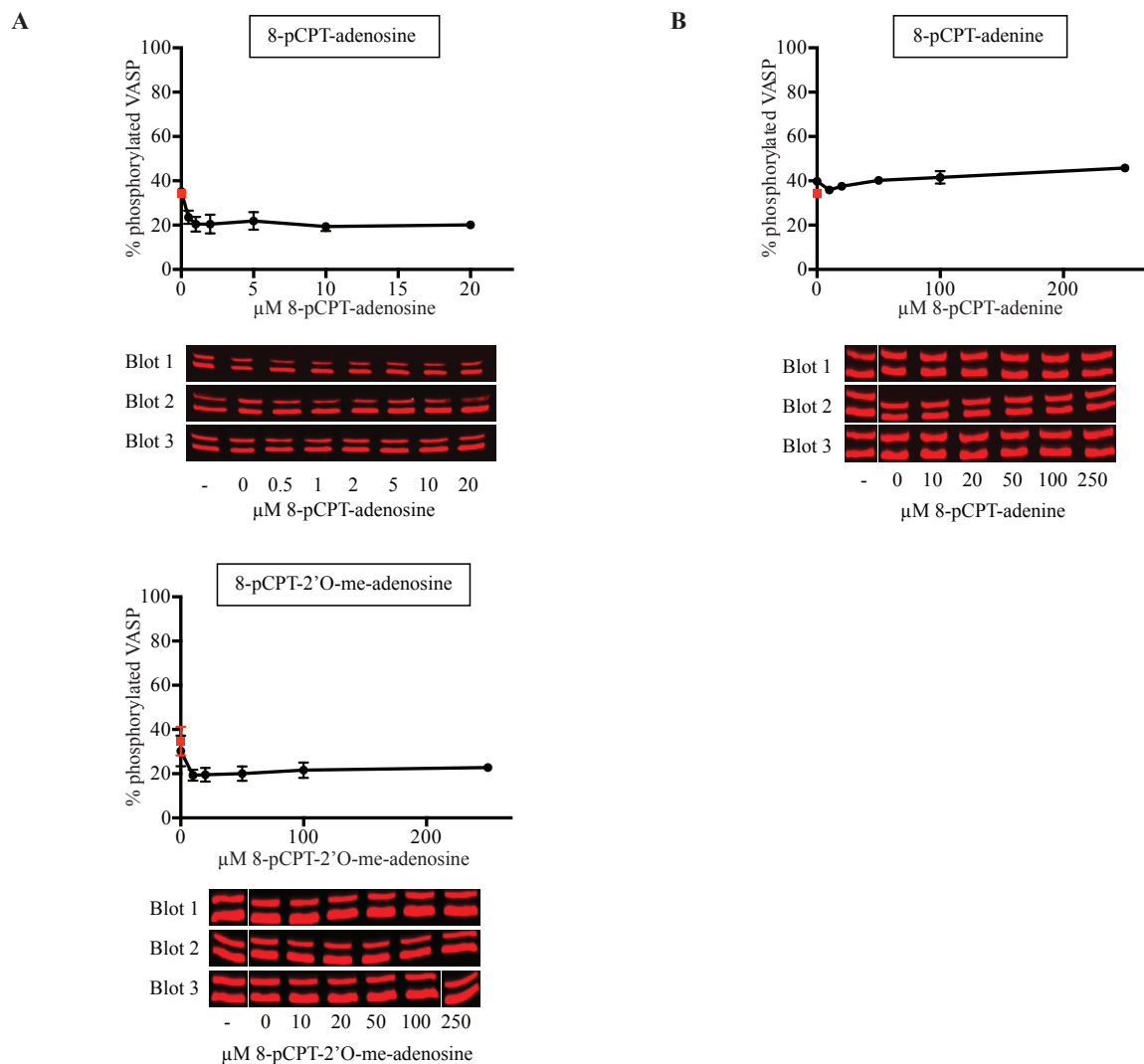


Figure S11: An *in vivo* small-scale screen identifies regulators of PKA activity in *T. brucei*.

The incubation time in all dose-response experiments was 15 min. Error bars represent SD of three independent biological replicates corresponding to the three Western blots shown for each experiment. For all compounds dissolved in DMSO, the untreated control is shown in the graphs as red dot.

A. Dose-response analysis of VASP phosphorylation upon incubation with 8-pCPT-adenosine or 8-pCPT-2'O-me-adenosine.

B. Dose-response analysis of VASP phosphorylation upon incubation with 8-pCPT-adenine.

C

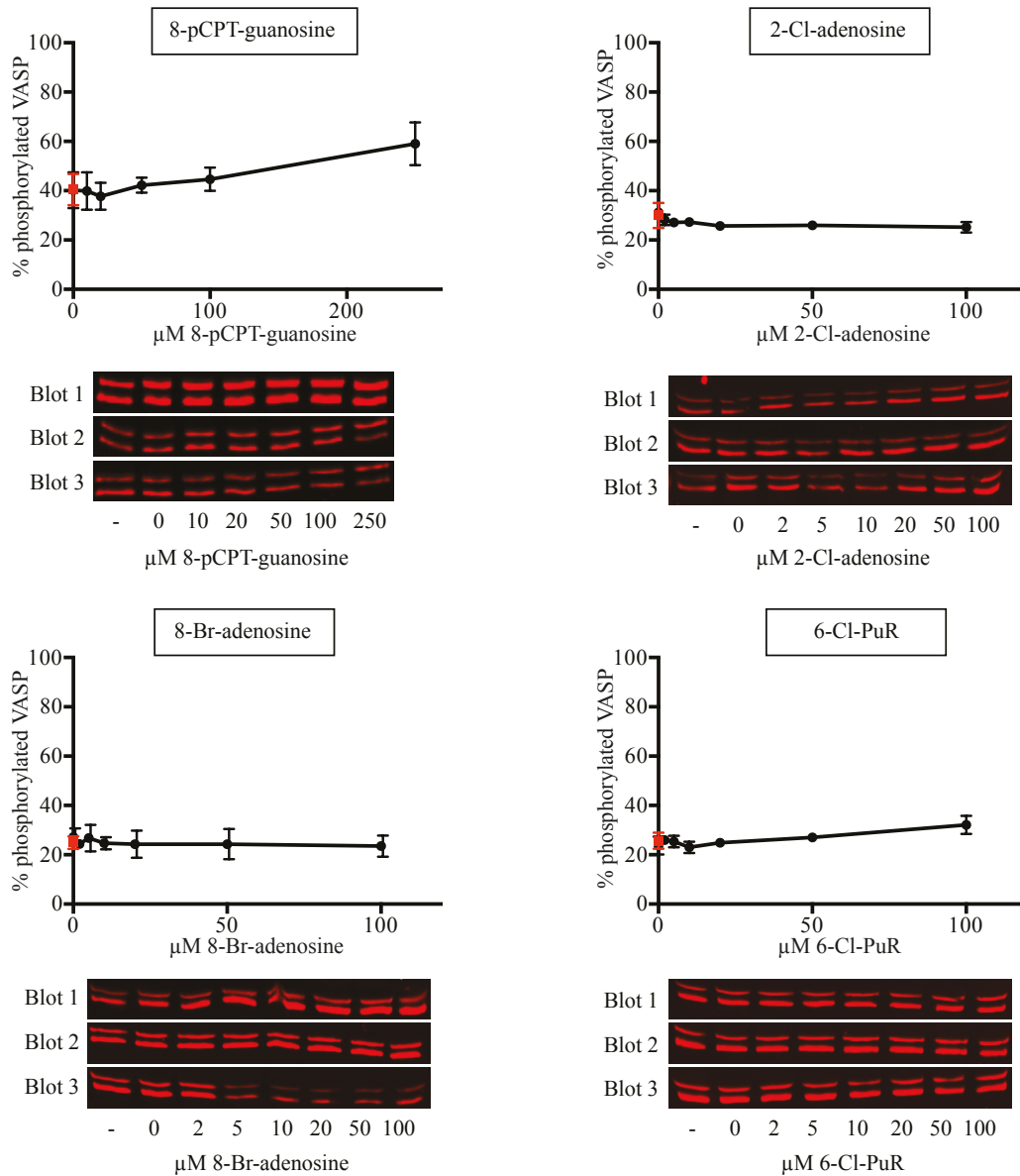


Figure S11: An *in vivo* small-scale screen identifies regulators of PKA activity in *T. brucei*.

C. Dose-response analysis of VASP phosphorylation upon incubation with the nucleoside derivatives 8-pCPT-guanosine, 2-Cl-adenosine, 8-Br-adenosine, or 6-Cl-purine riboside (6-Cl-PuR).

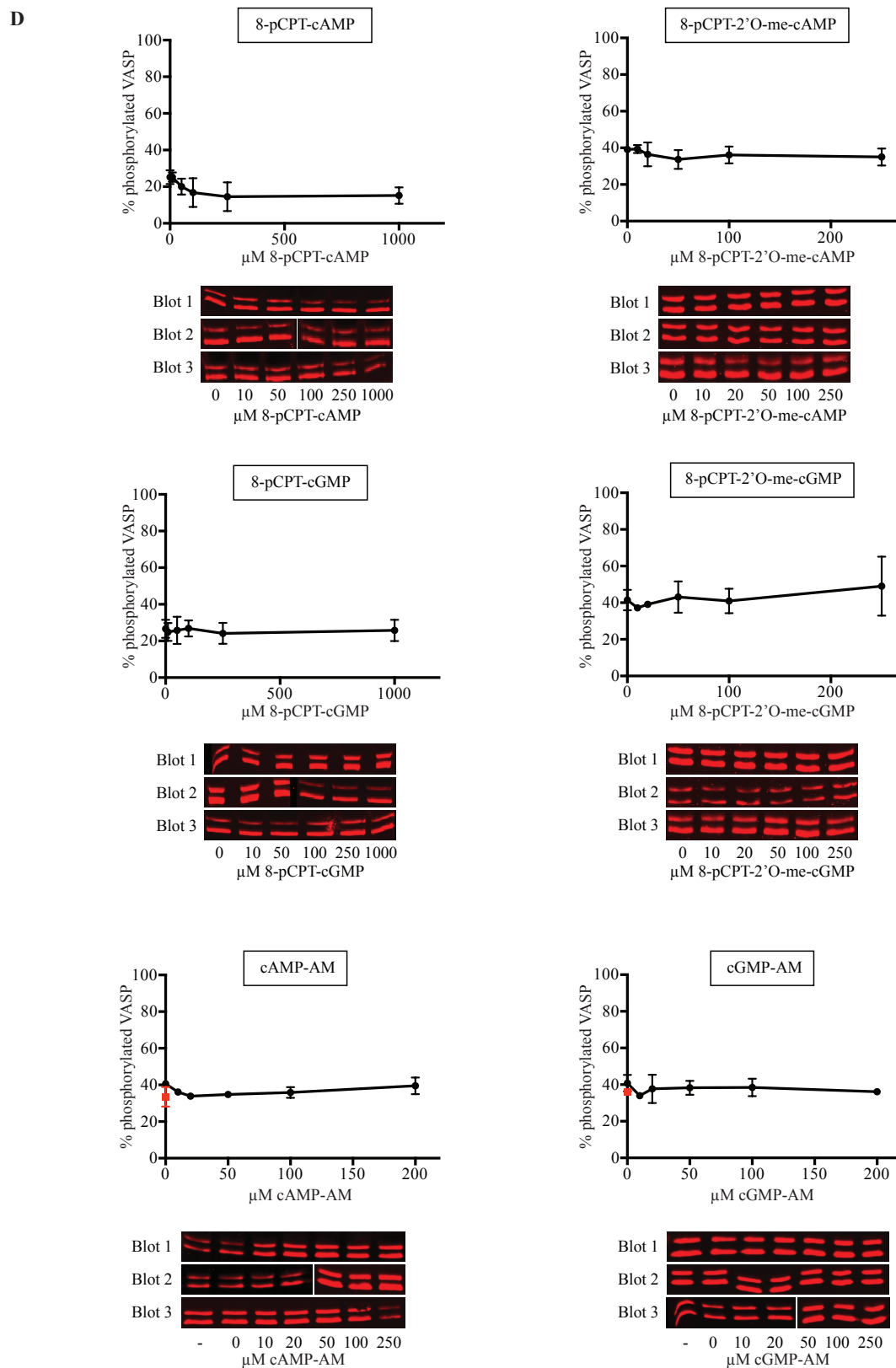


Figure S11: An *in vivo* small-scale screen identifies regulators of PKA activity in *T. brucei*.

D. Dose-response analysis of VASP phosphorylation upon incubation with the cAMP or cGMP derivatives 8-pCPT-cAMP, 8-pCPT-2'O-me-cAMP, 8-pCPT-cGMP, 8-pCPT-2'O-me-cGMP, cAMP-AM, or cGMP-AM.

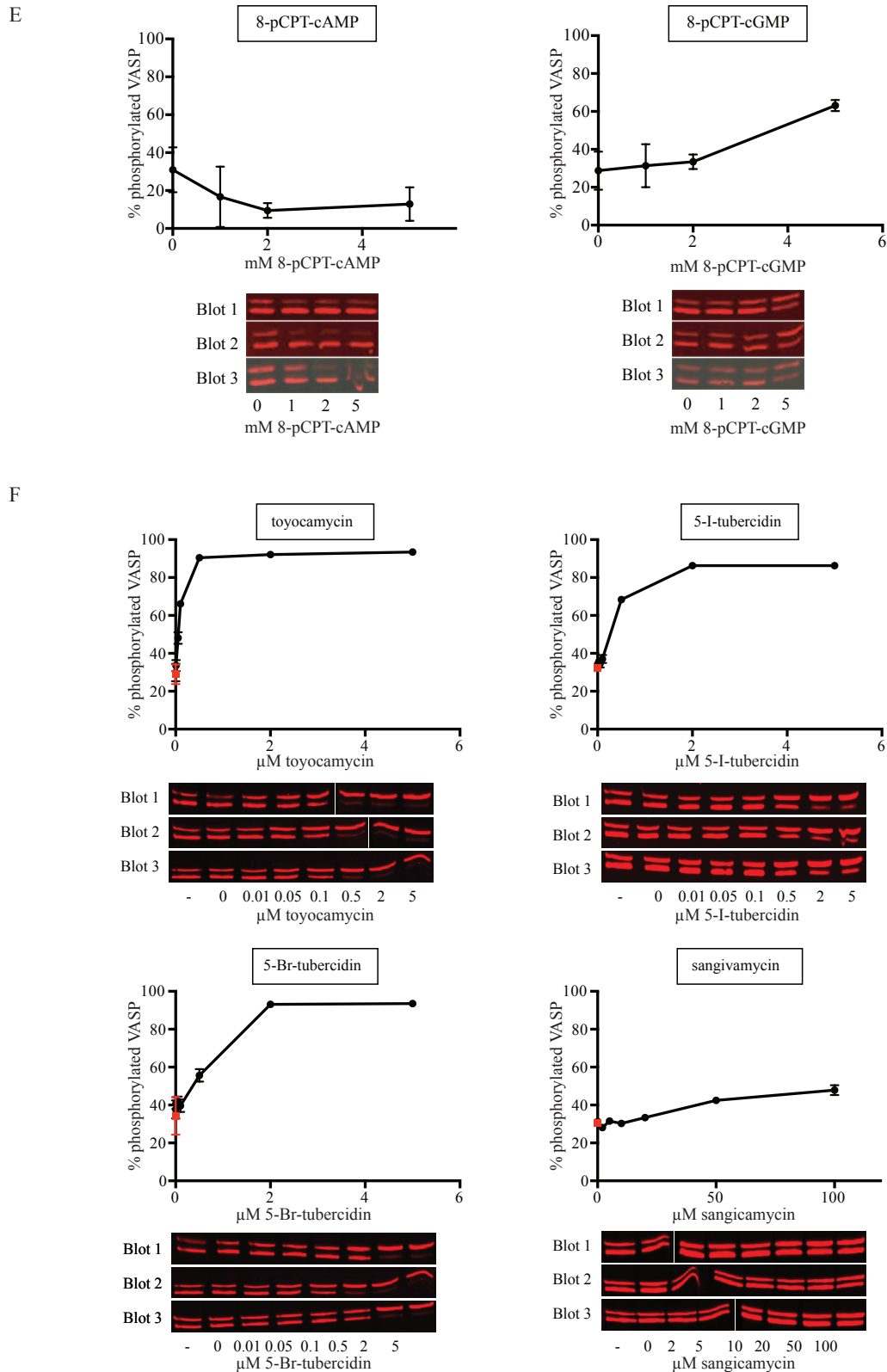
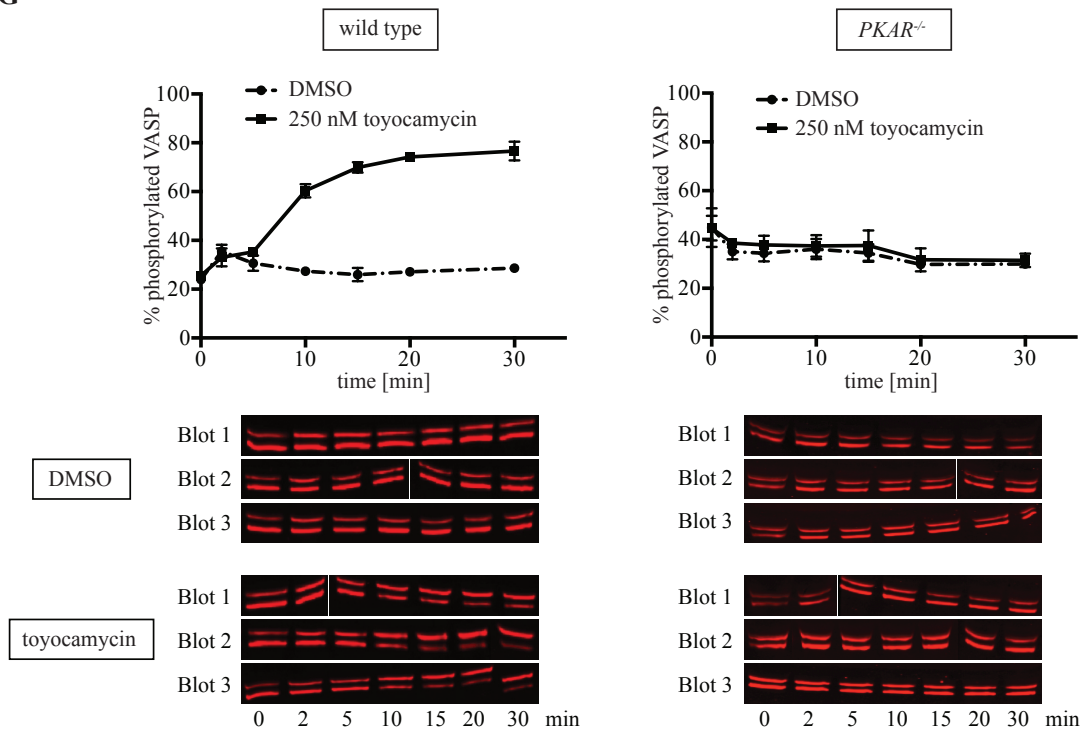


Figure S11: An *in vivo* small-scale screen identifies regulators of PKA activity in *T. brucei*.

E. Dose-response analysis of VASP phosphorylation upon incubation with high concentrations of 8-pCPT-cAMP or 8-pCPT-cGMP.

F. Dose-response analysis of VASP phosphorylation upon incubation with the 7-deazapurine derivatives toyocamycin, 5-I-tubercidin, 5-Br-tubercidin, or sangivamycin.

G



H

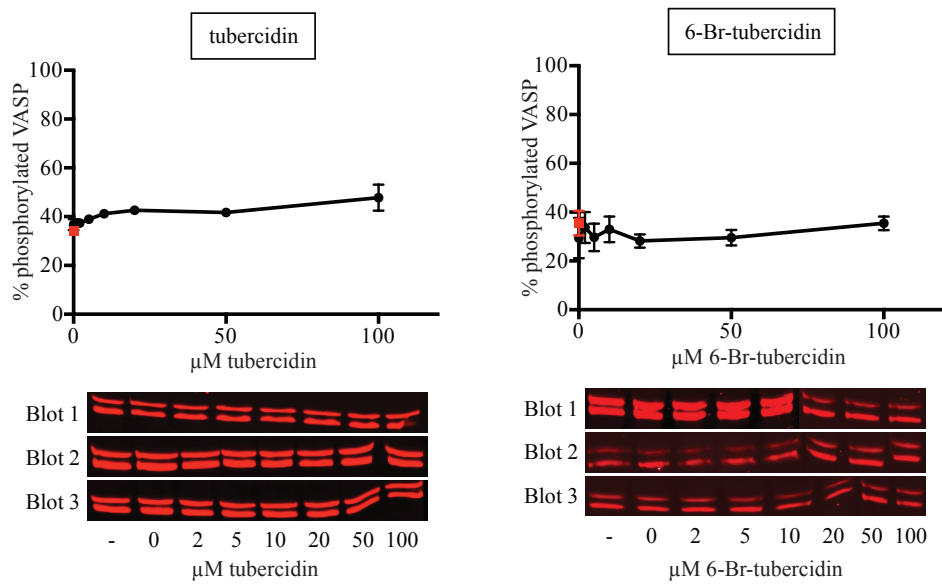


Figure S11: An *in vivo* small-scale screen identifies regulators of PKA activity in *T. brucei*.

G. Analysis of VASP phosphorylation in wild type cells or a homozygous deletion mutant of *PKAR* (*PKAR*^{-/-}) in the presence of 250 nM toyocamycin or 1% DMSO (solvent control) over 30 min.

H. Dose-response analysis of VASP phosphorylation upon incubation with tubercidin or 6-Br-tubercidin.

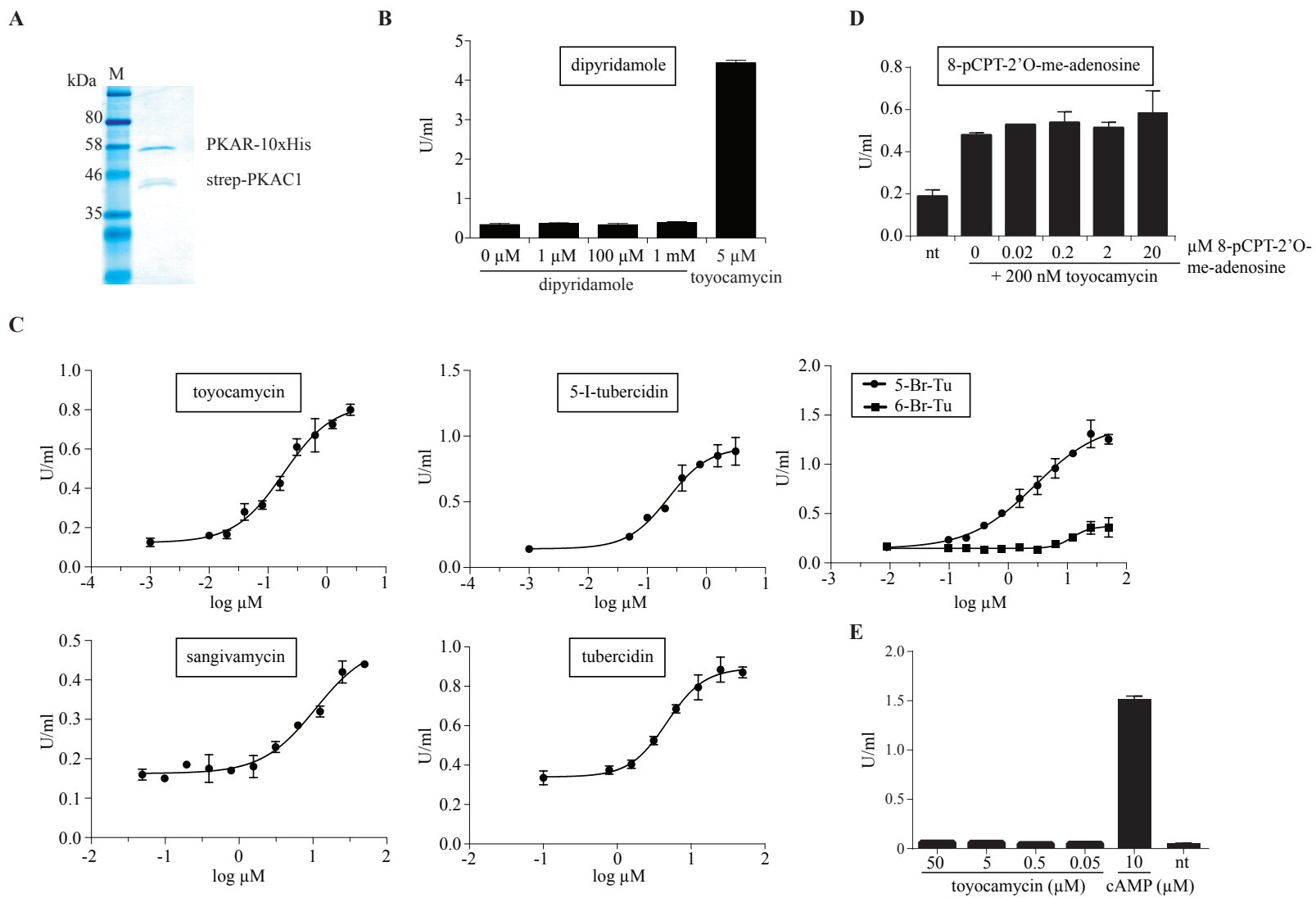


Figure S12: *In vitro* kinase assays with the identified *in vivo* regulators of *T. brucei* PKA.

A. *T. brucei* PKAR-10xHis and Strep-PKAC1 were recombinantly co-expressed using the *L. tarentolae* expression system (LEXSY). The holoenzyme was purified via His- and Strep-tag purification and subsequently used for *in vitro* kinase assays using kemptide as substrate.

B. Kemptide phosphorylation in the presence of dipyridamole (at the indicated concentrations) or 5 μ M toyocamycin (positive control). Data points represent the average of two determinations, and error bars represent the range.

C. Kemptide phosphorylation was analyzed in dose-response experiments upon incubation with toyocamycin, 5-I-tubercidin, 5-Br-tubercidin, sangivamycin, tubercidin or 6-Br-tubercidin. Data points are the average of two determinations, and error bars represent the range. This is a representative data set of at least two independent assays. The calculated EC₅₀ values (Graphpad Prism 6.0) are shown in Table 2.

D. Kemptide phosphorylation in the presence of 200 μ M toyocamycin (corresponds to the EC₅₀ concentration) and increasing concentrations of 8-pCPT-2'O-me-adenosine as indicated. The activity of the holoenzyme without compound treatment (nt) was included as control. Data points represent the average of two determinations, and error bars represent the range.

E. The human PKAR1 α holoenzyme complex (6xHis-PKAR and Strep-PKAC α) was co-expressed in *E. coli* and co-purified similarly to *T. brucei* PKA in A. *In vitro* kinase assays were performed in the presence of the indicated concentrations of toyocamycin. The activity of the holoenzyme upon treatment with 10 μ M cAMP or without compound treatment (nt), respectively, was included as control. Data points represent the average of two determinations, and error bars represent the range.

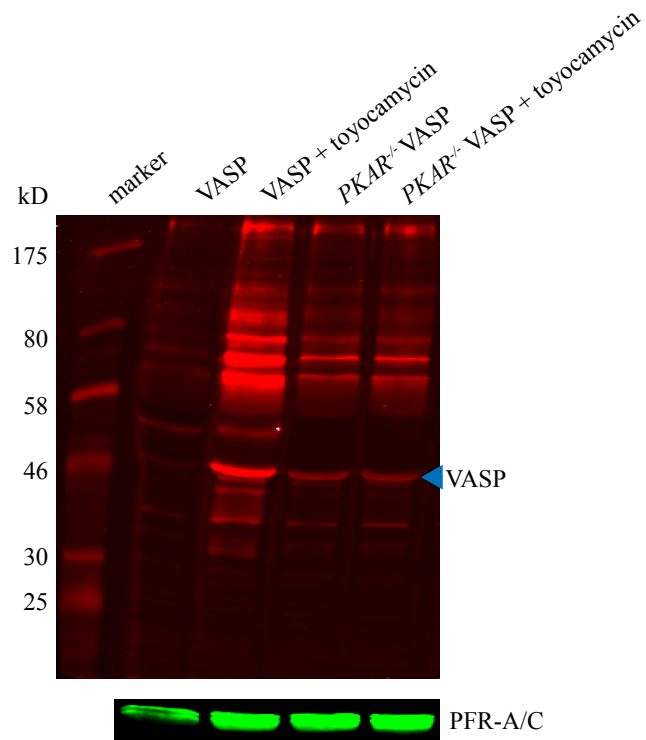


Figure S13: Increase in PKA-specific phosphorylations upon treatment with toyocamycin.

Western blot analysis of lysates from VASP expressing *T. brucei* wild type (VASP) or *PKAR*^{-/-} cells (*PKAR*^{-/-} VASP) treated or not with 2 μ M toyocamycin for 10 min. Proteins phosphorylated at RXXS/T motifs were detected by a Phospho-PKA substrate antibody (anti-RXXS*/T*; * = phosphorylation). The band corresponding to the size of the transgenically expressed PKA reporter substrate VASP is marked by a blue arrowhead. The monoclonal antibody L13D6 (Kohl et al., 1999) was used for detection of PFR-A/C as loading control.

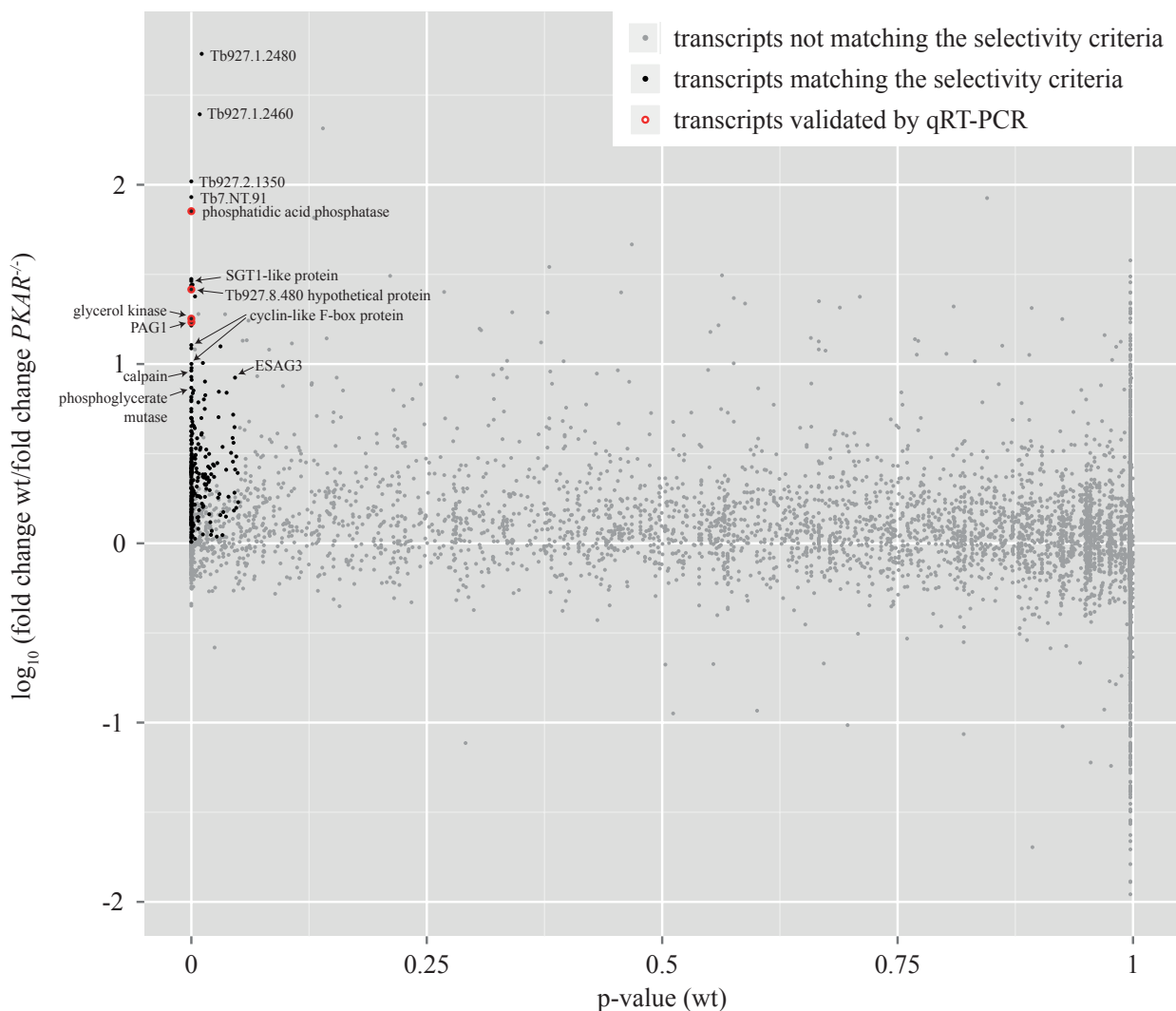


Figure S14: Scatter plot representing the RNAseq analysis of toyocamycin-treated wild type and *PKAR* knock out cells.

The logarithmic ratio of the fold change of transcripts detected in wild type (wt) cells versus the fold change in the *PKAR* deletion mutant was plotted against the p-value in wild type cells. The following selection criteria were applied: $p\text{-value wt} < 0.05$; fold change wt > 1.75 ; fold change wt / fold change *PKAR*^{-/-} > 1 ; < 2 changes in direction in both cell lines over the time course from 0 h to 8 h. Grey dots represent transcripts not matching these criteria, while transcripts matching these criteria are shown by black dots. Transcripts chosen for independent expression analysis by qRT-PCR are depicted by black dots encircled in red. The gene IDs (as TriTrypDB entries; www.tritrypdb.org) or annotated/predicted gene products are given for a selection of the transcripts matching the selectivity criteria.

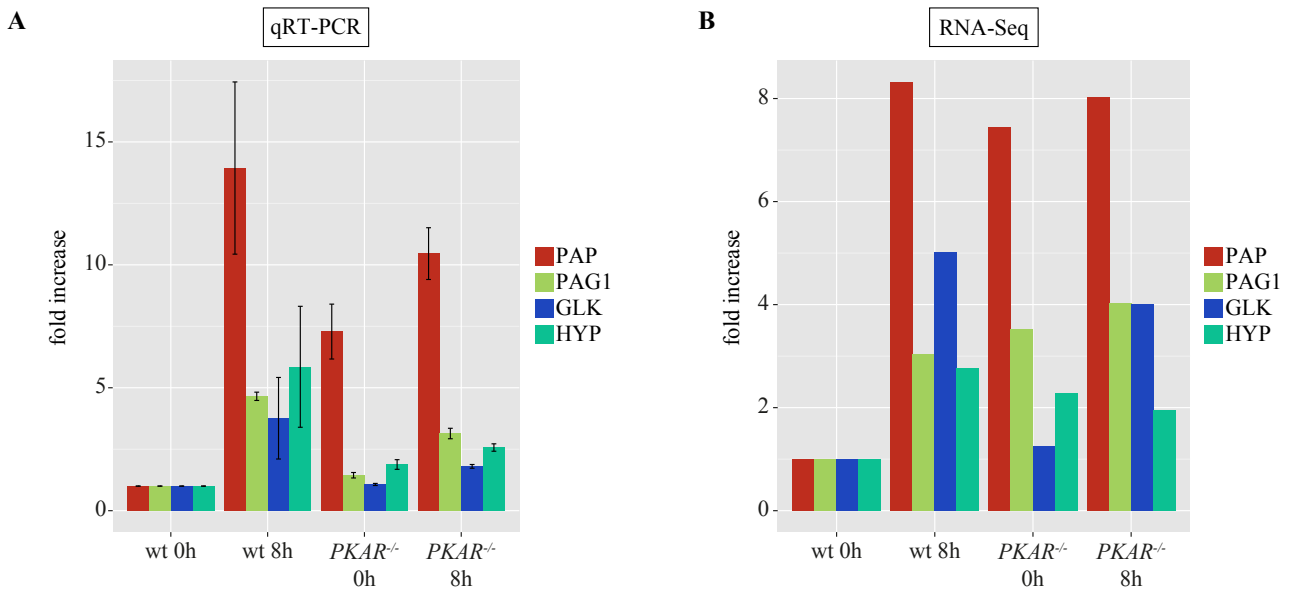


Figure S15: Validation of the RNAseq analysis by qRT-PCR.

A. Four transcripts (phosphatidic acid phosphatase (PAP; Tb927.8.480), procyclin associated gene 1 (PAG1; Tb927.10.10240), glycerol kinase 1 (GLK1; cluster of five nearly identical genes: Tb927.9.12550, Tb927.9.12570, Tb927.9.12590, Tb927.9.12610, Tb927.9.12630), and a hypothetical protein (HYP; Tb927.8.490)) matching the arbitrary defined selectivity criteria were chosen for independent expression analysis by qRT-PCR (highlighted in red in the scatter plot in Figure S14). RNA was extracted from wild type cells (wt) and the *PKAR* deletion mutant (*PKAR*^{-/-}) treated or not with toyocamycin for 8 h. Relative expression normalized to *TERT* as reference gene (Brenndorfer et al., 2010) and the wild type cell line is given with standard error (SEM) of three biological replicates.

B. Relative expression of the four transcripts chosen for the analysis shown in (A) revealed by the RNAseq study. Transcripts were normalized to the level in untreated wild type cells.

Table S1: Results of the RNAseq analysis: genes significantly regulated in wild type (wt) cells but not in the *PKAR* deletion mutant (*PKAR*^{-/-}) upon toyocamycin treatment in a time course over 8 h.

gene	product	wt 0 h	wt 0.5 h	wt 1 h	wt 4 h	wt 8 h	<i>PKAR</i> ^{-/-} 0 h	<i>PKAR</i> ^{-/-} 0.5 h	<i>PKAR</i> ^{-/-} 1 h	<i>PKAR</i> ^{-/-} 4 h	<i>PKAR</i> ^{-/-} 8 h	p-value wt	fold change wt	fold change <i>PKAR</i> ^{-/-}	fold change wt/ fold change <i>PKAR</i> ^{-/-}
Tb927.1.2480	hypothetical protein, unlikely	27	8	1	15	24	44	33	26	30	47	0,0110	27,21	1,77	15,34
Tb927.1.2460	hypothetical protein, unlikely	22	1	4	21	33	20	24	32	31	61	0,0089	33,45	3,05	10,95
Tb927.2.1350	retrotransposon hot spot protein (RHS, pseudogene), putative, retrotransposon hot spot protein 1 (RHS1), interrupted	5	26	56	150	77	8	8	20	33	29	0,0000	31,22	4,14	7,53
Tb7.NT.91		14	5	1	20	22	10	10	5	12	15	0,0000	21,64	3,14	6,90
Tb927.8.480	phosphatidic acid phosphatase protein, putative	364	565	636	1460	3030	2712	3540	2889	2962	2919	0,0000	8,32	1,31	6,38
Tb8.NT.2		25	66	66	147	205	100	120	123	126	189	0,0000	8,25	1,89	4,36
Tb927.1.3200	SGT1-like protein, putative	14	54	116	164	110	30	35	61	84	60	0,0000	12,09	2,80	4,32
Tb2.NT.37		17	79	116	51	44	28	34	45	41	37	0,0012	6,87	1,62	4,23
Tb927.11.17820_1	expression site-associated gene 3 (ESAG3), degenerate	2	29	36	49	50	4	12	10	22	30	0,0000	31,35	7,43	4,22
Tb3.NT.41		20	64	149	280	152	24	40	51	81	72	0,0000	14,01	3,36	4,17
Tb927.8.490	hypothetical protein	73	47	35	130	202	166	164	153	119	142	0,0000	5,73	1,39	4,12
Tb927.9.12590	glycerol kinase, glycosomal (glk1)	17	93	171	149	101	38	57	83	110	82	0,0000	10,15	2,91	3,49
Tb927.10.10240	procyclin-associated gene 1 (PAG1) protein (PAG1)	50	33	48	128	153	178	156	161	150	203	0,0000	4,64	1,35	3,43
Tb927.1.3770	hypothetical protein, unlikely	28	50	83	222	122	28	26	33	61	58	0,0000	7,93	2,35	3,37
Tb927.1.4630	cyclin-like F-box protein (CFB1E)	6	77	71	57	59	12	23	43	47	44	0,0000	11,97	3,96	3,02
Tb927.9.7300	hypothetical protein, unlikely	1	10	20	8	7	2	1	4	7	7	0,0309	19,85	6,62	3,00
Tb927.9.17800	hypothetical protein, unlikely	3	11	28	64	63	6	12	20	35	40	0,0000	20,00	6,74	2,97
Tb1.NT.33		145	71	54	142	213	146	152	165	195	210	0,0122	3,94	1,44	2,73
Tb927.1.4600	cyclin-like F-box protein (CFB1D)	12	61	90	78	60	18	26	42	50	43	0,0000	7,52	2,76	2,72
Tb927.8.510	hypothetical protein	64	42	50	100	173	176	179	150	115	163	0,0002	4,16	1,56	2,66

Tb927.7.4060	calpain-like cysteine peptidase, putative, cysteine peptidase, Clan CA, family C2, putative	16	75	119	160	137	22	26	54	77	84	0,0000	10,02	3,83	2,62
Tb927.10.9500	expression site-associated gene (ESAG) protein, putative, expression site-associated gene 3 (ESAG3) protein, putative	141	54	67	119	203	188	135	126	183	171	0,0463	3,76	1,49	2,52
Tb927.7.1290	hypothetical protein, conserved	33	120	143	105	96	52	61	79	88	91	0,0003	4,35	1,75	2,49
Tb927.11.10340	phosphoglycerate mutase family member 5, putative	639	427	463	1133	2027	996	790	699	1213	1391	0,0000	4,74	1,99	2,38
Tb927.7.6500	variant surface glycoprotein (VSG), putative	53	192	191	91	93	62	72	86	96	79	0,0023	3,64	1,55	2,34
Tb927.7.6880	hypothetical protein, conserved	51	29	23	73	97	44	43	43	77	66	0,0293	4,15	1,78	2,33
Tb927.2.3340	hypothetical protein	325	142	91	298	372	335	280	247	294	436	0,0015	4,08	1,77	2,31
Tb927.10.9360	hypothetical protein, conserved	162	54	69	203	201	224	168	181	246	278	0,0149	3,77	1,65	2,28
Tb927.9.6760	hypothetical protein, conserved	129	595	634	186	95	104	201	305	120	107	0,0000	6,65	2,94	2,26
Tb927.10.10610	protein tyrosine phosphatase, putative	638	204	227	512	658	509	432	353	424	507	0,0133	3,22	1,44	2,23
Tb927.9.12570	glycerol kinase, glycosomal (glk1)	18	101	156	160	112	22	43	81	89	82	0,0000	9,07	4,07	2,23
Tb7.NT.112		150	270	472	546	313	186	199	257	307	236	0,0000	3,65	1,65	2,21
Tb927.11.2690	succinyl-coA:3-ketoacid-coenzyme A transferase, mitochondrial precursor, putative	899	1649	1291	689	496	495	607	749	602	494	0,0074	3,33	1,51	2,20
Tb5.NT.25		64	37	42	116	124	52	60	73	77	82	0,0143	3,36	1,59	2,12
Tb8.NT.1		39	81	99	194	202	54	58	75	99	131	0,0000	5,14	2,43	2,12
Tb927.9.12610	glycerol kinase, glycosomal (glk1)	25	99	186	139	96	28	55	88	100	76	0,0000	7,49	3,59	2,09
Tb927.10.15020	protein kinase, putative	48	39	31	69	108	38	54	47	66	54	0,0288	3,53	1,74	2,02
Tb6.NT.31_homologue		82	113	139	185	279	154	171	184	126	212	0,0000	3,39	1,68	2,01
Tb927.11.9070	palmitoyl acyltransferase 4, putative	159	96	119	227	270	240	176	175	222	243	0,0106	2,79	1,39	2,01
Tb6.NT.31		247	407	399	527	825	481	498	553	416	690	0,0000	3,34	1,66	2,01
Tb927.1.470	hypothetical protein, conserved	193	82	91	245	301	182	151	140	228	255	0,0003	3,66	1,83	2,00
Tb927.3.2600	ATP-dependent DEAD/H RNA helicase, putative	332	393	375	228	143	341	273	325	336	245	0,0010	2,75	1,39	1,97
Tb927.11.14190	hypothetical protein, conserved	516	681	501	393	278	529	613	564	485	586	0,0015	2,45	1,26	1,94
Tb927.1.2330	beta tubulin	555	1369	2328	2581	1935	683	1050	1195	1653	1380	0,0000	4,65	2,42	1,92

Tb927.9.7230	ADP-ribosylation factor-like protein, putative (ARL1B)	35	108	108	91	100	54	50	41	65	61	0,0028	3,08	1,60	1,92
Tb927.2.1452	18S ribosomal RNA	22	28	61	98	62	28	28	27	65	40	0,0458	4,54	2,37	1,91
Tb927.11.7710	Gp63-1 surface protease homolog, putative	5	16	27	33	44	8	17	20	30	39	0,0036	9,22	4,85	1,90
Tb927.10.8520	glucose transporter, putative	16	86	124	87	104	24	46	41	92	99	0,0000	7,73	4,13	1,87
Tb927.10.10520	histone H2B, putative	27	103	188	257	221	26	69	87	131	117	0,0000	9,44	5,06	1,87
Tb7.NT.82		338	187	201	370	472	351	273	269	344	367	0,0111	2,52	1,36	1,85
Tb2.NT.20		127	125	173	339	219	114	130	138	169	164	0,0106	2,72	1,48	1,83
Tb927.6.2330	RGG protein (RGG1)	908	545	384	881	1137	758	749	643	1044	867	0,0000	2,96	1,62	1,82
Tb927.5.970	class I transcription factor A, subunit 6 (CITFA-6)	398	224	212	446	493	425	398	334	411	431	0,0439	2,32	1,29	1,80
Tb927.11.3150	hypothetical protein, conserved	61	41	43	68	141	58	56	41	64	78	0,0061	3,46	1,93	1,80
Tb927.1.270	hypothetical protein	410	227	210	598	796	311	283	288	578	601	0,0000	3,78	2,13	1,78
Tb927.9.12630	glycerol kinase, glycosomal (glk1)	19	113	190	139	100	20	53	76	111	94	0,0000	9,92	5,58	1,78
Tb927.11.13800	hypothetical protein, conserved	345	225	317	459	485	345	361	355	324	399	0,0448	2,15	1,23	1,75
Tb11.NT.105_1		78	46	59	84	181	124	90	111	158	200	0,0006	3,91	2,23	1,75
Tb927.6.2270	hypothetical protein, conserved	969	611	390	864	1071	796	769	670	1059	842	0,0074	2,75	1,58	1,74
Tb927.11.6440	hypothetical protein, conserved	320	317	300	193	110	317	355	372	278	222	0,0000	2,91	1,67	1,74
Tb7.NT.116		184	151	128	237	312	210	188	167	185	239	0,0098	2,43	1,43	1,70
Tb927.9.12550	glycerol kinase, glycosomal (glk1)	26	111	173	123	116	24	61	89	93	87	0,0000	6,56	3,87	1,70
Tb927.10.2470	hypothetical protein, conserved	743	364	388	843	824	854	643	622	821	759	0,0159	2,32	1,37	1,69
Tb927.11.12850	oligopeptidase b,serine peptidase, clan SC, family S9A-like protein (OPB)	1789	977	1410	1613	1251	1445	1476	1560	1543	1435	0,0091	1,83	1,09	1,68
Tb9.NT.99		286	226	195	385	563	345	301	301	405	517	0,0000	2,89	1,72	1,68
Tb927.11.9640	glycyl-tRNA synthetase, putative	438	563	539	339	271	423	413	387	366	337	0,0422	2,08	1,26	1,66
Tb927.7.2170	hypothetical protein, conserved	289	393	333	211	142	200	236	226	196	140	0,0188	2,78	1,69	1,65
Tb927.8.4820	eukaryotic translation initiation factor 4 gamma, putative	446	591	442	331	206	349	368	397	267	227	0,0003	2,88	1,75	1,65
Tb927.11.13870	hypothetical protein, conserved	326	260	220	463	478	397	321	315	416	418	0,0047	2,17	1,33	1,64
Tb927.9.15460	calcium motive p-type ATPase, putative	824	492	400	563	446	729	699	660	681	577	0,0001	2,06	1,26	1,63
Tb927.10.6630	ATP-dependent DEAD/H RNA helicase HEL64, putative (HEL64)	308	384	322	256	176	220	290	295	239	248	0,0477	2,18	1,34	1,62

Tb927.8.6390	lysophospholipase, putative,alpha/beta hydrolase, putative (TbLysoPLA)	531	203	203	540	547	579	520	558	546	864	0,0151	2,69	1,66	1,62
Tb927.10.9570	paraflagellar rod component, putative (PFC14)	1435	1666	1253	900	1003	1243	1263	1308	1217	1137	0,0005	1,85	1,15	1,61
Tb927.8.6760	IgE-dependent histamine-releasing factor, putative	1520	713	881	1012	1002	1483	1603	1518	1309	1211	0,0025	2,13	1,32	1,61
Tb927.6.1240	hypothetical protein, conserved	290	178	118	354	422	230	291	244	341	510	0,0000	3,57	2,22	1,61
Tb927.2.650	hypothetical protein	154	90	96	220	260	114	117	142	205	195	0,0041	2,89	1,80	1,60
Tb927.9.5320	nucleolar RNA binding protein, putative	581	689	766	446	291	395	468	496	398	301	0,0002	2,63	1,65	1,59
Tb927.8.6520	hypothetical protein, conserved	222	184	136	311	309	249	201	224	291	288	0,0442	2,28	1,45	1,58
Tb927.10.7410	succinyl-CoA ligase [GDP-forming] beta-chain, putative	1929	2211	3055	1698	1221	1627	1561	1899	1509	1193	0,0000	2,50	1,59	1,57
Tb3.NT.52		115	80	67	218	277	110	102	157	193	270	0,0000	4,15	2,65	1,57
Tb10.NT.107		210	136	127	248	316	170	158	170	250	242	0,0275	2,48	1,59	1,56
Tb927.10.6890	hypothetical protein	214	153	106	206	337	224	179	194	226	367	0,0038	3,20	2,05	1,56
Tb927.4.4730	amino acid transporter, putative (AATP11)	467	366	298	235	287	297	324	306	271	253	0,0230	1,99	1,28	1,55
Tb927.2.1810	transcription silencer (ISWI)	520	799	602	461	214	299	395	411	265	171	0,0001	3,73	2,40	1,55
Tb10.NT.74		1235	973	977	2165	2235	1271	1156	1062	1580	1384	0,0000	2,30	1,49	1,54
Tb927.4.1910	hypothetical protein, conserved	450	480	356	328	246	353	306	279	286	299	0,0022	1,95	1,27	1,54
Tb10.NT.193_1		272	196	135	314	366	234	259	273	323	409	0,0242	2,70	1,75	1,54
Tb927.3.1380	ATP synthase beta chain, mitochondrial precursor,ATP synthase F1, beta subunit	1528	1418	1667	1174	841	1066	1073	1240	967	958	0,0000	1,98	1,29	1,53
Tb927.9.3550	hypothetical protein, conserved	469	327	416	668	735	693	531	583	697	779	0,0002	2,25	1,47	1,53
Tb927.10.1630	unspecified product (RLI)	510	562	387	339	241	365	432	534	349	396	0,0000	2,33	1,53	1,52
Tb927.9.13820	kinetoplastid membrane protein KMP-11	43	181	335	408	409	58	121	135	292	361	0,0000	9,47	6,23	1,52
Tb927.10.3650	NADH-dependent fumarate reductase, putative	746	610	621	853	1081	822	716	777	705	810	0,0007	1,77	1,17	1,52
Tb927.10.8400	legume-like lectin, putative	462	320	256	496	630	537	400	338	523	546	0,0054	2,46	1,62	1,52
Tb927.7.6860	expression site-associated gene (ESAG) protein, putative,expression site-associated gene 5 (ESAG5) protein, putative	2865	1648	2140	3426	3842	3822	3744	3188	3661	4902	0,0000	2,33	1,54	1,52

Tb927.10.540	ATP-dependent DEAD/H RNA helicase, putative,DEAD box RNA helicase, putative	1512	1900	1530	1154	1018	1485	1582	1408	1318	1284	0,0000	1,87	1,23	1,51
Tb8.NT.73		62	77	92	69	131	96	78	68	86	86	0,0465	2,12	1,41	1,51
Tb3.NT.53		266	219	182	373	463	244	273	258	377	410	0,0001	2,54	1,68	1,51
Tb927.4.120	hypothetical protein	132	60	79	168	201	100	81	102	175	182	0,0370	3,37	2,23	1,51
Tb927.2.5980	ATP-dependent Clp protease subunit, heat shock protein 104 (HSP104), putative,atp-dependent chaperone (HSP104)	126	226	411	360	260	158	175	228	341	305	0,0003	3,25	2,16	1,50
Tb927.10.14710	40S ribosomal protein S2, putative (RPS2)	11337	14647	11370	14469	6976	10602	13453	11340	14868	12971	0,0000	2,10	1,40	1,50
Tb927.3.1630	casein kinase 1, putative (CK1)	3	33	37	19	17	2	8	6	15	12	0,0001	11,56	7,74	1,49
Tb927.11.11520	glycosomal membrane protein (PEX11)	3645	3875	2779	2048	2324	2720	2759	2962	2333	2591	0,0000	1,89	1,27	1,49
Tb7.NT.102		62	31	34	95	129	66	67	46	98	129	0,0056	4,13	2,77	1,49
Tb927.2.900	hypothetical protein	365	220	218	564	751	281	297	324	619	651	0,0000	3,44	2,31	1,49
Tb927.11.9850	hypothetical protein, conserved	370	394	304	437	601	327	335	329	436	375	0,0012	1,98	1,33	1,48
Tb927.9.10310	mitochondrial carrier protein (MCP11)	1115	1221	1144	817	694	982	913	1044	942	879	0,0000	1,76	1,19	1,48
Tb10.NT.193_3		659	526	467	929	1008	772	765	815	825	1115	0,0000	2,16	1,46	1,48
Tb927.9.6470	hypothetical protein, conserved	10	34	41	38	42	10	14	27	20	26	0,0491	4,07	2,75	1,48
Tb927.11.9610	eukaryotic translation initiation factor 3 subunit 2, putative (eIF-3 beta)	1130	1698	1659	931	662	858	946	1078	664	622	0,0002	2,56	1,73	1,48
Tb9.NT.106		71	48	77	102	153	134	78	95	120	170	0,0211	3,18	2,16	1,47
Tb1.NT.41		32	40	29	57	93	38	42	34	71	75	0,0147	3,24	2,20	1,47
Tb9.NT.1		110	47	65	166	175	150	85	102	181	213	0,0122	3,70	2,52	1,47
Tb927.11.11830	40S ribosomal protein S17, putative	15195	19012	18227	21302	27569	15574	18030	15521	19211	18980	0,0000	1,81	1,24	1,47
Tb927.7.6770	hypothetical protein, conserved	22	51	64	80	81	28	21	33	51	47	0,0144	3,60	2,46	1,46
Tb927.6.480	EP3-2 procyclin,PARP A-beta,surface protein EP3-2,surface protein EP3-2 procyclin precursor,procyclic form specific polypeptide A-beta precursor	378	528	445	554	709	515	624	573	487	611	0,0000	1,87	1,28	1,46
Tb927.8.6750	translationally controlled tumor protein (TCTP), putative	1555	790	920	1062	1102	1607	1691	1603	1399	1246	0,0133	1,97	1,36	1,45

Tb10.NT.111		1105	832	666	1440	1204	996	826	1234	992	1010	0,0241	2,16	1,49	1,45
Tb927.11.7380	glycerol-3-phosphate dehydrogenase (FAD-dependent), mitochondrial	1889	2293	1973	1525	1283	1958	2091	2142	1739	1735	0,0000	1,79	1,23	1,45
Tb927.11.7930	RNA polymerase B subunit RPB8, putative (RPB8)	532	349	361	646	699	613	527	442	576	588	0,0174	2,00	1,39	1,44
Tb927.8.3760	hypothetical protein	806	924	1097	800	542	788	664	789	673	563	0,0132	2,02	1,40	1,44
Tb927.8.7230	hypothetical protein, conserved	274	201	152	351	392	299	216	207	372	358	0,0072	2,59	1,80	1,44
Tb927.3.4530	hypothetical protein, conserved	282	258	187	365	416	222	280	239	307	344	0,0159	2,23	1,55	1,43
Tb8.NT.98		566	538	438	740	817	419	468	500	550	454	0,0021	1,87	1,31	1,42
Tb10.NT.193_2		254	179	158	338	366	236	241	254	257	384	0,0190	2,32	1,63	1,42
Tb927.7.1110	asparagine synthetase a, putative	2328	2749	2237	2001	1348	1659	1631	1867	1620	1301	0,0000	2,04	1,44	1,42
Tb927.3.3030	hypothetical protein, conserved	326	401	435	331	147	208	233	368	204	175	0,0065	2,97	2,10	1,42
Tb927.11.16760	T-complex protein 1, alpha subunit, putative (TCP-1-alpha)	2398	2852	2780	1807	1182	1828	1723	2330	1754	1361	0,0000	2,41	1,71	1,41
Tb927.4.4380	vacuolar-type proton translocating pyrophosphatase 1, putative (PPase1)	1115	1439	1533	936	800	1150	1299	1425	1046	1118		1,92	1,36	1,41
Tb927.11.17440	variant surface glycoprotein (VSG), degenerate	43	39	71	149	162	86	55	96	158	163	0,0000	4,19	2,98	1,40
Tb927.11.3250	dynein heavy chain, putative	2448	1768	1634	1363	1035	2058	2162	2321	1860	1368	0,0000	2,37	1,70	1,39
Tb927.9.6850	hypothetical protein, unlikely	101	47	65	143	176	80	58	53	122	142	0,0142	3,72	2,68	1,39
Tb11.NT.125		430	281	253	512	566	445	378	313	503	505	0,0158	2,24	1,61	1,39
Tb927.5.4420	nucleolar RNA helicase II, putative, nucleolar RNA helicase Gu, putative	853	1301	1145	757	557	774	669	725	699	459	0,0149	2,34	1,69	1,39
Tb927.10.14820	mitochondrial carrier protein, ADP/ATP translocase 1, putative (MCP5c)	769	922	752	547	512	565	629	639	486	594	0,0058	1,80	1,31	1,37
Tb927.10.14840	mitochondrial carrier protein (MCP5a)	763	876	800	530	473	493	633	630	467	553	0,0009	1,85	1,36	1,36
Tb927.10.1060	T-complex protein 1, delta subunit, putative (TCP-1-delta)	1884	2389	2402	1404	1089	1607	1570	2013	1543	1244	0,0000	2,21	1,62	1,36
Tb927.6.520	EP3-2 procyclin, PARP A-beta, surface protein EP3-3 procyclin precursor, procyclic form specific polypeptide A-beta precursor	373	520	511	539	682	473	634	549	499	607	0,0000	1,83	1,34	1,36

Tb927.6.510	GPEET2 procyclin precursor, PARP A-alpha, procyclin A-alpha, procyclic form specific polypeptide A-alpha precursor	371	532	467	528	664	457	601	592	482	592	0,0001	1,79	1,32	1,36
Tb927.8.4330	small GTP-binding protein Rab11 (RAB11)	961	1043	945	730	563	892	824	1013	741	792	0,0000	1,85	1,37	1,36
Tb927.11.1870	histone H1, putative	2160	1432	1988	2405	2648	2241	2251	1795	2447	2368	0,0005	1,85	1,36	1,36
Tb10.NT.182		202	140	124	198	321	204	188	213	251	359	0,0159	2,59	1,91	1,36
Tb927.1.275	expression site-associated gene (ESAG, pseudogene), putative, expression site-associated gene 4 (ESAG4), pseudogene	330	233	238	502	498	287	321	286	360	456	0,0012	2,16	1,60	1,35
Tb927.5.150	hypothetical protein, conserved	533	445	381	358	299	313	362	357	414	335	0,0008	1,78	1,32	1,35
Tb927.4.3600	hypothetical protein, conserved	333	233	199	336	475	405	292	229	289	330	0,0194	2,38	1,77	1,35
Tb927.11.6880	hypothetical protein	456	333	354	393	224	443	514	412	415	339	0,0010	2,03	1,51	1,34
Tb927.6.3590	hypothetical protein, conserved	202	223	246	285	388	206	210	193	276	265	0,0024	1,91	1,43	1,34
Tb927.10.16190	expression site-associated gene 4 (ESAG4) protein, putative, expression site-associated gene (ESAG) protein, putative, receptor-type adenylate cyclase	1930	3092	2555	1715	1299	1900	2619	2304	1901	1462	0,0002	2,38	1,79	1,33
Tb927.11.2430	Cytoplasmic dynein 2 heavy chain (DYNC2H1), putative, Cytoplasmic dynein 2 heavy chain (DYNC2H2), putative (DHC1b)	226	171	157	138	118	251	189	209	225	174	0,0458	1,92	1,45	1,33
Tb927.9.10650	hypothetical protein	339	464	410	501	628	393	335	468	424	447	0,0001	1,85	1,40	1,33
Tb10.NT.193		242	153	152	338	369	218	227	280	287	401	0,0037	2,43	1,84	1,32
Tb927.2.160	hypothetical protein, conserved	150	76	72	197	208	134	94	101	205	203	0,0298	2,88	2,19	1,32
Tb927.11.1530	expression site-associated gene (ESAG) protein, putative, expression site-associated gene 3 (ESAG3) protein, putative	274	203	191	258	462	347	257	297	350	475	0,0005	2,42	1,85	1,31
Tb927.6.4580	hypothetical protein, conserved	432	502	505	505	764	599	616	454	564	582	0,0000	1,77	1,36	1,30
Tb927.5.3810	orotidine-5-phosphate decarboxylase/ototate phosphoribosyltransferase, putative, OMPDCase-OPRTase, putative	791	1009	1101	637	473	854	865	892	632	499	0,0016	2,33	1,79	1,30

Tb1.NT.4		541	438	474	571	790	651	578	494	545	470	0,0060	1,80	1,39	1,30
Tb11.NT.105		114	86	87	151	225	160	143	187	203	288	0,0066	2,62	2,01	1,30
Tb8.NT.11		315	279	219	223	162	303	330	273	278	221	0,0084	1,94	1,49	1,30
Tb927.11.8270	hypothetical protein, conserved	206	241	229	161	97	136	161	187	125	98	0,0394	2,48	1,91	1,30
Tb927.10.4640	eukaryotic translation initiation factor 3 subunit L, putative	1038	1260	1097	866	667	796	985	1027	776	704	0,0002	1,89	1,46	1,30
Tb927.8.1730	hypothetical protein, conserved	374	361	310	484	564	339	302	366	424	380	0,0145	1,82	1,40	1,30
Tb927.10.4750	hypothetical protein, conserved	339	347	307	300	178	202	201	303	242	217	0,0096	1,95	1,51	1,29
Tb927.10.8110	hypothetical protein, conserved	518	590	474	507	331	341	333	459	384	331	0,0284	1,79	1,38	1,29
Tb927.10.10140	paraflagellar rod component, putative (PFC19)	2294	2890	2119	1955	1564	2297	1987	2253	2859	2041	0,0000	1,85	1,44	1,28
Tb11.NT.95		456	397	371	579	716	555	585	431	529	652	0,0008	1,93	1,51	1,28
Tb927.10.14830	mitochondrial carrier protein (MCP5b)	807	855	762	545	476	539	665	665	472	585	0,0001	1,80	1,41	1,27
Tb927.10.2370	RNA-binding protein, putative (LA)	579	718	630	398	322	581	598	531	429	341	0,0009	2,23	1,75	1,27
Tb927.10.14600	40S ribosomal protein S2, putative (RPS2)	10829	15508	12736	15637	8713	9227	12181	11769	13080	12209	0,0003	1,79	1,42	1,27
Tb927.10.5840	translation elongation factor 1-beta, putative	4700	5249	4683	3526	2830	3738	4948	5004	3953	3412	0,0000	1,85	1,47	1,26
Tb4.NT.1		1128	688	567	1164	1386	752	653	836	980	1267	0,0001	2,45	1,94	1,26
Tb927.6.4540	3-hydroxy-3-methylglutaryl-CoA reductase, putative	350	310	265	441	498	247	270	250	361	369	0,0498	1,88	1,49	1,26
Tb927.6.4480	valyl-tRNA synthetase, putative (ValRS)	462	459	446	403	243	429	412	464	304	320	0,0010	1,90	1,52	1,25
Tb927.4.1930	RNA-binding protein, putative (EIF3D)	1025	1420	1550	1000	693	862	849	1202	727	670	0,0112	2,24	1,79	1,25
Tb927.4.2000	ruvB-like DNA helicase, putative, ATP-dependent DNA helicase, putative	728	807	568	555	440	513	692	627	580	470	0,0006	1,83	1,47	1,24
Tb927.11.14840	chromosomal passenger protein (CTC2)	643	478	611	469	314	615	519	698	489	423	0,0000	2,05	1,65	1,24
Tb927.6.4370	eukaryotic translation initiation factor 3 subunit 7-like protein	687	635	726	488	392	631	657	677	583	455	0,0003	1,85	1,49	1,24
Tb927.10.12700	pyruvate dehydrogenase E1 alpha subunit, putative	73	196	232	186	153	62	90	116	159	107	0,0038	3,19	2,57	1,24
Tb927.10.2880	calcium channel protein, putative	486	351	336	287	262	411	449	492	335	328	0,0009	1,86	1,50	1,24
Tb927.8.4870	DIGIT	473	408	403	357	261	327	415	430	378	293	0,0015	1,81	1,47	1,24
Tb927.11.14090	hypothetical protein, conserved	636	587	578	324	321	531	586	511	419	365	0,0000	1,98	1,61	1,24

Tb927.10.7300	hypothetical protein, conserved	368	284	310	267	206	457	414	338	314	334	0,0128	1,79	1,45	1,23
Tb927.6.4590	glutamyl-tRNA synthetase, putative	1090	1111	962	804	611	912	884	1043	813	705	0,0000	1,82	1,48	1,23
Tb927.10.11340	hypothetical protein, conserved	334	264	224	259	175	295	293	286	299	192	0,0122	1,91	1,56	1,22
Tb927.2.1250	hypothetical protein	190	128	106	238	272	158	140	134	214	283	0,0477	2,57	2,11	1,22
Tb927.10.6070	universal minicircle sequence binding protein (UMSBP), putative, predicted zinc finger protein	14830	16947	18461	10279	8264	9561	13777	16420	8991	8915	0,0000	2,23	1,84	1,21
Tb927.8.1600	lysyl-tRNA synthetase, putative	913	1120	961	869	593	882	807	1085	835	695	0,0010	1,89	1,56	1,21
Tb927.10.16100	FK506-binding protein (FKBP)-type peptidyl-prolyl isomerase, putative	831	884	1564	2694	1973	1435	1351	1824	3632	2992	0,0000	3,24	2,69	1,21
Tb927.11.590	hypothetical protein, conserved	243	177	183	365	379	246	233	167	298	290	0,0082	2,14	1,78	1,20
Tb927.8.760	nucleolar RNA-binding protein (Nopp44/46)	2097	3227	3482	1698	1517	1962	1941	2543	1330	1397	0,0452	2,30	1,91	1,20
Tb927.9.11270	T-complex protein 1, eta subunit, putative, t-complex protein 1 (eta subunit), putative (TCP-1-eta)	2816	3291	3419	2263	1408	2146	2268	3392	1665	1761	0,0000	2,43	2,04	1,19
Tb927.11.14000	NRBD1 (NRBD1)	4040	5412	5467	3177	2567	2942	3050	4424	2572	2474	0,0000	2,13	1,79	1,19
Tb927.7.1060	hypothetical protein, conserved	545	484	585	527	263	363	432	553	403	296	0,0002	2,23	1,87	1,19
Tb5.NT.81		148	138	143	237	262	188	157	183	200	250	0,0340	1,89	1,59	1,19
Tb927.10.8510	glucose transporter, putative	14	85	98	94	92	18	50	66	110	104	0,0000	7,23	6,14	1,18
Tb927.8.4890	endoplasmic reticulum oxidoreductin, putative, pol-associated gene 1	995	1320	976	805	718	1265	1283	1175	831	821	0,0190	1,84	1,56	1,18
Tb927.7.4900	5'-3' exonuclease XRNA, putative, exoribonuclease 1, putative (XRNA)	282	278	297	236	151	168	217	281	213	185	0,0309	1,96	1,67	1,17
Tb927.10.4560	elongation factor 2	12871	15238	19557	10019	6530	9846	13320	17629	8014	6845	0,0000	3,00	2,58	1,16
Tb927.10.3560	arginine N-methyltransferase, putative	587	689	690	395	385	455	454	560	362	378	0,0368	1,79	1,55	1,16
Tb927.1.3190	hypothetical protein, unlikely	612	569	856	1261	1052	766	619	960	1166	1181	0,0000	2,21	1,91	1,16
Tb927.11.11080	Nucleoporin (TbNup149)	484	494	556	384	283	413	373	524	385	309	0,0074	1,96	1,70	1,16
Tb927.4.2310	asparaginyl-tRNA synthetase, putative	647	943	798	504	385	908	890	726	554	428	0,0063	2,45	2,12	1,15
Tb927.11.15370	hypothetical protein, conserved (TbKap123)	1115	984	1269	817	562	916	1077	1101	726	563	0,0000	2,26	1,96	1,15
Tb927.1.3390	hypothetical protein, conserved	353	516	596	632	621	471	437	542	662	679	0,0005	1,79	1,55	1,15

Tb927.8.3540	hypothetical protein, conserved	307	225	209	160	103	204	251	297	194	115	0,0000	2,97	2,59	1,15
Tb927.11.1990	arginyl-tRNA synthetase, putative	815	823	767	551	451	740	675	652	652	464	0,0000	1,83	1,60	1,14
Tb927.10.4570	elongation factor 2	13061	15137	19626	10068	6533	9978	13044	17536	8112	6660	0,0000	3,00	2,63	1,14
Tb927.7.3550	hypothetical protein, conserved	1648	1627	1734	1375	910	1762	1556	2105	1533	1259	0,0000	1,91	1,67	1,14
Tb927.6.3740	heat shock 70 kDa protein, mitochondrial precursor, putative	1121	1394	1413	712	754	1186	1293	1029	739	859	0,0074	1,98	1,75	1,13
Tb927.10.2090	elongation factor 1-alpha,EF-1-alpha (TEF1)	3214	4803	6380	6385	5289	3152	4274	4953	5532	3833	0,0000	1,99	1,76	1,13
Tb927.10.7190	D-tyrosyl-tRNA deacylase, putative	321	232	227	413	464	369	310	268	487	353	0,0201	2,05	1,82	1,13
Tb927.11.3240	T-complex protein 1, zeta subunit, putative (TCP-1-zeta)	1922	1842	1697	1177	934	1214	1373	1917	1046	1073	0,0000	2,06	1,83	1,12
Tb927.11.17040	expression site-associated gene (ESAG) protein, putative,expression site-associated gene 4 (ESAG4) protein, putative,receptor-type adenylate cyclase, putative	1830	2350	2492	1704	1352	1677	2283	2285	1753	1389	0,0013	1,84	1,65	1,12
Tb927.5.2570	translation initiation factor, putative (EIF3B)	1273	1511	1630	927	691	974	950	1286	868	610	0,0000	2,36	2,11	1,12
Tb927.11.1980	zinc finger protein family member, putative (ZC3H41)	3010	2738	3324	2477	1844	2411	2495	3205	2300	1990	0,0000	1,80	1,61	1,12
Tb927.1.4580	cyclin-like F-box protein (CFB1C)	8	69	107	66	43	4	28	48	44	33	0,0000	13,42	12,08	1,11
Tb927.7.4070	calpain-like cysteine peptidase, putative,cysteine peptidase, Clan CA, family C2, putative	3342	2292	2628	4366	4822	3589	3536	3299	4531	6255	0,0000	2,10	1,90	1,11
Tb7.NT.19		191	220	254	174	335	220	170	231	222	296	0,0024	1,93	1,74	1,11
Tb927.4.3590	translation elongation factor 1-beta, putative	4462	5463	5416	4104	3079	3457	3948	5440	3537	3390	0,0000	1,77	1,60	1,11
Tb927.8.750	nucleolar RNA-binding protein, putative	2024	2859	2985	1487	1402	1832	1848	2286	1330	1181	0,0016	2,13	1,94	1,10
Tb927.8.1510	ATP-dependent DEAD/H RNA helicase, putative	464	460	421	293	249	447	325	418	363	263	0,0010	1,86	1,70	1,10
Tb927.11.2290	hypothetical protein, conserved	417	409	394	362	236	283	347	377	337	232	0,0073	1,77	1,63	1,08
Tb927.10.14750	fibrillarin, putative	1986	3242	2738	1779	1319	1475	1478	2313	1470	1020	0,0002	2,46	2,27	1,08
Tb927.1.5280	expression site-associated gene (ESAG, pseudogene), putative,expression site-associated gene 3 (ESAG3), pseudogene	342	402	441	601	531	503	395	375	591	615	0,0217	1,76	1,64	1,07

Tb927.5.3800	glutamine hydrolysing (not ammonia-dependent) carbomoyl phosphate synthase, putative	586	710	674	459	338	547	548	657	431	335	0,0016	2,10	1,96	1,07
Tb927.8.3150	T-complex protein 1, gamma subunit, putative (TCP-1-gamma)	3668	3502	4334	2647	1750	2782	2997	4135	2611	1777	0,0000	2,48	2,33	1,06
Tb927.6.3490	zinc finger protein (ZFP1)	1119	1277	1531	871	782	1116	1047	1402	752	1109	0,0122	1,96	1,86	1,05
Tb927.11.4910	predicted ankyrin repeat family protein	1871	2104	1875	1487	1067	1108	1303	1929	1231	1027	0,0000	1,97	1,88	1,05
Tb927.10.13280	hypothetical protein, conserved	242	215	188	160	122	212	179	225	158	119	0,0208	1,99	1,90	1,05
Tb927.8.4370	hypothetical protein, conserved	350	364	414	339	199	238	214	328	243	165	0,0330	2,08	1,99	1,05
Tb927.10.2240	hypothetical protein, conserved	734	757	930	531	429	597	587	959	544	460	0,0011	2,17	2,09	1,04
Tb927.10.6060	universal minicircle sequence binding protein (UMSBP), putative, DNA-binding protein HEXBP, putative, zinc finger protein	3698	4372	3632	1950	1777	3184	4270	4545	2087	1917	0,0000	2,46	2,37	1,04
Tb927.1.5020	hypothetical protein, unlikely	68	49	54	98	145	44	59	55	111	124	0,0270	2,94	2,83	1,04
Tb927.9.13860		8166	5928	6623	8538	10915	8185	7543	7011	9862	12520	0,0000	1,84	1,79	1,03
Tb927.11.3730	leucyl-tRNA synthetase, putative (LeuRS)	710	646	797	581	449	599	627	777	517	449	0,0039	1,78	1,73	1,03
Tb927.9.13920	kinetoplastid membrane protein KMP-11 (KMP-11)	7986	5943	6475	8542	10811	8054	7487	7026	9980	12665	0,0000	1,82	1,80	1,01
Tb927.10.10480	histone H2B, putative	38	126	201	219	227	26	48	80	156	134	0,0000	6,04	5,99	1,01

Table S2A: GO enrichment analysis of PKA downstream targets using DAVID.

Annotation cluster 1		Enrichment score: 3.731590820350524									
Category	Term	Count	%	P-value	List total	Pop hits	Pop total	Fold enrichment	Bonferroni	Benjamini	FDR
GOTERM_BP_FAT	GO:0006072~glycerol-3-phosphate metabolic process	6	3,09	8,46E-07	72	8	2497	26,01	2,14E-04	2,14E-04	1,10E-03
INTERPRO	IPR018485: Carbohydrate kinase, FGGY, C-terminal	5	2,58	4,69E-06	85	5	2636	31,01	8,53E-04	8,53E-04	5,79E-03
INTERPRO	IPR018484: Carbohydrate kinase, FGGY, N-terminal	5	2,58	4,69E-06	85	5	2636	31,01	8,53E-04	8,53E-04	5,79E-03
INTERPRO	IPR000577: Carbohydrate kinase, FGGY	5	2,58	4,69E-06	85	5	2636	31,01	8,53E-04	8,53E-04	5,79E-03
INTERPRO	IPR018483: Carbohydrate kinase, FGGY, conserved site	5	2,58	4,69E-06	85	5	2636	31,01	8,53E-04	8,53E-04	5,79E-03
INTERPRO	IPR005999: Glycerol kinase	5	2,58	4,69E-06	85	5	2636	31,01	8,53E-04	8,53E-04	5,79E-03
GOTERM_MF_FAT	GO:0004370~glycerol kinase activity	5	2,58	4,92E-06	89	5	2730	30,67	7,93E-04	7,93E-04	5,95E-03
GOTERM_BP_FAT	GO:0006071~glycerol metabolic process	6	3,09	6,53E-06	72	11	2497	18,92	1,65E-03	8,26E-04	8,50E-03
GOTERM_BP_FAT	GO:0019400~alditol metabolic process	6	3,09	6,53E-06	72	11	2497	18,92	1,65E-03	8,26E-04	8,50E-03
GOTERM_BP_FAT	GO:0019751~polyol metabolic process	6	3,09	1,09E-05	72	12	2497	17,34	2,77E-03	5,54E-04	1,42E-02
PIR_SUPERFAMILY	PIRSF000538: xylulokinase	5	2,58	3,03E-05	36	5	670	18,61	9,08E-04	9,08E-04	2,58E-02
KEGG_PATHWAY	tbr00561: Glycerolipid metabolism	5	2,58	0,001442921	34	14	849	8,92	3,41E-02	1,72E-02	1,15E+00
GOTERM_BP_FAT	GO:0019637~organophosphate metabolic process	7	3,61	0,010082906	72	66	2497	3,68	9,23E-01	2,26E-01	1,24E+01
GOTERM_BP_FAT	GO:0006793~phosphorus metabolic process	9	4,64	0,551566733	72	280	2497	1,11	1,00E+00	1,00E+00	1,00E+02
GOTERM_BP_FAT	GO:0006796~phosphate metabolic process	9	4,64	0,551566733	72	280	2497	1,11	1,00E+00	1,00E+00	1,00E+02
SP_PIR_KEYWORDS	kinase	6	3,09	0,70941219	55	139	1291	1,01	1,00E+00	9,83E-01	1,00E+02
SP_PIR_KEYWORDS	transferase	7	3,61	0,870556298	55	201	1291	0,82	1,00E+00	9,96E-01	1,00E+02
Annotation cluster 2		Enrichment score: 3.6829780458417662									
Category	Term	Count	%	P-value	List total	Pop hits	Pop total	Fold enrichment	Bonferroni	Benjamini	FDR
GOTERM_BP_FAT	GO:0006418~tRNA aminoacylation for protein translation	8	4,12	8,20E-06	72	28	2497	9,91	2,07E-03	6,91E-04	1,07E-02
GOTERM_BP_FAT	GO:0043038~amino acid activation	8	4,12	1,06E-05	72	29	2497	9,57	2,67E-03	6,68E-04	1,38E-02
GOTERM_BP_FAT	GO:0043039~tRNA aminoacylation	8	4,12	1,06E-05	72	29	2497	9,57	2,67E-03	6,68E-04	1,38E-02
GOTERM_MF_FAT	GO:0004812~aminoacyl-tRNA ligase activity	8	4,12	1,14E-05	89	26	2730	9,44	1,83E-03	9,15E-04	1,38E-02
GOTERM_MF_FAT	GO:0016876~ligase activity, forming aminoacyl-tRNA and related compounds	8	4,12	1,14E-05	89	26	2730	9,44	1,83E-03	9,15E-04	1,38E-02

GOTERM_MF_FAT	GO:0016875~ligase activity, forming carbon-oxygen bonds	8	4,12	1,14E-05	89	26	2730	9,44	1,83E-03	9,15E-04	1,38E-02
KEGG_PATHWAY	tbr00970: Aminoacyl-tRNA biosynthesis	7	3,61	2,26E-04	34	25	849	6,99	5,40E-03	5,40E-03	1,81E-01
GOTERM_BP_FAT	GO:0006399~tRNA metabolic process	8	4,12	4,76E-04	72	51	2497	5,44	1,13E-01	1,99E-02	6,17E-01
GOTERM_BP_FAT	GO:0034660~ncRNA metabolic process	9	4,64	0,001149395	72	76	2497	4,11	2,52E-01	4,07E-02	1,49E+00
GOTERM_BP_FAT	GO:0006412~translation	17	8,76	0,001935562	72	260	2497	2,27	3,87E-01	5,30E-02	2,49E+00
SP_PIR_KEYWORDS	Aminoacyl-tRNA synthetase	3	1,55	0,074170061	55	11	1291	6,40	9,64E-01	6,69E-01	5,12E+01
SP_PIR_KEYWORDS	ligase	4	2,06	0,266636354	55	43	1291	2,18	1,00E+00	7,36E-01	9,44E+01

Annotation cluster 3 **Enrichment score: 2.366736896928375**

Category	Term	Count	%	P-value	List total	Pop hits	Pop total	Fold enrichment	Bonferroni	Benjamini	FDR
GOTERM_MF_FAT	GO:0032553~ribonucleotide binding	37	19,07	5,45E-04	89	678	2730	1,67	8,41E-02	2,89E-02	6,57E-01
GOTERM_MF_FAT	GO:0032555~purine ribonucleotide binding	37	19,07	5,45E-04	89	678	2730	1,67	8,41E-02	2,89E-02	6,57E-01
GOTERM_MF_FAT	GO:0000166~nucleotide binding	40	20,62	7,29E-04	89	769	2730	1,60	1,11E-01	2,89E-02	
GOTERM_MF_FAT	GO:0017076~purine nucleotide binding	37	19,07	9,55E-04	89	697	2730	1,63	1,43E-01	3,03E-02	1,15E+00
GOTERM_MF_FAT	GO:0005524~ATP binding	31	15,98	0,002991737	89	578	2730	1,65	3,83E-01	7,73E-02	3,56E+00
GOTERM_MF_FAT	GO:0032559~adenyl ribonucleotide binding	31	15,98	0,002991737	89	578	2730	1,65	3,83E-01	7,73E-02	3,56E+00
GOTERM_MF_FAT	GO:0030554~adenyl nucleotide binding	31	15,98	0,004858666	89	596	2730	1,60	5,43E-01	1,06E-01	5,72E+00
GOTERM_MF_FAT	GO:0001883~purine nucleoside binding	31	15,98	0,004858666	89	596	2730	1,60	5,43E-01	1,06E-01	5,72E+00
GOTERM_MF_FAT	GO:0001882~nucleoside binding	31	15,98	0,005251308	89	599	2730	1,59	5,72E-01	1,01E-01	6,17E+00
SP_PIR_KEYWORDS	nucleotide-binding	16	8,25	0,124678578	55	266	1291	1,41	9,97E-01	6,15E-01	7,10E+01
SP_PIR_KEYWORDS	ATP-binding	12	6,19	0,322508566	55	223	1291	1,26	1,00E+00	7,52E-01	9,73E+01

Annotation cluster 4 **Enrichment score: 2.048626865000886**

Category	Term	Count	%	P-value	List total	Pop hits	Pop total	Fold enrichment	Bonferroni	Benjamini	FDR
GOTERM_CC_FAT	GO:0005832~chaperonin-containing T-complex	5	2,58	8,48E-05	54	8	1513	17,51	5,67E-03	5,67E-03	8,70E-02
INTERPRO	IPR002194: Chaperonin TCP-1, conserved site	4	2,06	9,96E-04	85	7	2636	17,72	1,66E-01	8,67E-02	1,22E+00
INTERPRO	IPR017998: Chaperone, tailless complex polypeptide 1	4	2,06	9,96E-04	85	7	2636	17,72	1,66E-01	8,67E-02	1,22E+00
GOTERM_BP_FAT	GO:0051726~regulation of cell cycle	5	2,58	0,001684566	72	19	2497	9,13	3,47E-01	5,19E-02	2,17E+00
INTERPRO	IPR002423: Chaperonin Cpn60/TCP-1	4	2,06	0,004281377	85	11	2636	11,28	5,42E-01	1,77E-01	5,16E+00
GOTERM_CC_FAT	GO:0044445~cytosolic part	7	3,61	0,007415818	54	51	1513	3,85	3,93E-01	2,21E-01	7,35E+00
GOTERM_CC_FAT	GO:0005829~cytosol	8	4,12	0,018979082	54	80	1513	2,80	7,23E-01	3,48E-01	1,78E+01
PIR_SUPERFAMILY	PIRSF002584: molecular chaperone t-complex-type	3	1,55	0,024018991	36	5	670	11,17	5,18E-01	3,06E-01	1,87E+01
SP_PIR_KEYWORDS	Chaperone	5	2,58	0,033380787	55	30	1291	3,91	7,68E-01	5,18E-01	271E+01
SP_PIR_KEYWORDS	cytoplasm	4	2,06	0,07524734	55	24	1291	3,91	9,65E-01	5,69E-01	5,17E+01

GOTERM_MF_FAT	GO:0051082~unfolded protein binding	5	2,58	0,187307953	89	70	2730	2,19	1,00E+00	8,92E-01	9,18E+01
GOTERM_BP_FAT	GO:0006457~protein folding	6	3,09	0,2700358	72	123	2497	1,69	1,00E+00	9,95E-01	9,83E+01

Annotation cluster 5 **Enrichment score: 1.2601629776770822**

Category	Term	Count	%	P-value	List total	Pop hits	Pop total	Fold enrichment	Bonferroni	Benjamini	FDR
INTERPRO	IPR002113: Adenine nucleotide translocator 1	3	1,55	0,005775476	85	4	2636	23,26	6,52E-01	1,90E-01	6,90E+00
INTERPRO	IPR002067: Mitochondrial carrier protein	3	1,55	0,013849072	85	6	2636	15,51	9,21E-01	3,45E-01	1,58E+01
INTERPRO	IPR001993: Mitochondrial substrate carrier	4	2,06	0,018024939	85	18	2636	6,89	9,64E-01	3,77E-01	2,01E+01
INTERPRO	IPR018108: Mitochondrial substrate/solute carrier	4	2,06	0,02092073	85	19	2636	6,53	9,79E-01	3,82E-01	2,30E+01
GOTERM_CC_FAT	GO:0005743~mitochondrial inner membrane	5	2,58	0,025861844	54	33	1513	4,25	8,27E-01	3,55E-01	2,36E+01
GOTERM_CC_FAT	GO:0031966~mitochondrial membrane	5	2,58	0,025861844	54	33	1513	4,25	8,27E-01	3,55E-01	2,36E+01
GOTERM_CC_FAT	GO:0019866~organelle inner membrane	5	2,58	0,028564009	54	34	1513	4,12	8,57E-01	3,22E-01	2,57E+01
GOTERM_CC_FAT	GO:0005740~mitochondrial envelope	5	2,58	0,034459697	54	36	1513	3,89	9,05E-01	3,24E-01	3,02E+01
SP_PIR_KEYWORDS	transport	5	2,58	0,075990421	55	39	1291	3,01	9,67E-01	4,93E-01	5,21E+01
GOTERM_CC_FAT	GO:0031967~organelle envelope	5	2,58	0,078739793	54	47	1513	2,98	9,96E-01	4,97E-01	5,69E+01
GOTERM_CC_FAT	GO:0031975~envelope	5	2,58	0,094202564	54	50	1513	2,80	9,99E-01	4,85E-01	6,38E+01
GOTERM_CC_FAT	GO:0044429~mitochondrial part	5	2,58	0,1229241	54	55	1513	2,55	1,00E+00	5,50E-01	7,40E+01
SP_PIR_KEYWORDS	transmembrane	6	3,09	0,163754372	55	70	1291	2,01	1,00E+00	6,18E-01	8,11E+01
SP_PIR_KEYWORDS	membrane	5	2,58	0,277119958	55	64	1291	1,83	1,00E+00	7,19E-01	9,51E+01
GOTERM_CC_FAT	GO:0005739~mitochondrion	9	4,64	0,317264479	54	185	1513	1,36	1,00E+00	8,18E-01	9,80E+01
GOTERM_CC_FAT	GO:0031090~organelle membrane	5	2,58	0,34717512	54	85	1513	1,65	1,00E+00	8,32E-01	9,87E+01

Annotation cluster 6 **Enrichment score: 1.1918165215059067**

Category	Term	Count	%	P-value	List total	Pop hits	Pop total	Fold enrichment	Bonferroni	Benjamini	FDR
GOTERM_MF_FAT	GO:0003746~translation elongation factor activity	5	2,58	0,006537976	89	24	2730	6,39	6,52E-01	1,11E-01	7,62E+00
SP_PIR_KEYWORDS	elongation factor	4	2,06	0,026329228	55	16	1291	5,87	6,83E-01	6,83E-01	2,20E+01
GOTERM_MF_FAT	GO:0008135~translation factor activity, nucleic acid binding	6	3,09	0,028360472	89	54	2730	3,41	9,90E-01	3,71E-01	2,94E+01
GOTERM_BP_FAT	GO:0006414~translational elongation	4	2,06	0,043409712	72	28	2497	4,95	1,00E+00	6,40E-01	4,39E+01
INTERPRO	IPR004161: Translation elongation factor EFTu/EF1A, domain 2	3	1,55	0,045794652	85	11	2636	8,46	1,00E+00	5,74E-01	4,39E+01
GOTERM_MF_FAT	GO:0003924~GTPase activity	5	2,58	0,089299775	89	53	2730	2,89	1,00E+00	7,15E-01	6,77E+01
INTERPRO	IPR000795:Protein synthesis factor, GTP-binding	3	1,55	0,090224913	85	16	2636	5,81	1,00E+00	7,91E-01	6,89E+01
GOTERM_MF_FAT	GO:0005525~GTP binding	7	3,61	0,108329092	89	102	2730	2,11	1,00E+00	7,58E-01	7,50E+01
GOTERM_MF_FAT	GO:0032561~guanyl ribonucleotide binding	7	3,61	0,108329092	89	102	2730	2,11	1,00E+00	7,58E-01	7,50E+01
GOTERM_MF_FAT	GO:0019001~guanyl nucleotide binding	7	3,61	0,108329092	89	102	2730	2,11	1,00E+00	7,58E-01	7,50E+01

SP_PIR_KEYWORDS	GTP-binding	5	2,58	0,177087445	55	53	1291	2,21	1,00E+00	6,06E-01	8,37E+01
INTERPRO	IPR005225: Small GTP-binding protein	3	1,55	0,28353409	85	33	2636	2,82	1,00E+00	9,91E-01	9,84E+01

List total: number of genes in the gene list (transcripts regulated by PKA) mapped to any term in this ontology.

Pop hits (population hits): number of genes with this GO term on the background list (all transcripts identified by the RNAseq analysis).

Pop total (population total): number of genes on the background list mapped to any term in this ontology.

Table S2B: GO enrichment analysis of PKA downstream targets using TriTrypDB (www.tritrypdb.org).

Biological process

ID	Name	Background count	Result count	% of background	Fold enrichment	Odds ratio	P-value	Benjamini	Bonferroni
GO:0006072	glycerol-3-phosphate metabolic process	10	6	60	25,56	26,7	8,64E+04	3,63E+06	5,96E+06
GO:0006418	tRNA aminoacylation for protein translation	30	8	26,7	11,36	12,01	1,71E+05	3,63E+06	1,18E-04
GO:0043039	tRNA aminoacylation	31	8	25,8	10,99	11,62	2,10E+05	3,63E+06	1,45E-04
GO:0043038	amino acid activation	31	8	25,8	10,99	11,62	2,10E+05	3,63E+06	1,45E-4
GO:0006412	translation	327	21	6,4	2,74	3,05	3,65E+06	4,84E-04	2,52E-03
GO:0006399	tRNA metabolic process	65	9	13,8	5,9	6,25	4,21E+05	4,84E-04	2,90E-03
GO:0006520	cellular amino acid metabolic process	88	10	11,4	4,84	5,15	7,27E+06	7,16E-04	5,02E-03
GO:0051726	regulation of cell cycle	35	6	17,1	7,3	7,59	3,03E-04	2,61E-03	2,09E-02
GO:0044281	small molecule metabolic process	436	22	5	2,15	2,37	6,53E-04	5,01E-03	4,51E-02
GO:0044237	cellular metabolic process	2109	68	3,2	1,37	1,75	9,26E-04	6,39E-03	6,39E-02
GO:0034660	ncRNA metabolic process	105	9	8,6	3,65	3,84	1,14E-03	6,97E-03	7,85E-02
GO:0044238	primary metabolic process	2173	69	3,2	1,35	1,72	1,29E-03	6,97E-03	8,88E-02
GO:0034645	cellular macromolecule biosynthetic process	499	23	4,6	1,96	2,16	1,59E-03	6,97E-03	1,10E-01
GO:0043436	oxoacid metabolic process	134	10	7,5	3,18	3,35	1,63E-03	6,97E-03	1,12E-01
GO:0019752	carboxylic acid metabolic process	134	10	7,5	3,18	3,35	1,63E-03	6,97E-03	1,12E-01
GO:0006082	organic acid metabolic process	135	10	7,4	3,16	3,33	1,72E-03	6,97E-03	1,18E-01
GO:0009059	macromolecule biosynthetic process	502	23	4,6	1,95	2,15	1,72E-03	6,97E-03	1,18E-01
GO:0044282	small molecule catabolic process	20	4	20	8,52	8,75	1,97E-03	7,21E-03	1,36E-01

GO:0010467	gene expression	637	27	4,2	1,81	2,01	1,99E-03	7,21E-03	1,37E-01
GO:0044249	cellular biosynthetic process	810	32	4	1,68	1,89	2,19E-03	7,26E-03	1,51E-01
GO:0042180	cellular ketone metabolic process	140	10	7,1	3,04	3,21	2,21E-03	7,26E-03	1,52E-01
GO:0008284	positive regulation of cell proliferation	2	2	100	42,6	43,22	3,04E-03	9,27E-03	2,10E-01
GO:0009987	cellular process	2785	82	2,9	1,25	1,64	3,09E-03	9,27E-03	2,13E-01
GO:0009058	biosynthetic process	843	32	3,8	1,62	1,81	4,04E-03	1,15E-02	2,79E-01
GO:0008152	metabolic process	2513	75	3	1,27	1,61	4,18E-03	1,15E-02	2,88E-01
GO:0016070	RNA metabolic process	419	19	4,5	1,93	2,08	4,96E-03	1,32E-02	3,42E-01
GO:0034641	cellular nitrogen compound metabolic process	981	35	3,6	1,52	1,7	6,79E-03	1,74E-02	4,69E-01
GO:0019932	second-messenger-mediated signaling	4	2	50	21,3	21,6	7,37E-03	1,74E-02	5,09E-01
GO:0042127	regulation of cell proliferation	4	2	50	21,3	21,6	7,37E-03	1,74E-02	5,09E-01
GO:0006807	nitrogen compound metabolic process	988	35	3,5	1,51	1,69	7,57E-03	1,74E-02	5,22E-01
GO:0044267	cellular protein metabolic process	927	33	3,6	1,52	1,68	9,04E-03	2,01E-02	6,24E-01
GO:0019637	organophosphate metabolic process	98	7	7,1	3,04	3,15	1,01E-02	2,13E-02	6,95E-01
GO:0006402	mRNA catabolic process	5	2	40	17,04	17,28	1,02E-02	2,13E-02	7,02E-01
GO:0006139	nucleobase-containing compound metabolic process	944	33	3,5	1,49	1,65	1,17E-02	2,32E-02	8,07E-01
GO:0050789	regulation of biological process	457	19	4,2	1,77	1,9	1,18E-02	2,32E-02	8,14E-01
GO:0019538	protein metabolic process	1065	36	3,4	1,44	1,6	1,36E-02	2,61E-02	9,39E-01
GO:0050794	regulation of cellular process	368	16	4,3	1,85	1,97	1,41E-02	2,63E-02	9,74E-01
GO:0065007	biological regulation	485	19	3,9	1,67	1,78	2,06E-02	3,68E-02	1,00E+00
GO:0006401	RNA catabolic process	8	2	25	10,65	10,79	2,08E-02	3,68E-02	1,00E+00
GO:0006457	protein folding	142	8	5,6	2,4	2,49	2,14E-02	3,70E-02	1,00E+00
GO:0008150	biological_process	3816	101	2,6	1,13	1,5	2,35E-02	3,96E-02	1,00E+00
GO:0006414	translational elongation	25	3	12	5,11	5,21	2,54E-02	4,18E-02	1,00E+00
GO:0007051	spindle organization	10	2	20	8,52	8,63	2,96E-02	4,67E-02	1,00E+00
GO:0006413	translational initiation	29	3	10,3	4,41	4,48	3,61E-02	4,67E-02	1,00E+00
GO:0033043	regulation of organelle organization	13	2	15,4	6,55	6,64	4,51E-02	4,67E-02	1,00E+00
GO:0006438	valyl-tRNA aminoacylation	1	1	100	42,6	42,91	4,53E-02	4,67E-02	1,00E+00
GO:0019563	glycerol catabolic process	1	1	100	42,6	42,91	4,53E-02	4,67E-02	1,00E+00
GO:0044275	cellular carbohydrate catabolic process	1	1	100	42,6	42,91	4,53E-02	4,67E-02	1,00E+00

GO:0019405	alditol catabolic process	1	1	100	42,6	42,91	4,53E-02	4,67E-02	1,00E+00
GO:0070408	carbamoyl phosphate metabolic process	1	1	100	42,6	42,91	4,53E-02	4,67E-02	1,00E+00
GO:0033044	regulation of chromosome organization	1	1	100	42,6	42,91	4,53E-02	4,67E-02	1,00E+00
GO:0006467	protein thiol-disulfide exchange	1	1	100	42,6	42,91	4,53E-02	4,67E-02	1,00E+00
GO:0033047	regulation of mitotic sister chromatid segregation	1	1	100	42,6	42,91	4,53E-02	4,67E-02	1,00E+00
GO:0006420	arginyl-tRNA aminoacylation	1	1	100	42,6	42,91	4,53E-02	4,67E-02	1,00E+00
GO:0046164	alcohol catabolic process	1	1	100	42,6	42,91	4,53E-02	4,67E-02	1,00E+00
GO:0046174	polyol catabolic process	1	1	100	42,6	42,91	4,53E-02	4,67E-02	1,00E+00
GO:0006424	glutamyl-tRNA aminoacylation	1	1	100	42,6	42,91	4,53E-02	4,67E-02	1,00E+00
GO:0070409	carbamoyl phosphate biosynthetic process	1	1	100	42,6	42,91	4,53E-02	4,67E-02	1,00E+00
GO:0006543	glutamine catabolic process	1	1	100	42,6	42,91	4,53E-02	4,67E-02	1,00E+00
GO:0006426	glycyl-tRNA aminoacylation	1	1	100	42,6	42,91	4,53E-02	4,67E-02	1,00E+00
GO:0019933	cAMP-mediated signaling	1	1	100	42,6	42,91	4,53E-02	4,67E-02	1,00E+00
GO:0006429	leucyl-tRNA aminoacylation	1	1	100	42,6	42,91	4,53E-02	4,67E-02	1,00E+00
GO:0033045	regulation of sister chromatid segregation	1	1	100	42,6	42,91	4,53E-02	4,67E-02	1,00E+00
GO:0019935	cyclic-nucleotide-mediated signaling	1	1	100	42,6	42,91	4,53E-02	4,67E-02	1,00E+00
GO:0000291	nuclear-transcribed mRNA catabolic process, exonucleolytic	1	1	100	42,6	42,91	4,53E-02	4,67E-02	1,00E+00
GO:0043044	ATP-dependent chromatin remodeling	1	1	100	42,6	42,91	4,53E-02	4,67E-02	1,00E+00
GO:0046952	ketone body catabolic process	1	1	100	42,6	42,91	4,53E-02	4,67E-02	1,00E+00
GO:0044260	cellular macromolecule metabolic process	1520	45	3	1,26	1,39	4,74E-02	4,81E-02	1,00E+00
GO:0000226	microtubule cytoskeleton organization	33	3	9,1	3,87	3,94	4,86E-02	4,86E-02	1,00E+00

Molecular function

ID	Name	Background count	Result count	% of background	Fold enrichment	Odds ratio	P-value	Benjamini	Bonferroni
GO:0035639	purine ribonucleoside triphosphate binding	815	42	5,2	2,2	2,73	5,88E+04	8,58E+05	3,35E+06
GO:0032555	purine ribonucleotide binding	816	42	5,1	2,19	2,73	6,07E+04	8,58E+05	3,46E+06
GO:0032553	ribonucleotide binding	816	42	5,1	2,19	2,73	6,07E+04	8,58E+05	3,46E+06
GO:0017076	purine nucleotide binding	818	42	5,1	2,19	2,72	6,48E+04	8,58E+05	3,69E+06
GO:0016876	ligase activity, forming aminoacyl-tRNA and related compounds	28	8	28,6	12,17	12,87	1,10E+05	8,58E+05	6,25E+06

GO:0016875	ligase activity, forming carbon-oxygen bonds	28	8	28,6	12,17	12,87	1,10E+05	8,58E+05	6,25E+06
GO:0004812	aminoacyl-tRNA ligase activity	28	8	28,6	12,17	12,87	1,10E+05	8,58E+05	6,25E+06
GO:0000166	nucleotide binding	870	43	4,9	2,11	2,62	1,24E+05	8,58E+05	7,04E+05
GO:0004370	glycerol kinase activity	5	5	100	42,6	44,19	1,35E+04	8,58E+05	7,72E+06
GO:0036094	small molecule binding	907	43	4,7	2,02	2,49	3,64E+05	1,92E+06	2,08E-04
GO:0005524	ATP binding	692	36	5,2	2,22	2,65	4,11E+05	1,92E+06	2,34E-04
GO:0032559	adenyl ribonucleotide binding	693	36	5,2	2,21	2,65	4,24E+05	1,92E+06	2,42E-04
GO:0030554	adenyl nucleotide binding	694	36	5,2	2,21	2,65	4,38E+05	1,92E+06	2,50E-04
GO:0008135	translation factor activity, nucleic acid binding	53	7	13,2	5,63	5,88	4,01E-04	1,63E-03	2,28E-02
GO:0005488	binding	2862	87	3	1,3	1,82	4,99E-04	1,90E-03	2,84E-02
GO:0003723	RNA binding	384	20	5,2	2,22	2,43	8,09E-04	2,88E-03	4,61E-02
GO:0016462	pyrophosphatase activity	418	21	5	2,14	2,35	9,26E-04	3,02E-03	5,28E-02
GO:0016818	hydrolase activity, acting on acid anhydrides, in phosphorus-containing anhydrides	419	21	5	2,14	2,34	9,53E-04	3,02E-03	5,43E-02
GO:0003676	nucleic acid binding	807	33	4,1	1,74	1,98	1,04E-03	3,05E-03	5,91E-02
GO:0016817	hydrolase activity, acting on acid anhydrides	423	21	5	2,12	2,32	1,07E-03	3,05E-03	6,10E-02
GO:0004386	helicase activity	106	9	8,5	3,62	3,8	1,21E-03	3,28E-03	6,90E-02
GO:0017111	nucleoside-triphosphatase activity	410	20	4,9	2,08	2,26	1,74E-03	4,51E-03	9,93E-02
GO:0016874	ligase activity	113	9	8	3,39	3,56	1,83E-03	4,54E-03	1,04E-01
GO:0003674	molecular_function	4258	114	2,7	1,14	1,87	3,29E-03	7,81E-03	1,88E-01
GO:0016887	ATPase activity	202	12	5,9	2,53	2,68	3,52E-03	8,03E-03	2,01E-01
GO:0002161	aminoacyl-tRNA editing activity	3	2	66,7	28,4	28,81	4,99E-03	1,09E-02	2,84E-01
GO:0003746	translation elongation factor activity	16	3	18,8	7,99	8,15	8,74E-03	1,80E-02	4,98E-01
GO:0003743	translation initiation factor activity	32	4	12,5	5,33	5,46	8,83E-03	1,80E-02	5,03E-01
GO:0016787	hydrolase activity	898	32	3,6	1,52	1,68	1,01E-02	1,98E-02	5,75E-01
GO:0003824	catalytic activity	2232	66	3	1,26	1,5	1,20E-02	2,27E-02	6,82E-01
GO:0008026	ATP-dependent helicase activity	83	6	7,2	3,08	3,18	1,60E-02	2,85E-02	9,11E-01
GO:0070035	purine NTP-dependent helicase activity	83	6	7,2	3,08	3,18	1,60E-02	2,85E-02	9,11E-01
GO:0052689	carboxylic ester hydrolase activity	23	3	13	5,56	5,66	2,09E-02	3,60E-02	1,00E+00
GO:0051082	unfolded protein binding	92	6	6,5	2,78	2,86	2,45E-02	4,11E-02	1,00E+00
GO:0003924	GTPase activity	68	5	7,4	3,13	3,21	2,55E-02	4,15E-02	1,00E+00

GO:0032561	guanyl ribonucleotide binding	124	7	5,6	2,41	2,48	3,03E-02	4,53E-02	1,00E+00
GO:0005525	GTP binding	124	7	5,6	2,41	2,48	3,03E-02	4,53E-02	1,00E+00
GO:0019001	guanyl nucleotide binding	124	7	5,6	2,41	2,48	3,03E-02	4,53E-02	1,00E+00
GO:0030246	carbohydrate binding	11	2	18,2	7,75	7,85	3,45E-02	4,53E-02	1,00E+00
GO:0042623	ATPase activity, coupled	158	8	5,1	2,16	2,23	3,63E-02	4,53E-02	1,00E+00
GO:0030295	protein kinase activator activity	1	1	100	42,6	42,91	4,53E-02	4,53E-02	1,00E+00
GO:0004832	valine-tRNA ligase activity	1	1	100	42,6	42,91	4,53E-02	4,53E-02	1,00E+00
GO:0031491	nucleosome binding	1	1	100	42,6	42,91	4,53E-02	4,53E-02	1,00E+00
GO:0004420	hydroxymethylglutaryl-CoA reductase (NADPH) activity	1	1	100	42,6	42,91	4,53E-02	4,53E-02	1,00E+00
GO:0019209	kinase activator activity	1	1	100	42,6	42,91	4,53E-02	4,53E-02	1,00E+00
GO:0004814	arginine-tRNA ligase activity	1	1	100	42,6	42,91	4,53E-02	4,53E-02	1,00E+00
GO:0004590	orotidine-5'-phosphate decarboxylase activity	1	1	100	42,6	42,91	4,53E-02	4,53E-02	1,00E+00
GO:0004071	aspartate-ammonia ligase activity	1	1	100	42,6	42,91	4,53E-02	4,53E-02	1,00E+00
GO:0004588	orotate phosphoribosyltransferase activity	1	1	100	42,6	42,91	4,53E-02	4,53E-02	1,00E+00
GO:0032574	5'-3' RNA helicase activity	1	1	100	42,6	42,91	4,53E-02	4,53E-02	1,00E+00
GO:0032575	ATP-dependent 5'-3' RNA helicase activity	1	1	100	42,6	42,91	4,53E-02	4,53E-02	1,00E+00
GO:0004823	leucine-tRNA ligase activity	1	1	100	42,6	42,91	4,53E-02	4,53E-02	1,00E+00
GO:0004055	argininosuccinate synthase activity	1	1	100	42,6	42,91	4,53E-02	4,53E-02	1,00E+00
GO:0043539	protein serine/threonine kinase activator activity	1	1	100	42,6	42,91	4,53E-02	4,53E-02	1,00E+00
GO:0004820	glycine-tRNA ligase activity	1	1	100	42,6	42,91	4,53E-02	4,53E-02	1,00E+00
GO:0008410	CoA-transferase activity	1	1	100	42,6	42,91	4,53E-02	4,53E-02	1,00E+00
GO:0004818	glutamate-tRNA ligase activity	1	1	100	42,6	42,91	4,53E-02	4,53E-02	1,00E+00

Cellular compartment

ID	Name	Background count	Result count	% of background	Fold enrichment	Odds ratio	P-value	Benjamini	Bonferroni
GO:0005832	chaperonin-containing T-complex	8	5	62,5	26,63	27,6	6,55E+05	2,23E-04	2,23E-04
GO:0020015	glycosome	46	7	15,2	6,48	6,78	1,83E-04	1,75E-03	6,21E-03
GO:0044445	cytosolic part	22	5	22,7	9,68	10,01	3,17E-04	1,75E-03	1,08E-02
GO:0005623	cell	2707	84	3,1	1,32	1,84	3,48E-04	1,75E-03	1,18E-02
GO:0044464	cell part	2707	84	3,1	1,32	1,84	3,48E-04	1,75E-03	1,18E-02
GO:0005777	peroxisome	52	7	13,5	5,74	5,99	3,61E-04	1,75E-03	1,23E-02
GO:0042579	microbody	52	7	13,5	5,74	5,99	3,61E-04	1,75E-03	1,23E-02
GO:0005575	cellular_component	3314	96	2,9	1,23	1,8	1,01E-03	3,93E-03	3,44E-02
GO:0044424	intracellular part	2446	76	3,1	1,32	1,73	1,04E-03	3,93E-03	3,53E-02
GO:0005622	intracellular	2624	79	3	1,28	1,67	2,05E-03	6,98E-03	6,98E-02
GO:0005743	mitochondrial inner membrane	83	7	8,4	3,59	3,73	4,39E-03	1,24E-02	1,49E-01
GO:0019866	organelle inner membrane	83	7	8,4	3,59	3,73	4,39E-03	1,24E-02	1,49E-01
GO:0043234	protein complex	489	21	4,3	1,83	1,98	5,74E-03	1,50E-02	1,95E-01
GO:0005737	cytoplasm	1820	57	3,1	1,33	1,58	6,91E-03	1,68E-02	2,35E-01
GO:0005852	eukaryotic translation initiation factor 3 complex	6	2	33,3	14,2	14,4	1,34E-02	2,63E-02	4,54E-01
GO:0005853	eukaryotic translation elongation factor 1 complex	6	2	33,3	14,2	14,4	1,34E-02	2,63E-02	4,54E-01
GO:0032991	macromolecular complex	776	28	3,6	1,54	1,68	1,41E-02	2,63E-02	4,79E-01
GO:0044446	intracellular organelle part	637	24	3,8	1,61	1,73	1,45E-02	2,63E-02	4,93E-01
GO:0031966	mitochondrial membrane	106	7	6,6	2,81	2,91	1,47E-02	2,63E-02	5,00E-01
GO:0031090	organelle membrane	191	10	5,2	2,23	2,33	1,67E-02	2,83E-02	5,66E-01
GO:0044422	organelle part	650	24	3,7	1,57	1,7	1,81E-02	2,93E-02	6,14E-01
GO:0031967	organelle envelope	139	8	5,8	2,45	2,54	1,92E-02	2,93E-02	6,54E-01
GO:0031975	envelope	140	8	5,7	2,43	2,52	2,00E-02	2,93E-02	6,78E-01
GO:0005740	mitochondrial envelope	114	7	6,1	2,62	2,7	2,07E-02	2,93E-02	7,04E-01
GO:0005829	cytosol	92	6	6,5	2,78	2,86	2,45E-02	3,34E-02	8,34E-01
GO:0009986	cell surface	30	3	10	4,26	4,33	3,90E-02	4,53E-02	1,00E+00
GO:0005730	nucleolus	30	3	10	4,26	4,33	3,90E-02	4,53E-02	1,00E+00
GO:0000331	contractile vacuole	12	2	16,7	7,1	7,19	3,97E-02	4,53E-02	1,00E+00

GO:0031981	nuclear lumen	54	4	7,4	3,16	3,22	4,33E-02	4,53E-02	1,00E+00
GO:0005876	spindle microtubule	1	1	100	42,6	42,91	4,53E-02	4,53E-02	1,00E+00
GO:0009345	glycine-tRNA ligase complex	1	1	100	42,6	42,91	4,53E-02	4,53E-02	1,00E+00
GO:0031332	RNAi effector complex	1	1	100	42,6	42,91	4,53E-02	4,53E-02	1,00E+00
GO:0035097	histone methyltransferase complex	1	1	100	42,6	42,91	4,53E-02	4,53E-02	1,00E+00
GO:0016442	RNA-induced silencing complex	1	1	100	42,6	42,91	4,53E-02	4,53E-02	1,00E+00

Background count: number of genes in the background (all transcripts identified by the RNAseq analysis) with this term.

Result count: number of genes in the gene list (transcripts regulated by PKA) with this term.

% of background: of the genes in the background with this term, the percent that are present in the gene list.

Supplemental material – Chapter 4.2

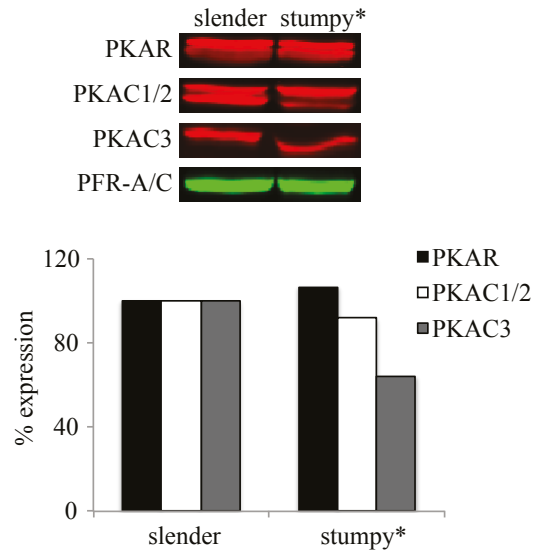


Figure S1: Developmental regulation of PKA subunit expression in monomorphic *T. brucei* cells. Protein expression of PKA subunits in slender and stumpy-like (stumpy*) MiTat 1.2 cells was analyzed by Western blotting using specific antibodies against PKAC1/2, PKAC3 and PKAR (Bachmaier et al., submitted manuscript, see chapter 5; Bachmaier et al, manuscript, see chapter 4.1). PFR-A/C detected by the monoclonal antibody L13D6 (Kohl et al., 1999) was used for normalization. The diagram shows the percentage of PKAR, PKAC1/2 and PKAC3 in the two different life cycle stages (slender was set to 100%).

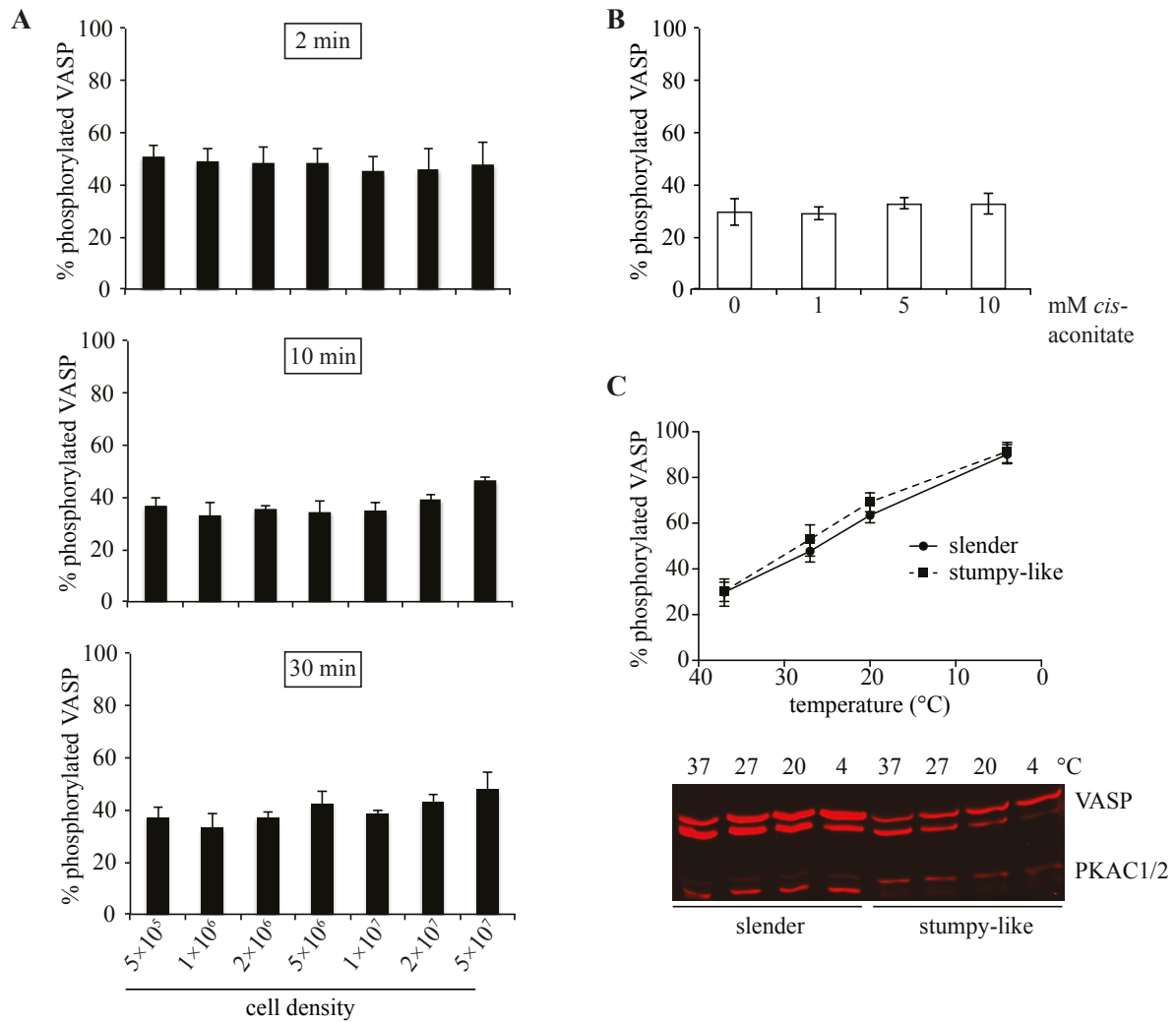


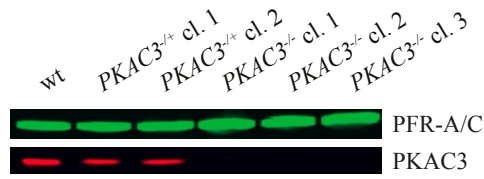
Figure S2: Activation of *T. brucei* PKA by cold shock.

A. VASP phosphorylation is independent of the cell density. Phosphorylation of the transgenically expressed PKA reporter substrate VASP was analyzed at the indicated cell densities and incubation times (2 min, 10 min, 30 min). Error bars represent SD of three independent biological replicates.

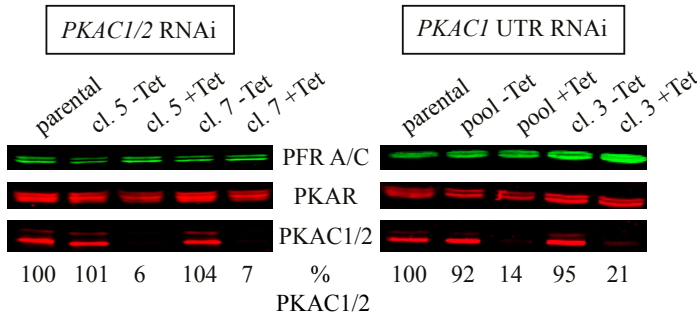
B. PKA activity is not regulated by *cis*-aconitate *in vivo*. VASP phosphorylation was analyzed upon incubation with the indicated concentrations of *cis*-aconitate for 10 minutes. The diagram shows the average and range of two independent biological replicates.

C. Analysis of VASP phosphorylation in slender versus stumpy-like monomorphic BSF trypanosomes at 37°C, 27°C, 20°C or 4°C, respectively. VASP expressing cells were incubated at the indicated temperatures for 10 minutes, followed by quantitative Western blotting to determine the percentage of phosphorylated VASP and the extent of the ‘stumpy-specific’ phosphorylation of PKAC1/2. Error bars represent SD of three independent biological replicates. The Western blot below the graph shows one representative experiment.

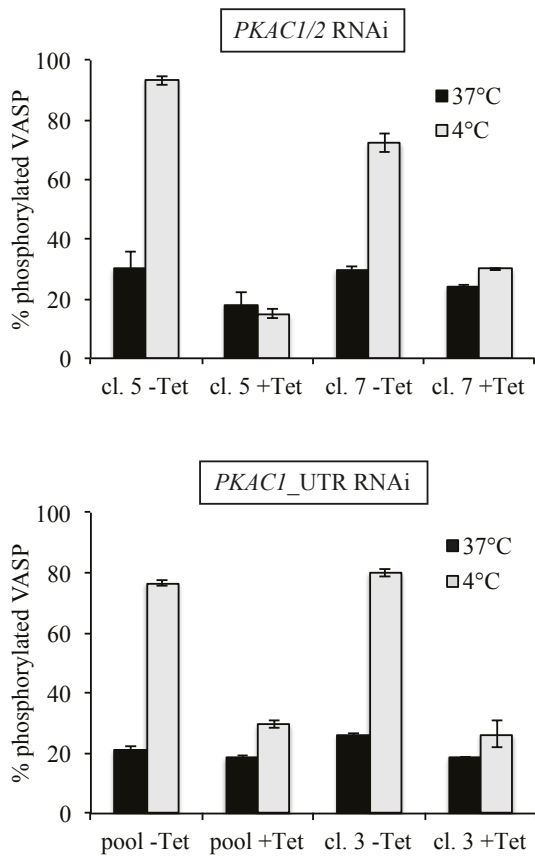
A



B



C



incubation at 37°C or 4°C, respectively, for 10 min. Error bars represent SD of three independent biological replicates.

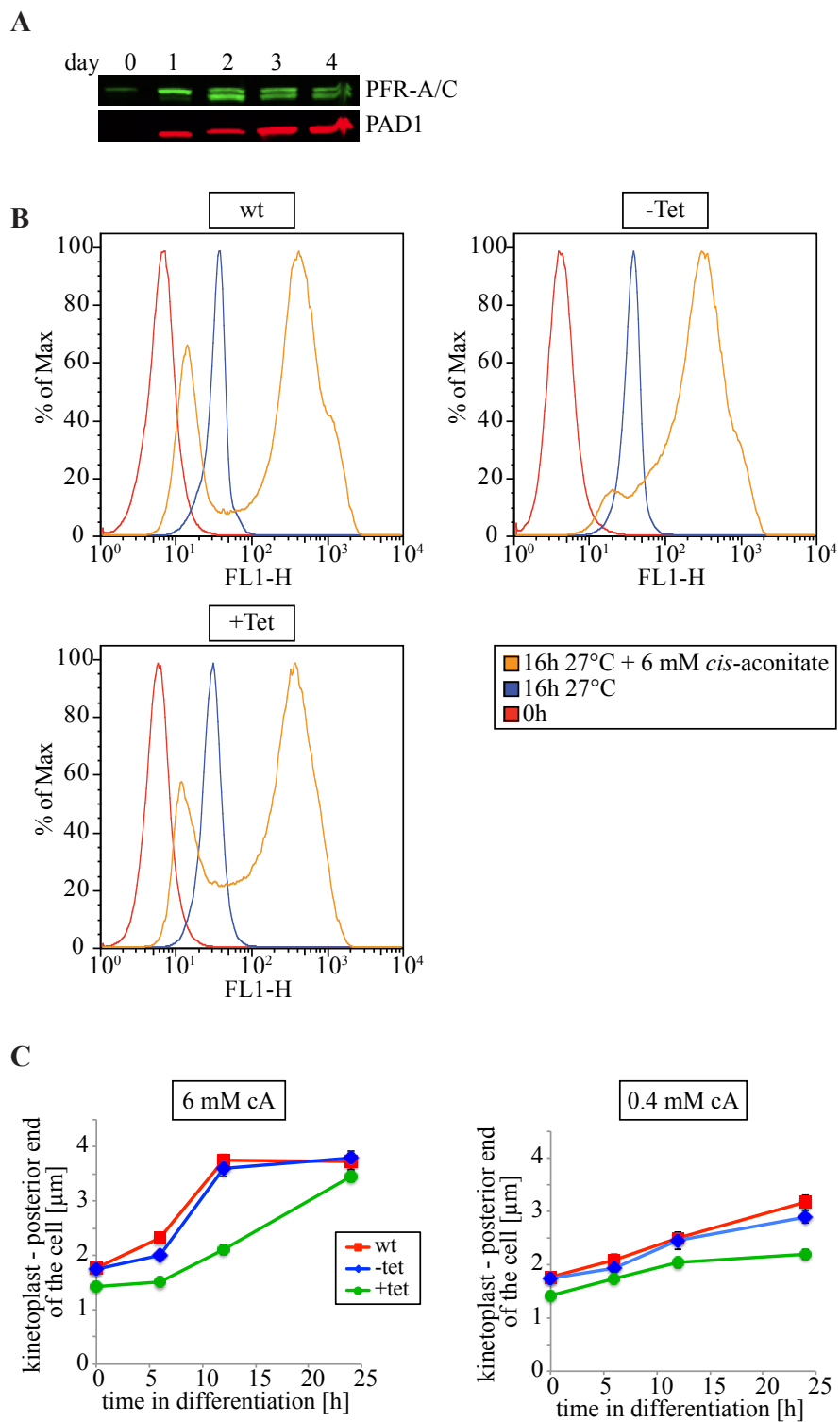
Figure S3: PKA subunit expression and VASP phosphorylation in PKA mutants.

A. Western blot analysis of MiTat 1.2 wild type (wt) and hemizygous (*PKAC3*^{+/+}, clones 1 and 2) and homozygous (*PKAC3*^{-/-}, clones 1, 2 and 3) deletion mutants of *PKAC3*. *PKAC3* expression was analyzed using an anti-*PKAC3* antibody (Bachmaier et al., manuscript; see chapter 4.1). The monoclonal antibody L13D6 detecting PFR-A/C (Kohl et al., 1999) was used as loading control.

B. Western blot analysis of the cell lines *PKAC1/2* RNAi (clones 5 and 7) and *PKAC1* UTR RNAi (pool and clone 3) in the presence (+Tet) or absence (-Tet) of 10 µg/ml tetracycline (induced 24 h). The parental cell line MiTat 1.2 1313 was included as control. The following antibodies were used: anti-*PKAC1/2* (Bachmaier et al., manuscript; see chapter 4.1), anti-*PKAR* (Bachmaier et al., submitted manuscript; see chapter 5) and anti-PFR-A/C (loading control; Kohl et al., 1999). The normalized *PKAC1/2* signal of the parental cells was set to 100%. Quantification of the *PKAC1/2* signal is indicated (in %) below the Western blots.

C. Analysis of VASP phosphorylation in cell lines with inducible RNAi against *PKAC1/2* (clones 5 and 7; upper panel) or *PKAC1* (pool and clone 3; lower panel), respectively.

Phosphorylation of the PKA reporter substrate was analyzed in cells with (+Tet) or without (-Tet) induction of RNAi with 10 µg/ml tetracycline for 24 h followed by



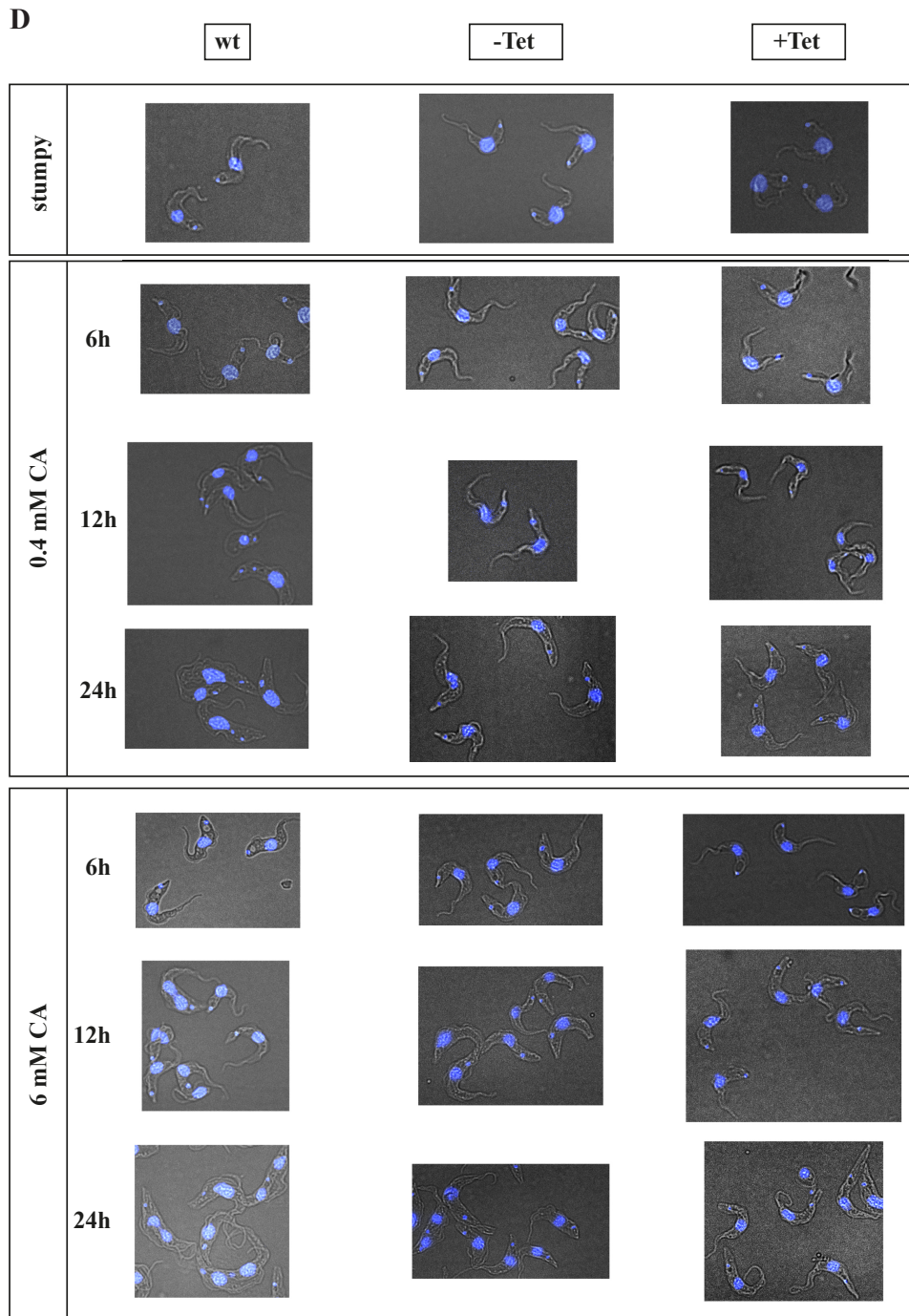


Figure S4: Analysis of differentiation markers in cells with depleted PKAC1/2.

A. Western blot analysis of PAD1 expression in pleomorphic AnTat 1.1 p cells grown on agarose plates. Slender cells derived from infected rats were plated on agarose plates. In a time course over four days cells were harvested from one plate each day, and PAD1 expression was analyzed by Western blot. PFR-A/C detected by the monoclonal antibody L13D6 (Kohl et al., 1999) was used as loading control.

B. Surface expression of EP procyclin was analyzed by flow cytometry of AnTat 1.1 p wild type (wt) and *PKAC1/2* RNAi cells induced (+Tet) or not (-Tet) with 10 µg/ml tetracycline. Samples for flow cytometry were taken from stumpy cells harvested from agarose plates followed by cultivation in DTM for 0 h or for 16 h at 27°C with or without addition of 6 mM *cis*-aconitate.

C. Kinetoplast repositioning during SS to PCF differentiation was analyzed in pleomorphic AnTat 1.1 p wild type cells as well as in the derived *PKAC1/2* RNAi cell line in the presence (+ Tet) or absence (- Tet) of 10 μ g/ml tetracycline. The distance between kinetoplast and posterior end of the cell was determined at the indicated time points after initiation of differentiation by addition of 0.4 mM or 6 mM *cis*-aconitate, respectively, using the software ImageJ.

D. Representative microscopic images showing the kinetoplast repositioning during SS to PCF differentiation of AnTat 1.1 wild type cells and the derived *PKAC1/2* RNAi cell line (RNAi induced: +Tet; RNAi non-induced: -Tet).

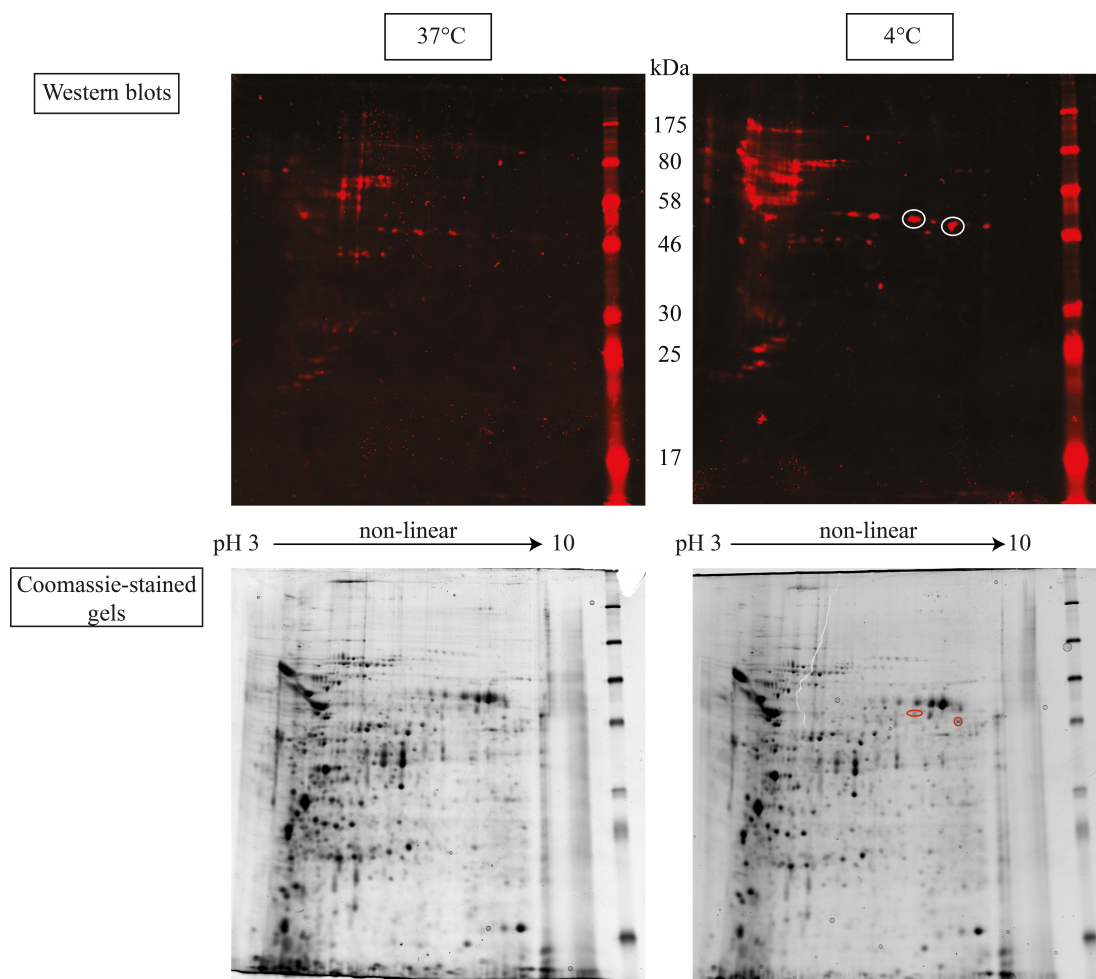


Figure S5: Detection of RXXS*/T*-phosphorylated proteins in *T. brucei* BSF cells expressing the PKA reporter substrate VASP by 2D gel electrophoresis followed by Western blotting.

BSF trypanosomes expressing the PKA reporter substrate VASP were incubated for 10 min at 37°C or 4°C, respectively, followed by lysis and separation of the proteins by isoelectric focusing (IEF) and SDS PAGE. Each sample was run in duplicates. While one gel was stained with Colloidal Coomassie (bottom), the other one was blotted to a PVDF membrane (top). Detection of phosphorylated RXXS*/T* proteins was carried out using the anti-RXXS*/T* antibody. The spots encircled in the Western blot and in the Coomassie-stained gel with the cold shocked sample represent spots, which were cut and subjected to MS/MS. They represent the transgenically expressed PKA reporter substrate VASP.

Table S1: Identified candidate substrates of *T. brucei* PKA.

# of peptides	gene ID ¹	product description ¹	predicted GO function ¹	predicted GO process ¹	functional category	conservation ²	phospho-RXXS/T identified	NetPhosK 1.0 prediction PKA ³	detected in plasma membrane (PM) and/or cytoskeleton (CS) proteomes ⁴	detected in flagellar proteomes ^{5, 6, 7, 8}	detected in glycosomal proteomes ^{9, 10, 11}	putative involvement in Ca ²⁺ signaling
136	Tb927.7.3550	hypothetical protein, conserved	null	null	unknown function	c	P-peptide identified (RELS* (S587))	not predicted to be a PKA site	PM, CS	x		x (C2 domain)
65	Tb927.1.4310	hypothetical protein, conserved	protein binding	null	unknown function	k			PM, CS	x		
63	Tb927.8.6660	paraflagellar rod component, putative (PFC1)	null	null	unknown function	k	P-peptide identified (RRQT (T477))	0,71	PM, CS	x	x	x (EF hand)
53	Tb11.01.0680	leucine rich repeat (TbLRRP1)	null	null	motility	c	P-peptide identified (RPPS (S559); RSAS (S608); RRRS (S620))	0.74; 0.65; 0.89	PM CS	x		
51	Tb927.4.2920	hypothetical protein, conserved	null	null	unknown function	t	P-peptide identified (RRLS (S395))	0,85	PM	x		
41	Tb09.160.1160	nucleolar protein (NOP86)	null	null	other	k			PM, CS	x		
39	Tb927.8.8330	calpain, putative, cysteine peptidase, putative	calcium-dependent cysteine-type endopeptidase activity	proteolysis	protein transport and maturation	k	P-peptide identified (RRPS (S261))	0,81	PM, CS	x		x (calcium-dep. cystein peptidase)
38	Tb927.10.840	hypothetical protein, conserved	null	null	other	k	P-peptide identified (RLHS (S1112 or S1240))	0.54; 0.66	PM, CS	x		

# of peptides	gene ID ¹	product description ¹	predicted GO function ¹	predicted GO process ¹	functional category	conservation ²	phospho-RXXS/T identified	NetPhosK 1.0 prediction PKA ³	detected in plasma membrane (PM) and/or cytoskeleton (CS) proteomes ⁴	detected in flagellar proteomes ^{5, 6, 7, 8}	detected in glycosomal proteomes ^{9, 10, 11}	putative involvement in Ca ²⁺ signaling
33	Tb927.1.2330	beta tubulin	GTP binding, GTPase activity, structural molecule activity	microtubule-based movement, microtubule-based process, protein polymerization	motility	c			PM, CS	x	x	
31	Tb927.10.10980	heat shock protein 83, heat shock protein	ATP binding, unfolded protein binding	protein folding, response to stress	protein folding	c	P-peptide identified (RFHS (S442))	0,51	PM	x		
31	Tb927.1.2340	alpha tubulin	GTP binding, GTPase activity, structural molecule activity	microtubule-based movement, microtubule-based process, protein polymerization	motility	c			PM, CS		x	
30	Tb927.10.5620	fructose-bisphosphate aldolase, glycosomal (ALD)	84	glycolysis	carbohydrate metabolism	c			PM, CS	x	x	
29	Tb11.02.1085	40S ribosomal protein S4, putative	RNA binding, structural constituent of ribosome	translation	ribosome biogenesis / translation	c			PM, CS			

# of peptides	gene ID ¹	product description ¹	predicted GO function ¹	predicted GO process ¹	functional category	conservation ²	phospho-RXXS/T identified	NetPhosK 1.0 prediction PKA ³	detected in plasma membrane (PM) and/or cytoskeleton (CS) proteomes ⁴	detected in flagellar proteomes ^{5, 6, 7, 8}	detected in glycosomal proteomes ^{9, 10, 11}	putative involvement in Ca ²⁺ signaling
27	Tb927.2.2720	protein kinase, putative	ATP binding, protein kinase activity, protein serine/threonine kinase activity, protein tyrosine kinase activity	protein phosphorylation	signaling	k	P-peptide identified (RPHS (S492); RRTS (S1427))	not predicted to be a PKA site; 0.88				
24	Tb927.4.2080	C2 domain containing protein (CC2D)	null	null	other	k	P-peptide identified (RNNS (S488))	0,76	PM, CS	x		x (C2 domain)
24	Tb927.6.4280	glyceraldehyde 3-phosphate dehydrogenase, glycosomal (GAPDH)	NAD or NADH binding, catalytic activity, glyceraldehyde-3-phosphate dehydrogenase activity	glucose metabolic process, metabolic process	carbohydrate metabolism	c			PM, CS	x	x	
22	Tb927.10.2110	elongation factor 1-alpha (TEF1)	GTP binding, GTPase activity, translation elongation factor activity	translational elongation	ribosome biogenesis / translation	c			PM, CS	x	x	
22	Tb11.02.5450	glucose-regulated protein 78, putative, luminal binding protein 1 (BiP), putative	ATP binding	null	protein folding	c			PM		x	

# of peptides	gene ID ¹	product description ¹	predicted GO function ¹	predicted GO process ¹	functional category	conservation ²	phospho-RXXS/T identified	NetPhosK 1.0 prediction PKA ³	detected in plasma membrane (PM) and/or cytoskeleton (CS) proteomes ⁴	detected in flagellar proteomes ^{5, 6, 7, 8}	detected in glycosomal proteomes ^{9, 10, 11}	putative involvement in Ca ²⁺ signaling
20	Tb927.3.3270	ATP-dependent phosphofructokinase (TbPFK)	6-phosphofructokinase activity, ATP binding	glycolysis	carbohydrate metabolism	c			PM, CS	x	x	
20	Tb09.160.5250	adenosine monophosphate deaminase, putative, AMP deaminase, putative	deaminase activity	purine ribonucleoside monophosphate biosynthetic process	other metabolism	c			PM, CS	x		
20	Tb927.4.1800	ribosomal protein L3, mitochondrial, putative	structural constituent of ribosome	translation	ribosome biogenesis / translation	c						
19	Tb927.10.6050	clathrin heavy chain (CHC)	binding, protein binding, structural molecule activity	intracellular protein transport, vesicle-mediated transport	protein transport and maturation	c			PM	x		
18	Tb09.211.0620	actin A	protein binding	null	other	c			PM, CS			
18	Tb927.10.4560	elongation factor 2	GTP binding, GTPase activity	null	ribosome biogenesis / translation	c			PM, CS			
17	Tb927.1.1100	hypothetical protein, conserved	null	null	motility	k						
16	Tb09.211.3550	glycerol kinase, glycosomal (glk1)	glycerol kinase activity	carbohydrate metabolic process, glycerol-3-phosphate metabolic process	carbohydrate metabolism	c			PM, CS	x	x	
16	Tb927.10.5910	hypothetical protein, conserved	null	null	unknown function	k						

# of peptides	gene ID ¹	product description ¹	predicted GO function ¹	predicted GO process ¹	functional category	conservation ²	phospho-RXXS/T identified	NetPhosK 1.0 prediction PKA ³	detected in plasma membrane (PM) and/or cytoskeleton (CS) proteomes ⁴	detected in flagellar proteomes ^{5, 6, 7, 8}	detected in glycosomal proteomes ^{9, 10, 11}	putative involvement in Ca ²⁺ signaling
14	Tb11.02.2210	protein kinase A regulatory subunit (PKA-R)	cAMP-dependent protein kinase regulator activity	regulation of protein phosphorylation	signaling	c			PM, CS	x		
14	Tb927.10.8940	hypothetical protein, conserved	null	null	protein transport and maturation	k			PM, CS	x		
14	Tb11.02.4190	MRB1-associated protein	protein binding	null	unknown function	k						
13	Tb11.02.0170	hypothetical protein, conserved	null	null	unknown function	t	P-peptide identified (RTLS (S357))	0,74	PM, CS	x		
13	Tb11.55.0006	intraflagellar transport protein IFT88 (IFT88)	null	null	protein transport and maturation	c						
13	Tb11.01.5570	NRBD1 (NRBD1)	nucleic acid binding	null	RNA associated	k			CS			
12	Tb927.10.2890	enolase	phosphopyruvate hydratase activity	glycolysis	carbohydrate metabolism	c				x		
12	Tb09.244.2630	40S ribosomal protein S6, putative	structural constituent of ribosome	translation	ribosome biogenesis / translation	c			PM, CS	x		
12	Tb927.3.5050	60S ribosomal protein L4	structural constituent of ribosome	translation	ribosome biogenesis / translation	c			PM, CS	x		
12	Tb927.3.3300	hypothetical protein, conserved	null	null	unknown function	t			PM, CS	x		
12	Tb09.211.1620	hypothetical protein, conserved	null	null	unknown function	c						

# of peptides	gene ID ¹	product description ¹	predicted GO function ¹	predicted GO process ¹	functional category	conservation ²	phospho-RXXS/T identified	NetPhosK 1.0 prediction PKA ³	detected in plasma membrane (PM) and/or cytoskeleton (CS) proteomes ⁴	detected in flagellar proteomes ^{5, 6, 7, 8}	detected in glycosomal proteomes ^{9, 10, 11}	putative involvement in Ca ²⁺ signaling
12	Tb927.3.1010	hypothetical protein, conserved	null	null	unknown function	t			PM, CS			
11	Tb927.10.11390	60S ribosomal protein L6, putative	structural constituent of ribosome	translation	ribosome biogenesis / translation	c			CS	x		
11	Tb927.3.3310	60S ribosomal protein L13, putative	structural constituent of ribosome	translation	ribosome biogenesis / translation	c			CS	x		
11	Tb927.2.4710	RNA-binding protein, putative (TRRM1)	nucleic acid binding, zinc ion binding	null	RNA associated	c			PM	x		
11	Tb927.7.2450	hypothetical protein, conserved	null	null	unknown function	k						
11	Tb927.10.1510	NOT1 (NOT1)	null	null	unknown function	c			PM			
11	Tb927.10.8830	hypothetical protein, conserved	heat shock protein binding	null	protein folding	k			PM			
10	Tb927.10.2010	hexokinase (HK1)	ATP binding	carbohydrate metabolic process	carbohydrate metabolism	c			PM	x	x	
10	Tb927.10.890	kinesin, putative	ATP binding, microtubule motor activity, nucleotide binding	microtubule-based movement	motility	t				x		

# of peptides	gene ID ¹	product description ¹	predicted GO function ¹	predicted GO process ¹	functional category	conservation ²	phospho-RXXS/T identified	NetPhosK 1.0 prediction PKA ³	detected in plasma membrane (PM) and/or cytoskeleton (CS) proteomes ⁴	detected in flagellar proteomes ^{5, 6, 7, 8}	detected in glycosomal proteomes ^{9, 10, 11}	putative involvement in Ca ²⁺ signaling
10	Tb11.02.0760	dynein heavy chain, putative	ATP binding, ATPase activity, microtubule motor activity, nucleoside-triphosphatase activity, nucleotide binding	bioluminescence, microtubule-based movement, protein-chromophore linkage	motility	c			PM, CS	x		
10	Tb927.6.3740	heat shock 70 kDa protein, mitochondrial precursor, putative	ATP binding, unfolded protein binding	protein folding	protein folding	c			PM	x	x	
10	Tb927.10.450	hypothetical protein, conserved	null	null	motility	c				x		
10	Tb11.01.4940	AAA ATPase, putative	ATP binding, nucleoside-triphosphatase activity, nucleotide binding	null	metabolism	c						
10	Tb927.8.1330	60S ribosomal protein L7a, putative	null	null	ribosome biogenesis / translation	c			PM, CS			

# of peptides	gene ID ¹	product description ¹	predicted GO function ¹	predicted GO process ¹	functional category	conservation ²	phospho-RXXS/T identified	NetPhosK 1.0 prediction PKA ³	detected in plasma membrane (PM) and/or cytoskeleton (CS) proteomes ⁴	detected in flagellar proteomes ^{5, 6, 7, 8}	detected in glycosomal proteomes ^{9, 10, 11}	putative involvement in Ca ²⁺ signaling
10	Tb927.10.13720	RNA-binding protein, putative (RBP29)	nucleic acid binding	null	RNA associated	k						
10	Tb927.10.5140	protein kinase, putative, mitogen-activated protein kinase 2, putative	ATP binding, protein kinase activity, protein serine/threonine kinase activity, protein tyrosine kinase activity	protein phosphorylation	signaling	c			PM			
10	Tb11.02.1540	hypothetical protein, conserved	null	null	unknown function	k						
9	Tb927.1.700	phosphoglycerate kinase (PGKC)	phosphoglycerate kinase activity	glycolysis	carbohydrate metabolism	c				x	x	
9	Tb11.01.3110	heat shock protein 70	ATP binding	null	protein folding	c			PM, CS	x	x	
9	Tb927.2.5160	chaperone protein DNAj, putative	heat shock protein binding, unfolded protein binding	protein folding	protein folding	c				x		
9	Tb927.7.5000	60S ribosomal protein L19, putative	structural constituent of ribosome	translation	ribosome biogenesis / translation	c			CS	x		

# of peptides	gene ID ¹	product description ¹	predicted GO function ¹	predicted GO process ¹	functional category	conservation ²	phospho-RXXS/T identified	NetPhosK 1.0 prediction PKA ³	detected in plasma membrane (PM) and/or cytoskeleton (CS) proteomes ⁴	detected in flagellar proteomes ^{5, 6, 7, 8}	detected in glycosomal proteomes ^{9, 10, 11}	putative involvement in Ca ²⁺ signaling
9	Tb09.211.2150	Polyadenylate-binding protein 2 (Poly(A)-binding protein 2) (Poly(A)-binding protein II) (PABII) (Polyadenylate-binding nuclear protein 1) (Nuclear poly(A)-binding protein 1) (PABP2), putative (PABP2)	RNA binding, nucleic acid binding	null	RNA associated	c			PM, CS	x		
9	Tb927.8.900	splicing factor TSR1 (TSR1)	nucleic acid binding	null	RNA associated	c				x		
9	Tb11.02.0810	hypothetical protein, conserved	null	null	unknown function	c			PM, CS	x		
9	Tb927.10.3930	40S ribosomal protein S3A, putative	structural constituent of ribosome	translation	ribosome biogenesis / translation	c	no RXXS/T		CS			
9	Tb927.7.1730	60S ribosomal protein L7, putative	structural constituent of ribosome, transcription regulator activity	translation	ribosome biogenesis / translation	c			CS			
9	Tb927.10.14550	ATP-dependent DEAD/H RNA helicase, putative	ATP binding, ATP-dependent helicase activity, helicase activity, nucleic acid binding	null	RNA associated	c						
9	Tb927.7.6730	hypothetical protein, conserved	null	null	unknown function	k						

# of peptides	gene ID ¹	product description ¹	predicted GO function ¹	predicted GO process ¹	functional category	conservation ²	phospho-RXXS/T identified	NetPhosK 1.0 prediction PKA ³	detected in plasma membrane (PM) and/or cytoskeleton (CS) proteomes ⁴	detected in flagellar proteomes ^{5, 6, 7, 8}	detected in glycosomal proteomes ^{9, 10, 11}	putative involvement in Ca ²⁺ signaling
9	Tb927.8.5710	recombination initiation protein NBS1, putative	null	null	unknown function	k			PM			
8	Tb927.3.930	dynein heavy chain, putative	ATP binding, ATPase activity, microtubule motor activity, nucleoside-triphosphatase activity, nucleotide binding	microtubule-based movement	motility	c			PM, CS	x		
8	Tb927.10.8190	T-complex protein 1, theta subunit, putative, CCT-theta, putative (TCP-1-theta)	ATP binding, protein binding, unfolded protein binding	cellular protein metabolic process, protein folding	protein folding	c				x		
8	Tb11.01.7960	60S ribosomal protein L2, putative, 60S ribosomal protein L8, putative	structural constituent of ribosome	translation	ribosome biogenesis / translation	c	no RXXS/T		CS	x		
8	Tb927.8.6150	40S ribosomal protein S8, putative	null	null	ribosome biogenesis / translation	c			CS	x		
8	Tb927.10.2880	calcium channel protein, putative	ion channel activity	ion transport	transport	c			PM	x		x (calcium channel)
8	Tb09.160.0650	hypothetical protein, conserved	null	null	unknown function	k			PM, CS	x		

# of peptides	gene ID ¹	product description ¹	predicted GO function ¹	predicted GO process ¹	functional category	conservation ²	phospho-RXXS/T identified	NetPhosK 1.0 prediction PKA ³	detected in plasma membrane (PM) and/or cytoskeleton (CS) proteomes ⁴	detected in flagellar proteomes ^{5, 6, 7, 8}	detected in glycosomal proteomes ^{9, 10, 11}	putative involvement in Ca ²⁺ signaling
8	Tb927.4.4570	hypothetical protein, conserved	sequence-specific DNA binding transcription factor activity	regulation of transcription	other	k						
8	Tb09.244.2730	unspecified product	5S rRNA binding, structural constituent of ribosome	translation	ribosome biogenesis / translation	c			CS			
8	Tb11.01.3420	eukaryotic translation initiation factor, putative	null	null	ribosome biogenesis / translation	c						
8	Tb927.10.2240	hypothetical protein, conserved	null	transport	transport	k						
8	Tb09.160.5060	hypothetical protein, conserved	null	null	unknown function	k			PM, CS			
8	Tb927.7.7190	hypothetical protein, conserved	null	null	unknown function	t						
7	Tb927.3.4720	dynammin, putative, vacuolar sortin protein 1, putative	GTP binding, GTPase activity	null	other	c			PM	x		
7	Tb11.02.4700	14-3-3 protein	protein domain specific binding	null	other	c				x		
7	Tb11.01.5860	T-complex protein 1, epsilon subunit, putative (TCP-1-epsilon)	ATP binding, protein binding, unfolded protein binding	cellular protein metabolic process, protein folding	protein folding	c			PM	x		
7	Tb927.7.710	heat shock 70 kDa protein, putative (HSP70)	ATP binding	null	protein folding	c			PM	x		

# of peptides	gene ID ¹	product description ¹	predicted GO function ¹	predicted GO process ¹	functional category	conservation ²	phospho-RXXS/T identified	NetPhosK 1.0 prediction PKA ³	detected in plasma membrane (PM) and/or cytoskeleton (CS) proteomes ⁴	detected in flagellar proteomes ^{5, 6, 7, 8}	detected in glycosomal proteomes ^{9, 10, 11}	putative involvement in Ca ²⁺ signaling
7	Tb09.211.3610	ubiquitin-activating enzyme E1, putative (UBA2)	ATP binding, catalytic activity, small protein activating enzyme activity	protein modification process	protein transport and maturation	k				x		
7	Tb927.10.1170	intraflagellar transport protein IFT172, putative (IFT172)	null	null	protein transport and maturation	c				x	x	
7	Tb927.3.2600	ATP-dependent DEAD/H RNA helicase, putative	ATP binding, ATP-dependent helicase activity, helicase activity, nucleic acid binding	null	RNA associated	c				x		
7	Tb927.4.2180	60S ribosomal protein L35a, putative	structural constituent of ribosome	translation	ribosome biogenesis / translation	c			CS	x		
7	Tb11.01.8770	leucine-rich repeat protein (LRRP), putative	carbohydrate binding, protein binding	null	motility	c			PM, CS	x		
7	Tb927.10.14710	40S ribosomal protein S2, putative (RPS2)	RNA binding, structural constituent of ribosome	translation	ribosome biogenesis / translation	c			PM, CS	x		
7	Tb927.10.12680	60S ribosomal protein L34, putative	structural constituent of ribosome	translation	ribosome biogenesis / translation	c	no RXXS/T			x		

# of peptides	gene ID ¹	product description ¹	predicted GO function ¹	predicted GO process ¹	functional category	conservation ²	phospho-RXXS/T identified	NetPhosK 1.0 prediction PKA ³	detected in plasma membrane (PM) and/or cytoskeleton (CS) proteomes ⁴	detected in flagellar proteomes ^{5, 6, 7, 8}	detected in glycosomal proteomes ^{9, 10, 11}	putative involvement in Ca ²⁺ signaling
7	Tb927.2.5870	hypothetical protein, conserved	null	null	unknown function	k	P-peptide identified (RRAS (S1678))	0,8	CS			
7	Tb11.02.5050	protein kinase, putative	ATP binding, protein kinase activity, protein serine/threonine kinase activity, protein tyrosine kinase activity	protein phosphorylation	signaling	c						
7	Tb09.160.4610	unspecified product	null	null	unknown function	t						
7	Tb927.5.3240	hypothetical protein, conserved	null	null	unknown function	k						
7	Tb927.6.2210	hypothetical protein, conserved	binding	null	unknown function	c						
7	Tb11.01.2560	40S ribosomal protein SA, putative	structural constituent of ribosome	translation	ribosome biogenesis / translation	c			PM, CS			
7	Tb927.1.4280	hypothetical protein, conserved	protein binding	null	unknown function	t			PM, CS			

# of peptides	gene ID ¹	product description ¹	predicted GO function ¹	predicted GO process ¹	functional category	conservation ²	phospho-RXXS/T identified	NetPhosK 1.0 prediction PKA ³	detected in plasma membrane (PM) and/or cytoskeleton (CS) proteomes ⁴	detected in flagellar proteomes ^{5, 6, 7, 8}	detected in glycosomal proteomes ^{9, 10, 11}	putative involvement in Ca ²⁺ signaling
6	Tb927.5.800	casein kinase I, isoform 2 (CK1.2)	ATP binding, protein kinase activity, protein serine/threonine kinase activity, protein tyrosine kinase activity	protein phosphorylation	signaling	c	P-peptide identified (RYCS (S186))	0,7	PM, CS	x		
6	Tb09.211.3180	6-phosphogluconate dehydrogenase, decarboxylating (gnD)	NADP or NADPH binding, binding, catalytic activity, oxidoreductase activity	metabolic process, oxidation-reduction process, pentose-phosphate shunt	metabolism	c				x	x	
6	Tb927.10.540	ATP-dependent DEAD/H RNA helicase, putative, DEAD box RNA helicase, putative	ATP binding, ATP-dependent helicase activity, helicase activity, nucleic acid binding	null	RNA associated	c				x		
6	Tb09.211.3510	ATP-dependent DEAD/H RNA helicase, putative (DED1)	ATP binding, ATP-dependent helicase activity, helicase activity, nucleic acid binding	null	RNA associated	c				x		

# of peptides	gene ID ¹	product description ¹	predicted GO function ¹	predicted GO process ¹	functional category	conservation ²	phospho-RXXS/T identified	NetPhosK 1.0 prediction PKA ³	detected in plasma membrane (PM) and/or cytoskeleton (CS) proteomes ⁴	detected in flagellar proteomes ^{5, 6, 7, 8}	detected in glycosomal proteomes ^{9, 10, 11}	putative involvement in Ca ²⁺ signaling
6	Tb927.8.2390	hypothetical protein, conserved	null	null	unknown function	k				x		
6	Tb927.10.14890	C-terminal motor kinesin, putative (TBKIFC1)	ATP binding, microtubule motor activity	intracellular protein transport, microtubule-based movement	motility	c			PM	x		
6	Tb11.02.0250	heat shock protein 84, putative	ATP binding, unfolded protein binding	protein folding, response to stress	protein folding	c			PM	x	x	
6	Tb09.160.3270	ATP-dependent DEAD box helicase, putative	ATP binding, ATP-dependent helicase activity, helicase activity, nucleic acid binding	null	RNA associated	c			PM	x		
6	Tb11.02.0030	Cytoplasmic dynein 2 heavy chain (DYNC2H1), putative, Cytoplasmic dynein 2 heavy chain (DYNC2H2), putative (DHC1b)	ATP binding, ATPase activity, microtubule motor activity, nucleotide binding	microtubule-based movement	motility	c			PM	x		

# of peptides	gene ID ¹	product description ¹	predicted GO function ¹	predicted GO process ¹	functional category	conservation ²	phospho-RXXS/T identified	NetPhosK 1.0 prediction PKA ³	detected in plasma membrane (PM) and/or cytoskeleton (CS) proteomes ⁴	detected in flagellar proteomes ^{5, 6, 7, 8}	detected in glycosomal proteomes ^{9, 10, 11}	putative involvement in Ca ²⁺ signaling
6	Tb927.8.3530	glycerol-3-phosphate dehydrogenase [NAD ⁺], glycosomal	NAD or NADH binding, catalytic activity, oxidoreductase activity, protein homodimerization activity	carbohydrate metabolic process, glycerol-3-phosphate catabolic process, glycerol-3-phosphate metabolic process, metabolic process, oxidation-reduction process	carbohydrate metabolism	c			PM, CS	x	x	
6	Tb927.2.340	retrotransposon hot spot protein 4 (RHS4), putative	null	null	unknown function	t			PM, CS	x		
6	Tb927.10.6510	chaperonin HSP60, mitochondrial precursor (HSP60)	ATP binding, protein binding	cellular protein metabolic process	protein folding	c			PM, CS	x	x	
6	Tb09.211.0110	60S ribosomal protein L10, putative, QM-like protein (QM)	structural constituent of ribosome	translation	ribosome biogenesis / translation	c				x		
6	Tb11.46.0001	60S acidic ribosomal subunit protein, putative	structural constituent of ribosome	ribosome biogenesis, translational elongation	ribosome biogenesis / translation	c	no RXXS/T		CS		x	
6	Tb927.10.13180	hypothetical protein, conserved	null	null	RNA associated	c			CS			
6	Tb927.3.4750	aminopeptidase, putative, metallo-peptidase, Clan MA(E) Family M1	metallopeptidase activity, zinc ion binding	null	protein transport and maturation	c				x		

# of peptides	gene ID ¹	product description ¹	predicted GO function ¹	predicted GO process ¹	functional category	conservation ²	phospho-RXXS/T identified	NetPhosK 1.0 prediction PKA ³	detected in plasma membrane (PM) and/or cytoskeleton (CS) proteomes ⁴	detected in flagellar proteomes ^{5, 6, 7, 8}	detected in glycosomal proteomes ^{9, 10, 11}	putative involvement in Ca ²⁺ signaling
6	Tb09.211.3270	unspecified product	structural constituent of ribosome	translation	ribosome biogenesis / translation	c						
6	Tb927.8.4450	RNA-binding protein, putative (RBP11)	nucleic acid binding	null	RNA associated	c						
6	Tb927.5.1560	ATP-dependent DEAD/H RNA helicase, putative	ATP binding, ATP-dependent helicase activity, helicase activity, nucleic acid binding	null	RNA associated	c						
6	Tb11.01.4230	protein kinase, putative	ATP binding, protein kinase activity, protein serine/threonine kinase activity, protein tyrosine kinase activity	protein phosphorylation	signaling	c						

# of peptides	gene ID ¹	product description ¹	predicted GO function ¹	predicted GO process ¹	functional category	conservation ²	phospho-RXXS/T identified	NetPhosK 1.0 prediction PKA ³	detected in plasma membrane (PM) and/or cytoskeleton (CS) proteomes ⁴	detected in flagellar proteomes ^{5, 6, 7, 8}	detected in glycosomal proteomes ^{9, 10, 11}	putative involvement in Ca ²⁺ signaling
6	Tb927.10.13780	glycogen synthase kinase 3 (GSK3)	ATP binding, protein kinase activity, protein serine/threonine kinase activity, protein tyrosine kinase activity	protein phosphorylation	signaling	c						
6	Tb09.160.5670	predicted tetratricopeptide repeat protein	null	null	protein transport and maturation	c						
6	Tb927.8.3840	hypothetical protein, conserved	null	null	unknown function	k						
5	Tb927.8.3150	T-complex protein 1, gamma subunit, putative (TCP-1-gamma)	ATP binding, protein binding, unfolded protein binding	cellular protein metabolic process, protein folding	protein folding	c				x		
5	Tb927.7.900	hypothetical protein, conserved	null	null	unknown function	k			PM	x	x	
5	Tb927.3.4290	PFR1 (PFR1)	calmodulin binding	null	motility	k			PM, CS	x	x	x (calmodulin binding)
5	Tb927.8.3060	cytosolic leucyl aminopeptidase, putative, metallo-peptidase, Clan MF, Family M17	aminopeptidase activity	proteolysis	protein transport and maturation	c			PM, CS	x		
5	Tb927.10.13500	60S ribosomal protein L10a	RNA binding	RNA processing	ribosome biogenesis / translation	c	no RXXS/T		PM, CS	x		

# of peptides	gene ID ¹	product description ¹	predicted GO function ¹	predicted GO process ¹	functional category	conservation ²	phospho-RXXS/T identified	NetPhosK 1.0 prediction PKA ³	detected in plasma membrane (PM) and/or cytoskeleton (CS) proteomes ⁴	detected in flagellar proteomes ^{5, 6, 7, 8}	detected in glycosomal proteomes ^{9, 10, 11}	putative involvement in Ca ²⁺ signaling
5	Tb927.8.1590	ubiquitin-protein ligase, putative (upl3)	acid-amino acid ligase activity, zinc ion binding	protein modification process	protein transport and maturation	c			CS			
5	Tb927.10.12490	kinesin, putative	ATP binding, microtubule motor activity, sequence-specific DNA binding	microtubule-based movement	motility	k						
5	Tb11.03.0880	predicted WD40 repeat protein (PIFTF6)	null	null	protein transport and maturation	c						
5	Tb927.7.3180	Mu-adaptin 1, putative, adaptor complex AP-1 medium subunit, putative	protein binding	intracellular protein transport, transport, vesicle-mediated transport	protein transport and maturation	c						
5	Tb927.10.14680	ribosome biogenesis protein, putative	null	null	ribosome biogenesis / translation	c						
5	Tb927.3.2470	pumilio RNA binding protein, putative (PUF8)	RNA binding, binding	null	RNA associated	c						
5	Tb927.3.4600	hypothetical protein, conserved	binding	null	protein transport and maturation	k						

# of peptides	gene ID ¹	product description ¹	predicted GO function ¹	predicted GO process ¹	functional category	conservation ²	phospho-RXXS/T identified	NetPhosK 1.0 prediction PKA ³	detected in plasma membrane (PM) and/or cytoskeleton (CS) proteomes ⁴	detected in flagellar proteomes ^{5, 6, 7, 8}	detected in glycosomal proteomes ^{9, 10, 11}	putative involvement in Ca ²⁺ signaling
5	Tb927.10.180	ATP synthase F1 subunit gamma protein, putative	null	ATP synthesis coupled proton transport	metabolism	c			PM			
5	Tb927.3.4070	hypothetical protein, conserved	null	null	transport	k			PM			
5	Tb11.47.0011	hypothetical protein, conserved	null	null	unknown function	c			PM			
5	Tb927.10.15660	hypothetical protein, conserved	null	null	unknown function	t			PM			
5	Tb09.211.4511	kinetoplastid membrane protein KMP-11	null	defense response, positive regulation of cell proliferation	other	k			PM, CS		x	
5	Tb09.211.1800	hypothetical protein, conserved	null	null	other	c			PM, CS			
5	Tb11.01.6790	hypothetical protein, conserved	null	null	unknown function	t			PM, CS			
4	Tb927.10.12710	heat shock protein 110, putative	ATP binding	null	protein folding	c				x		
4	Tb927.10.3660	aspartate aminotransferase	pyridoxal phosphate binding, transaminase activity	biosynthetic process, cellular amino acid metabolic process	other metabolism	c				x		
4	Tb927.7.5610	hypothetical protein, conserved	null	null	unknown function	k				x		
4	Tb11.02.1420	hypothetical protein, conserved	null	null	unknown function	k				x		
4	Tb11.02.5280	glycerol-3-phosphate dehydrogenase (FAD-dependent), mitochondrial	glycerol-3-phosphate dehydrogenase activity, oxidoreductase activity	glycerol-3-phosphate metabolic process	carbohydrate metabolism	c			PM	x	x	

# of peptides	gene ID ¹	product description ¹	predicted GO function ¹	predicted GO process ¹	functional category	conservation ²	phospho-RXXS/T identified	NetPhosK 1.0 prediction PKA ³	detected in plasma membrane (PM) and/or cytoskeleton (CS) proteomes ⁴	detected in flagellar proteomes ^{5, 6, 7, 8}	detected in glycosomal proteomes ^{9, 10, 11}	putative involvement in Ca ²⁺ signaling
4	Tb927.10.14140	pyruvate kinase 1 (PYK1)	catalytic activity, magnesium ion binding, potassium ion binding, pyruvate kinase activity	glycolysis	carbohydrate metabolism	c			PM, CS	x	x	
4	Tb927.3.2310	PACRGA	binding	null	motility	c	no RXXS/T		PM, CS	x	x	
4	Tb11.01.1960	hypothetical protein, conserved	null	null	unknown function	k			PM, CS	x		
4	Tb927.7.2390	hypothetical protein, conserved	null	null	unknown function	k			PM, CS	x		
4	Tb10.v4.0052	microtubule-associated protein 2_chrX additional, unordered contigs	null	null	unknown function	c				x		
4	Tb09.211.0180	hypothetical protein, conserved	null	cell proliferation	ribosome biogenesis / translation	c			CS			
4	Tb927.7.2170	hypothetical protein, conserved	protein binding, telomeric DNA binding	telomere maintenance via telomerase	other	k			CS			

# of peptides	gene ID ¹	product description ¹	predicted GO function ¹	predicted GO process ¹	functional category	conservation ²	phospho-RXXS/T identified	NetPhosK 1.0 prediction PKA ³	detected in plasma membrane (PM) and/or cytoskeleton (CS) proteomes ⁴	detected in flagellar proteomes ^{5, 6, 7, 8}	detected in glycosomal proteomes ^{9, 10, 11}	putative involvement in Ca ²⁺ signaling
4	Tb11.02.3360	replication factor C, subunit 1, putative, replication factor C large subunit, putative	ATP binding, ATP-dependent peptidase activity, DNA binding, DNA clamp loader activity, nucleoside-triphosphatase activity, nucleotide binding, serine-type endopeptidase activity	DNA replication, proteolysis	other	c						
4	Tb927.10.15520	signal recognition particle protein, putative	7S RNA binding	SRP-dependent cotranslational protein targeting to membrane	protein transport and maturation	c						
4	Tb09.160.5580	60S ribosomal protein L11, putative	structural constituent of ribosome	translation	ribosome biogenesis / translation	c						

# of peptides	gene ID ¹	product description ¹	predicted GO function ¹	predicted GO process ¹	functional category	conservation ²	phospho-RXXS/T identified	NetPhosK 1.0 prediction PKA ³	detected in plasma membrane (PM) and/or cytoskeleton (CS) proteomes ⁴	detected in flagellar proteomes ^{5, 6, 7, 8}	detected in glycosomal proteomes ^{9, 10, 11}	putative involvement in Ca ²⁺ signaling
4	Tb11.01.1050	hypothetical protein, conserved	ATP binding, protein kinase activity, protein serine/threonine kinase activity, protein tyrosine kinase activity	protein phosphorylation	signaling	k						
4	Tb09.160.1790	hypothetical protein, conserved	null	null	RNA associated	k						
4	Tb11.02.5580	hypothetical protein, conserved	null	null	unknown function	t						
4	Tb927.10.12430	hypothetical protein, conserved	binding	null	unknown function	c						
4	Tb927.10.850	hypothetical protein, conserved	null	null	unknown function	c						
4	Tb927.5.2770	hypothetical protein, conserved	null	null	unknown function	k						
4	Tb927.7.4410	hypothetical protein, conserved	null	null	unknown function	t						
4	Tb927.10.14840	mitochondrial carrier protein (MCP5a)	binding, transporter activity	transport	transport	c			PM, CS			
4	Tb927.3.2050	hypothetical protein, conserved	null	null	unknown function	k			PM, CS			
4	Tb927.3.5370	hypothetical protein, conserved	null	null	unknown function	k			PM, CS			
4	Tb927.5.2330	hypothetical protein, conserved	binding	null	unknown function	k			PM, CS			
4	Tb927.8.6980	hypothetical protein, conserved	null	null	unknown function	c			PM, CS			

# of peptides	gene ID ¹	product description ¹	predicted GO function ¹	predicted GO process ¹	functional category	conservation ²	phospho-RXXS/T identified	NetPhosK 1.0 prediction PKA ³	detected in plasma membrane (PM) and/or cytoskeleton (CS) proteomes ⁴	detected in flagellar proteomes ^{5, 6, 7, 8}	detected in glycosomal proteomes ^{9, 10, 11}	putative involvement in Ca ²⁺ signaling
3	Tb927.3.2230	succinyl-CoA synthetase alpha subunit, putative	binding, catalytic activity	metabolic process	carbohydrate metabolism	c				x	x	
3	Tb927.10.3990	DHH1 (DHH1)	ATP binding, ATP-dependent helicase activity, helicase activity, nucleic acid binding	null	RNA associated	c				x		
3	Tb927.4.1080	V-type ATPase, A subunit, putative	null	ATP metabolic process, ATP synthesis coupled proton transport, proton transport	transport	c				x		
3	Tb927.8.980	phosphoacetylglucosamine mutase, putative, acetylglucosamine phosphomutase, putative, N-acetylglucosamine-phosphate mutase, putative	phosphoacetylglucosamine mutase activity	carbohydrate metabolic process	carbohydrate metabolism	c				x		
3	Tb11.01.8510	T-complex protein 1, alpha subunit, putative (TCP-1-alpha)	ATP binding, protein binding	cellular protein metabolic process	protein folding	c			PM	x		

# of peptides	gene ID ¹	product description ¹	predicted GO function ¹	predicted GO process ¹	functional category	conservation ²	phospho-RXXS/T identified	NetPhosK 1.0 prediction PKA ³	detected in plasma membrane (PM) and/or cytoskeleton (CS) proteomes ⁴	detected in flagellar proteomes ^{5, 6, 7, 8}	detected in glycosomal proteomes ^{9, 10, 11}	putative involvement in Ca ²⁺ signaling
3	Tb927.10.12510	P-type H -ATPase, putative	ATP binding, ATPase activity, catalytic activity	ATP biosynthetic process, cation transport, metabolic process	transport	c			PM	x		
3	Tb09.211.1750	mitochondrial carrier protein (MCP11)	binding	transport	transport	c	no RXXS/T		PM, CS	x	x	
3	Tb927.3.1120	GTP-binding nuclear protein rtb2, putative (rtb2)	GTP binding, GTPase activity, protein binding	intracellular protein transport, nucleocytoplasmic transport, protein transport, signal transduction, small GTPase mediated signal transduction	protein transport and maturation	c			PM, CS	x		
3	Tb927.10.14580	60S ribosomal protein L17, putative	structural constituent of ribosome	translation	ribosome biogenesis / translation	c			PM, CS	x		
3	Tb927.5.3800	glutamine hydrolysing (not ammonia-dependent) carbomoyl phosphate synthase, putative	ATP binding, argininosuccinate synthase activity, carbamoyl-phosphate synthase activity, catalytic activity	arginine biosynthetic process, glutamine metabolic process, metabolic process, nitrogen compound metabolic process	other metabolism	c						

# of peptides	gene ID ¹	product description ¹	predicted GO function ¹	predicted GO process ¹	functional category	conservation ²	phospho-RXXS/T identified	NetPhosK 1.0 prediction PKA ³	detected in plasma membrane (PM) and/or cytoskeleton (CS) proteomes ⁴	detected in flagellar proteomes ^{5, 6, 7, 8}	detected in glycosomal proteomes ^{9, 10, 11}	putative involvement in Ca ²⁺ signaling
3	Tb927.2.380	retrotransposon hot spot protein 2 (RHS2), putative	null	null	unknown function	t						
3	Tb11.01.4370	hypothetical protein, conserved	null	null	unknown function	k			PM, CS			

¹ www.tritrypdb.org² www.orthomcl.org³ www.cbs.dtu.dk/services/NetPhosK/⁴ Bridges et al., 2007⁵ Broadhead et al., 2006⁶ Zhou et al., 2010⁷ Oberholzer et al., 2011⁸ Subota et al., 2014⁹ Vertommen et al., 2008¹⁰ Colasante et al., 2006¹¹ Güther et al., 2014

c: conserved; k: kinetoplastid-specific; t: *Trypanosoma*-specific; PM: plasma membrane; CS: cytoskeleton
green: phospho-RXXS*/T* identified; orange: no RXXS/T in primary amino acid sequence

Table S2: Kinases identified as putative substrates of *T. brucei* PKA.

gene ID ¹	description ¹	kinase group ²	putative dual specificity kinase	phospho-RXXS/T identified	NetPhosK prediction PKA ³
Tb927.10.5140	protein kinase, putative,mitogen-activated protein kinase 2, putative	CMGC	no		
Tb927.5.800	casein kinase I, isoform 2	CK	yes	S186	0,7
Tb11.01.4230	protein kinase, putative	CMGC/CLK	maybe		
Tb11.01.1050	hypothetical protein, conserved	unique	maybe		
Tb927.10.13780	glycogen synthase kinase 3	CMGC/GSK	yes (but only autophosphorylation at Tyr)		
Tb11.02.5050	protein kinase, putative	other/PEK	no		
Tb927.2.2720	protein kinase, putative	unique	maybe	S492, S1427	-- , 0.88

¹ www.tritrypdb.org

² Parsons et al., 2005

³ www.cbs.dtu.dk/services/NetPhosK

Supplemental material – Chapter 5

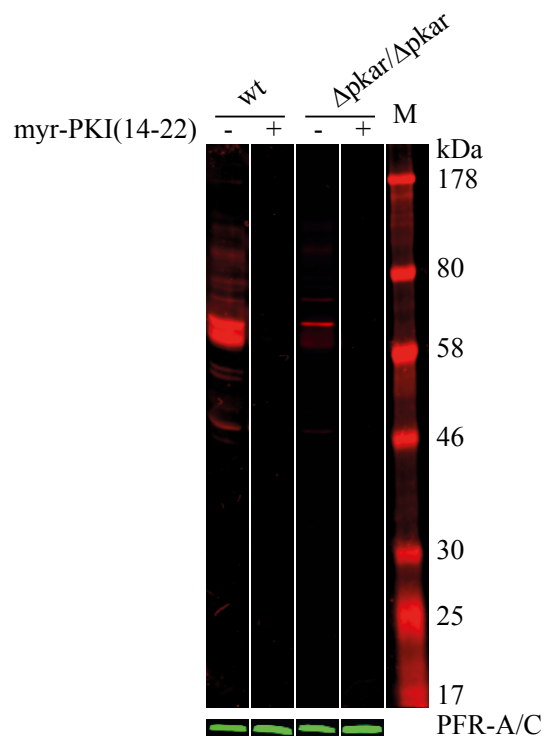


Figure S1: PKA-specificity of global RXXS/T site phosphorylation. Western blot analysis of lysates of *T. brucei* wild type (wt) cells and a homozygous *PKAR* deletion mutant ($\Delta pkar/\Delta pkar$) with a phospho-specific RXXS*/T* antibody. Cells were treated (+) or not (-) with 200 μ M PKA-specific inhibitor peptide myr-PKI(14-22) for 10 minutes. PFR-A/C was used as loading control and detected by the monoclonal antibody L13D6 (Kohl et al., 1999).

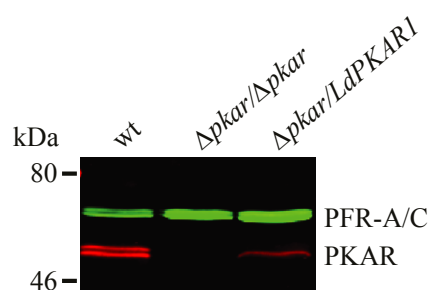


Figure S2: Specificity of the anti-PKAR antibody. A Western blot loaded with lysates from *T. brucei* MiTat 1.2 bloodstream parasites (wt), a homozygous deletion mutant of *PKAR* ($\Delta pkar/\Delta pkar$) and an endogenous rescue with *L. donovani* *PKAR* ($\Delta pkar/ /LdPKAR1$) shows that the serum raised against *T. brucei* *PKAR* (Tb427tmp.02.2210) cross-reacts with *L. donovani* *PKAR* (LdBPK_130160.1). PFR-A/C detected by the monoclonal antibody L13D6 (Kohl et al., 1999) was used as loading control. The endogenous *PKAR* of both *T. brucei* and *L. donovani* (see Figure 4B) comes in two molecular mass variants, suggesting allelic polymorphisms.

Supplemental material – Discussion

Table S1: *T. brucei* PKA substrate candidates with known or putative role in motility control.

gene ID ¹	product description ¹	annotated/predicted GO function ¹	annotated/predicted GO process ¹	annotated/predicted GO component ¹	conservation ²	phospho-RXXS/T identified	NetPhosK1.0 prediction PKA ³	flagellar proteome ^{4,5,6,7}	motility phenotype upon RNAi in <i>T. brucei</i>	motility phenotype in other flagellated eukaryotic cells or organisms ^{1,5}	other remarks	known PKA substrate in other organism
Tb927.1.2340	alpha tubulin	GTP binding, GTPase activity, structural molecule activity	microtubule-based movement, microtubule-based process, protein polymerization	microtubule, protein complex	c							X (Boudreau et al., 2009)
Tb927.1.2330	beta tubulin	GTP binding, GTPase activity, structural molecule activity	microtubule-based movement, microtubule-based process, protein polymerization	microtubule, protein complex	c			x				X (Loza-Huerta et al., 2013)
Tb11.02.0760	dynein heavy chain, putative	ATP binding, ATPase activity, microtubule motor activity, nucleoside-triphosphatase activity, nucleotide binding	bioluminescence, microtubule-based movement, protein-chromophore linkage	dynein complex	c			x		linked to ciliary disease in humans		

gene ID ¹	product description ¹	annotated/predicted GO function ¹	annotated/predicted GO process ¹	annotated/predicted GO component ¹	conservation ²	phospho-RXXS/T identified	NetPhosK1.0 prediction PKA ³	flagellar proteome ^{4, 5, 6, 7}	motility phenotype upon RNAi in <i>T. brucei</i>	motility phenotype in other flagellated eukaryotic cells or organisms ^{1, 5}	other remarks	known PKA substrate in other organism
Tb927.3.930	dynein heavy chain, putative	ATP binding, ATPase activity, microtubule motor activity, nucleoside-triphosphatase activity, nucleotide binding	microtubule-based movement	dynein complex	c			x	motility defect in BSF and PCF (Monnerat et al., 2009)	linked to ciliary disease in humans		
Tb11.02.0030	Cytoplasmic dynein 2 heavy chain (DYNC2H1), putative, Cytoplasmic dynein 2 heavy chain (DYNC2H2), putative (DHC1b)	ATP binding, ATPase activity, microtubule motor activity, nucleotide binding	microtubule-based movement	dynein complex	c			x		linked to ciliary disease in humans	predicted to be cytoplasmic, but observed to be localized in the basal bodies and the flagellum (TriTryp DB user comment ID 24800)	
Tb927.10.14890	C-terminal motor kinesin, putative (TBKIFC1)	ATP binding, microtubule motor activity	intracellular protein transport, microtubule-based movement	null	c			x				
Tb927.10.890	kinesin, putative	ATP binding, microtubule motor activity, nucleotide binding	microtubule-based movement	null	t			x		linked to ciliary disease in humans		

gene ID ¹	product description ¹	annotated/predicted GO function ¹	annotated/predicted GO process ¹	annotated/predicted GO component ₁	conservation ²	phospho-RXXS/T identified	NetPhosK1.0 prediction PKA ³	flagellar proteome ^{4,5,6,7}	motility phenotype upon RNAi in <i>T. brucei</i>	motility phenotype in other flagellated eukaryotic cells or organisms ^{1,5}	other remarks	known PKA substrate in other organism
Tb927.10.12490	kinesin, putative	ATP binding, microtubule motor activity, sequence-specific DNA binding	microtubule-based movement	null	k							
Tb927.10.1170	intraflagellar transport protein IFT172, putative (IFT172)	null	null	null	c			x				
Tb11.55.0006	intraflagellar transport protein IFT88 (IFT88)	null	null	null	c							
Tb11.03.0880	predicted WD40 repeat protein (PIFTF6)	null	null	null	c							

gene ID ¹	product description ¹	annotated/predicted GO function ¹	annotated/predicted GO process ¹	annotated/predicted GO component ¹	conservation ²	phospho-RXXS/T identified	NetPhosK1.0 prediction PKA ³	flagellar proteome ^{4,5,6,7}	motility phenotype upon RNAi in <i>T. brucei</i>	motility phenotype in other flagellated eukaryotic cells or organisms ^{1,5}	other remarks	known PKA substrate in other organism
Tb927.10.450	hypothetical protein, conserved (CMF62)	null	null	null	c			x	motility defect in PCFs upon RNAi (Baron et al., 2007)	homologous to Traf3ip1 of other eukaryotes (44% identity to human Traf3ip1); in <i>C. elegans</i> , <i>Danio rerio</i> , <i>Chlamydomonas reinhardtii</i> as well as in mammalian cells (Kunitomo and Iino 2008; Li et al., 2008; Omori et al., 2008; Berbari et al., 2011) Traf3ip1 localizes to the cilium and is required for ciliogenesis		
Tb927.3.4290	PFR1 (PFR1)	calmodulin binding	null	microtubule-based Flagellum	k			x	motility defect in PCFs upon RNAi (Bastin et al., 1998, 1999; Durand-Dubief et al., 2003)			
Tb927.8.6660	paraflagellar rod component, putative (PFC1)	null	null	null	k	P-peptide identified (RRQT (T477))	0,71	x				

gene ID ¹	product description ¹	annotated/predicted GO function ¹	annotated/predicted GO process ¹	annotated/predicted GO component ¹	conservation ²	phospho-RXXS/T identified	NetPhosK1.0 prediction PKA ³	flagellar proteome ^{4,5,6,7}	motility phenotype upon RNAi in <i>T. brucei</i>	motility phenotype in other flagellated eukaryotic cells or organisms ^{1,5}	other remarks	known PKA substrate in other organism
Tb11.01.0680	leucine rich repeat (TbLRRP1)	null	null	null	k	P-peptide identified (RPPS (S559); RSAS (S608); RRRS (S620))	0.74; 0.65; 0.89	x	motility defect in PCFs upon RNAi (Broadhead et al., 2006)		interacts with Ran (Brasseur et al., 2014); Ran identified as putative PKA substrate devoid of a PKA phosphorylation site; Ran is involved in ciliary protein targeting in various eukaryotes	
Tb927.8.8330	calpain, putative, cysteine peptidase, putative	calcium-dependent cysteine-type endopeptidase activity	proteolysis	intracellular	k	P-peptide identified (RRPS (S261))	0,81	x	growth and CC phenotype, lethal in BSF	suggested to control cell motility in human cells (reviewed in Wells et al., 2005)		X
Tb927.4.2080	C2 domain containing protein (CC2D)	null	flagellum assembly	null	k	P-peptide identified (RNNS (S488))	0,76	x			human protein CC2D2A with similar domain organization implicated in ciliogenesis and ciliopathies	

gene ID ¹	product description ¹	annotated/predicted GO function ¹	annotated/predicted GO process ¹	annotated/predicted GO component ¹	conservation ²	phospho-RXXS/T identified	NetPhosK1.0 prediction PKA ³	flagellar proteome ^{4,5,6,7}	motility phenotype upon RNAi in <i>T. brucei</i>	motility phenotype in other flagellated eukaryotic cells or organisms ^{1,5}	other remarks	known PKA substrate in other organism
Tb927.5.800	casein kinase I, isoform 2 (CK1.2)	ATP binding, protein kinase activity, protein serine/threonine kinase activity, protein tyrosine kinase activity	protein phosphorylation	null	c	P-peptide identified (RYCS (S186))	0,7	x		important for proper motility in <i>Chlamydomonas</i> (Gokhale et al., 2009; Boesger et al., 2012) or <i>Paramecium</i> (Walczak and Nelson, 1993)		
Tb11.02.4700	14-3-3 protein	protein domain specific binding	null	null	c			x	motility defect in PCFs upon RNAi (Inoue et al., 2005)	regulation of cell motility in cancer cells (Goc et al., 2012)		X

¹ www.tritrypdb.org² www.orthomcl.org³ www.cbs.dtu.dk/services/NetPhosK/⁴ Broadhead et al., 2006⁵ Zhou et al., 2010⁶ Oberholzer et al., 2011⁷ Subota et al., 2014c: conserved; k: kinetoplastid-specific; t: *Trypanosoma*-specific

Acknowledgements

First, I would like to express my special gratitude to my supervisor Prof. Michael Boshart for the opportunity to work on this exiting project and with this fascinating organism, for innumerable highly interesting and fruitful discussions, and for enabling me to participate in many international scientific conferences.

I am very grateful to Prof. Martin Parniske for being the second examiner of this thesis and for his continuous interest in this project. I also would like to thank Prof. Angelika Böttger, Dr. Ralf Heermann, Prof. Dirk Eick and Prof. Heinrich Leonhardt for serving as members of my thesis committee.

Special thanks goes to all our collaborators (Etienne Pays and Didier Salmon, Harry de Koning, Dan Zilberstein, Frank Schwede and Hans-Gottfried Genieser, Axel Imhof, and Lars Israel), whose contributions were essential for successful completion of our joint projects. Many thanks to Dan for the great time in his lab and the great stay at the very comfortable and luxurious guesthouse at the campus of the Technion University.

A big thank goes to all the former and present members of the AG Boshart and the AG Janzen for the great atmosphere, the fruitful scientific discussions, and their support in all respects. Thank you for the many nice evenings we had in and outside of the lab with plenty of scientific and non-scientific discussions, beer and lots of fun. Thanks to all lab members for their great baking skills and the many tasty cakes we had in the last years.

Special thanks to Larissa for her continuous support by preparing media or buffers and by always having nice and motivating words and lots of chocolate.

I am especially grateful to my family and friends for their continuous sympathy and support in every respect.

Curriculum Vitae

Personal details

Name	Sabine Bachmaier
Date of birth	September 11, 1981
Place of birth	Pfarrkirchen

University

since 06/2008	<p>PhD thesis, LMU Munich, Section of Genetics, group of Prof. Dr. Michael Boshart</p> <ul style="list-style-type: none"> • thesis title: “Evolutionary repurposing of cAMP and PKA signaling pathways in kinetoplastids” • member of the international graduate school “Life Science Munich” (LSM) • member of the mentoring program LMUMentoring (12/2012-09/2014)
09/2002 – 04/2008	<p>Study of Biology (diploma) LMU Munich</p> <ul style="list-style-type: none"> • degree: <i>Dipl.-Biol.</i> (grade: 1.0) • thesis title: “Charakterisierung einer PKA-ähnlichen Kinase in <i>Trypanosoma brucei</i>”

Education

06/2000	<p>University-entrance diploma, Gymnasium Pfarrkirchen</p> <ul style="list-style-type: none"> • degree: Abitur (grade: 1.7)
---------	---

Publications

Bachmaier, S., Kramer, S., Pepperl, J., Githure, G., Israel, L., Imhof, A., Boshart, M. (2015). A cold-inducible protein kinase A regulates stage differentiation in trypanosomes. **Manuscript**.

Bachmaier, S., Kramer, S., Githure, G., Scharf, F., Polatoglou, E., Klöckner, T., Krumbholz, C., Böttger, F., Pepperl, J., Schulte zu Sodingen, C., Schwede, F., Gunasekera, K., Ochsenreiter, T., Genieser, H.-G., Boshart, M. (2015). Cyclic AMP-independent signaling from a conserved PKA. **Manuscript**.

Bachmaier, S.*, Witztum, R. *, Tsigankov, P., Koren, R., Boshart, M., Zilberstein, D. (2015). Bidirectional axenic differentiation of *Leishmania* implicates changes in protein kinase A signaling. **Manuscript** submitted to Int J Parasitol.

* these authors contributed equally to this article.

Bachmaier, S., and Boshart, M. (2013). Kinetoplastid AGC Kinases. In Protein Phosphorylation in Parasites (Wiley-VCH Verlag GmbH & Co. KGaA), pp. 99-122.

Gould, M.K.*, Bachmaier, S.*, Ali, J.A., Alsford, S., Tagoe, D.N., Munday, J.C., Schnauffer, A.C., Horn, D., Boshart, M., and de Koning, H.P. (2013). Cyclic AMP effectors in African trypanosomes revealed by genome-scale RNA interference library screening for resistance to the phosphodiesterase inhibitor CpdA. *Antimicrob Agents Chemother* 57, 4882-4893.

* these authors contributed equally to this article.

Salmon, D., Vanwalleghem, G., Morias, Y., Denoeud, J., Krumbholz, C., Lhomme, F., Bachmaier, S., Kador, M., Gossmann, J., Dias, F.B., *et al.* (2012b). Adenylate cyclases of *Trypanosoma brucei* inhibit the innate immune response of the host. *Science* 337, 463-466.

Salmon, D., Bachmaier, S., Krumbholz, C., Kador, M., Gossmann, J.A., Uzureau, P., Pays, E., and Boshart, M. (2012a). Cytokinesis of *Trypanosoma brucei* bloodstream forms depends on expression of adenylyl cyclases of the ESAG4 or ESAG4-like subfamily. *Mol Microbiol* 84, 225-242.

National and international conferences

- 2015 **4th Conference on Protein Kinases of Parasitic Protozoa: Targeting signaling pathways in parasites** (Haifa, Israel)
Talk: Cyclic AMP-independent signaling from a conserved PKA.
- 2013 **ASTMH annual meeting** (Washington, USA)
Talk (invited speaker): A novel cAMP signaling pathway in *T. brucei*.
- 2013 **PAI 7/41 meeting “Tolerance and resistance to parasite infection: Trypanosomatidae as paradigm (TRIT)”** (Antwerp, Belgium)
Talk: A novel kinetoplastid-specific pathway for cAMP signaling.
- 2013 **5th Kinetoplastid Molecular Cell Biology Meeting** (Woods Hole, MA, USA)
Talk: A novel cAMP signaling pathway in *T. brucei*.
Prize for best talk: invitation to the ASTMH annual meeting 2013 (Washington, USA)
- 2013 **3rd ACETOTRYP Meeting** (Frauenchiemsee, Germany)
- 2011 **4th Kinetoplastid Molecular Cell Biology Meeting** (Woods Hole, MA, USA)
Poster: Screening for downstream effectors of cAMP and PKA-like kinases in *T. brucei*.
- 2011 **Life Science Munich (LSM) conference** (Schliersee, Germany)
Talk: Screening for downstream effectors of cAMP and PKA-like kinases in *T. brucei*.

- 2010 **“Molecular Dialogue in Host-Parasite Interaction”** (Brussels, Belgium)
Poster: Identification of downstream substrates of cold-inducible *T. brucei* PKA-like kinase.
- 2010 **3rd Conference on Protein Kinases of Parasitic Protozoa** (Lausanne, Switzerland)
Poster: *T. brucei* PKA-like kinases: no activation by cAMP but by cold shock.
- 2009 **3rd Kinetoplastid Molecular Cell Biology Meeting** (Woods Hole, MA, USA)
Talk: Cold-inducible PKA-like kinase of *Trypanosoma brucei*.

Workshops / training

- proteomics workshop (BioRad, EMBL Heidelberg, Germany)
- training in *Leishmania* cell culture and *in vivo* kinase assays (Technion University, Haifa, Israel)
- training in sample preparation for mass spectrometry (Adolf-Butenandt Institute, Munich, Germany)
- soft skill workshops: poster presentation, literature management using Endnote, Adobe Illustrator CS5 (Graduate Center LMU); Projektmanagement (Student und Arbeitsmarkt, LMU); Professionelle Mitarbeiterauswahl, Konfliktmanagement (LMUMentoring); Produktives Selbstmanagement (LMU)

Teaching

- 2008 – 2014 Supervision of practical courses
- Phosphoproteomics
 - Genetik II
 - Methods for protein kinase analysis *in vivo* and *in vitro*
 - Parasitäre Tropenkrankheiten: Einzeller und ihre tödlichen Strategien (for medical students)
 - Methods in Molecular Biology – applied to pathogen biology (for Brazilian exchange students, funded by “Science without borders”)
 - Analysis of signal protein regulation *in vitro* and by reverse genetics
- 2009 – 2012 Supervision of bachelor / diploma theses
- “Großpraktikum” Gisela Schimmak
 - diploma thesis Andrea Forkert
 - diploma thesis Felizitas Schmitz
 - bachelor thesis Matthias Noll
 - bachelor thesis Anna Krauthloher
- 2010 – 2011 Supervision of “Summer School” students
- Marko Ristic (AMGEN)
 - Fatma Bathawab (AMGEN)

- Bahar Degirmenci (LSM)

2006 – 2007 Student research assistant

- Fortgeschrittenen-Praktikum Genetik
- Biologisches Praktikum für Mediziner